

**Teil 1: „Studies on the extracellular matrix enzyme
lysyl oxidase (LOX) in epithelial cells“**

**Teil 2: „Gene expression signatures of circulating peripheral blood
cells associated with early-onset coronary artery disease“**

Inaugural-Dissertation
zur
Erlangung des Doktorgrades
der Mathematisch-Naturwissenschaftlichen Fakultät
der Universität zu Köln
vorgelegt von
Matthias Jansen
aus Köln

Hundt Druck GmbH, Köln
2012

Berichterstatter:

(Gutachter)

Tag der mündlichen Prüfung:

Prof. Dr. Arnd Baumann

Prof. Dr. Thomas Wiehe

16. April 2012

Teil 1:
„Studies on the extracellular matrix enzyme
lysyl oxidase (LOX) in epithelial cells“

Durchführung der experimentellen Arbeiten am
Cardiovascular Research Center, University of Hawaii, Honolulu

vorgelegt von
Matthias Jansen

Köln, im Februar 2012

Table of contents

I. Introduction	5
1. Lysyl oxidase	5
1.1 Amine oxidases	5
Table 1. Characteristics of mammalian amine oxidases.	6
1.2 The lysyl oxidase family	6
Figure 1. Domain organization of the five members of the mammalian lysyl oxidase enzyme family.	7
Figure 2. Sequence alignment for the copper-binding motif of the human lysyl oxidase enzymes.	7
Figure 3. Sequence alignment for the LTQ cofactor of the human lysyl oxidase enzymes.	8
Figure 4. Chemical structure of the LTQ cofactor in mature LOX with the lysine and tyrosine residue involved numbered according to the rat LOX sequence (from Smith-Mungo & Kagan, 1998).	8
Figure 5. Sequence alignment of the cytokine receptor-like (CRL) domain of the human lysyl oxidase enzymes and its homology to the N Domain of class I cytokine receptor.	9
1.3 Biosynthesis and processing of LOX	10
2. Significance of LOX for connective tissue homeostasis	10
Figure 6. Stoichiometry of the LOX-catalyzed reaction.	12
Figure 7. LOX-catalyzed oxidation of primary amines in lysine residues and crosslink formation by spontaneous condensation of the resulting aldehydes (from Kagan & Cai, 1995).	12
Figure 8. Space-filling model of the sequences adjacent to the lysine and tyrosine that form the LTQ cofactor within the catalytic site of LOX.	14
Figure 9. Schematic depiction of a fibroblast secreting precursors of collagen and elastin.	14
3. LOX in cancer: tumor suppressor versus metastasis promoter	15
Table 2. Genes and their respective proteins that are up- or down-regulated during EMT.	18
Figure 10. Epithelial-mesenchymal transition (EMT) during development and cancer.	19
4. Dissertation hypothesis and specific aims	21
II. Material and methods	23
1. Cell Culture	23
<i>MDCK II cells</i>	23
<i>MCF-10A cells</i>	23
2. RNA purification	23

Table of contents

3. cDNA synthesis	24
4. Polymerase chain reaction (PCR)	24
Table 3: Primers for RT-PCR detection of LOX in MDCK II cells and MCF-10A cells.	26
5. Cloning of lysyl oxidase constructs	26
5.1 PCR and agarose gel electrophoresis of amplified DNA fragments	26
Table 4: PCR primers for the generation of LOX expression constructs.	26
5.2 DNA purification from agarose gels	27
5.3 Restriction enzyme digestion	27
5.4 DNA ligations	28
5.5 Bacterial transformation	28
5.6 Plasmid purification	28
6. Site-directed mutagenesis	29
Table 5: Mutagenic primers for generation of mutated mature LOX constructs.	30
Table 6: Cycle parameters for synthesis and amplification of the mutated pcDNA-LOX30-Y355F construct.	31
7. Generation of stable MDCK cell lines	31
8. Preparation of protein extracts from whole cell lysates	32
9. Preparation of protein extracts from conditioned cell medium	32
10. Measuring protein concentration with the Bradford Assay	33
11. SDS Polyacrylamid Gel-Electrophoresis (PAGE)	33
12. Western blot analysis	34
13. Immunofluorescence staining	34
14. Primary antibodies	35
15. Secondary antibodies	36
Table 7: Secondary antibodies used for western blot analysis or immunofluorescence studies.	36
16. Assay for lysyl oxidase enzyme activity	37
III. Results	38
Rationale to study LOX in epithelial cells	38

Table of contents

1. Characterization of LOX expression in MDCK II and MCF-10A cells	38
Figure 11. (A) MDCK II and (B) MCF-10A cells display the characteristic “cobblestone” morphology of polarized epithelial cells in culture.	40
Figure 12: MDCK II cells express (A) E-Cadherin and (B) ZO-1, two characteristic cell-cell junction proteins for epithelial cells.	40
Figure 13. Expression of LOX mRNA in MDCK II and MCF-10A cells as detected by RT-PCR with gene-specific primers.	41
Figure 14. Alignment of the annotated amino acid sequences of the human and putative dog LOX protein.	42
Figure 15. Detection of LOX protein by western blot analysis in cell lysates and media fractions of (A + B) MDCK II and (C) MCF-10A cells.	45
Figure 17. Detection of fibronectin in conditioned cell medium of MDCK II and MCF-10A cells.	47
Figure 18. Immunofluorescence staining of LOX in MDCK II cells.	48
Figure 19. Principle of the assay for LOX activity measurements.	50
Figure 20. BAPN-inhibitable lysyl oxidase enzyme activity in conditioned cell medium of MDCK II (top panel) cells and MCF-10A (bottom panel) cells.	51
Summary	52
2. Increased LOX expression during scattering of MDCK II cells	53
Figure 21. Scattering of MDCK II cells induced by HGF treatment.	54
Figure 22. Increased expression of vimentin and cytoplasmic re-localization of E-cadherin during scattering of MDCK II cells.	55
Summary	56
Figure 23. Examination of vimentin and E-cadherin expression during scattering of MDCK II cells by western blot analysis.	57
Figure 24. Standard graph for LOX copy numbers after linear amplification from a pcDNA-LOX plasmid template.	58
Figure 25. Increased LOX transcript levels after scattering of MDCK II cells.	59
3. Generation of stable MDCK II cell lines over-expressing LOX	60
3.1 Stable MDCK II cell lines that over-express LOX-EGFP constructs	60
Figure 26. Schematic depiction of the cloning strategy for LOX-EGFP expression constructs.	61
Figure 27. Analysis of LOX-EGFP constructs by restriction digest.	62
Figure 28. Morphology of stable MDCK II LOX-EGFP cell lines.	64
Figure 29. Examination of LOX30-EGFP expression in stable MDCK cell lines.	65
Figure 30. Examination of LOX50-EGFP expression in stable MDCK cell lines by western blot analysis.	67

Table of contents

Figure 31. Examination of LOX50-EGFP expression in stable transfected MDCK II cell lines by immunofluorescence analysis.	68
Figure 32. BAPN-inhibitable lysyl oxidase enzyme activity in conditioned cell medium of LOX-EGFP expressing MDCK II cells.	69
3.2 Stable cell lines that over-express pcDNA-LOX(-V5) constructs	70
Figure 33. Schematic depiction of the cloning strategy for pcDNA-LOX(-V5) expression constructs.	70
Figure 34. Restriction digest of pcDNA-LOX constructs.	72
Figure 35. Morphology of stable MDCK II pcDNA-LOX cell lines.	73
Figure 36. Examination of pcDNA-LOX30 expression in stable transfected MDCK cell lines by western blot analysis.	75
Figure 37. Examination of pcDNA-LOX50 expression in stable transfected MDCK cell lines by western blot analysis.	76
Figure 38. BAPN-inhibitable lysyl oxidase enzyme activity in conditioned cell medium of pcDNA-LOX expressing MDCK II cells.	78
Summary	79
Table 8. Qualitative characteristics of stable MDCK-LOX cell lines.	79
IV. Discussion and future perspectives	81
V. Abstract	88
VI. Zusammenfassung	90
VII. Literature	92

I. Introduction

1. Lysyl oxidase

The discovery of the matrix enzyme lysyl oxidase (LOX) emerged from the convergence of mainly two research areas. Already the greek philosopher Hippocrates reported that chronic ingestion of the sweet pea *Lathyrus odoratus* can result in a disease today referred to as lathyrism. Studies with experimental animal models in the first half of the 20th century demonstrated increased connective tissue fragility and increased collagen solubility in the individuals affected {Geiger et al., 1933}. Scientific research in the 1950s revealed that the symptoms are caused by the chemical compound beta-aminopropionitrile (BAPN) present in *L. odoratus* extracts {McKay et al., 1954}. Further studies showed that lathyritic connective tissue contained collagen and elastin with reduced levels of covalent crosslinks resulting in their increased solubility {Tanzer, 1965; Piez, 1968}.

Around the same time nutritional copper deficiency had been demonstrated to cause similar connective tissue symptoms with reduced covalent crosslinks between lysine residues in collagen and elastin fibers {O'Dell et al., 1961; Savage et al.; 1966; O'Dell et al., 1966}. These findings led to the hypothesis of a putative copper-dependent enzyme that was inhibitable by the lathyric factor BAPN and that catalyzed the oxidative deamination of lysine residues resulting in spontaneous intra- and intermolecular crosslink formation of collagen and elastin fibers. Pinnell and Martin published in 1968 their landmark paper demonstrating that BAPN was an irreversible inhibitor of an extracellular enzyme with substrate specificity for peptidyl lysine residues {Pinnell & Martin, 1968}. This enzyme was later given the name lysyl oxidase {Siegel et al., 1970}.

1.1 Amine oxidases

Lysyl oxidase belongs to the family of amine oxidases including monoamine oxidases A and B (MAO A and B), polyamine oxidase (PAO), semicarbazide-sensitive amine oxidase (SSAO) also called vascular adhesion protein 1 (VAP-1) and diamine oxidase (DAO) {Jalkanen & Salmi, 2001}. This enzyme family is classified into different subgroups based on their cofactors, either a flavin-adenine dinucleotide (FAD) or a copper atom in conjunction with a quinone cofactor (Table 1). FAD-containing amine oxidases have the ability to oxidize primary, secondary or tertiary amines whereas the copper-containing amine oxidases (CuAO) oxidize exclusively primary amine substrates. In contrast to most amine oxidases, which act primarily on small molecule amines such

Introduction

as neurotransmitters in the case of MAOs, LOX is known for its catalytic action on lysine residues of macromolecular substrates such as fibrillar collagen and elastin.

Amine Oxidase	Cofactor	Substrates
MAO A & B	FAD	Monoamines (e.g. dopamine, serotonin)
PAO	FAD	Polyamines (e.g. spermine, spermidine)
DAO	Copper and topaquinone (TPQ)	Diamines (e.g. histamines, spermine)
SSAO or VAP-1	Copper and topaquinone (TPQ)	Monoamines (e.g. dopamine, tyramine)
LOX and LOX-like 1-4	Copper and lysyl-tyrosylquinone (LTQ)	Peptidyl lysines (e.g. collagen, elastin, cadaverine)

Table 1. Characteristics of mammalian amine oxidases.

1.2 The lysyl oxidase family

The mammalian lysyl oxidase gene family consists of the prototypic LOX and four additional LOX-like genes encoding proteins that share a highly conserved C-terminus but are rather diverse at their N-termini (Figure 1). Researchers observed from early on that chromatographic separation of purified LOX from tissue extracts yielded multiple isoforms leading to the hypothesis that several LOX isozymes may exist {Narayanan et al., 1974; Stassen, 1974; Kagan et al. 1979}. However, it was not until the 1990s that four additional LOX-like genes were identified and subsequently cloned {reviewed in Csiszar, 2001}. All five members of the lysyl oxidase enzyme family contain a catalytic domain and a cytokine-receptor-like domain at the N-terminus (Figure 1). The catalytic domain consists of the copper-binding motif and a unique lysyl-tyrosylquinone (LTQ) cofactor. The copper-binding motif contains four histidines that are thought to coordinate binding of copper into the active site (Figure 2) {Gacheru et al., 1990; Kosonen et al., 1997}. The LTQ cofactor is formed through covalent linkage between lysine 314 (K314) and tyrosine 349 (Y349) in the rat LOX protein and is conserved in all LOX-like proteins (Figures 3 and 4). This cofactor is unique to the lysyl oxidase enzyme family and is essential for the catalytic activity of LOX. In mutagenesis studies with rat LOX where the LTQ tyrosine residue was replaced by phenylalanine, activity of the LOX enzyme was diminished {Wang et al., 1996; Wang et al., 1997}. Partially overlapping with the LTQ site is the cytokine receptor-like (CRL) domain whose name results from its sequence homology to the N-terminal consensus sequence of class I cytokine receptors (Figure 5) {Bazan, 1990}. The function of this domain in the lysyl oxidase family of proteins is not known.

Introduction

As much as the C-terminus is conserved, the N-terminus displays a great diversity among LOX and the LOX-like proteins implicating potential differences in their function (Figure 1). LOXL, the first LOX-like protein identified after the prototypic LOX, contains a distinct proline-rich region whose functional significance has not been clarified yet {Kenyon et al., 1993; Kim et al., 1995}.

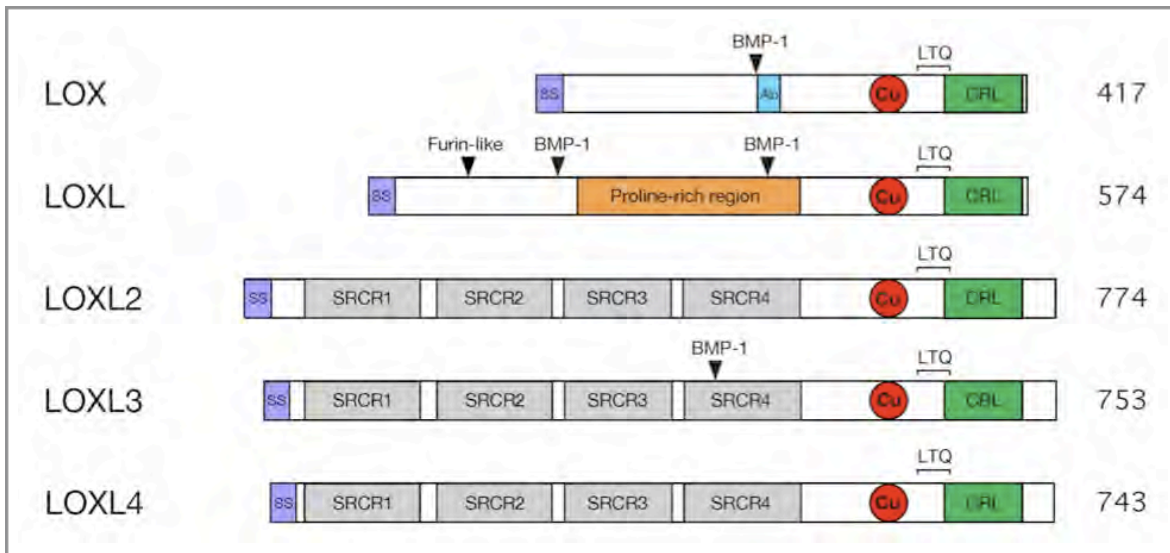


Figure 1. Domain organization of the five members of the mammalian lysyl oxidase enzyme family.

The name and number of amino acids of each protein are indicated on the left and right side, respectively. The signal sequence (SS) for each protein is shown in magenta, the copper-binding motif (Cu) in red, the cytokine-receptor-like (CRL) domain in green and the location of the lysyl-tyrosylquinone (LTQ) cofactor is indicated with a bracket. In addition, known processing sites for proteases, such as bone-morphogenetic protein 1 (BMP-1), are marked with an arrow. A 22-mer peptide within the LOX sequence that was used as an epitope to generate a polyclonal antibody used in this study is shown in light blue. A proline-rich region in LOXL is marked in orange. The four scavenger-receptor cysteine-rich (SRCR) modules present in LOXL2, LOXL3 and LOXL4 are highlighted in grey (from Csiszar, 2001).

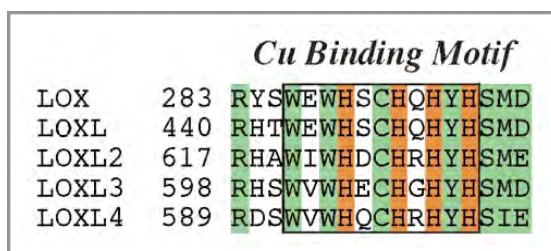


Figure 2. Sequence alignment for the copper-binding motif of the human lysyl oxidase enzymes.

Conserved amino acids among the proteins are shown in green. The four histidine residues thought to coordinate the copper atom within the catalytic site are depicted in orange (from Csiszar, 2001).

Introduction

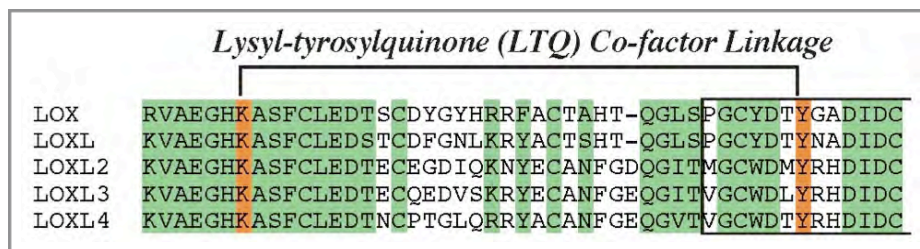


Figure 3. Sequence alignment for the LTQ cofactor of the human lysyl oxidase enzymes.

Conserved amino acids among the proteins are shown in green. The lysine residue and the tyrosine residue forming the lysyl-tyrosylquinone (LTQ) cofactor linkage are highlighted in orange (from Csiszar, 2001).

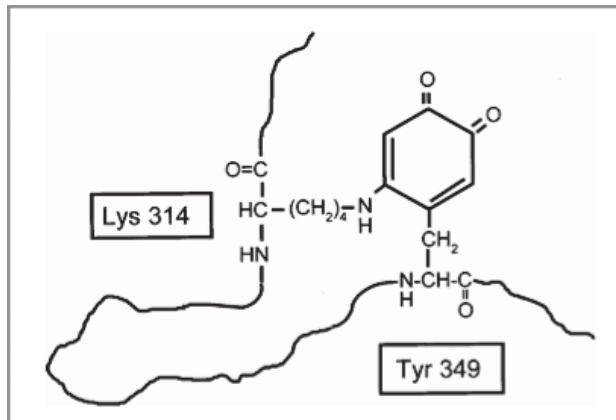


Figure 4. Chemical structure of the LTQ cofactor in mature LOX with the lysine and tyrosine residue involved numbered according to the rat LOX sequence (from Smith-Mungo & Kagan, 1998).

Introduction

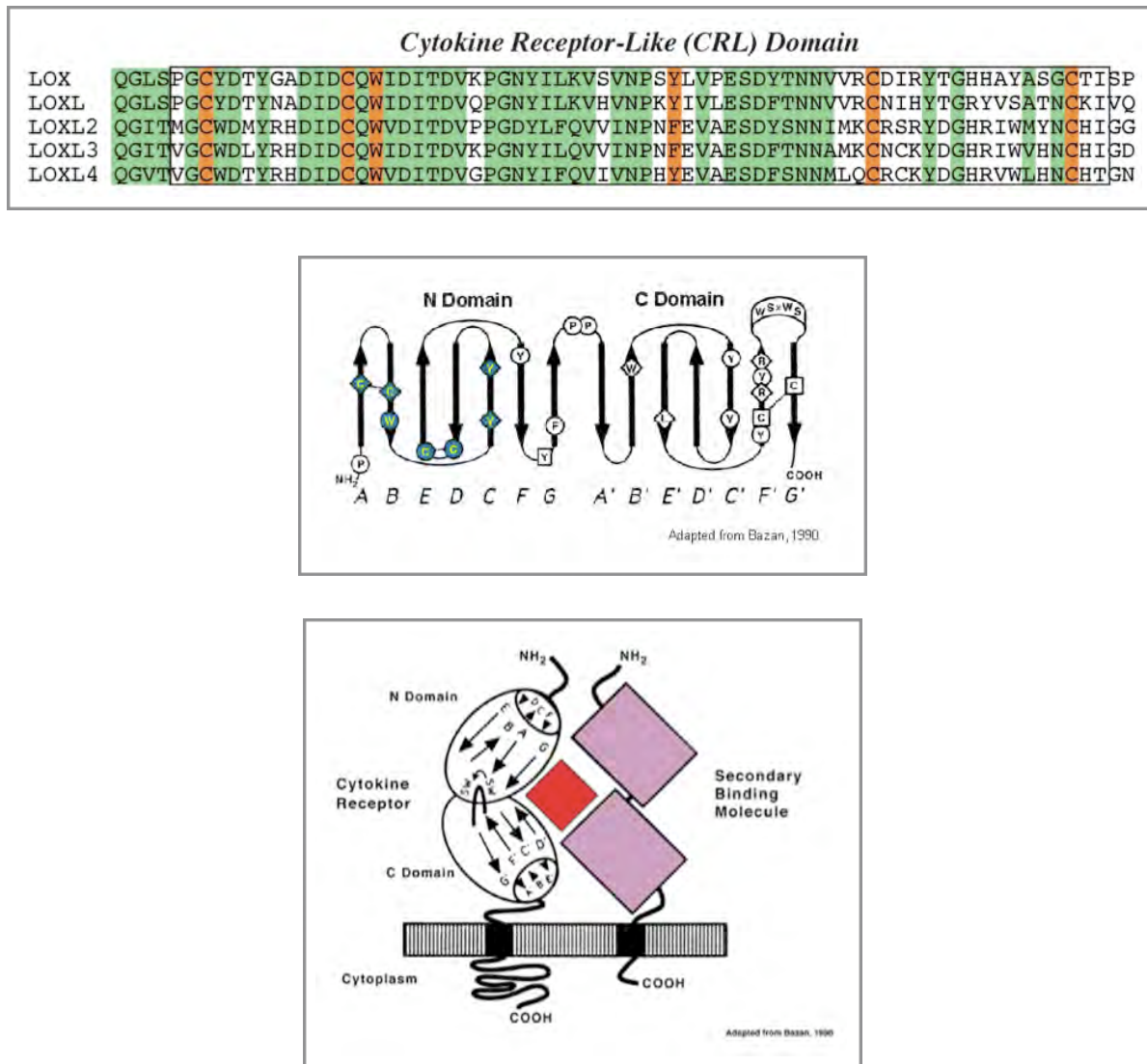


Figure 5. Sequence alignment of the cytokine receptor-like (CRL) domain of the human lysyl oxidase enzymes and its homology to the N Domain of class I cytokine receptor.

Top panel: Conserved amino acids among lysyl oxidase proteins are shown in green. Residues highlighted in orange match the type I cytokine receptor consensus sequence. *Middle panel:* Schematic depiction of the beta-sheets forming the N and C Domain in class I cytokine receptors. Residues matching the CRL domain of lysyl oxidase proteins are highlighted in blue. *Bottom panel:* Diagram of the cytokine receptor as it dimerizes with a secondary binding molecule (magenta) to bind a cytokine ligand (red) (from Csiszar, 2001).

Introduction

However, it is known from the literature that proline-rich sequences can interact with other protein domains such as SH3 (Src-homology 3) domains {Kay et al., 2000}. Future studies will have to determine whether the proline-rich region in LOXL mediates interactions with other proteins. LOXL2, LOXL3 and LOXL4 define a subgroup of the lysyl oxidase enzyme family that is characterized by the four scavenger-receptor cysteine-rich (SRCR) domains at the N-termini {Saito et al., 1997; Jourdan Le Saux et al., 1998; Maki et al., 2001a; Huang et al., 2001; Jourdan Le Saux et al., 2001; Asuncion et al., 2001; Maki et al., 2001b}. The function of the repetitive SRCR domains in LOX-like proteins remains unknown. SRCR domains are highly conserved ancient protein modules that are found in membrane-bound or soluble receptors in a variety of cell types in all species throughout the animal kingdom {Resnick et al. 1994; Sarrias et al., 2004}.

1.3 Biosynthesis and processing of LOX

After cloning and sequencing of the LOX gene, the molecular weight of the corresponding protein was predicted to be 48 kD thus differing from the previously characterized 32 kD active enzyme purified from bovine aorta {Kagan et al., 1979; Mariani et al., 1992}. Subsequent studies revealed that LOX is synthesized as a pre-proenzyme with the signal sequence being cleaved off in the endoplasmatic reticulum followed by multiple N-glycosylation during the secretory pathway in the Golgi network {Trackman et al., 1992}. Therefore, the LOX proenzyme emerges from the cell as a 50 kD glycosylated inactive precursor protein. After secretion into the extracellular space human proLOX is processed by proteolytic cleavage of the propeptide between Gly 168 and Asp 169 through bone morphogenetic protein 1 (BMP-1) into the mature form of the enzyme {Cronshaw et al., 1995; Panchenko et al., 1996}. Further studies showed that other extracellular proteases, including mammalian tolloid and tolloid-like 1 and 2, are also capable to convert proLOX into the mature active form, although with less efficiency compared to BMP-1 {Uzel et al., 2001}. Notably, BMP-1 is also known as procollagen-C-proteinase, and is the same protease that processes type I collagen precursors into mature collagen, one of the major substrates of LOX in the extracellular matrix {Prockop et al., 1998}.

2. Significance of LOX for connective tissue homeostasis

The connective tissue gives major structural support for all organs and provides with the skeleton also the scaffold that builds the internal frame of the vertebrate body {Olsen et al., 2000}. It consists of a highly complex and organized proteinaceous mixture called extracellular matrix

Introduction

(ECM) that is inhabited by different cell types of mesodermal origin {Mecham, 2011}. The connective tissue provides mainly two mechanical functions: tensile strength and elasticity. Collagen fibers, made of triple-helical ordered microfibrils, are the molecular basis for the tensile strength of bones {Knott & Bailey, 1998}. Elastic fibers, made of the protein elastin, ensure the elasticity of skin {Mecham, 1991}. More recently, the extracellular matrix of the connective tissue has also become appreciated as a reservoir of growth factors and effector of diverse cell functions {Nelson & Bissell, 2006}.

LOX is primarily known as an enzyme of outstanding importance for the formation of covalent crosslinks in collagen and elastin fibers, a crucial process for the maturation of these extracellular matrix macromolecules {Trackman & Kagan, 1991; Smith-Mungo & Kagan, 1998}. In this context, LOX is best characterized as the catalyst of the oxidative deamination of ϵ -amino groups in specific lysine residues of fibrillar collagen and elastin {Siegel, 1974; Bedell-Hogan et al., 1993}. The stoichiometry of this reaction is depicted in Figure 6. In the presence of molecular oxygen and water, the ϵ -amino group is transformed into an aldehyde group during the LOX-catalyzed reaction. The resulting allysine can then condensate in a spontaneous reaction with either another allysine or lysine residue to form covalent crosslinkages (Figure 7). Notably, hydrogen peroxide is generated as a side product during each reaction cycle. The specific detection of LOX-generated hydrogen peroxide has been used since many years as a sensitive indicator for the measurement of LOX activity {Trackman et al., 1981; Palamakumbura & Trackman, 2002}. The physiological importance of lysyl oxidase mediated crosslinking in soluble collagen and elastin precursors is illustrated by the phenotype of LOX knockout mice. These mice die either before, or shortly after birth, due to severe fragility of the connective tissue supporting the cardiovascular system, which is indicated by numerous aneurysms in major blood vessels {Maki et al., 2002; Hornstra et al., 2003; Maki et al., 2005}. Ultrastructural analysis of LOX knockout mice by electron microscopy revealed dramatic disturbances in connective tissue organization with strongly fragmented collagen and elastic fiber formation in cardiovascular, respiratory and skin tissues. Thus, LOX-initiated crosslinking is essential for both, the tensile strength of collagen fibers and for the elasticity of elastin fibers thereby mediating connective tissue integrity. Although it was assumed that soluble precursors of fibrillar collagen and elastin were the unique substrates of LOX, biochemical studies soon demonstrated this view as too limited. *In vitro* studies on the substrate specificity of LOX showed that the purified enzyme is able to oxidize a number of basic globular proteins with pI values > 8.0 including the H1 histone protein {Kagan et al., 1984}.

Introduction

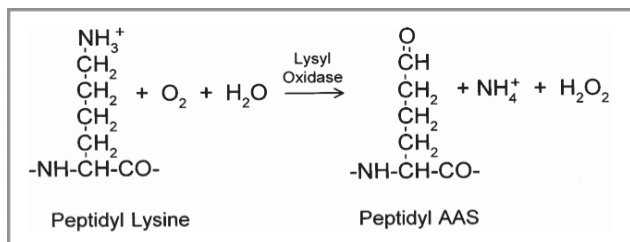


Figure 6. Stoichiometry of the LOX-catalyzed reaction.

LOX catalyzes the oxidative deamination of ϵ -amino groups in a peptidyl lysines resulting in the peptidyl aldehyde α -amino adipic- δ -semialdehyde (AAS). The catalytic reaction also requires the presence of molecular oxygen and water and yields in addition ammonia and hydrogen peroxide as side-products (from Lucero & Kagan, 2006).

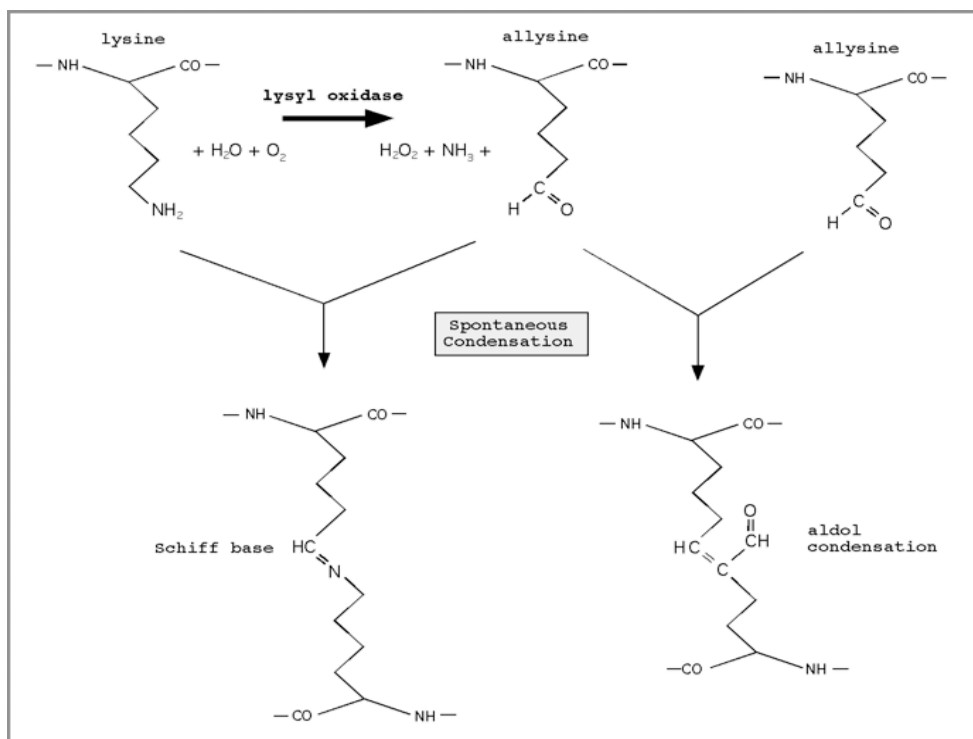


Figure 7. LOX-catalyzed oxidation of primary amines in lysine residues and crosslink formation by spontaneous condensation of the resulting aldehydes (from Kagan & Cai, 1995).

LOX-catalyzed deamination of lysine residues results in allysine (or α -amino adipic- δ -semialdehyde) where the ϵ -amino group is replaced by an aldehyde function. The aldehyde group in allysine can then spontaneously condense with the aldehyde group of another allysine (via aldol condensation) or with the ϵ -amino group of another lysine residue (via Schiff base).

Introduction

Notably, bovine serum albumine (BSA), a rather acidic protein, was oxidized by LOX, too, when glutamate and aspartate residues were converted into their basic counterparts glutamine and asparagines resulting in a basic protein. In addition, LOX can also oxidize non-peptidyl amine substrates such as cadaverine (1, 5-diaminopentane), which is commonly used as a substrate for the detection of LOX activity during *in vitro* assays {Palamakumbura & Trackman, 2002}. But until today there is no clear evidence for LOX activity towards other substrates than collagen and elastin *in vivo*.

These studies indicated that LOX may have a preference for cationic protein substrates. Attempts to elucidate the three-dimensional structure of LOX have not been successful yet due to difficulties in crystallizing sufficient amounts of the purified enzyme. However, analysis of the amino acid sequence suggests that anionic residues are indeed distributed in a manner that likely provides a localized density of anionic charge in the microenvironment of the catalytic site of LOX {Kagan et al., 1979}. The sequences surrounding the lysine and tyrosine residues forming the LTQ cofactor are both enriched in anionic residues (Figure 8). The notion that LOX seems to exhibit a strong preference for cationic protein substrates is also supported by the fact that the elastin precursor tropoelastin, a cationic protein, is easily oxidized by LOX *in vitro* {Bedell-Hogan et al., 1993}. In contrast, susceptible lysine residues in type I collagen that are known to be oxidized by LOX *in vivo* are located within hydrophilic sequences enriched in anionic residues. Synthetic peptides of these sequences of the N-terminal region of type I collagen were not oxidized by LOX *in vitro* {Nagan & Kagan, 1994}. This may indeed explain why collagen precursors have to undergo a self-assembly into microfibrillar arrays that presumably allow a favorable distribution of ionic charges along the protein prior to their oxidation by LOX {Siegel, 1974}. Thus, the electrostatic properties of the LOX protein and in particular of the catalytic region seem to reflect an important determinant for substrate specificity of this enzyme. At the same time it may provide an effective mechanism to prevent the random modification of abundant lysine residues in other proteins.

Since its discovery, research on lysyl oxidase has been conducted almost exclusively in mesenchymal cell types such as vascular smooth muscle cells in blood vessels, osteoblasts in cartilage or fibroblasts {reviewed in Kagan & Li, 2003}. These cell types, reside within the connective tissue and are traditionally known to produce and secrete most of the extracellular matrix proteins, such as collagen and elastin, into the surrounding stroma (Figure 9) {Gordon & Olsen, 1990}. Originally, it was believed these cell types may be the only source producing matrix

Introduction

proteins for the tissue stroma. However, accumulating evidence in the 1970s suggested that matrix proteins are not exclusively synthesized by mesenchymal cell types.

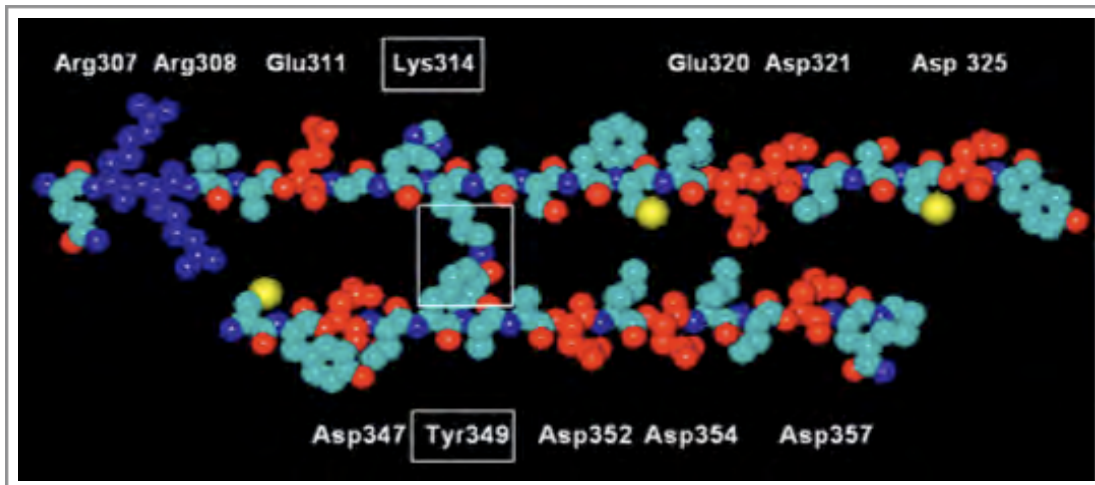


Figure 8. Space-filling model of the sequences adjacent to the lysine and tyrosine that form the LTQ cofactor within the catalytic site of LOX.

The square highlights the covalent link between Lys314 and Tyr349 in rat LOX. Shown in red are anionic residues such as glutamine and asparagines and in dark blue two cationic arginines. All remaining amino acids are highlighted in magenta (from Lucero & Kagan, 2006).

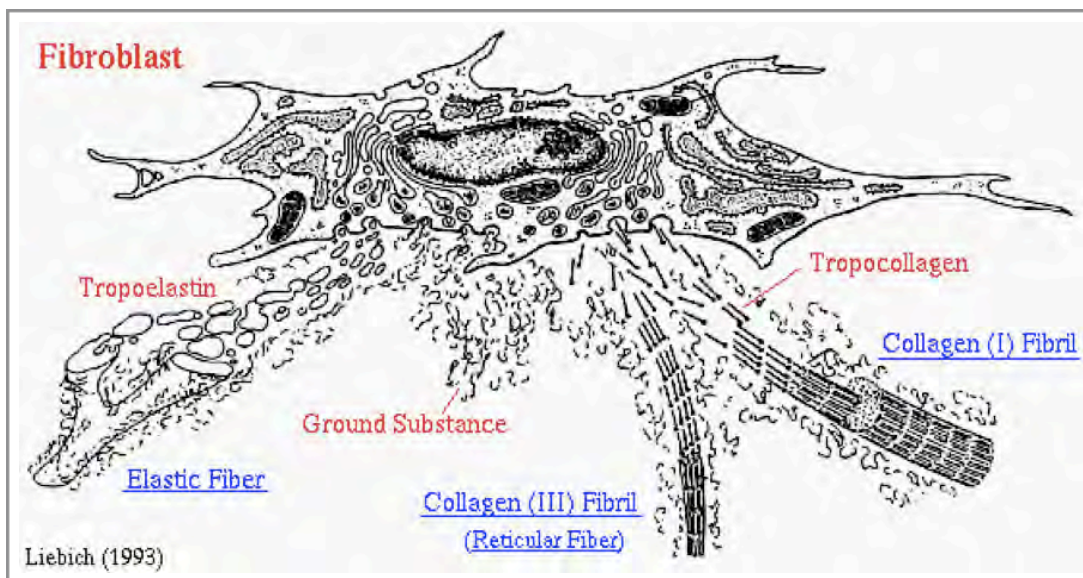


Figure 9. Schematic depiction of a fibroblast secreting precursors of collagen and elastin.

Fibroblasts are residential cells of the connective tissue. They synthesize and secrete typical matrix proteins such as collagen and elastin precursors. After secretion into the extracellular space these proteins assemble into their mature fibrillar structure (from Liebich, 1993).

Introduction

Hay and colleagues were the first to demonstrate that epithelial cells can produce and secrete fibrillar collagen into the tissue stroma {Dodson & Hay, 1971}. In subsequent years it was well established that many epithelial tissues contribute significant amounts of diverse matrix proteins to the stromal compartment {Hay, 1979}. Nevertheless, until today connective tissue research focuses primarily on mesenchymal cell types and so does lysyl oxidase research.

Although LOX expression has been detected in several epithelial tissues by immunohistochemistry, its potential role in epithelial cells has never been investigated. In recent studies LOX protein expression was observed in epithelial cell layers of the skin, kidney, liver and in reproductive organs such as the uterus and placenta {Hayashi et al., 2004; Noblesse et al., 2004; Fogelgren et al., 2005}. Some of the stainings imply intracellular localization of LOX but it remains unclear whether intracellular signals detected by LOX antibodies correspond to the proenzyme or to the mature form. However, because there is evidence for expression of LOX in epithelial tissues, it would be interesting to probe into the molecular function of LOX in epithelial cells.

3. LOX in cancer: tumor suppressor versus metastasis promoter

Lysyl oxidase research has traditionally focused on its matrix function within the connective tissue. However, one additional area of major interest arose in the early 1990s and suggested that LOX may also act as a tumor suppressor gene. The first evidence came already from a study a few years earlier where Kivirikko and colleagues observed decreased LOX activity in cancer cell lines of several sarcomas {Kuvianemi et al., 1986}. Around the same time when the LOX gene was cloned, Friedman and colleagues identified a gene that was not expressed in ras-transformants of NIH 3T3 fibroblasts but re-appeared in spontaneous revertants after prolonged interferon treatment {Contente et al., 1990}. Further investigation revealed that this gene, which was given the name ras-recision gene (rrg), was identical to LOX {Kenyon et al., 1991; Mariani et al., 1992}. These findings led to the hypothesis that LOX acts as a phenotypic suppressor of the ras oncogene. Subsequent studies demonstrated that LOX expression is downregulated in several malignantly transformed human cell lines {Hamalainen et al., 1995}. Decreased LOX expression was also observed in gastric, prostate and colorectal cancer tissues {Ren et al., 1998; Csiszar et al. 2002, Kaneda et al. 2004}. However, these studies did not investigate whether the decrease in LOX expression was related to ras-transformation in the corresponding tumor tissue. In fact, two reports indicated that loss-of-heterozygosity due to chromosomal aberrations in tumor cells was the cause for down-regulation of LOX expression rather than transformation by the ras oncogene {Csiszar et al., 2002; Kaneda et al.,

Introduction

2004}. Until today the exact mechanism(s) underlying the down-regulation of LOX in ras-transformed cells remains elusive. Although numerous consensus sequences for binding sites of transcription factors were identified within the promoter region of LOX, so far none of these have been linked mechanistically to decreased LOX mRNA levels in ras-transformed cells {Hamalainen et al., 1995; Csiszar et al., 1996}. However, DNA methylation of the LOX gene has been shown in ras-transformed fibroblasts as well as in gastric cancer tissues suggesting epigenetic inhibition of LOX expression {Contente et al., 1999; Kaneda et al., 2004}.

Evidence for a tumor suppressor role of LOX came also from other areas of research. Di Donato and colleagues demonstrated that knockdown of LOX in normal rat kidney fibroblasts by stable transfection of antisense constructs resulted in a transformed phenotype of these cells, that was characterized by anchorage-independent growth, reduced cell-matrix attachment and most importantly increased ras-expression {Giampuzzi et al., 2001}. In addition, these cells proved highly tumorigenic in nude mice. Subsequent studies provided evidence the transformed phenotype in cells of this model system was mediated by nuclear accumulation of beta-catenin in concert with up-regulation of cyclin D1 (Giampuzzi et al., 2003; Giampuzzi et al., 2005}. In contrast, the phenotype in ras-transformed NIH 3T3 fibroblasts seems to be mediated, at least partially, by the transcription factor NF- κ B as ectopic LOX expression inhibited NF- κ B activity indirectly through upstream signaling pathways that have not been clarified yet {Jeay et al., 2003}. More recently, Trackman and colleagues made the interesting observation that the phenotypic reversion of ras-transformed fibroblasts was independent of LOX catalytic activity. Further investigation revealed that the cleaved propeptide and not the mature enzyme inhibits ras-mediated transformation {Palamakumbura et al., 2004}. Subsequent studies using a mice Her-2/neu breast cancer model demonstrated that the LOX-propeptide inhibits Her-2/neu-driven transformation in these tumor cells, as well as tumor growth in nude mice and invasive properties {Min et al., 2007}. Her-2/neu is a member of the EGF receptor family and upstream activator of ras that has been found constitutively active in many breast cancers {Yarden & Sliwkowski, 2001}. In addition, ectopic expression of the LOX propeptide in lung and pancreatic cancer cells has been shown to inhibit their transformed phenotype via Bcl-2, a target gene of NF- κ B {Wu et al., 2007}.

On the other hand, there has been evidence accumulating in recent years that LOX may also act as a metastasis promoter during cancer progression. Gene expression profiling of cancer cells reflecting different stages of the disease showed a significant increase of LOX expression when tumors acquire a more invasive phenotype and start to metastasize distant tissue sites.

Introduction

While comparing gene expression profiles in human breast carcinoma cell lines from different disease stages by differential display analysis, Kirschmann and colleagues observed strongly elevated LOX mRNA levels in invasive breast cancer cells compared to non-invasive cell lines {Kirschmann et al., 1999}. Similarly, LOX was detected in a panel of genes up-regulated in renal cell carcinomas which were in particular aggressive and resistant to chemo- and radiation therapy {Stassar et al., 2001}. Strongly increased expression of LOX in invasive compared to non-invasive breast carcinoma cells was later also confirmed in microarray and proteomic expression profiling studies {Nagaraja et al., 2006; Mbenkui et al., 2007}. The first mechanistic link between LOX and cancer cell invasion came from a study showing that over-expression of LOX in a non-invasive breast cancer cell line resulted in a two-fold increase of invasiveness that was reversible upon treatment with the LOX-specific inhibitor BAPN in a dose-dependent manner {Kirschmann et al., 2002}. Similarly, antisense knock-down or BAPN-mediated inhibition of endogenous LOX in invasive breast cancer cells greatly reduced their invasive potential {Kirschmann et al., 2002}. Since BAPN treatment abolished invasiveness, these findings suggested that LOX-facilitated invasion depends on its catalytic activity. Further investigation revealed that LOX promotes breast cancer cell migration via a hydrogen peroxide-mediated mechanism involving focal adhesion kinase (FAK) and Src kinase signaling pathways {Payne et al., 2005}.

In addition, LOX expression was found elevated in hypoxic tumor cells that were in particular aggressive and invasive {Denko et al.; 2003}. Hypoxia is a characteristic feature of tumors > 1 mm in diameter and inflicts a selective pressure on tumor cells favoring angiogenesis and invasion of the tissue environment. Clinically, hypoxia is associated with poor distant metastasis-free survival in patients {Hockel & Vaupel, 2001}. Detailed analysis in breast carcinoma cells demonstrated that LOX expression is up-regulated under hypoxic conditions by the transcription factor hypoxia-inducible factor 1 (HIF-1) {Erler et al., 2006}. Furthermore, the authors showed that inhibition of LOX eliminates metastasis of orthotopically grown breast carcinomas in mice. The data indicated that LOX facilitated breast cancer cell invasion in this hypoxic tumor model through focal adhesion kinase signaling as suggested by other studies under normoxic conditions earlier as well. A follow-up study complemented these findings with the notion that hypoxia alone leads only to an increase in LOX expression but that subsequent reoxygenation is required for LOX catalytic activity, which in turn is essential for the induction of migratory properties during cancer cell invasion {Postovit et al., 2007}. Finally, most recently LOX was also identified as a critical factor for cellular invasiveness in malignant astrocytes.

Introduction

In line with previous observations in breast carcinomas, increased LOX expression and catalytic activity seems to be critical for invasive cell behavior in astrocytomas, which account for the most aggressive form of brain tumors {Laczko et al., 2007}.

A general observation is that LOX seems to play a role when tumors start to form metastases at distant tissue sites. As a prerequisite, cells within the primary tumor have to lose critical epithelial characteristics and have instead to acquire migratory properties that allow them to spread away from the tumor mass {Fidler, 2003}. Indeed, research over the last years has shown that malignant cells of primary tumors can undergo such a phenotypic change and this process is referred to as epithelial-mesenchymal transition (EMT) {Thiery, 2002; Huber et al., 2005}. In the field of developmental biology EMT has been already recognized for a long time as a critical process for metazoan organ development (Figure 10) {Hay, 2005}. During EMT, transcriptional programs become activated that lead to down-regulation of cell-cell adhesion molecules, such as E-cadherin, and up-regulation of mesenchymal marker proteins, such as vimentin or fibroblast-specific protein 1 (FSP-1) (Table 2). Researchers have discovered that often the same transcriptional programs become active during cancer metastasis {Kang & Massagué, 2004}. Therefore, LOX could be possibly one of the many target genes being up-regulated during EMT reprogramming of cancer cells.

Up-regulated genes	Down-regulated genes
Vimentin	E-cadherin
Fibroblast-specific protein 1 (FSP-1)	Ocludins
Snail	Claudins
Slug	Desmoplakin
α -smooth muscle actin	Cytokeratins

Table 2. Genes and their respective proteins that are up- or down-regulated during EMT.

Interestingly, the notion that LOX can induce cell motility is not completely new. Studies in the late 1980s showed that BAPN treatment of sea urchin embryos in the blastula stage prevented them from entering gastrulation {Wessel & McClay, 1987; Butler et al., 1987}. Gastrulation is a developmental process that is characterized by massive cell migration of cell clusters within the embryo and results in the formation of the three germ layers. Around the same time, wound healing studies demonstrated that migration of fibroblasts into fibrin clots was inhibited by BAPN in a dose-dependent manner {Nelson et al., 1988}.

Introduction

The first direct evidence that LOX can induce cell migration followed almost a decade later. Lazarus et al. could show that addition of purified mature LOX to human monocyte cultures in subnanomolar concentrations resulted in a chemotactic response, which was prevented by heat inactivation of the enzyme or inhibition with BAPN {Lazarus et al., 1995}.

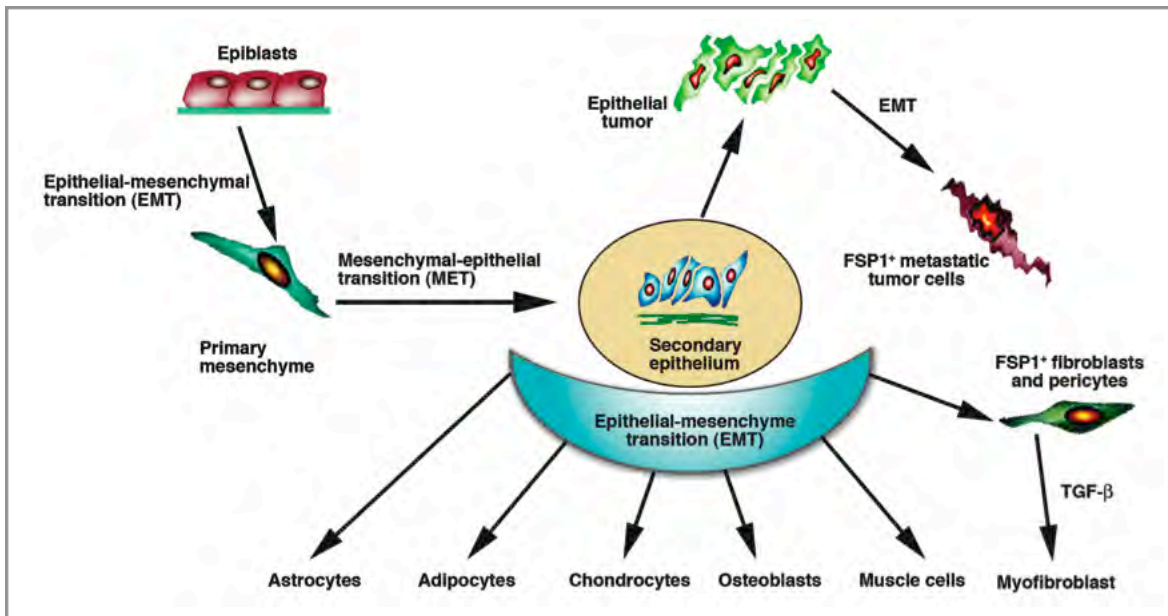


Figure 10. Epithelial-mesenchymal transition (EMT) during development and cancer.

EMT occurs first during gastrulation of the embryo when epiblasts of the blastula start to migrate into the hollow lumen forming the primary mesenchyme (*top left*). Mesenchymal-epithelial transition of the primary mesenchyme results in the secondary epithelium, which can undergo again EMT during organ development to differentiate into specialized cell types (*center and bottom*). The secondary epithelium can also give rise to epithelial tumors, that can undergo EMT during the formation of metastases at distant tissue sites. (*top right*). Recently, it was also discovered that EMT of the secondary epithelium can result in formation of fibroblasts and pericytes during organ fibrosis (*bottom right*). During EMT in both, cancer and fibrosis, the generated cells express the mesenchymal marker protein FSP-1 (from Kalluri & Neilson, 2003).

Introduction

Finally, Kagan and colleagues demonstrated that LOX induces chemotaxis in vascular smooth muscle cells in a hydrogen peroxide-dependent manner, providing more evidence that catalytic activity of LOX is required to induce the chemotactic response {Li et al., 2000}. Thus, LOX-induced cell migration seems not to be limited to malignantly transformed cells but can also occur in diverse normal non-transformed cell types.

The question arises of how the apparent paradox of LOX being both, a tumor suppressor and metastasis promoter, can be reconciled. Most of the data pointing towards a tumor suppressor role of LOX was obtained from studies with either transformed fibroblasts or sarcomas, which are both of mesenchymal origin. In contrast, data indicating LOX as a metastasis promoter result exclusively from studies with carcinoma cells, which are of epithelial origin. It is possible that the opposing effects of LOX observed in malignant mesenchymal versus epithelial cells is at least in part the result of different gene expression programs in these cell types due to their different ontological background. However, most recent studies demonstrating the LOX pro-peptide causes reversion of the ras-transformed phenotype provide for the first time more detailed molecular evidence for the tumor suppressor effect of LOX not only in mesenchymal but also in cancer cells of epithelial origin {Palamakumbura et al., 2004; Min et al., 2007; Wu et al., 2007}. In contrast, the metastasis promoting effect of LOX in carcinomas seems to be clearly linked to the mature enzyme and requires catalytic activity, although the potential substrate(s) remain unknown {Payne et al., 2005; Erler et al., 2006}. Genomic mutations and gene expression patterns among cancer cells display a great diversity. Therefore, the LOX propeptide may have the ability to counterbalance the tumor promoting effect of the mature protein only in cancer cells with aberrant ras-signaling. But this compensation may be not effective in cells that are transformed independently of ras-signaling, or in later stages of malignancies, for example under hypoxic conditions. This hypothesis is supported indirectly by a recent study that suggested fibroblasts may be not appropriate to investigate ras oncogenic activation in tumors of epithelial origin (carcinomas) because they do not respond the same way to ras-transformation as epithelial cells {Skinner et al., 2004}.

So far it is completely unknown whether the function of LOX in normal epithelial cells is potentially associated with its metastasis-promoting effect in progressive stages of carcinomas. Detailed knowledge about the role of LOX in normal epithelia could therefore complement and facilitate efforts to characterize its role in cancer.

4. Dissertation hypothesis and specific aims

LOX is traditionally known as a copper-dependent enzyme that catalyzes the initial step of collagen and elastin crosslinking within the extracellular matrix. LOX is synthesized as a proenzyme that is secreted into the extracellular space where it is proteolytically processed into the mature protein and catalytically active enzyme. LOX catalyzes the oxidative deamination of peptidyl lysine residues in fibrillar collagen and elastin to allysine, which can then spontaneously condense with other lysine or allysine residues of neighboring fibrils to form covalent cross-linkages. The formation of cross-links in collagen- and elastin fibers is essential for connective tissue integrity. Until today the role of LOX in the ECM has been studied almost exclusively in mesenchymal cell types that reside within the tissue stroma. Although epithelia face the ECM with their basal surfaces, it is still unclear whether epithelial cells secrete active LOX protein into the ECM and whether epithelial LOX may have additional - so far unknown - functions as well. Over the last two decades, extensive research has also revealed a context-dependent role for LOX in cancer, either as a tumor suppressor or as a metastasis promotor. In ras-transformed cells the LOX propeptide seems to exhibit a tumor suppressive function. In contrast, during cancer progression the active LOX enzyme is capable to promote invasion of primary tumor cells. Interestingly, most cancers are carcinomas, tumors of epithelial origin. The question emerges whether and how LOX function in normal epithelial cells may be altered during the course of malignancies.

In all multicellular organisms, epithelial tissues serve as critical barriers and communication windows to the external environment. The goal of this PhD project was to investigate the role of LOX in epithelial cells and its potential significance for connective tissue homeostasis and cancer.

Specific Aim 1. Establish an *in vitro* model system to study LOX in epithelial cells.

- a) Characterize extra- and potentially intracellular LOX expression
- b) Determine whether LOX expression is dependent on the differentiation state of epithelial cells
- c) Test whether epithelial cells produce catalytically active LOX enzyme

Specific Aim 2. Recapitulate characteristic features of cancer progression *in vivo* using the epithelial *in vitro* model.

- a) Establish an assay reflecting hallmarks of cancer invasion
- b) Analyze changes of LOX expression between normal and cancer-like states

Introduction

Specific Aim 3. Analyze the effect of LOX over-expression in normal epithelial cells.

- a) Design and generate mammalian LOX expression constructs
- b) Stable transfection of LOX into normal epithelial cells
- c) Characterize exogenous LOX expression
- d) Analyze potential changes of the epithelial phenotype in stable cell lines

II. Material and methods

1. Cell Culture

All cell culture work was performed under a sterile hood. In this study two mammalian cell lines of epithelial origin were grown as adherent monolayers in tissue culture flasks. Cells were cultured at 37°C in a humidified atmosphere supplemented with 5% CO₂ content.

MDCK II cells

Madine Darby Canine Kidney II (MDCK II) cells were cultured in DMEM low Glucose (Invitrogen) supplemented with 10 % (w/v) fetal bovine serum (Mediatech), 1 x penicillin/streptomycin (Invitrogen). After reaching 80 % confluence the culture medium was aspirated and cells were rinsed with sterile PBS. Subsequently, cells were detached in Trypsin/EDTA solution (Invitrogen) and split in a ratio of 1:10 to 1:15 into new cell culture flasks.

MCF-10A cells

MCF-10A (human mammary epithelial) cells were grown in DMEM/F12 (Invitrogen) supplemented with 5 % (w/v) horse serum (Invitrogen), 20 ng/ml EGF (Peprotech), 500 ng/ml hydrocortisone (Sigma), 100 ng/ml cholera toxin (Sigma), 10 µg/ml insulin (Sigma) and penicillin/streptomycin (Invitrogen). At 80 % confluence cells were split in a ratio of 1:6 to 1:10 into new cell culture flasks.

2. RNA purification

Total RNA was isolated from cells using the RNeasy® Mini Kit from Qiagen. This protocol is based on the selective binding of RNA to a silica membrane in the presence of chaotropic salts and allows purification of RNA molecules longer than 200 nucleotides thereby eliminating small rRNAs and tRNAs that make up to 15-20 % of total RNA.

Initially, cells were lysed in a highly denaturating salt buffer containing guanidine-thiocyanate, which inactivates RNases thereby ensuring isolation of intact RNA. By using a non-ionic detergent in the lysis buffer, nuclei remained intact during cell lysis and were removed during subsequent homogenization minimizing potential DNA contamination of the samples. Ethanol was then added to allow selective binding of cytoplasmic RNA to a silica membrane whereas contaminants were washed away during additional steps. Finally, almost pure RNA was eluted into RNase-free water.

Material and methods

RNA concentration was determined by OD 260 measurement with a Nanodrop™ spectrophotometer. RNA was stored at -80°C.

3. cDNA synthesis

Reverse transcriptases were initially discovered in the 1970s as enzymes from retroviruses. Because of their unique ability to synthesize DNA from RNA templates these viral DNA polymerases have become an important tool for the analysis of gene expression at the mRNA level. After isolation of cellular mRNA they are commonly used to generate copy DNA for subsequent PCR amplification of a specific gene of interest.

First-strand cDNA was synthesized from total RNA preparations with SuperScript™II Reverse Transcriptase Kit from Invitrogen. SuperScript™II RT has been engineered to retain the full DNA polymerase activity of Mouse-Moloney Leukemia Virus (M-MLV) RT combined with a reduced intrinsic RNase H⁺ activity. Therefore SuperScript™II RT has greater yields and improved capabilities to copy long RNA templates in comparison to many viral reverse transcriptases.

1-2 µg of total RNA was used as template for first-strand cDNA synthesis reactions. Briefly, RNA was denatured at 65°C to eliminate potential secondary structures and then incubated with Oligo (dT)₁₂₋₁₈ primer to allow selective amplification of mRNA only. Through addition of an RNase inhibitor to the reaction mix RNA templates were further protected from enzymatic degradation resulting from potential RNase contamination in the samples that could possibly affect RNA integrity. Then first strand cDNA synthesis was performed in the presence of SuperScript™II RT at 42°C for 50 minutes. In the final step the RNA template was removed from the cDNA:RNA hybrid molecule by digestion with RNase H at 37°C for 20 minutes. cDNA was stored at -20°C.

4. Polymerase chain reaction (PCR)

In the 1980s Kary Mullis and colleagues invented a method that allows the synthetic amplification of DNA *in vitro* {Mullis et al., 1986}. This method was called polymerase chain reaction (PCR) and has revolutionized modern molecular biology because of its capability to selectively amplify DNA from tiny amounts of starting material. The principle is fairly simple: DNA template, primer pair, buffer, nucleotides and DNA polymerase are mixed in a test tube where a specific section of the template DNA (defined by the primer pair) is amplified in repetitive cycles. One reaction cycle encompasses the following steps:

Material and methods

1. Denaturation of the double-stranded DNA template molecule (*denaturation*)
2. Annealing of the primer pair to the template sequence (*primer annealing*)
3. DNA synthesis (*synthesis*)

For PCR reactions in this study Deep Vent_R™ Polymerase (New England Biolabs) was used. Deep Vent_R™ Polymerase is a genetically modified thermophilic DNA polymerase with 3'→ 5' proofreading exonuclease activity for high fidelity. PCR was performed to amplify gene-specific templates from first-strand cDNA for gene expression analysis on the mRNA level.

The reaction mix for each sample was assembled as follows:

- 5 µl 10 x Thermopol buffer (New England Biolabs)
- 1 µl sense primer (20 µM)
- 1 µl antisense primer (20 µM)
- 4 µl 2.5 mM dNTP mix (New England Biolabs)
- 1 µl template DNA
- 0.5 µl (2 U/µl) Deep Vent_R™ Polymerase (New England Biolabs)
- 37.5 µl dH₂O (nuclease-free)

50 µl total volume

The cycle parameters were adjusted as follows for a total of 35 cycles:

- 5 min. at 95°C (start)

- 30 sec. at 95°C
- 30 sec. at 59-62°C (depending on primer)
- 45 sec. at 72°C

- 10 min. at 72°C (end)

Material and methods

Gene	Primer	Primer Sequence	Size of amplified fragment
canine LOX	sense	5'-AATGGCACAGTTGTCACCAA-3'	289 bp
	antisense	5'-CTGGGGTTCACACTGACCTT-3'	
human LOX	sense	5'-GACGGCATGGTGGCGACGAC-3'	572 bp
	antisense	5'-GGTATCATAACAGCCAGGACTCAA-3'	
human LOX	sense	5'-GATCCTGCTGATCCGCGACAA-3'	368 bp
	antisense	5'-GGGAGACCGTACTGGAAGTAGCCAGT-3'	
human β -actin	sense	5'-GGAAATCGTGCCTGACATTA-3'	372 bp
	antisense	5'-GGAGCAATGATCTTGATCTTC-3'	

Table 3: Primers for RT-PCR detection of LOX in MDCK II cells and MCF-10A cells.

The primers in Table 3 (see above) were used to analyze LOX mRNA expression in MDCK II cells and MCF-10A cells. The first human LOX primer amplified due to the high sequence homology, both canine and human LOX. This primer was utilized to quantify canine LOX mRNA levels by means of copy numbers using amplification of a human LOX plasmid as a reference (see Results).

5. Cloning of lysyl oxidase constructs

5.1 PCR and agarose gel electrophoresis of amplified DNA fragments

Full-length LOX constructs (with and without V5-tag) were previously generated in our laboratory and had only to be subcloned into the pcDNA3.1(-) vector from Invitrogen or the pEGFP-N1 vector from BD Biosciences. Constructs carrying the sequence for mature LOX were engineered from the full-length constructs by PCR amplification with restriction sites, Kozak sequence, start and stop codons designed into the primer sequence (Table 4).

Construct	Primer	Primer sequence	Restriction Site
<i>pcDNA-LOX30</i>	sense	5'-CGGAATTCTGTTATGGACG ACCCTTACAACCCCTAC-3'	<i>EcoRI</i>
	antisense	5'-CCGGGATCCCTAAT ACGGTGAAATTGTGCA-3'	<i>BamHI</i>
<i>pcDNA-LOX30-V5</i>	sense	5'-CGGAATTCTGTTATGGACG ACCCTTACAACCCCTAC-3'	<i>EcoRI</i>
	antisense	5'-CGGGATCCTCAACG CGTAGAACATGAGACC-3'	<i>BamHI</i>
<i>pEGFP-LOX30</i>	sense	5'-CGGAATTCTGTTATGGACG ACCCTTACAACCCCTAC-3'	<i>EcoRI</i>
	antisense	5'-CGGATCCCGA TACGGTGAAAT-3'	<i>BamHI</i>

Table 4: PCR primers for the generation of LOX expression constructs.

Material and methods

The amplified DNA fragments were separated by agarose gel-electrophoresis. Briefly, 10 µl of 6 x loading dye (0.25 % (w/v) bromophenol blue, 40 % (w/v) sucrose in H₂O) were added to each 50 µl PCR reaction. 15 µl aliquots of each sample were then separated on 1 % agarose gels in TE-buffer containing ethidium bromide (0.5 µl EtBr/10 ml TE-buffer) at 100 V for 45 to 60 minutes. Log-2 DNA ladder from New England Biolabs was used as a molecular weight marker. The separated DNA fragments were visualized with a UV transilluminator connected to a Kodak EDAS 290 Imaging System.

5.2 DNA purification from agarose gels

DNA fragments were purified from agarose gels using the Geneclean Spin Kit from Q-Biogene. DNA fragments were excised from agarose gels under UV illumination with a razor blade and then melted for 5-10 minutes in 400 µl glassmilk at 55°C. The mixture was incubated for 5 min. at room temperature to allow DNA binding to the silica particles. After two washes with EtOH-containing wash buffer the DNA was eluted from the column.

5.3 Restriction enzyme digestion

Purified DNA fragments were digested with EcoRI and BamHI restriction enzymes (New England Biolabs) to create sticky ends for ligation into the vector. 20 µl reaction mixes were assembled as follows and incubated for 30 min. at 37°C:

- 11 µl gel-purified DNA
- 2 µl 10 x restriction digest buffer (New England Biolabs)
- 1 µl EcoRI [20 U/µl] (New England Biolabs)
- 1 µl BamHI [20 U/µl] (New England Biolabs)
- 5 µl dH₂O (nuclease-free)

20 µl total volume

To stop the reaction samples were placed on ice for 2 minutes. To eliminate restriction enzymes from the samples for downstream processing (e.g. DNA ligations) DNA was purified again with the Geneclean Spin Kit (see above).

Material and methods

5.4 DNA ligations

The digested LOX fragments were ligated into the corresponding plasmid vector (pcDNA3.1(-) or pEGFP-N1) in a 10 µl reaction with an insert/vector ratio of ~ 4:1. The reaction mix was incubated at room temperature for 20 minutes.

- 3 µl dH₂O (sterile)
 - 4 µl LOX insert
 - 1 µl plasmid vector
 - 1 µl 10 x ligase buffer (New England Biolabs)
 - 1 µl T4 DNA ligase [400 U/µl] (New England Biolabs)
-

10 µl total volume

5.5 Bacterial transformation

Transformation of plasmid DNA into competent XL-1 Blue *E. coli* bacteria (Stratagene) was performed using the heat-shock method. Competent cells were thawed for 10 minutes on ice. 100 µl aliquots of competent cells per transformation were transferred to a sterile tube. After addition of 1.7 µl 1.42 M β-mercaptoethanol the mix was incubated for 10 minutes on ice. Then 5 µl of the ligation reaction were added and incubated for 30 minutes on ice. The cells were now heat-shocked at 42°C for 45 seconds and placed on ice for 2 minutes. To allow expression of the antibiotic resistance gene on the plasmids, 900 µl of LB-medium were added to the cells and then incubated on a shaker (250 rpm) at 37°C for 1 hour. Finally, 200 µl of transformed cells were spread on LB-agar plates containing the corresponding antibiotic (ampicillin for pcDNA3.1(-) vector and kanamycin for pEGFP-N1 vector) and incubated overnight at 37°C. Single colonies were picked after 15-18h the next day with a sterile wire loop and were grown overnight in 30 ml LB-media at 37°C/250 rpm for plasmid purifications the next day.

5.6 Plasmid purification

Plasmid purifications for transfection-grade plasmid DNA were performed using the “QIAfilter Plasmid Midi Kit” from Qiagen. The principle of this plasmid purification protocol is based on a modified alkaline lysis procedure, followed by binding of plasmid DNA to an anion-exchange resin under appropriate low-salt and pH conditions.

Material and methods

RNA, proteins, dyes and low-molecular-weight impurities are removed by a medium-salt wash. Finally, plasmid DNA is eluted in a high-salt buffer and then concentrated and desalting by isopropanol precipitation.

Bacterial cells were harvested by centrifugation at 4000 rpm for 15 min. at 4°C. The bacterial pellet was resuspended in 4 ml Buffer P1 (50 mM Tris-HCl, pH 8.0; 10 mM EDTA; 100µg/ml RNase A). Cells were lysed for 5 min. at room temperature through addition of 4 ml Buffer P2 (200 mM NaOH; 1 % (w/v) SDS). Bacterial lysis was stopped and genomic DNA, proteins and cell debris were precipitated by addition 4 ml of neutralizing Buffer P3 (3 M potassium acetate, pH 5.0). The neutralized bacterial lysate was then transferred into a QIAfilter Cartridge and incubated at room temperature for 10 minutes. After equilibrating a Qiagen-tip 100 column with 4 ml of Buffer QBT (750 mM NaCl; 50 mM MOPS, pH 7.0; 15 % (w/v) isopropanol; 0.15 % (w/v) Triton-X-100) the cell lysate was filtered into the column and allowed to enter the resin by gravity flow. The column was washed twice with 10 ml Buffer QC (1.0 M NaCl; 50 mM MOPS, pH 7.0; 15 % (w/v) isopropanol) before the DNA was eluted with 5 ml Buffer QF (1.25 M NaCl; 50 mM Tris-HCl, pH 8.5; 15 % (w/v) isopropanol). The eluted plasmid DNA was precipitated with 3.5 ml isopropanol and centrifuged at 4000 rpm for 60 minutes at 4°C. The DNA pellet was washed twice with 2 ml 70 % (w/v) EtOH and then allowed to air-dry. Purified plasmid DNA was redissolved in 500 TE buffer (pH 8.0). To determine the yield, concentration of the plasmid DNA was determined by OD 260 measurement with a Nanodrop™ spectrophotometer.

6. Site-directed mutagenesis

A mature LOX construct was generated where the tyrosine at position 355 was converted into phenylalanine through exchange of one base in the codon from TAT to TTT. This point mutation yields in a catalytically inactive enzyme because tyrosine 355 is essential for formation of the lysyl tyrosyl quinone (LTQ) cofactor of LOX. Site-directed mutagenesis in vitro was performed using the “QuikChange II Site-directed Mutagenesis Kit” from Stratagene.

The method is basically a mutagenic primer-directed replication of both plasmid strands with *PfuUltra*™ high fidelity DNA polymerase. The procedure utilizes a supercoiled double-stranded DNA vector with an insert of interest and two synthetic oligonucleotide primers, both containing the desired mutation.

Material and methods

The oligonucleotide primers, each complementary to opposite strands of the vector, are extended during temperature cycling by *PfuUltra*TM high fidelity DNA polymerase, without primer displacement. Extension of the oligonucleotide primers generates a mutated plasmid containing staggered nicks. Following temperature cycling, the product is treated with *Dpn* I. The *Dpn* I endonuclease is specific for methylated and hemimethylated DNA and is used to digest the parental DNA template. DNA from *E. coli* is *dam* methylated and therefore susceptible to *Dpn* I digestion whereas the mutated newly synthesized strands are not. The nicked vector DNA containing the desired mutations is then transformed into XL1-Blue competent cells.

As a template served the pcDNA-LOX30(-V5) construct(s) carrying the sequence for the mature 30 kD LOX. Mutagenic primers carrying the point mutation TAT (tyrosine) to TTT (phenylalanine) were designed for, both the sense and antisense strand of the vector (Table 5).

Construct	Primer	Primer sequence
<i>pcDNA-LOX30-Y355F(-V5)</i>	sense	5'-GGCTGTTATGATAC CTTG GTGCAGACATAGACTGCC-3'
	antisense	5'-GGCAGTCTATGTCTGCAC CAAAGGTATCATAAACAGCC-3'

Table 5: Mutagenic primers for generation of mutated mature LOX constructs.

The reaction mix was assembled as outlined below:

- 5 µl 10 x reaction buffer
- 2.5 µl plasmid DNA template (20 ng/µl dilution from plasmid stock)
- 5 µl sense primer (2 µM)
- 5 µl antisense primer (2 µM)
- 1 µl dNTP mix (10 mM)
- 1 µl (2.5 U/µl) *PfuUltra* DNA polymerase
- 30.5 µl dH₂O (nuclease-free)

50 µl total volume

The vector containing the mutated sequence of mature LOX was then synthesized during temperature cycling as depicted in Table 4. After completion the reaction was placed on ice for 2 minutes to cool the reaction mix below 37°C.

Material and methods

Cycles	Temperature	Time
1	95°C	30 seconds
12	95°C	30 seconds
	55°C	1 minute
	68°C	6 minutes

Table 6: Cycle parameters for synthesis and amplification of the mutated pcDNA-LOX30-Y355F construct.

To digest and eliminate the non-mutated template plasmid 1 µl of *Dpn* I restriction enzyme (10 U/µl) were added to the reaction mixture and incubated at 37°C for 1 hour. The newly generated mutated pcDNA-LOX30-Y355F(-V5) vector was then transformed into XL-1 Blue competent cells and the cloning process completed as described for the constructs above.

7. Generation of stable MDCK cell lines

To generate stable cell lines MDCK II cells were transfected with the generated LOX constructs using Lipofectamine reagent from Invitrogen. Lipofectamine consists of a cationic lipid formulation that is widely used to transfect plasmid DNA into cells and to force exogenous expression of a gene of interest. The exact molecular mechanism is not completely understood but there is evidence that cationic lipid vesicles form stable complexes with DNA. These complexes are delivered into the cell by fusion of the DNA-lipid vesicles with the plasma membrane and can then subsequently enter the nucleus by an unknown mechanism to allow gene expression from the transfected plasmid DNA.

MDCK II cells were seeded in six-well plates overnight so that monolayers reached 60-70 % confluence the next day. For each transfection 1 µg of purified plasmid DNA was mixed with Lipofectamine in a ratio of 1:3 in a total volume of 500 µl in Opti-MEM® reduced serum medium (Invitrogen) and incubated at room temperature for 20 minutes to allow DNA-lipid complex formation. The regular cell culture medium was removed and cells were washed in sterile PBS to eliminate serum and antibiotics from the culture. The DNA-Lipofectamine mixture was added to the cells and after incubation at 37°C for 4 h the transfection mixture was replaced by normal cell culture medium. Stable expressing clones were selected starting 24 h after transfection for two weeks by addition of 500 µg/ml G418 (Geneticin) to the normal culture medium. The selection medium was replaced every two days to ensure proper nutrient supply and active antibiotics.

Material and methods

After 7-10 days most of the cells that were not carrying the transfected construct died and stable-expressing clones became evident as isolated growing clusters of cells. Stable clones were brought up to T75 flasks and freezing stocks were generated prior to gene expression analysis and further experiments. Usually, each transfection resulted in at least 5-10 stable clones which were maintained as polyclonal cultures under the continuous selection pressure of G418.

8. Preparation of protein extracts from whole cell lysates

Crude cytoplasmic fractions were prepared from whole cell lysates using a mild detergent-based method. As a lysis buffer served “M-PER Mammalian Protein Extraction Reagent” (Pierce) containing a proprietary detergent formulation in 25 mM bicine buffer (pH 7.6) including “Halt Protease Inhibitor Cocktail” (Pierce).

The whole protein extraction procedure was performed on ice. First, the cell culture medium was aspirated and monolayers were washed once with PBS. After addition of the lysis buffer cells were detached using a plastic cell scraper. The mixture of detached cells and lysis buffer was transferred into a microcentrifuge tube and incubated for 10 minutes to allow efficient cell lysis. Cell debris and nuclei were pelleted at 3500 rpm for 10 minutes. The supernatant containing a crude cytoplasmic fraction was transferred into a new tube and aliquots were taken to measure protein concentration. SDS sample buffer (final concentration: 50 mM Tris-HCl pH 6.8; 5 % (w/v) glycerol; 100 mM Di-thio-threitol; 1 % (w/v) SDS; 0.01 % (w/v) bromo-phenolblue) was added to keep proteins in a denatured state and samples were stored at -20°C until further usage.

9. Preparation of protein extracts from conditioned cell medium

For preparation of protein extracts from medium supernatants the regular cell culture medium was replaced by phenol-red-free and serum-free medium 48 h prior to protein harvest to avoid interference with measurement of protein concentration and contamination of serum proteins, respectively.

The medium supernatant was transferred into a tube and potential cellular contaminations were pelleted at 1500 rpm for 2 minutes. The “supernatant” was transferred into a new tube, stored on ice and aliquots were taken to measure protein concentration. Because the absolute protein concentration in medium supernatants was relatively low, aliquots equivalent to 20 µg of total protein each were concentrated by incubation with 1 µl of “Strataclean Resin” per 100 µl medium supernatant on a rocker at 4 °C for 30 minutes. The bound protein on the resin was pelleted for 1

Material and methods

min. at full speed and the supernatant subsequently discarded. The pellet was resuspended in SDS sample buffer (50 mM Tris-HCl pH 6.8; 5 % (w/v) glycerol; 100 mM Di-thio-threitol; 1 % (w/v) SDS; 0.01 % (w/v) bromo-phenolblue) and stored at -20°C.

10. Measuring protein concentration with the Bradford Assay

The Bradford Assay takes advantage of the fact that Coomassie brilliant blue G-250 dye forms a complex with amino acids of proteins {Bradford, 1976}. Upon complex formation the absorption maximum of the Coomassie dye transitions from 465 nm to 595 nm. The OD₅₉₅ is directly proportional to the protein concentration in the solution.

We used a Bradford Assay that was adapted for microtiter plate format and utilized bovine serum albumin (BSA) standards from 5 to 25 µg protein/ml to generate a calibration graph. Aliquots of samples from protein extracts were diluted in 160 µl PBS before 40 µl of Bradford reagent were added to a total volume of 200 µl. The OD 595 was measured in a Polarstar Optima plate reader from BMG Labtechnologies Inc. and the protein concentration was determined based on the calibration graph and the dilution factor of the corresponding sample aliquot. Each sample was assayed in triplicate to minimize systematic errors.

11. SDS Polyacrylamid Gel-Electrophoresis (PAGE)

Protein extracts of whole cell lysates and conditioned cell medium were separated based on their molecular weight using SDS-PAGE. Sodium-dodecyl sulfate (SDS) is a detergent that is able to bind and denature proteins thereby forming a SDS-protein complex with constant mass-/charge-ratio. When applying an electric field the proteins are separated within a polyacrylamide gel matrix according to their molecular weight, with smaller proteins running faster relative to bigger proteins. Laemmli and colleagues were the first to introduce this method in 1970 {Laemmli, 1970}.

We used the NuPAGE precast gel system from Invitrogen for our SDS-PAGE analyses. Protein samples were boiled for 5 minutes in a water bath and then incubated on ice for 2 minutes. Bis-Tris buffered 4-12 % gradient gels were loaded with 20 µg of total protein for each sample and also with molecular weight protein standards from Invitrogen for SDS-PAGE (SeeBlue Plus2) and for subsequent western blot analysis (MagicMark XP). Protein extracts were separated by gel-electrophoresis at 200 V for 50 minutes.

12. Western blot analysis

Resolved proteins on SDS-PAGE gels were transferred onto PVDF (Polyvinylidene fluoride) membranes by western blotting. The tank blot system “XCell II” from Invitrogen was used for wet protein transfer. The SDS-PAGE gel was placed on top of an Immobilon-P PVDF membrane (Millipore) inside the tank blot apparatus and submerged in NuPAGE transfer buffer. The proteins were then transferred for 90 minutes at 30 V onto the PVDF membrane. Successful transfer of proteins was verified by Ponceau-S staining. The blot membrane was now blocked with 5 % (w/v) Carnation non-fat dry milk in PBS-T (PBS containing 0.2 % (w/v) Tween-20) for 1 h. The primary antibody was incubated for 1 h and after 3 washes in PBS-T the secondary horseradish peroxidase-coupled antibody was incubated for an additional hour. Prior to chemiluminescence detection with ECLplus substrate (Amersham) the blot membrane was thoroughly washed in PBS-T and PBS, respectively. Finally, the blot membrane was exposed to x-ray film for 30 sec. to 5 min. depending on the signal intensity. The film was then developed, fixed and air-dried before analysis of the detected antibody signals.

13. Immunofluorescence staining

MDCK II cells were seeded overnight on cover-slips in six-well plates and fixed in 2 % para-formaldehyde for 15 minutes the next day at approximately 60-70 % confluency. Cells were permeabilized in 0.1 % (w/v) Triton-X-100 for 15 minutes and then blocked in 3 % (w/v) BSA for 30 minutes. Cells were incubated with the primary antibody for 1 h and then with the fluorophore-coupled secondary antibody for 45 minutes. To visualize nuclei and the actin cytoskeleton, cells were stained in selected experiments with Hoechst 33258 dye and fluorophore-coupled Phalloidin in PBS for 20 minutes, respectively. After each of the steps described above, cells were washed 3 times in PBS. Finally, cover-slips were mounted in anti-fading fluorescence mounting medium (Molecular Probes) and stored at 4°C in the dark. Images were recorded with a Zeiss LSM 5 confocal microscope unit and figures were assembled with Adobe Photoshop 7.0 software.

14. Primary antibodies

α-LOX antibody

LOX protein was detected using two rabbit polyclonal antibodies (“DK 1” and “KF 00116”) raised against the peptide sequence KYSDDNPYYNYYDTYERPRPGG of human LOX, seven amino acids down from the BMP-1 cleavage site (N-terminus of the mature LOX protein) {Hayashi et al., 2004, Fogelgren et al., 2005}. The antibodies were used at a concentration of 1-2 µg/ml for western blot analysis and 10 µg/ml for immunofluorescence stainings.

α-BMP-1 antibody

Bone morphogenetic protein 1 (BMP-1) was detected using a rabbit polyclonal antibody from Affinity Bioreagents that was raised against the CUB-2 domain of human BMP-1. The antibody was used at a dilution of 1:5000 for western blot analysis.

α-Fibronectin

Fibronectin was detected using a mouse monoclonal antibody (clone P5F3) from Santa Cruz Biotechnology Inc. that recognizes the highly conserved adhesive peptide FN CH/1 within the carboxy Hep II region. The antibody was used at a concentration of 1 µg/ml for western blot analysis.

α-E-cadherin antibody

E-cadherin was detected using a mouse monoclonal antibody (clone 36) from BD Biosciences that was raised against an epitope at the C-terminus. The antibody was used at a dilution of 1:2000 for western blot analysis and 1:1000 for immunofluorescence stainings.

α-vimentin

Vimentin was detected using a mouse monoclonal antibody (clone) from Chemicon International that was raised against the epitope. The antibody was used at a dilution of 1:1000 for western blot analysis and immunofluorescence stainings.

Material and methods

α -GFP

Green fluorescent protein (GFP) was detected using a mouse monoclonal antibody (clone 11E5) from Molecular Probes that was raised against native GFP from *Aequorea victoria*. The antibody was used at a dilution of 1:1000 for western blot analysis and immunofluorescence stainings.

α -GAPDH

Glyceraldehyde phosphate dehydrogenase (GAPDH) was detected using a goat polyclonal antibody from Acris Antibodies GmbH that was raised against a C-terminal epitope of human GAPDH. The antibody was used at a dilution of 1:1000 for western blot analysis.

α -V5

The V5-tag was detected using a mouse monoclonal antibody from Invitrogen that was raised against the V5-epitope found in P and V proteins of the paramyxovirus SV5. The antibody was used at a dilution of 1:2000 for western blot analysis.

α -ZO-1

Zonula occludens protein 1 (ZO-1) was detected using a mouse monoclonal antibody (clone 1520) from Chemicon International that was raised against a tight junction-containing fraction from mouse liver. The antibody was used at a dilution of 1:1000 for immunofluorescence stainings.

15. Secondary antibodies

The following list comprises all secondary antibodies that were used for western blot or immunofluorescence experiments throughout this study.

Antibody	Application	Dilution	Company
<i>HRP-coupled anti-rabbit IgG</i>	western blot	1:4000	Amersham
<i>HRP-coupled anti-mouse IgG</i>	western blot	1:2000	Amersham
<i>HRP-coupled anti-goat IgG</i>	western blot	1:20.000	Jackson Laboratories
<i>AF488-labeled anti-rat IgG</i>	immunofluorescence	1:1000	Molecular Probes
<i>AF488-labeled anti-rabbit IgG</i>	immunofluorescence	1:1000	Molecular Probes
<i>AF546-labeled anti-rabbit IgG</i>	immunofluorescence	1:1000	Molecular Probes
<i>AF546-labeled anti-mouse</i>	immunofluorescence	1:1000	Molecular Probes

Table 7: Secondary antibodies used for western blot analysis or immunofluorescence studies.

16. Assay for lysyl oxidase enzyme activity

The principle of measuring enzyme activity of LOX is based on the detection of hydrogen peroxide which is generated in stoichiometric proportions as a side product during each catalytic cycle. Addition of beta-aminopropionitrile BAPN, a specific and irreversible inhibitor of LOX activity, to the reaction mix allows the detection of hydrogen peroxide that originates specifically from LOX catalytic activity.

We used an adapted microplate version of a fluorometric assay recently developed by Trackman and colleagues {Palamakumbura & Trackman, 2002}. This assay uses 1,5-diaminopentane as a synthetic substrate and the Amplex Red dye (Molecular Probes) in conjunction with horseradish peroxidase (HRP) as a sensor to detect LOX generated hydrogen peroxide. In the presence of hydrogen peroxide HRP converts Amplex Red into the fluorescent product resorufin. Conditioned cell medium was concentrated in sequential centrifugation steps using Amicon 10 kD cut-off filter devices (Millipore). Aliquots equal to 100 µg of total protein were added to the final reaction mix (50 mM sodium borate, pH 8.2; 1.2 M urea; 50 µM Amplex Red; 1 U/ml horseradish peroxidase, 10 mM 1,5-diaminopentane substrate) in the presence or absence of 500 µM BAPN and incubated at 37°C. The fluorescent product was excited at 560 nm and the emission was read at 590 nm every 5 minutes for 3 h using a Polarstar Optima plate reader (BMG Labtechnologies Inc.). Activity assays were repeated three times and samples for each experiment were performed at least in triplicates. Purified LOX (300 ng per assay) from bovine aorta, kindly provided by Dr. Kagan from Boston University, was used as a positive control. BAPN-inhibitable lysyl oxidase enzyme activity was calculated by subtracting the detected fluorescence in BAPN-treated samples from the values detected in non-treated samples.

III. Results

Rationale to study LOX in epithelial cells

There are two major rationales to study LOX in epithelial cells. The first rationale results from the traditional role of LOX during initiation of collagen and elastin cross-linkages in the extracellular matrix (ECM), a crucial process for connective tissue integrity. Up to date LOX studies have been conducted almost exclusively in mesenchymal cell types because they are the residential cells within the tissue stroma that produce most of the matrix proteins. However, epithelia face the extracellular matrix with their basal surfaces and although for a long time not recognized, it is now well established that epithelial cells contribute a significant amount of extracellular matrix proteins to the connective tissue, in particular to basement membranes {Hay, 1980; Kalluri & Neilson, 2003; Quondamatteo, 2002; Yurchenco et al., 2004}. Preliminary evidence provided by immunohistochemistry data from several laboratories suggests that LOX is among the matrix proteins that are not only expressed by mesenchymal cells within the tissue stroma but also by cells of surrounding epithelia {Hayashi et al., 2004; Noblesse et al., 2004; Fogelgren et al. 2005}.

The second rationale is related to more recent findings in cancer research where increased LOX expression has been observed during progression of carcinomas towards a migratory and more invasive phenotype {Kirschmann et al., 1999; Payne et al. 2005; Erler et al. 2006}. As carcinomas are cancers of epithelial origin these findings raise the question if there is a change of LOX function during the transition from a normal to a malignant state in epithelial cells.

1. Characterization of LOX expression in MDCK II and MCF-10A cells

The first goal of this dissertation was to verify and characterize LOX expression and enzyme activity in epithelial cells using an *in vitro* cell culture model that reflects key features of normal epithelia *in vivo*.

We decided to use MDCK II dog kidney epithelial cells and MCF-10A human mammary epithelial cells for our studies. Both cell lines have been extensively characterized and have been shown to possess crucial properties of epithelial tissues *in vivo* {Yeaman et al., 1999; Debnath et al., 2003}. The characteristic “cobblestone” morphology as displayed in Figure 11 is a direct consequence of the epithelial phenotype.

Results

In addition, expression and localization pattern of the cell-cell adhesion protein E-Cadherin and the tight junction protein ZO-1 as detected by immunofluorescence in MDCK II cells confirmed important epithelial characteristics at the molecular level (Figure 12).

It has been established that cultured normal epithelial cells in a pre-confluent stage possess many features of undifferentiated epithelia *in vivo*, whereas post-confluent monolayers reflect many properties of differentiated epithelia *in vivo* {Simons & Fuller, 1985}. Therefore we wanted to analyze LOX expression in both pre- and post-confluent cultures of MDCK II and MCF-10A cells. Initially, we examined LOX expression at the mRNA level and detected LOX transcripts by semi-quantitative RT-PCR in each cell line (Figure 13). To determine LOX protein expression, we subjected cell lysates as well as protein fractions from conditioned cell medium to western blot analysis. Cell lysates were basically crude cytoplasmic fractions cleared from nuclei. Protein from conditioned cell medium was concentrated with 10 kD cut-off centrifugal filter devices up to applicable levels for western blot analysis.

In these studies we have used two rabbit polyclonal antibodies, named “DK1” and “KF30116”, that were both raised independently against the same epitope at the N-terminus of the mature human LOX protein, seven amino acids down from the BMP-1 cleavage site {Li et al., 2004; Hayashi et al., 2004, Fogelgren et al., 2005}.

MDCK II cells are dog cells and because the antibodies were generated against the human LOX protein we examined sequence homology of the epitope between dog LOX and human LOX. Sequence analysis revealed that all of the 22 amino acids within the antibody epitope were identical except for the last amino acid where glycine in the human LOX sequence was replaced by serine in the dog LOX sequence (Figure 14). The amino acid sequence of essential functional domains such as the copper-binding site, the BMP-1 cleavage site and the amino acids forming the LTQ cofactor were also identical between dog and human LOX suggesting the putative dog LOX protein may have the same functional capabilities as the human enzyme (Figure 14). This was important information as the dog genome has been sequenced but the canine LOX gene has not been cloned yet and no functional studies with the dog LOX protein have been conducted before.

Results

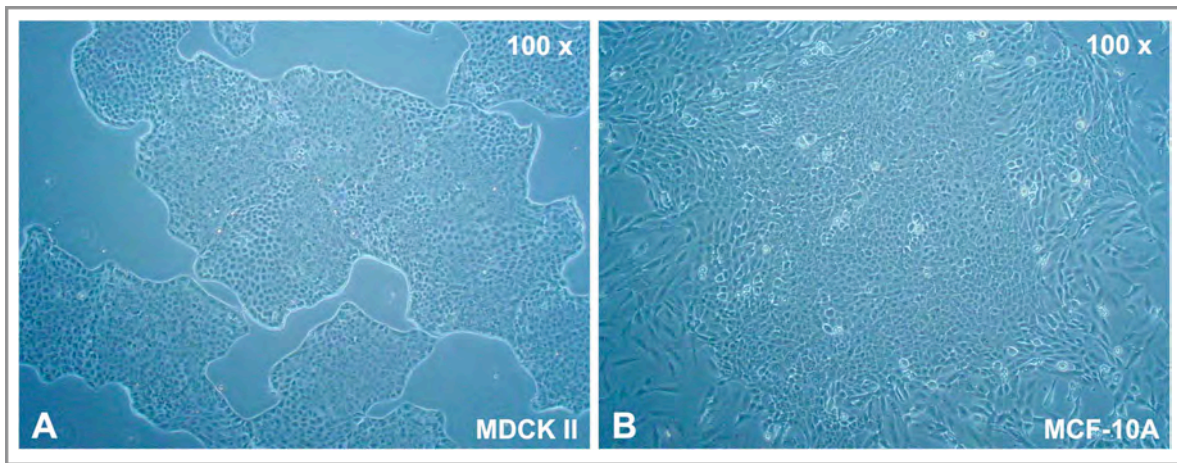


Figure 11. (A) MDCK II and (B) MCF-10A cells display the characteristic “cobblestone” morphology of polarized epithelial cells in culture.

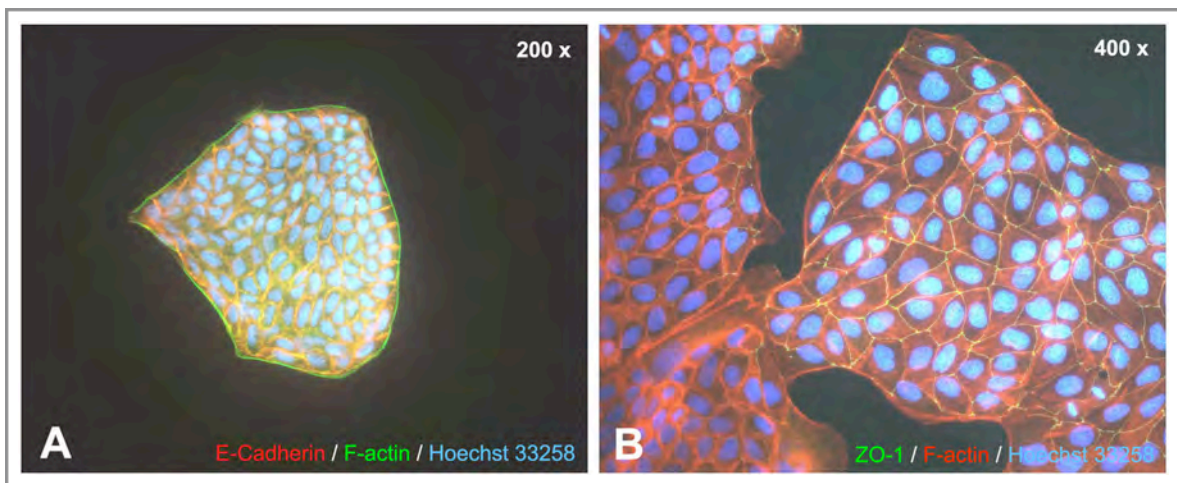


Figure 12: MDCK II cells express (A) E-Cadherin and (B) ZO-1, two characteristic cell-cell junction proteins for epithelial cells.

MDCK II cells were seeded overnight on glass cover slips and then fixed in 2 % para-formaldehyde at 70-80% confluence the next day. Cells were stained with anti-E-Cadherin (A) and anti-ZO-1 (B) antibody. In addition the actin cytoskeleton was counterstained with fluorophore-conjugated phalloidin and nuclei were visualized with Hoechst 33258 dye. Images were recorded with a Zeiss Axioskop fluorescence microscope set-up.

Results

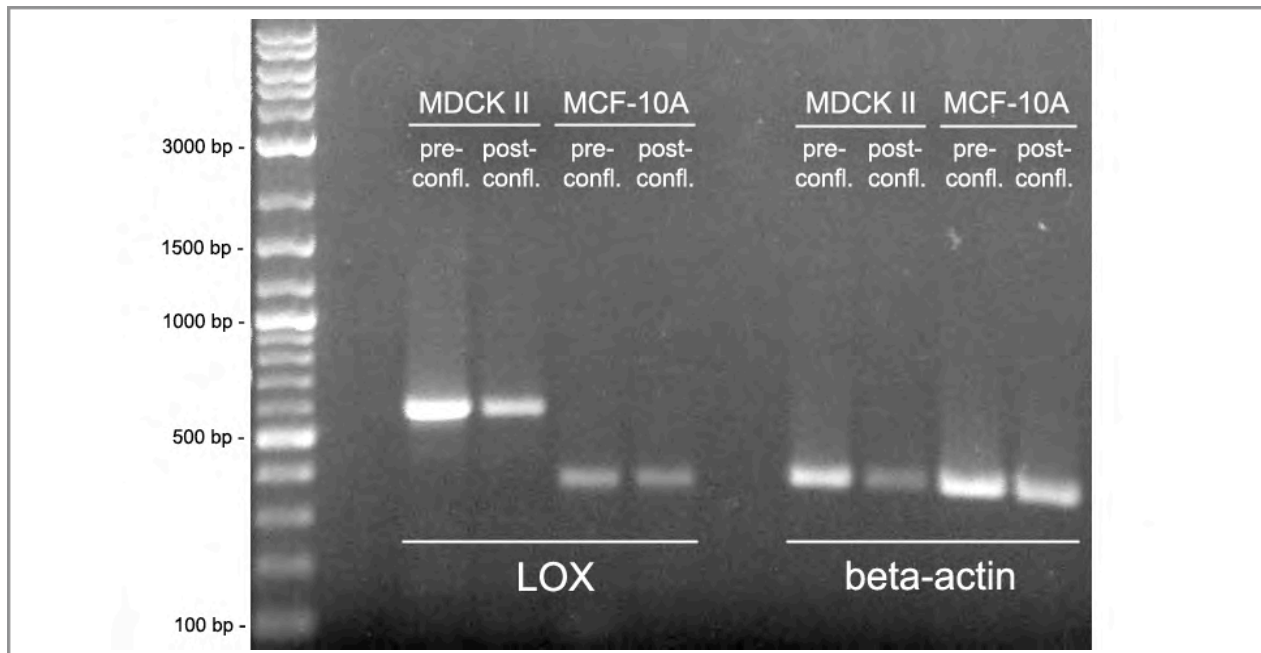


Figure 13. Expression of LOX mRNA in MDCK II and MCF-10A cells as detected by RT-PCR with gene-specific primers.

Dog LOX (MDCK II cells) was amplified with a primer pair yielding in a fragment of 572 bp and human LOX (MCF-10A cells) was amplified with primers resulting in a fragment of 368 bp. As an internal control beta-actin was amplified with a primer pair yielding a 372 bp fragment. Signal intensities in samples amplified for beta-actin indicate lower mRNA template inputs from post-confluent MDCK II samples.

Results

<i>canine LOX</i>	MRFATALLGPLQLCALLR	C	P	P	A	A	G	Q	Q	P	R	P	P	A	A	W	R	Q	R	I	Q	W	E	N	N	Q	V																						
<i>human LOX</i>	MRFATVLLLGPLQLCALVH	C	P	P	A	A	G	Q	Q	P	R	P	P	E	P	P	A	G	W	R	Q	Q	I	Q	W	E	N	N	Q	V																			
<i>canine LOX</i>	SLLSLGSQYQPQR	R	D	P	G	T	T	A	P	G	A	N	A	A	P	Q	P	R	T	P	I	L	L	R	N	R	T	A	A	R	E	A	G	T	A	G													
<i>human LOX</i>	SLLSLGSQYQPQR	R	D	P	G	A	A	V	P	G	A	N	A	S	A	Q	P	R	T	P	I	L	I	R	D	N	R	T	A	A	R	T	R	T	A	G	S												
<i>canine LOX</i>	GAGRPRPAARHW	F	Q	A	G	Y	S	A	S	G	A	D	A	N	Q	T	A	P	G	E	P	A	S	N	L	R	P	S	R	V	D	G	M	V	GDDPYN														
<i>human LOX</i>	GVTAGRPRPTARHW	F	Q	A	G	Y	S	T	S	R	A	E	A	G	S	R	A	E	N	Q	T	A	P	G	E	V	P	A	S	N	L	R	P	S	R	V	D												
<i>canine LOX</i>	PYKYSDDNPYYNYD	T	Y	E	R	P	R	P	G	S	R	Y	R	P	G	Y	G	T	G	F	Q	Y	G	L	P	D	L	V	P	D	P	Y	Y	I	Q	A	S	T	Y	V									
<i>human LOX</i>	MVGDDPYNPYKYSDDN	P	Y	K	Y	S	D	D	N	P	Y	Y	N	Y	D	T	Y	E	R	P	R	P	G	G	R	Y	R	P	G	Y	T	G	F	Q	Y	G	L	P	D	L	V	A	D	P	Y				
<i>canine LOX</i>	QKMSMYNLRC	A	E	N	C	L	A	S	A	Y	R	A	V	R	D	Y	D	H	R	V	L	L	R	F	P	Q	R	V	K	N	Q	G	T	S	D	F	L	P	S	R	R								
<i>human LOX</i>	YI	Q	A	S	T	Y	V	Q	K	M	S	M	Y	N	L	R	C	A	E	N	C	L	A	S	A	Y	R	A	V	R	D	Y	D	H	R	V	L	L	R	F	P	Q	R	V	K	N	Q	G	T
<i>canine LOX</i>	YSWEWH	S	C	H	Q	Y	H	S	M	D	E	F	S	H	Y	D	L	L	D	A	S	T	Q	R	R	V	A	E	G	H	K	A	S	F	C	L	E	D	T	S	C	D	Y	G	Y	H	R	R	
<i>human LOX</i>	DFLPSR	P	R	Y	S	W	E	H	S	C	H	Q	Y	H	S	M	D	E	F	S	H	Y	D	L	L	D	A	S	T	Q	R	R	V	A	E	G	H	K	A	S	F	C	L	E	D	T	S		
<i>canine LOX</i>	ACTAHTQGLSP	G	C	Y	D	T	Y	N	A	D	I	D	C	Q	W	I	D	I	T	D	V	K	P	G	N	Y	I	L	K	V	S	V	N	P	S	L	V	P	E	D	Y	S							
<i>human LOX</i>	DYGYHRR	F	A	C	T	A	H	T	Q	G	L	S	P	G	C	Y	D	T	Y	N	A	D	I	D	C	Q	W	I	D	I	T	D	V	K	P	G	N	Y	I	L	K	V	S	V	N	P	S	L	
<i>canine LOX</i>	NVVRCEIRYTGH	H	A	Y	S	G	C	T	I	S	P																																						
<i>human LOX</i>	VPESDYTNNVVRC	D	I	R	Y	T	G	H	A	Y	S	G	C	T	I	S	P																																

Figure 14. Alignment of the annotated amino acid sequences of the human and putative dog LOX protein.

Highlighted are the *signal peptide cleavage site* in yellow, the *BMP-1 cleavage site* of the pro-peptide in red, the *copper-binding site* in blue, the lysine and tyrosine residue generating the *lysyl-tyrosyl quinone cofactor* in orange and the *cytokine-receptor-like domain* in green. Notably, the annotated dog LOX protein is lacking 8 amino acids in the pro-peptide region compared to human LOX. However, the sequence of the mature proteins is highly conserved between both species and is identical for important functional domains (highlighted in colors). In addition, the epitope sequence of the two anti-LOX antibodies used in this study is highlighted in black.

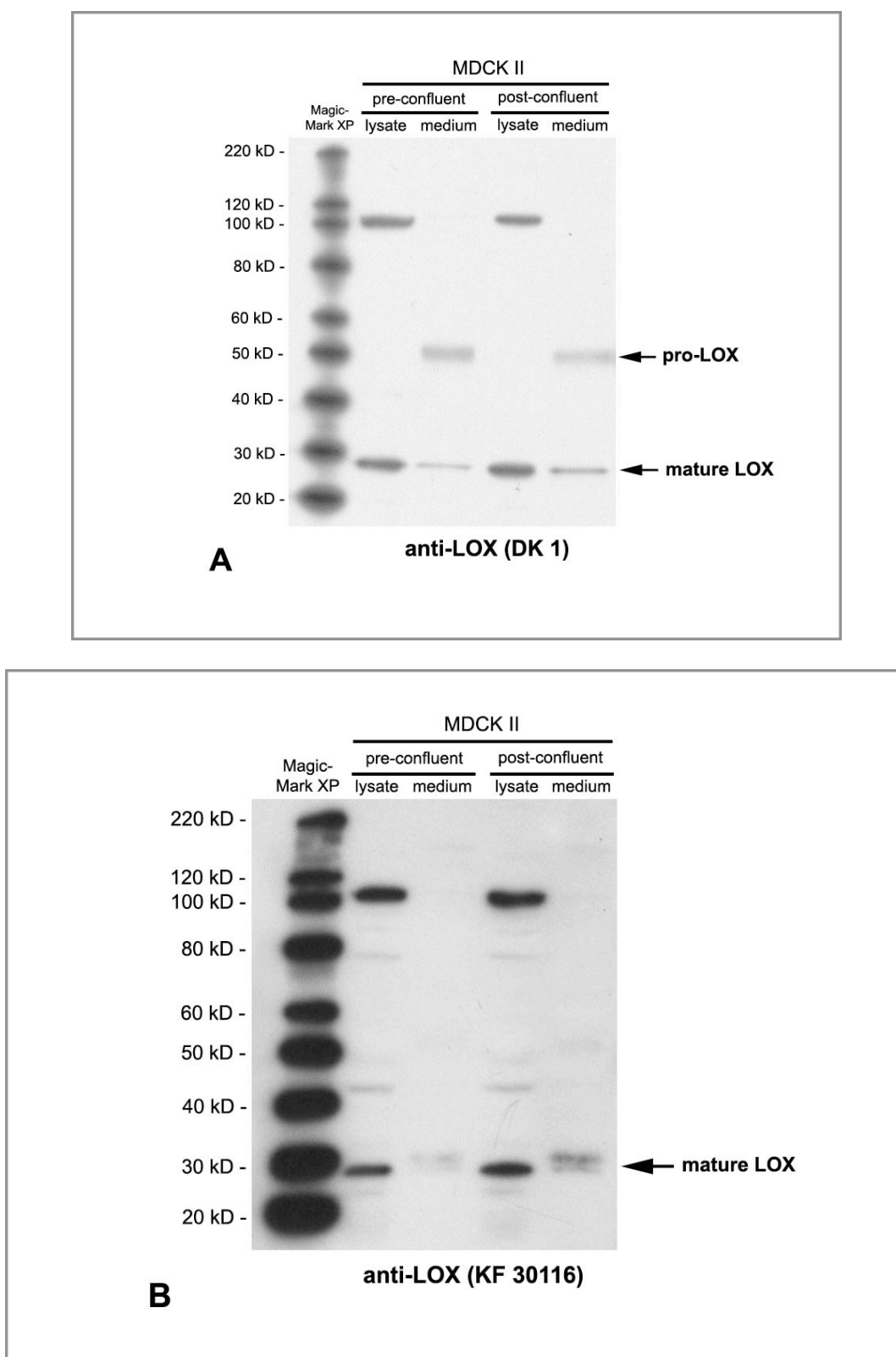
Results

In media fractions of MDCK II cells the “DK1” antibody detected one signal close to 30 kD and another signal at 50 kD corresponding to the expected size of mature and pro-LOX, respectively (Figure 15 A). The 50 kD signal was slightly stronger in media fractions from pre-confluent cultures whereas the 30 kD signal was more pronounced in media fractions from post-confluent cultures probably reflecting advanced processing of pro-LOX into the mature form within the extracellular space during the transition from pre- to post-confluent stages. Surprisingly, we detected an even stronger 30 kD signal in cell lysates of both pre- and post-confluent cultures suggesting the presence of mature LOX in the cytoplasm of MDCK II cells. In addition, a strong band of approximately 100 kD was observed in cell lysates. The identity of this band is unclear but signals of similar molecular weight have been observed with different LOX antibodies in other cell types and by other laboratories as well (personal communication with H. Kagan and P. Sommer). In previous biochemical studies it has also been observed that LOX is a rather insoluble protein in physiological buffer systems. Therefore, researchers have speculated that the 100 kD signal could result from aggregation of LOX monomers and may represent a homodimer of the 50 kD full-length LOX (personal communication with H. Kagan and P. Sommer). However, this band could also be the result of the antibody cross-reacting with another protein.

As the supply of the anti-LOX “DK 1” antibody was limited, we were forced to switch to another antibody (anti-LOX “KF 30116” that was raised against the same epitope, see above) where sufficient stocks were available from our own laboratory. Western blot results were almost identical except that the anti-LOX “KF 30116” antibody did only barely detect the 50 kD signal of the LOX pro-enzyme in MDCK II cells (Figure 15 B). This observation was confirmed in other cell types such as NIH3T3 fibroblasts and vascular smooth muscle cells by our laboratory and may be due to the source of a different animal for antibody generation (personal communication with K. Fong). However, after long exposures of western blots, weak signals between 45 kD and 50 kD corresponding to the size of the LOX pro-enzyme were detected as well (data not shown).

Using the anti-LOX “KF 30116” antibody we then analyzed LOX protein expression in MCF-10A. As in MDCK II cells we detected mature LOX in media fractions of predominantly post-confluent cultures and even stronger 30 kD signals in cell lysates (Figure 15 C). In addition, cell lysates of MCF-10A cells showed a signal of approximately 35 kD and a double band between 40 kD and 50 kD. Although substantially weaker, the latter signals could be also seen in MDCK II cells after long exposures and might correspond to non-glycosylated forms of the LOX pro-enzyme.

Results



Results

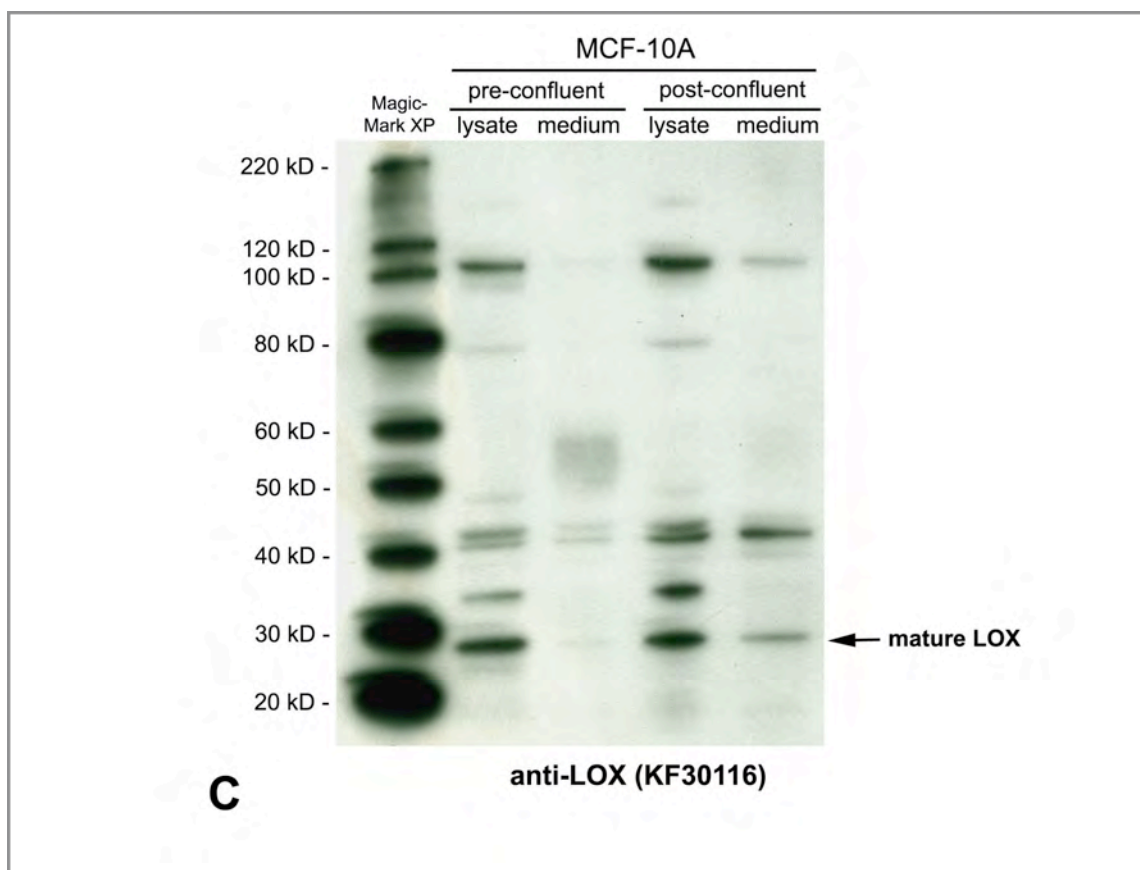


Figure 15. Detection of LOX protein by western blot analysis in cell lysates and media fractions of (A + B) MDCK II and (C) MCF-10A cells.

Protein extracts of pre- and post-confluent MDCK II and MCF-10A cells were prepared from crude cytoplasmic fractions and conditioned cell medium. 20 µg of total protein were loaded for each sample. Western blots were probed with a rabbit polyclonal anti-LOX antibodies “DK 1” (A) and “KF 30116” (B + C) that both target an epitope 7 amino acids down from the BMP-1 cleavage site but were generated in different animals.

Results

Interestingly, the 35 kD signal was not detected in MDCK II cells and in MCF-10A cells was only observed in the cytoplasmic fraction. The 35 kD band could result from a cross-reaction of the antibody with a protein that is expressed in MCF-10A but not in MDCK II cells. Alternatively, it could also represent a novel post-translational modified form of the 30 kD mature LOX in the cytoplasm that is specific for mammary epithelial cells. Notably, MCF-10A cells are not only supplemented with serum during cell culture but also with 20 ng/ml EGF and 10 ug/ml Insulin, two potent growth factors and activators of tyrosine kinase receptor signaling pathways that result in phosphorylation of multiple target proteins in the cytoplasm {Bublil & Yarden, 2007; Saltiel & Pessin, 2002}. However, phosphorylation of the LOX protein has not been published so far although there is preliminary evidence from other laboratories that it may occur (personal communication, Dr. Aukhil Ikramuddin).

In most fibrogenic cells LOX is synthesized as a glycosylated 50 kD pro-enzyme that is secreted into the extracellular space where according to current knowledge it is being processed into the 30 kD catalytically active form by procollagen-C-proteinase, now often referred to as bone morphogenetic protein 1 (BMP-1) {Cronshaw et al., 1995; Panchenko et al., 1996; Uzel et al., 2001}. To address the question whether epithelial cells do possess the cellular machinery required for adequate processing of LOX we examined the expression of BMP-1 in MDCK II and MCF-10A cells. Western blots showed expression of the 70 kD mature BMP-1 not only in extracellular media fractions but also in cell lysates of both cell lines implying that MDCK II and MCF-10A cells might have the ability to process LOX not only in the extracellular space but also inside the cell (Figure 16). Besides the 70 kD band corresponding to mature BMP-1, the antibody also detected bands at 50 kD and 30 kD, especially in media fractions of both cell lines. This antibody was designed against the CUB-2 domain of BMP-1, a motif that is shared by a BMP-1-interacting protein named Procollagen C Proteinase Enhancer Protein (PCOLCE). These signals most likely represent the uncleaved 50 kD and the processed 30 kD form of the enhancer protein that is known to act in concert with BMP-1 on collagen-processing in the extracellular matrix {Takahara et al., 1994}.

In addition, we wanted to exclude the possibility that detection of 30 kD mature LOX in cytoplasmic fractions was an artifact due to extracellular contaminations during preparation of protein extracts. Therefore we decided to probe our samples with an antibody against fibronectin, one of the most abundant proteins in the extracellular matrix {Pankov & Yamada, 2002}.

Results

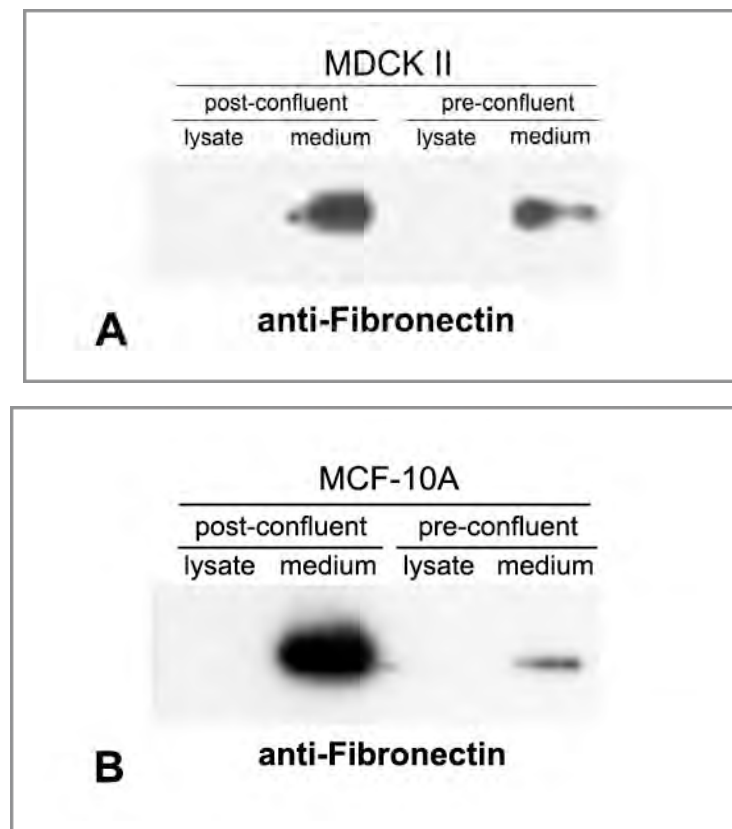


Figure 17. Detection of fibronectin in conditioned cell medium of MDCK II and MCF-10A cells.

Western blots probed with anti-LOX antibodies were stripped and then reprobed with anti-fibronectin antibody to examine the presence of fibronectin in cell lysates and media fractions of MDCK II (A) and MCF-10A cells (B).

Results

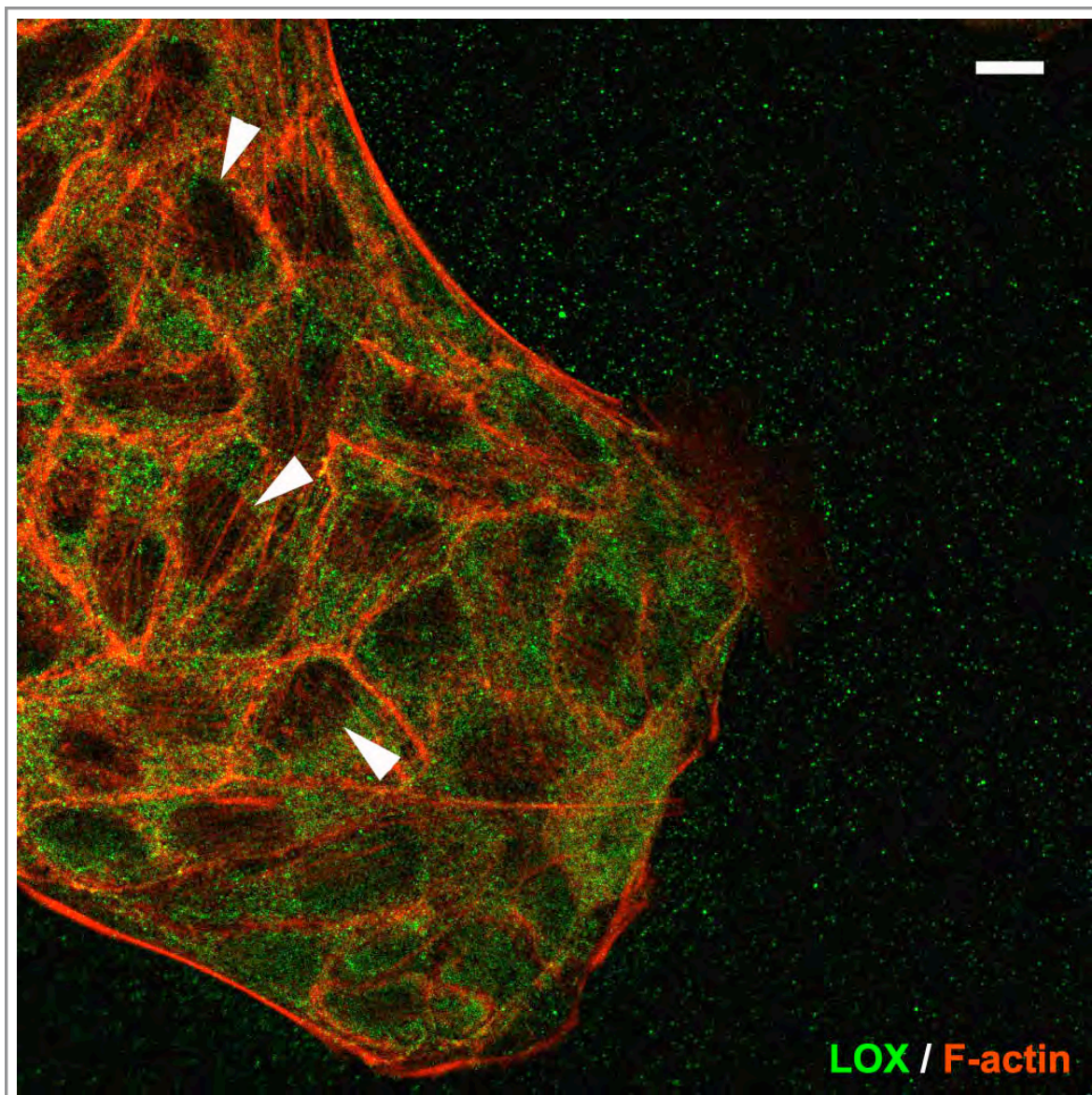


Figure 18. Immunofluorescence staining of LOX in MDCK II cells.

MDCK II cells were seeded overnight on glass coverslips and fixed in 2 % para-formaldehyde at 70-80 % confluence the following day. Cells were stained with anti-LOX (KF 30116) antibody and the actin cytoskeleton was visualized with Palloidin-TRITC. Images were recorded with a Zeiss LSM confocal microscope. Nuclei were counterstained with Hoechst 33258 dye but no images could be recorded on the UV-channel due to technical limitations. Scale bar indicates 10 μ m.

Results

Fibronectin signals were detected only in media fractions but not in cell lysates of both cell lines suggesting validity of the detected LOX signals and high purity of the cytoplasmic fractions (Figure 17). Furthermore, immunofluorescence stainings with MDCK II cells reinforced the observations made during western blot analysis. LOX was detected in a broadly distributed punctate staining pattern throughout the cytoplasm (Figure 18). In contrast, no significant LOX staining was seen within nuclei (indicated by arrows) of MDCK II cells. Interestingly, although MDCK II cells were cultured on plain tissue culture plasticware, fluorescent signals were also detected in the extracellular space surrounding the cells. These LOX signals could indicate early stages of a developing extracellular matrix which is supported by the fact that fibronectin was detected by western blot analysis in extracellular medium fractions of MDCK II cells (Figure 17 A).

So far the results provided evidence for expression of mature LOX in both MDCK II and MCF-10A cells but it was not clear from those data if the LOX enzyme was catalytically active. As the question of catalytic activity is critical with respect to the functional relevance of the observed LOX expression in those epithelial cell lines we performed *in vitro* assays to measure LOX enzyme activity. Trackman and colleagues developed and recently optimized a sensitive fluorometric assay that uses 1, 5-diaminopentane, a non-peptidyl alkyl amine, as a substrate {Trackman et al., 1981; Palamakumbura & Trackman, 2002}. An adapted version of this assay for microplate formats has been used by our laboratory since 2003 for the routine detection of LOX activity from conditioned cell medium of fibrogenic cells (Fogelgren et al., 2005). The principle of the assay is based on the detection of hydrogen peroxide that is generated in stoichiometric proportions as a side-product during the catalytic reaction (Figure 19). In the presence of hydrogen peroxide, horseradish peroxidase converts Amplex Red dye into the fluorescing reagent resorufin. To determine the amount of hydrogen peroxide that is generated only by LOX catalytic activity, reactions were run in parallel in the presence of excess amounts of the irreversible LOX-inhibitor beta-aminopropionitrile (BAPN).

In conditioned cell medium of both, MDCK II and MCF-10A cells, significant lysyl oxidase enzyme activity was measured in post-confluent cultures but only little activity was detected from pre-confluent cultures (Figure 20). These data confirmed previous western blot results where prominent signals of 30 kD LOX were detected in medium fractions from post-confluent cells and weak signals in pre-confluent cells. We also tried to measure LOX activity from cell lysates but those attempts were not successful (data not shown).

Results

The limitation here may have been the assay itself. Hydrogen peroxide is produced by a variety of sources within the cytoplasm, such as superoxid dismutase and NADPH oxidase {Veal et al., 2007}. All of these sources could mask the hydrogen peroxide generated by LOX. However, it cannot be excluded that intracellular mature LOX may not be catalytically active, for example due to interaction(s) with other proteins that keep it in an inactive conformation.

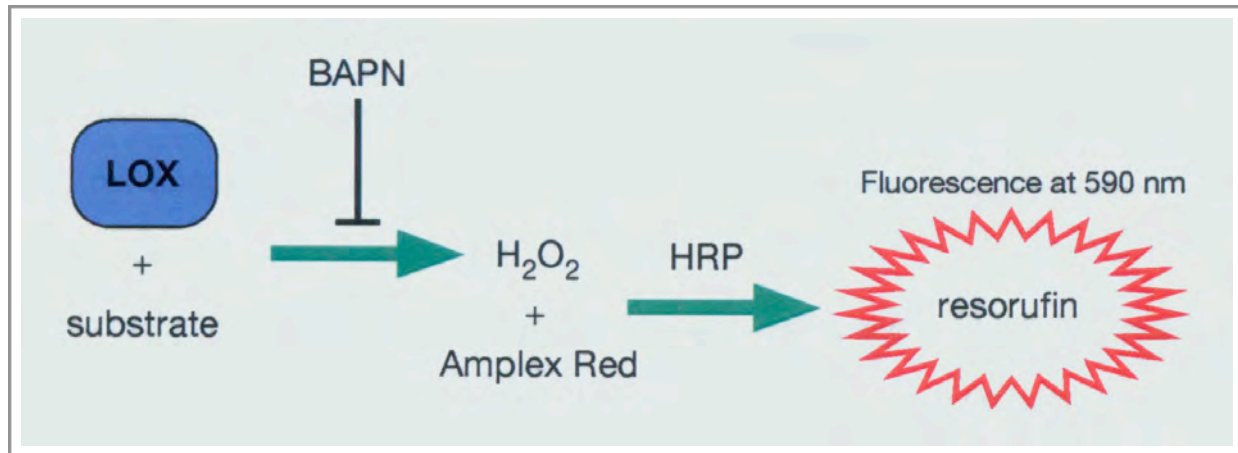


Figure 19. Principle of the assay for LOX activity measurements.

LOX protein (e.g. from conditioned cell medium and/or purified LOX) is incubated with a substrate (e.g. cadaverine) yielding H₂O₂ as a side product. In the presence of H₂O₂, Amplex Red is converted by horse radish peroxidase (HRP) into resorufin whose fluorescence signal can be measured at 590 nm. The amount of BAPN-inhibitable H₂O₂ generation is defined as LOX activity.

Results

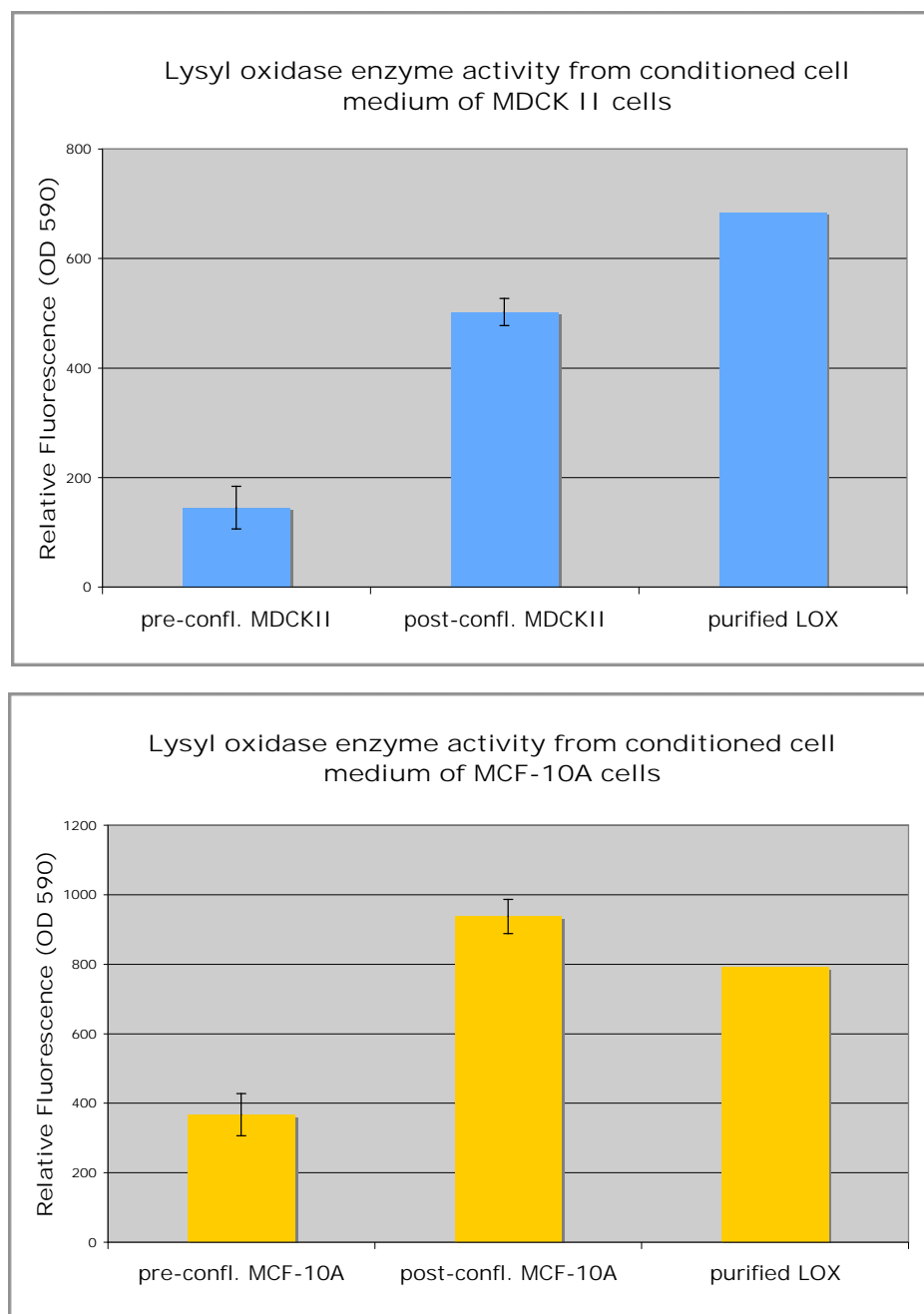


Figure 20. BAPN-inhibitable lysyl oxidase enzyme activity in conditioned cell medium of MDCK II (top panel) cells and MCF-10A (bottom panel) cells.

100 µg of total protein from conditioned cell medium of MDCK II and MCF-10A cells were assayed for BAPN-inhibitable lysyl oxidase enzyme activity with 1, 5-diaminopentane as a synthetic substrate. 300 ng of purified LOX protein from bovine aorta (kindly provided by Dr. Kagan, Boston University) were used as a positive control.

Results

Summary

Using MDCK II dog kidney epithelial cells and MCF-10A human mammary epithelial cells, two well characterized cell lines that exhibit important features of epithelia *in vivo*, we could demonstrate for the first time the expression of catalytically active LOX in epithelial cells {published in Jansen & Csiszar, 2007}. During western blot analyses mature 30 kD LOX was detected in conditioned cell medium especially from post-confluent cultures of both cell lines. These results suggest that cells in differentiated epithelial tissues might contribute to LOX-catalyzed crosslinking of ECM fibrils at their underlying basal surfaces and basement membranes. Enzyme activity assays with media fractions confirmed these findings as significant BAPN-inhibitable LOX activity was observed. Furthermore, high amounts of 30 kD LOX were detected in cell lysates that were cleared from nuclei, indicating the presence of mature LOX in the cytoplasm of these cells. Immunofluorescence stainings of MDCK II monolayers reinforced this observation as LOX was detected in a punctate staining pattern throughout the cytoplasm but could not be seen within nuclei. Together these results raise the intriguing option for a novel intracellular function of LOX in the cytoplasm of epithelial cells. The presence of BMP-1 in cell lysates and media fractions underlined that MDCK II and MCF-10A cells possess the molecular machinery to process LOX into its mature form both, intracellularly and extracellularly. Interestingly though, LOX activity could not be measured in cytoplasmic fractions yet. It remains to be resolved whether mature LOX in the cytoplasm does not possess catalytic activity or if the conditions of the current standard assay are not applicable for intracellular activity measurements.

2. Increased LOX expression during scattering of MDCK II cells

The second goal of the first dissertation project was to simulate phenotypical events of cellular invasion during malignant progression using our established epithelial cell model system and to analyze potential changes of LOX expression. For this purpose we utilized a well characterized *in vitro* assay that recapitulates important features of epithelial-mesenchymal transition (EMT), a cellular phenotype transition that is widely considered to be one of the hallmarks of tumor metastasis {Thiery, 2002}. After treatment with hepatocyte growth factor (HGF) MDCK II cells start to scatter and dissolve their cell-cell contacts within hours and acquire a migratory and motile phenotype {Stoker et al., 1987}. During this process the cells loose important epithelial characteristics whereas typical mesenchymal features are gained. However, the “Scatter Assay”, although a valuable model, is not a true EMT per definition as it is transient and completely reversible upon HGF withdrawal.

After testing several lots of commercially available recombinant HGF we established a protocol using 5 ng/ml HGF which was added to the cell culture medium for the duration of the assay. After incubation with HGF for 15 hours, MDCK II cells showed a dramatic change in their morphology (Figure 21). The cells lost contact to neighboring cells resulting in flattened and elongated fibroblast-like cell shapes (Figure 21 C and D) whereas cells from control assays without HGF treatment retained the typical “cobblestone” morphology of polarized epithelial cells in culture (Figure 21 A and B).

Analysis of characteristic marker proteins confirmed phenotypical changes from an epithelial towards a mesenchymal phenotype during scattering of MDCK II cells. Increased expression of vimentin, an intermediate filament protein and marker for mesenchymal cell types {Helfand et al., 2004}, was observed in immunofluorescence stainings after induction of scattering in MDCK II cells (Figure 22 A and B). In contrast, E-cadherin, a homophilic cell-cell adhesion protein characteristic for epithelial cells {Gumbiner, 2005}, was massively relocated from cell-cell junctions into the cytoplasm (Figure 22 C and D). It is known that down-regulation of E-cadherin during EMT is initiated through E-cadherin internalization into the cytoplasm where it becomes subject to proteasomal degradation {Yap et al., 2007}.

Results

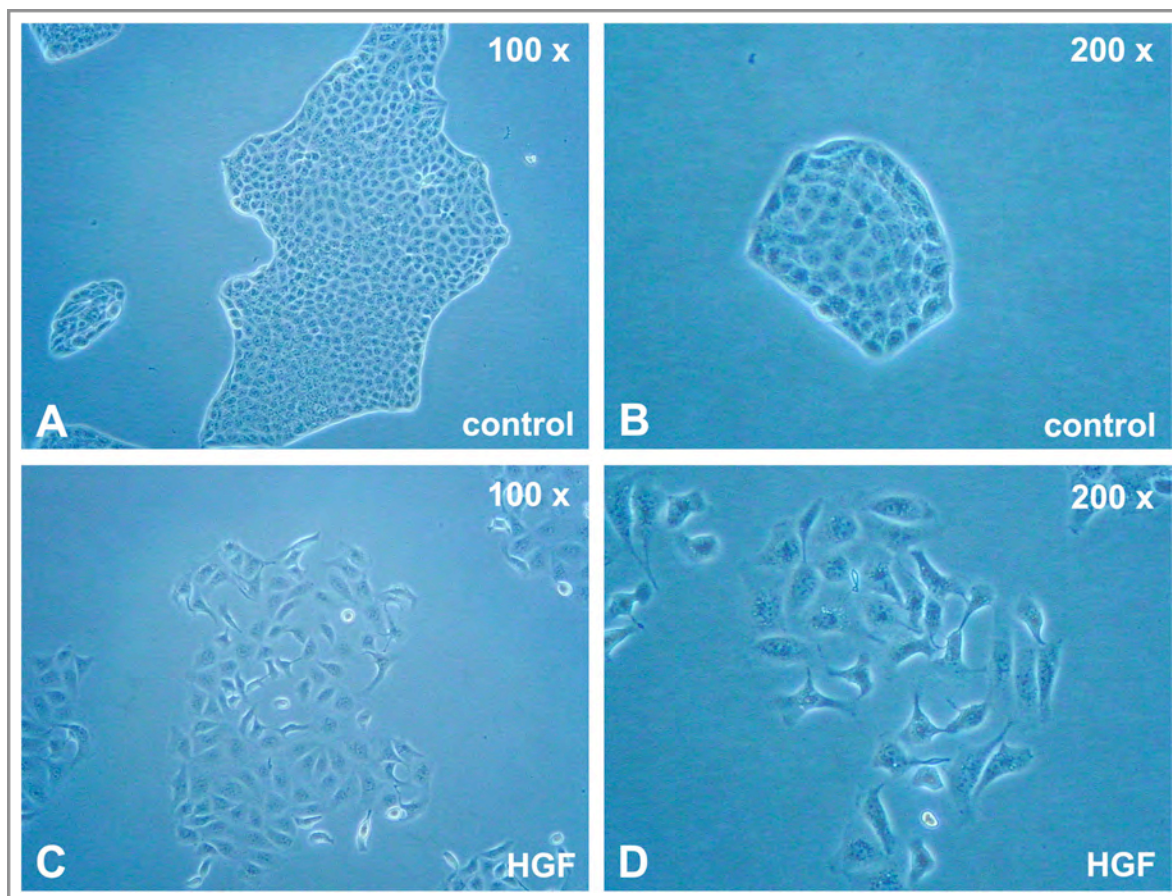


Figure 21. Scattering of MDCK II cells induced by HGF treatment.

Pre-confluent (< 50 % confluence) cultures of MDCK II cells were supplemented with 5 ng/ml HGF for 15 hours. Morphological changes in HGF-treated (C + D) compared to control (A + B) cells were documented with a Zeiss Axiovert brightfield microscope.

Results

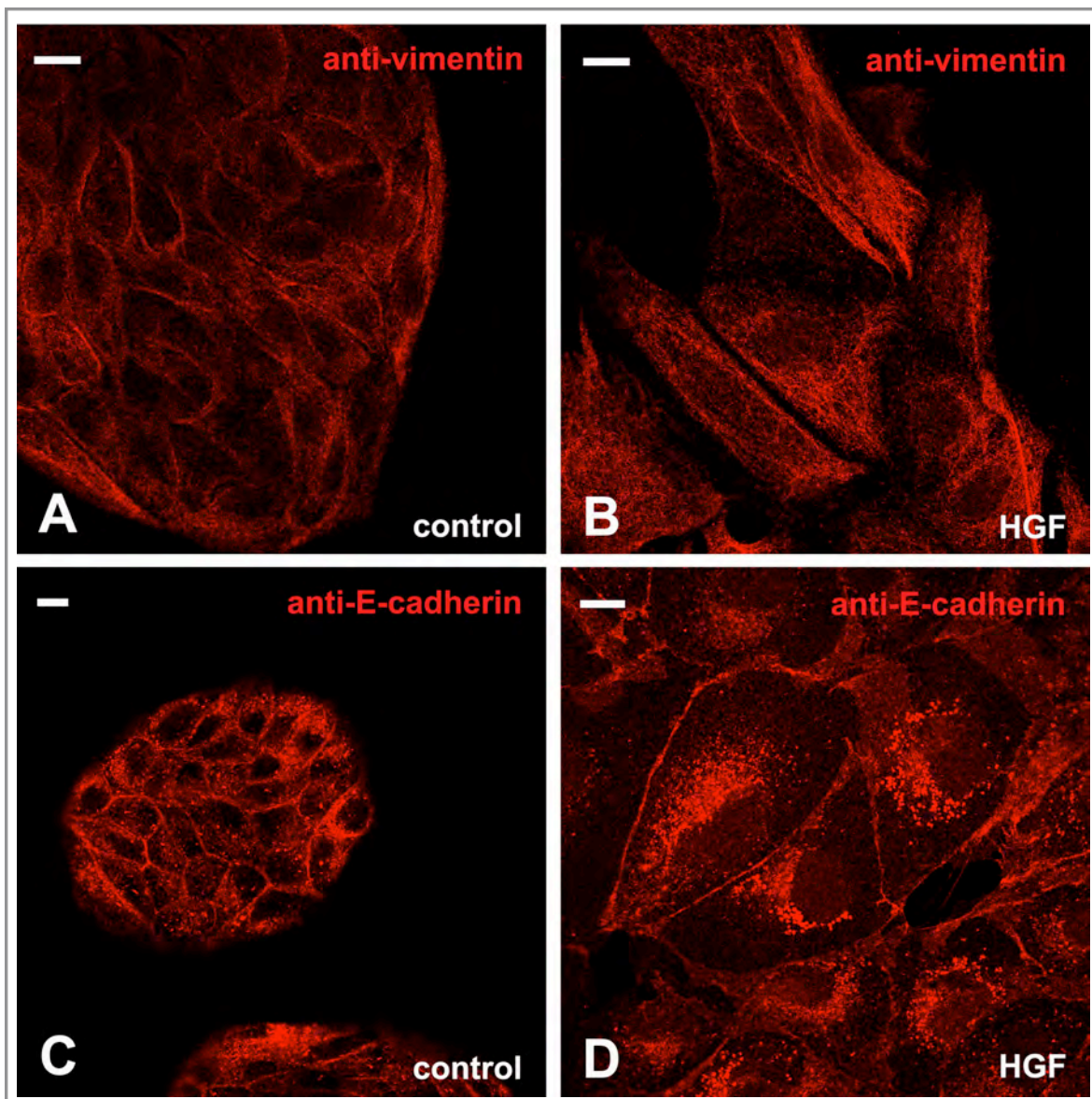


Figure 22. Increased expression of vimentin and cytoplasmic re-localization of E-cadherin during scattering of MDCK II cells.

After induction of scattering with 5 ng/ml HGF for 15 hours, MDCK II cells were fixed in 2 % paraformaldehyde and stained with antibodies against vimentin (A + B) and E-cadherin (C + D). Images were recorded with a Zeiss LSM confocal microscope. Scale bars correspond to 10 μ m.

Results

Western blot analysis emphasized these findings showing both, a strong increase of vimentin expression and accumulation of E-cadherin in the cytoplasmic fraction during scattering of MDCK II cells (Figure 23). In fact, the E-cadherin signal in cell lysates of HGF-treated samples was so strong that the film was bleached in the center of the signal. Furthermore, we detected an increase of 30 kD mature LOX in the cytoplasm of MDCK II cells after HGF treatment (Figure 23). This raised the question whether increased amounts of intracellular 30 kD LOX were due to post-translational changes, for example through increased protein stability, or whether these observations were due to transcriptional up-regulation of LOX expression. It was therefore decided to perform quantitative real-time PCR experiments to assess the transcript levels of LOX. Total RNA was extracted from control and HGF-treated MDCK II cells and cDNA was generated. Initially, housekeeping genes, i.e. GAPDH, β -actin and ribosomal RNA genes, were used as internal standards for relative quantification of LOX expression in control and HGF-treated samples. However, as all of those genes showed significant changes in transcript levels themselves (data not shown), we decided to quantify LOX transcript copy numbers directly. Serial dilutions of LOX-plasmid DNA were amplified with gene-specific primers for LOX to generate a standard graph where the C(t) value for each dilution was plotted against the copy number of LOX template DNA (Figure 24). Based on the standard graph it was now possible to determine and compare the transcript levels of LOX in control and HGF-induced samples by means of absolute copy numbers. The results showed a more than two-fold increase of LOX mRNA levels in HGF-treated versus control cells indicating a significant transcriptional up-regulation of LOX during scattering of MDCK II cells (Figure 25).

Summary

Applying the “Scatter Assay” with MDCK II cells as an *in vitro* model for EMT, increased amounts of intracellular 30 kD mature LOX were detected during the transition from an epithelial towards a mesenchymal phenotype. The increase in LOX protein expression most likely resulted from increased transcriptional activity of the LOX gene as quantitative real-time PCR experiments revealed a strong increase of LOX mRNA levels in HGF-treated versus untreated cells. Using a simple *in vitro* cell culture assay, we were able to recapitulate transcriptional up-regulation of LOX expression as it has been previously observed during tumor metastasis *in vivo*.

Results

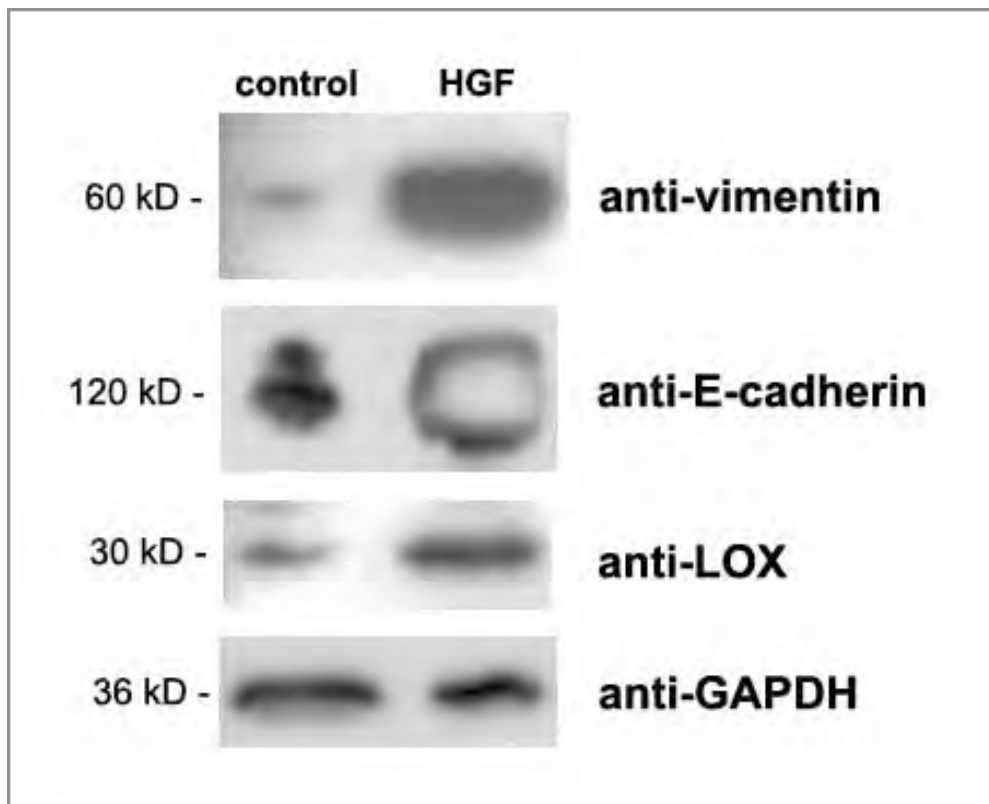


Figure 23. Examination of vimentin and E-cadherin expression during scattering of MDCK II cells by western blot analysis.

After induction of scattering with 5 ng/ml HGF for 15 hours, cell lysates from MDCK II cells were collected. 20 µg of total protein from each sample were subjected to western blot analysis. Western blots were probed with specific antibodies against vimentin, E-cadherin, LOX and GAPDH. The latter was used as a loading control.

Results

PCR amplification of LOX from serial dilutions of a pcDNA-LOX plasmid template

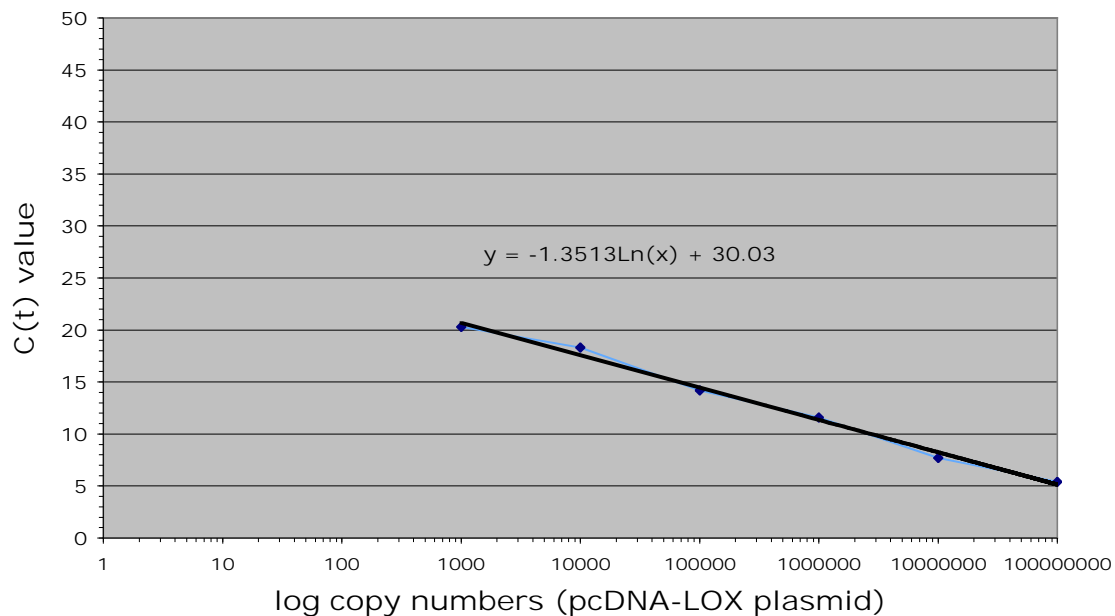


Figure 24. Standard graph for LOX copy numbers after linear amplification from a pcDNA-LOX plasmid template.

Serial dilutions of pcDNA-LOX plasmid were amplified with gene-specific LOX primers. The C(t) values were then plotted against the LOX copy numbers on a logarithmic scale. LOX copy numbers were calculated based on size and concentration of the pcDNA-LOX plasmid.

Results

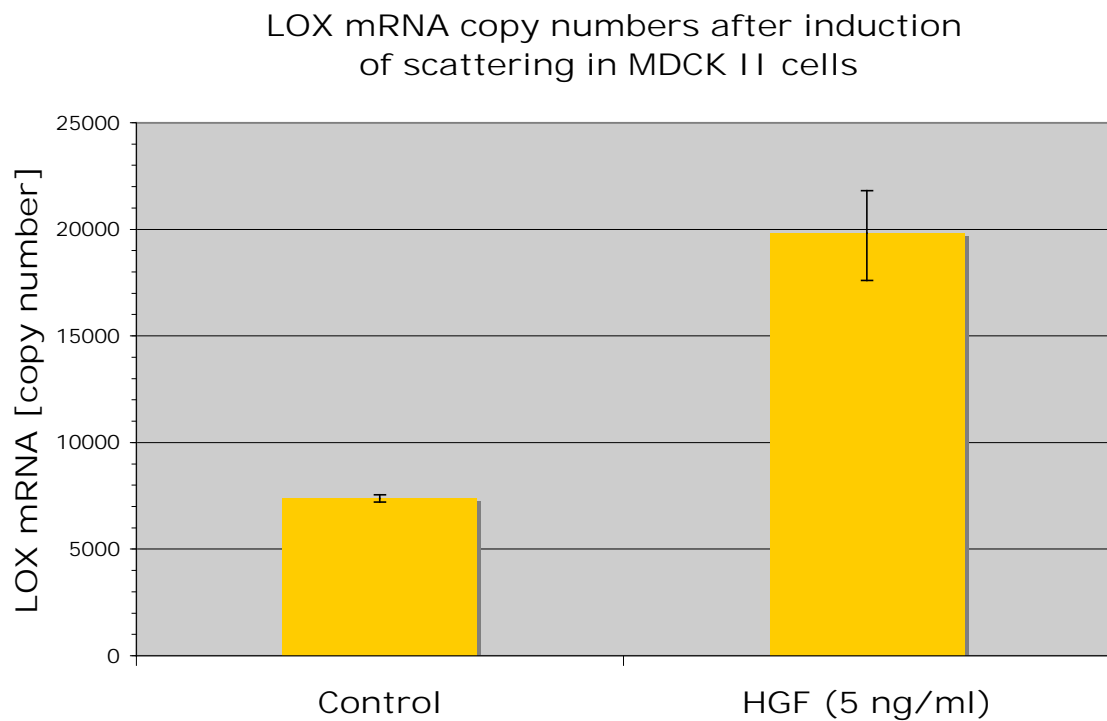


Figure 25. Increased LOX transcript levels after scattering of MDCK II cells.

Total RNA was harvested and reverse transcribed into cDNA from control cells and HGF-treated cells for 15 h. LOX mRNA expression was assessed with gene-specific primers using quantitative real-time PCR as described in the text.

3. Generation of stable MDCK II cell lines over-expressing LOX

Almost a decade ago, analysis of differential gene expression patterns in breast cancer cell lines detected LOX in a set of highly up-regulated genes in cell lines with a metastatic phenotype {Kirschmann et al., 1999}. Subsequent *in vitro* and *in vivo* studies revealed LOX as a key factor for cellular invasiveness and tumor metastasis in breast carcinomas {Kirschmann et al., 2002; Payne et al., 2005; Erler et al., 2006}. Although carcinomas are tumors of epithelial origin, until now the effect of increased LOX expression on the cellular phenotype in normal epithelia has not been addressed. Therefore, the aim was to investigate the consequence of LOX over-expression in normal, non-transformed epithelial cells. Consequently, the third goal of this dissertation was to generate stable MDCK II cell lines over-expressing LOX. The rationale was to utilize forced over-expression of LOX as a tool to test if LOX can induce a phenotype that could be further dissected at the molecular level. As the presence of mature LOX was detected to our surprise within the cytoplasm of MDCK II cells earlier in this study, one particular interest was to analyze the epithelial phenotype after intracellular over-expression of mature LOX.

3.1 Stable MDCK II cell lines that over-express LOX-EGFP constructs

Green fluorescent protein (GFP) is an auto-fluorescing protein that was originally discovered in the jellyfish *Aequorea* in the 1960s by Shimoura et al. and then later cloned by Prasher et al. in 1992 {reviewed in Tsien, 1998}. In contrast to many fluorescent dyes GFP can be introduced into mammalian cells without cellular toxicity. It is often expressed as a fusion protein together with the gene of interest and has become an excellent tool to study intracellular localization and dynamics of proteins {Ward & Lippincott-Schwartz, 2006}. Due to its auto-fluorescing properties GFP is widely used for “live-cell imaging” experiments where localization patterns and movements of the GFP-fusion protein in different cellular compartments can be tracked with a microscope {Rizzuto et al., 1995; Kanda et al., 1998; Riesen et al., 2002}. Considering the potential applications of LOX-GFP-fusion proteins for intracellular LOX studies constructs were generated that express mature or full-length LOX as a fusion protein with GFP at the C-terminus. To build the LOX-GFP construct, the pEGFP-N1 vector (BD Biosciences) which encodes a red-shifted GFP-variant optimized for brighter fluorescence and higher expression efficiency in mammalian cells was used {Chalfie et al., 1994}. A diagram of the pEGFP-N1 vector is shown in Figure 26.

Results

A cDNA fragment encoding the full-length human LOX protein was cloned into the *EcoRI* and *BamHI* restriction sites of pEGFP-N1. Restriction analysis of this construct yielded an expected fragment of ~ 1.25 kb fragment (Figure 27 A). Interestingly, an additional fragment of ~ 600 bp also occurred. The cause of this band has never been determined but sequencing of purified plasmid DNA ruled out any contaminants (data not shown).

In addition, a construct coding for mature LOX (amino acids 169-417) was generated by PCR. The insert was ligated into the *EcoRI* and *BamHI* sites of the pEGFP-N1 vector. Positive recombinants were identified by restriction digest yielding in a ~ 750 bp fragment (Figure 27 B) as well as by DNA sequencing (data not shown).

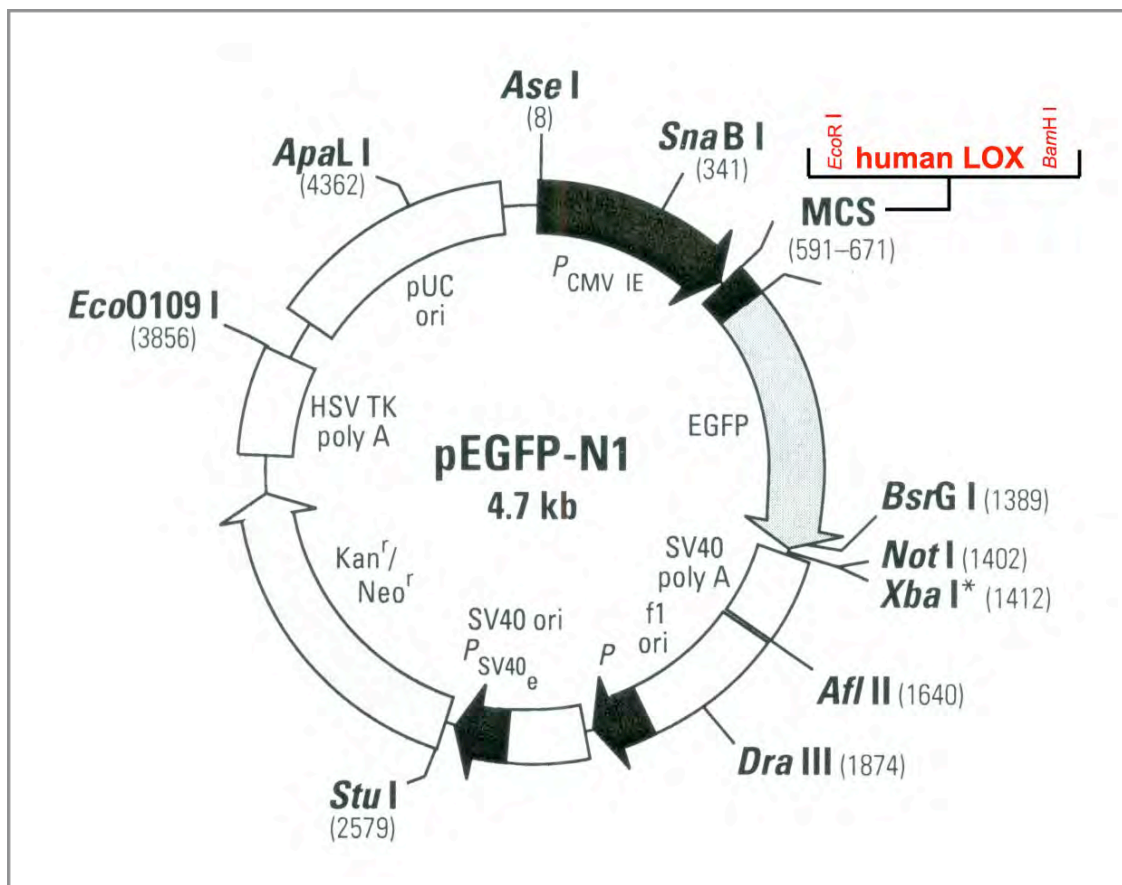
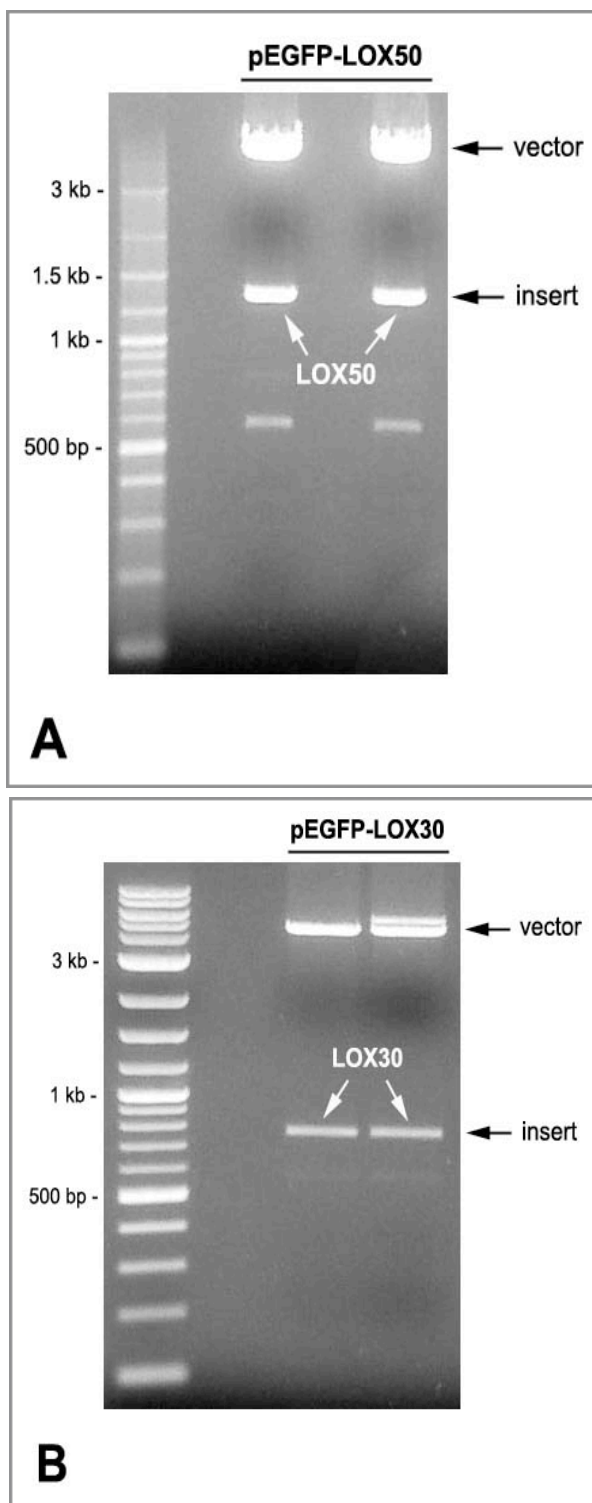


Figure 26. Schematic depiction of the cloning strategy for LOX-EGFP expression constructs.

The human LOX gene, flanked by *EcoRI* and *BamHI* restriction sites, was ligated into the multiple cloning site of the pEGFP-N1 vector from BD Biosciences. As a consequence LOX-EGFP is expressed as a fusion protein where EGFP is expressed in frame and C-terminal of LOX.

Results



Results

The mature LOX30-EGFP and full-length LOX50-EGFP constructs were transfected into MDCK II cells. Cells stably expressing the LOX-EGFP constructs were selected by antibiotic treatment with 500 µg/ml G418 for two weeks. After cell culture propagation, stable clones were initially analyzed for phenotype changes based on their morphology (Figure 28). Parental MDCK II cells (Figure 28 A) displayed the characteristic cuboidal morphology of epithelial cells as did MDCK II cells transfected with the pEGFP-N1 vector only (Figure 28 B). Also cells transfected with the mature LOX30-EGFP construct did not change their morphology (Figure 28 C). In contrast, especially one particular clone of MDCK II cells transfected with LOX50-EGFP showed a remarkable change in morphology (Figure 28 D). The cell shapes were flattened out and strongly elongated but interestingly cells were still growing in clusters and seemed to maintain adhesive contacts with most adjacent cells (see insert of Figure 28 D).

In the next step expression of the transfected constructs was examined by western blot analysis using anti-GFP and anti-LOX antibodies. In cell lysates from LOX30-EGFP cells the anti-GFP antibody did not detect any signal except for two background bands at approximately 65 kD and 120 kD that were also seen in the parental cell line (Figure 29, left panel). Because the secondary antibody alone did not yield any signal (data not shown), the background bands were probably due to cross-reaction of the primary antibody with other protein(s) in MDCK II cells. The anti-LOX antibody detected endogenous mature LOX and the glycosylated and non-glycosylated forms of proLOX, both in parental and LOX30-EGFP cells (Figure 29, right panel). Based on the molecular weight of mature LOX (~ 30 kD) and EGFP (~ 30 kD) the fusion protein would be expected at an approximate molecular weight of 60 kD. A signal of this size was detected with neither the anti-GFP nor the anti-LOX antibody suggesting a LOX30-EGFP fusion protein was not successfully expressed in these cells. We did not test expression of the LOX30-EGFP fusion gene on the mRNA level but due to the constantly stringent selection conditions (cells were continuously cultured in the presence of G418), only cells expressing the construct presumably had a chance to survive. However, it is possible that expressed LOX30-EGFP may have become subject to a pre-translational mRNA decay mechanism or to post-translational degradation, for example due to misfolding of the fusion protein {Isken & Maquat, 2007; Herbert & Molinari, 2007}.

Results

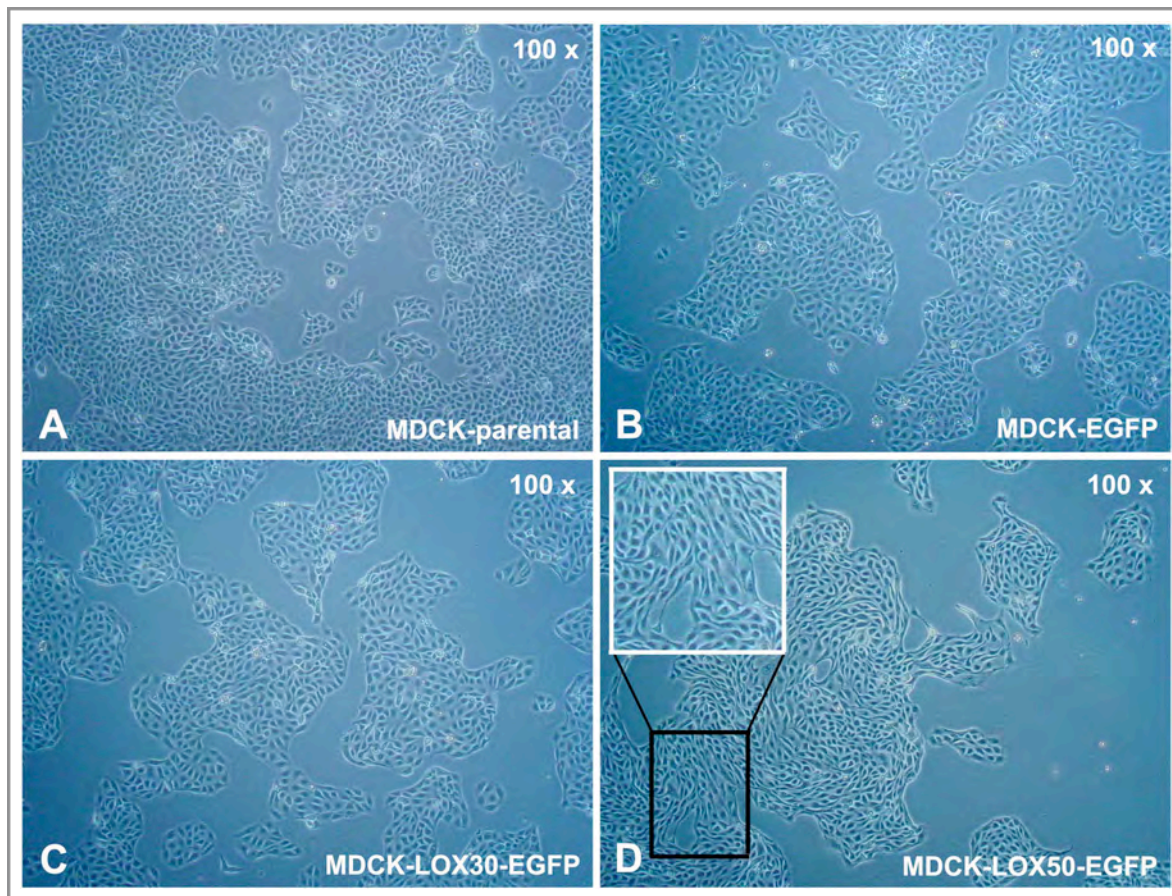


Figure 28. Morphology of stable MDCK II LOX-EGFP cell lines.

MDCK II cells were transfected with (B) EGFP-vector, (C) LOX30-EGFP construct, and (D) LOX50-EGFP construct. After selection of stable clones with G418 for two weeks, clonal populations were propagated. Images were taken with a Zeiss Axiovert 25 microscope.

Results

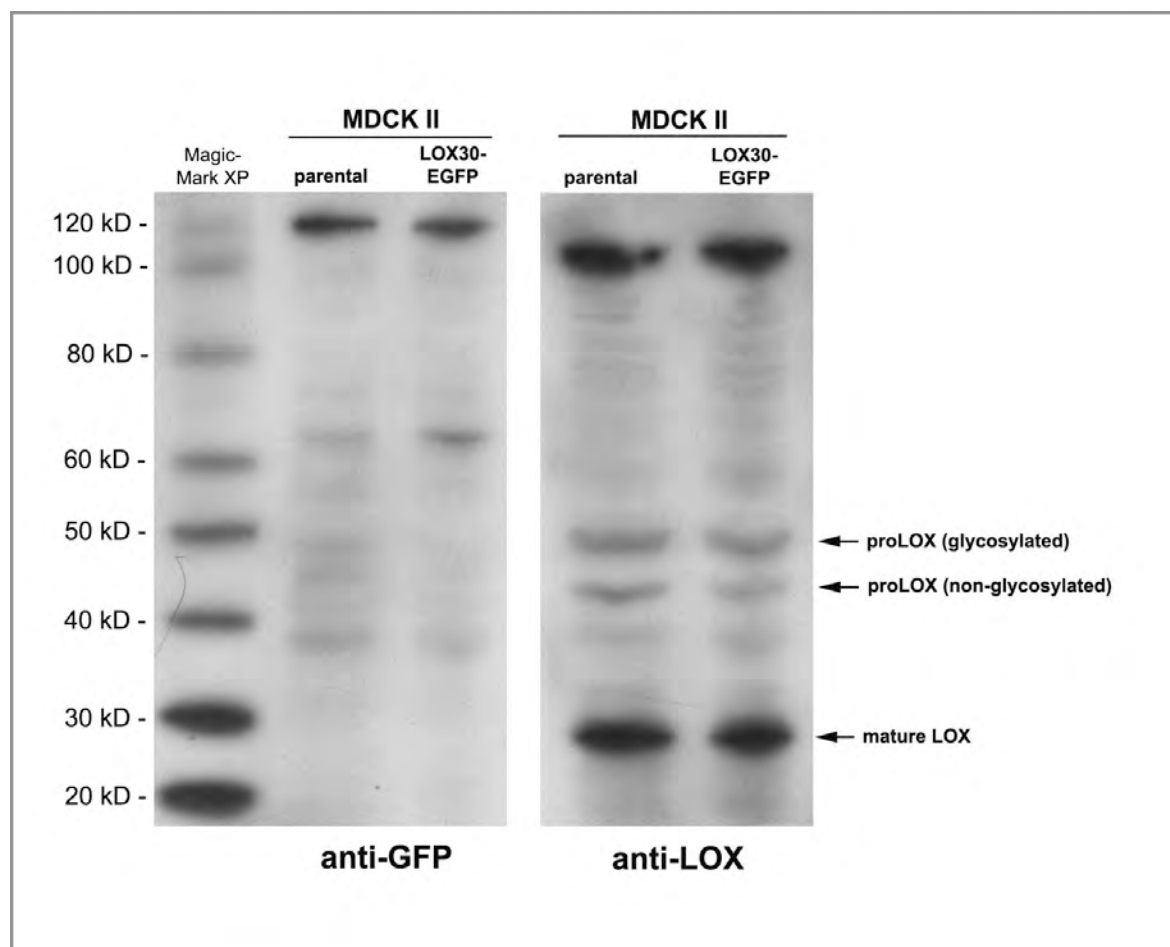


Figure 29. Examination of LOX30-EGFP expression in stable MDCK cell lines.

Protein extracts of MDCK-LOX30-EGFP cells were prepared from cell lysates. 20 µg of total protein were loaded for each sample. Western blots were probed with anti-LOX and anti-GFP antibody to detect LOX30-EGFP expression.

Results

Western blots with anti-LOX antibody on protein extracts from LOX50-EGFP cells detected a signal at ~ 80 kD in cell lysates and at ~ 85 kD in conditioned cell medium (Figure 30 A, far right). The same two bands were also detected by the anti-GFP antibody (Figure 30 B, far right). The predicted molecular weight of the full-length LOX-EGFP fusion protein is approximately 80 kD suggesting that the 80 kD signal in cell lysates and the 85 kD signal in conditioned cell medium represent non-glycosylated and glycosylated forms of the fusion protein, respectively. Interestingly, in conditioned cell medium of LOX50-EGFP cells the anti-LOX antibody also detected a weak signal close to 60 kD which may correspond to the processed mature LOX-EGFP protein (Figure 30 A). In addition, endogenous 30 kD mature LOX and the previously discussed unspecified 100 kD band were seen in cell lysates of LOX50-EGFP, parental and EGFP-expressing cells (Figure 30 A). As expected, the anti-GFP antibody also detected a strong signal of EGFP close to 30 kD in the cell lysate of EGFP-expressing cells and two previously described background signals at 65 kD and at 120 kD in all three cell lines (Figure 30 B). To further analyze the morphological change in LOX50-EGFP cells, immunofluorescence stainings with anti-LOX and anti-GFP antibodies were performed (Figure 31). Both antibodies showed strong cytoplasmic LOX staining and a good overlap with EGFP fluorescence resulting in a yellow staining pattern (Figure 31 A and B). As this clone of LOX50-EGFP expressing cells displayed, in comparison to the parental MDCK II cell line, a very distinct and elongated almost spindle-like morphology similar to mesenchymal cells (Figure 3), we examined if any changes occurred in the expression and localization pattern of the epithelial marker protein E-cadherin (Figure 31 C). However, even in cells with a very elongated cell shape, E-cadherin staining was observed as a pronounced line between adjacent cells indicating the presence of intact cell-cell junctions typical for epithelial cells (indicated by arrows). Using western blot analysis significant amounts of proLOX-EGFP but only tiny levels of the processed mature LOX-EGFP were detected in conditioned cell medium of LOX50-EGFP cells (Figure 30 A). As the conversion of the LOX pro-enzyme into the mature catalytically active form is important for its function and relevant for the evaluation of the observed phenotype of these cells, LOX activity measurements were conducted. Lysyl oxidase enzyme activity in conditioned medium of MDCK-LOX50-EGFP cells was not increased compared to the parental cell line or to EGFP-expressing MDCK II cells (Figure 32). These results suggest that the expressed LOX-EGFP fusion protein does not possess detectable LOX activity. It could not be determined if the lack of enzyme activity was a result of low processing rates of proLOX-EGFP into mature LOX-EGFP or if the mature fusion protein simply does not possess catalytic activity in these cells.

Results

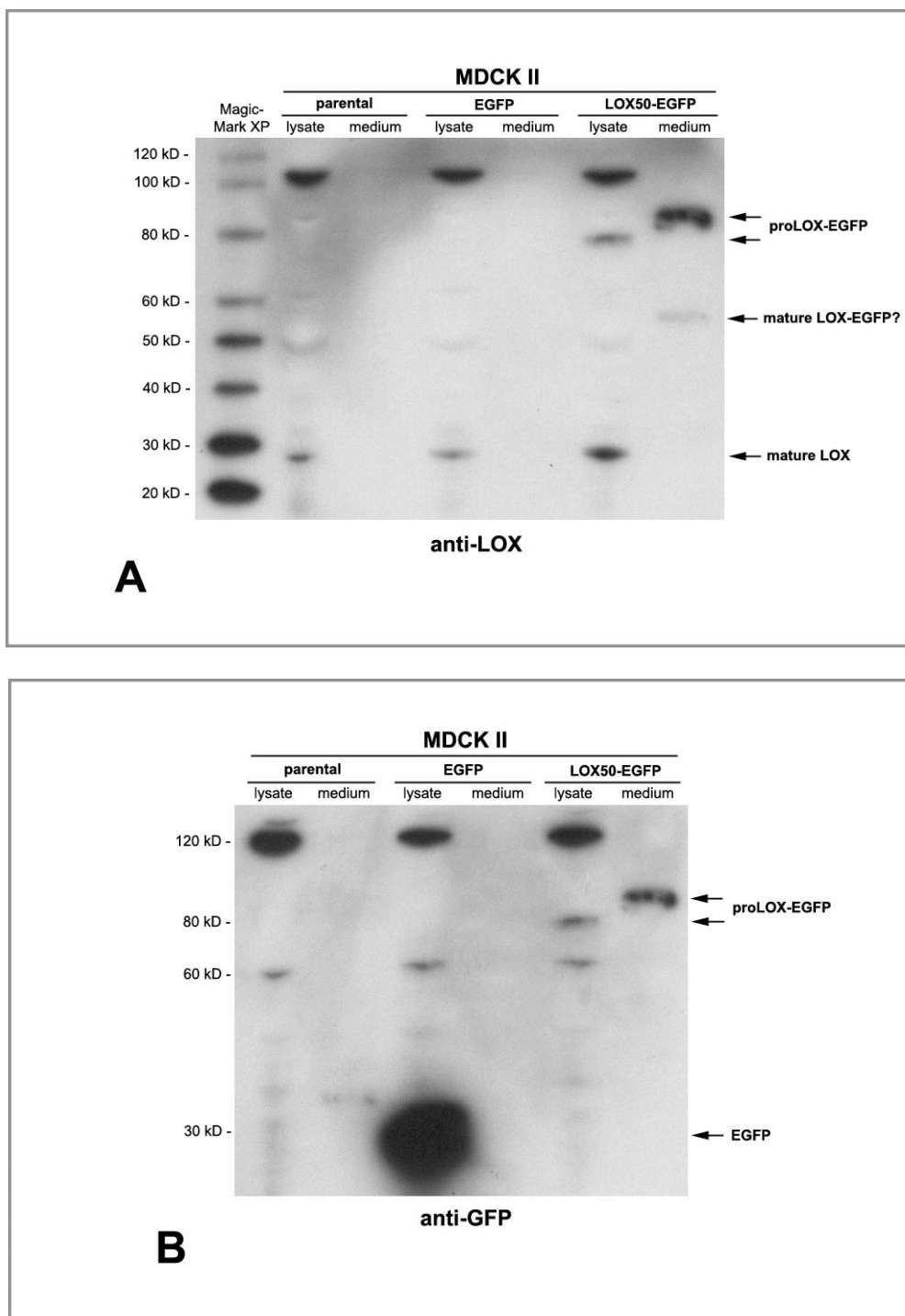


Figure 30. Examination of LOX50-EGFP expression in stable MDCK cell lines by western blot analysis.

Protein extracts of MDCK-LOX50-EGFP cells were prepared from cell lysates and conditioned cell medium. 20 µg of total protein were loaded for each sample. Western blots were probed with (A) anti-LOX and (B) anti-GFP antibody to analyze LOX50-EGFP expression.

Results

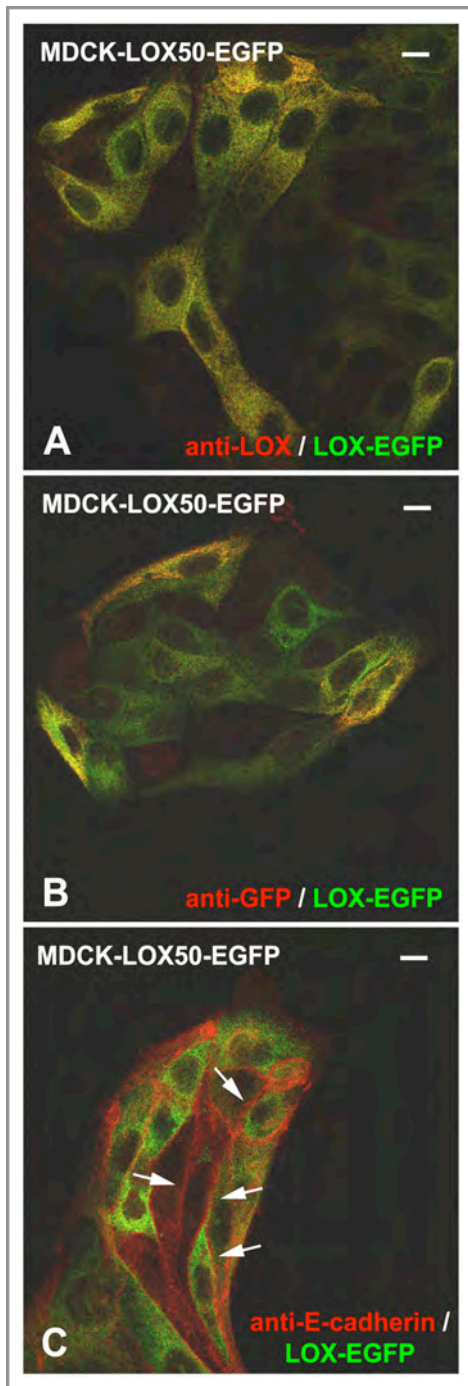


Figure 31. Examination of LOX50-EGFP expression in stable transfected MDCK II cell lines by immunofluorescence analysis.

MDCK-LOX50-EGFP cells were seeded overnight on cover slips and fixed in 2 % para-formaldehyde the following day. Cells were stained with (A) anti-LOX antibody, (B) anti-GFP antibody and (C) anti-E-cadherin antibody. In addition, LOX-EGFP expression was monitored by EGFP fluorescence. Images were recorded with a Zeiss LSM 5 confocal microscope. Scale bars correspond to 10 μ m.

Results

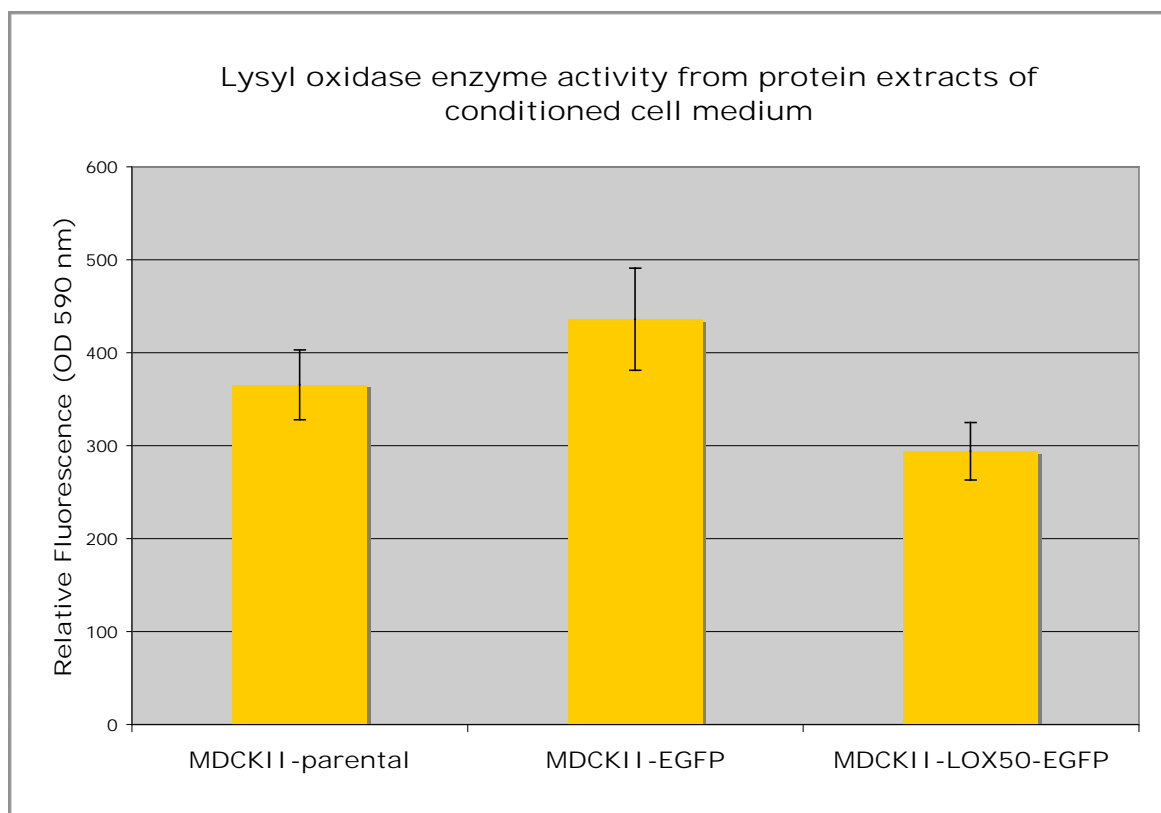


Figure 32. BAPN-inhibitable lysyl oxidase enzyme activity in conditioned cell medium of LOX-EGFP expressing MDCK II cells.

100 µg of total protein from conditioned cell medium of different cell lines were assayed for BAPN-inhibitable lysyl oxidase enzyme activity using 1, 5-diaminopentane as a synthetic substrate.

3.2 Stable cell lines that over-express pcDNA-LOX(-V5) constructs

The LOX-EGFP cell lines could not be successfully established as an experimental system generating sufficient LOX-EGFP fusion protein that is properly processed and catalytically active. One reason for these difficulties might be the fact that EGFP is almost as big as the mature LOX protein and could possibly cause steric hindrance that may interfere with the maturation of the LOX pro-enzyme and/or the catalytic function of mature LOX. The experimental strategy was redesigned and it was decided to generate expression constructs where LOX is tagged with a V5-epitope. The V5-tag was originally discovered as a C-terminal epitope on P- and V-proteins of simian virus 5 and contains only 14 amino acids resulting in a short peptide of ~ 1.4 kD {Southern et al., 1991}. The V5-epitope is commonly used as a tag on recombinant proteins and in most cases does not interfere with the conformation and function of the expressed protein of interest. Due to the difficulties to generate a functional LOX-EGFP fusion protein it seemed a reasonable approach to attempt expression of recombinant LOX with a small tag only. Full-length and mature human LOX were ligated each, with and without a V5-tag, into the pcDNA3.1(-) expression vector from Invitrogen (Figure 33).

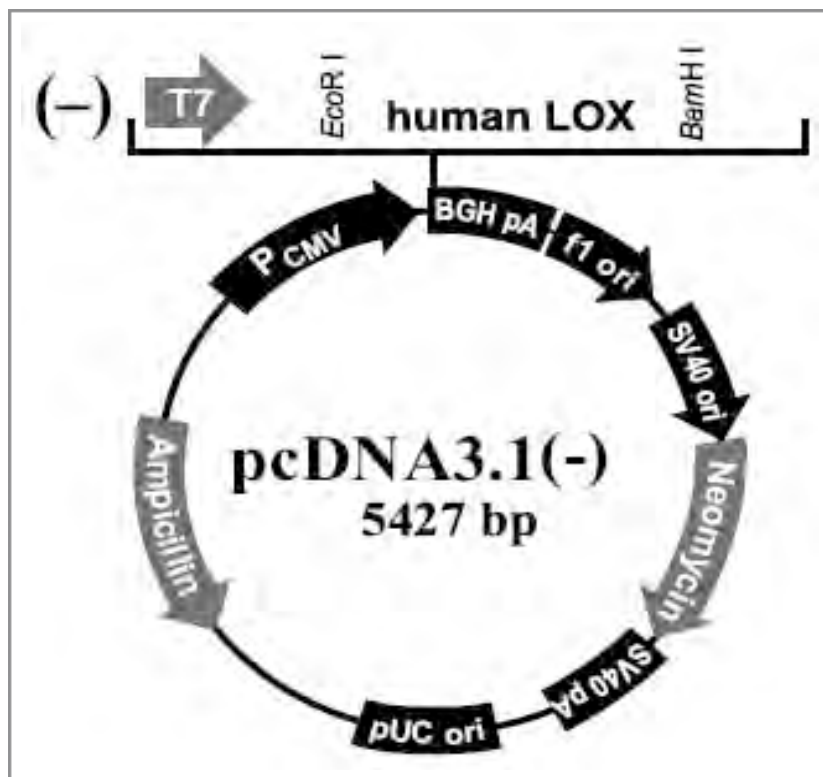
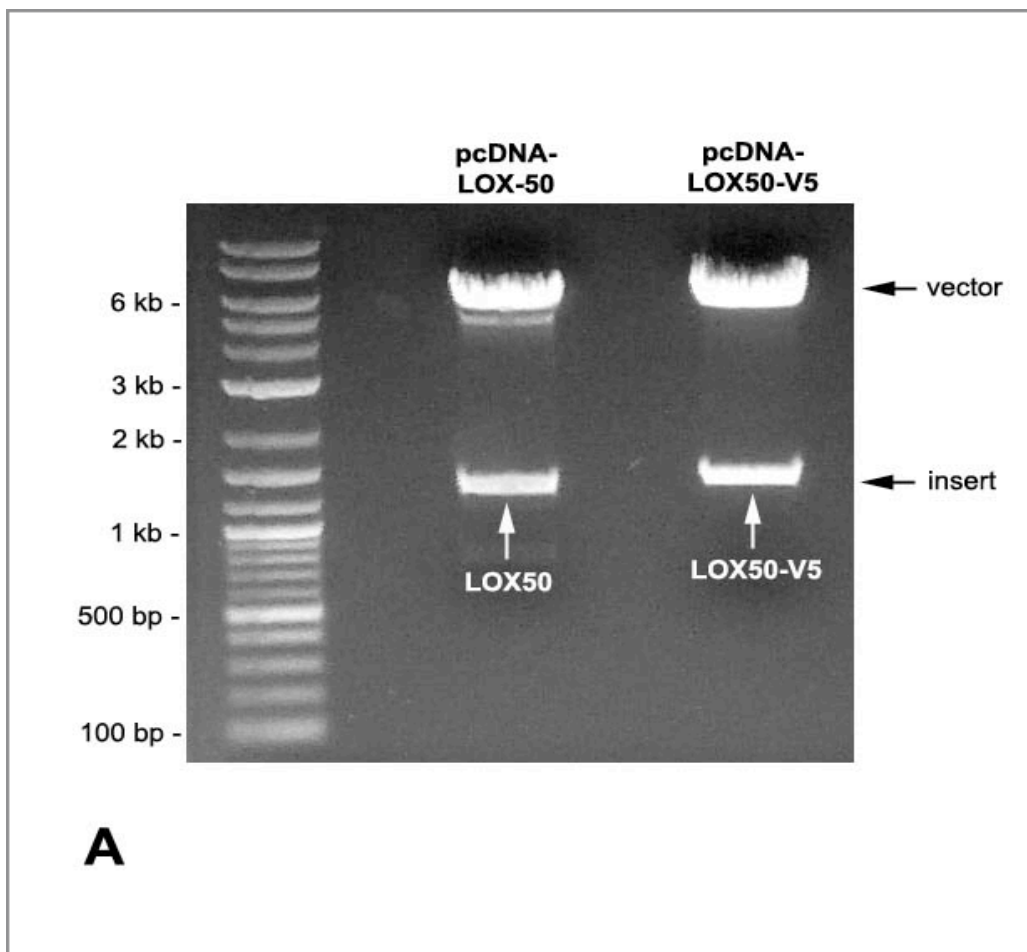


Figure 33. Schematic depiction of the cloning strategy for pcDNA-LOX(-V5) expression constructs.

The human LOX gene, flanked by EcoRI and BamHI restriction sites, was ligated into the multiple cloning site of the pcDNA3.1(-) vector from Invitrogen. LOX was expressed with and without a C-terminal V5 tag.

Results

Restriction digest verified the corresponding inserts at the correct size (Figure 34). Full-length LOX yielded a fragment of ~ 1.25 kb and with the V5-tag about 1.3 kb (Figure 34 A). Mature LOX resulted in a fragment of ~ 750 bp and with V5-tag about 800 bp (Figure 34 B). In addition, a construct was generated encoding a catalytically inactive mature LOX variant resulting from a point mutation where the tyrosine forming the LTQ-cofactor at position 355 was converted into phenylalanine (Figure 34 C) {Chang et al., 1996}. This particular construct was generated with the intention to test the possibility of reversing a potential phenotype that may be caused by stable over-expression of the mature LOX construct in MDCK II cells. All pcDNA-LOX constructs were additionally verified by DNA sequencing (data not shown).



Results

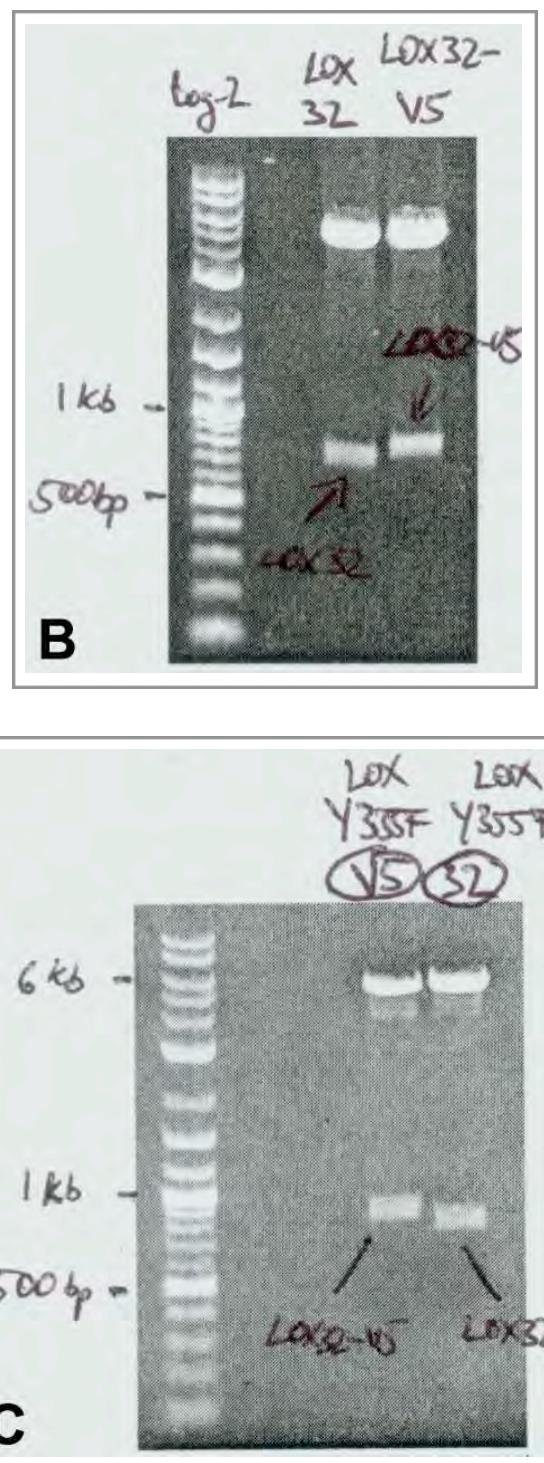


Figure 34. Restriction digest of pcDNA-LOX constructs.

pcDNA-constructs carrying (A) LOX50(-V5), (B) LOX30(-V5) and (C) LOXY355F(-V5) where tyrosine (Y) at position 355 was mutated into phenylalanine yielding in an inactive enzyme, were digested with EcoRI and BamHI restriction enzymes for 30 min. at 37°C. An aliquot of each restriction digest was loaded on a 1% agarose gel to visualize the fragments.

Results

The mature and full-length LOX constructs were transfected into the parental MDCK II cell line and stable-expressing clones were selected for two weeks by G418 treatment. Morphological examination with a brightfield microscope did not reveal a striking phenotype change in any of the stable cell lines (Figure 35). However, cells of the LOX30 and LOX30-V5 clones displayed a slightly flattened cell shape (indicated by arrows) and therefore showed subtle differences compared to the parental and the vector-only expressing cell line (Figure 35 C, D, A and B, respectively).

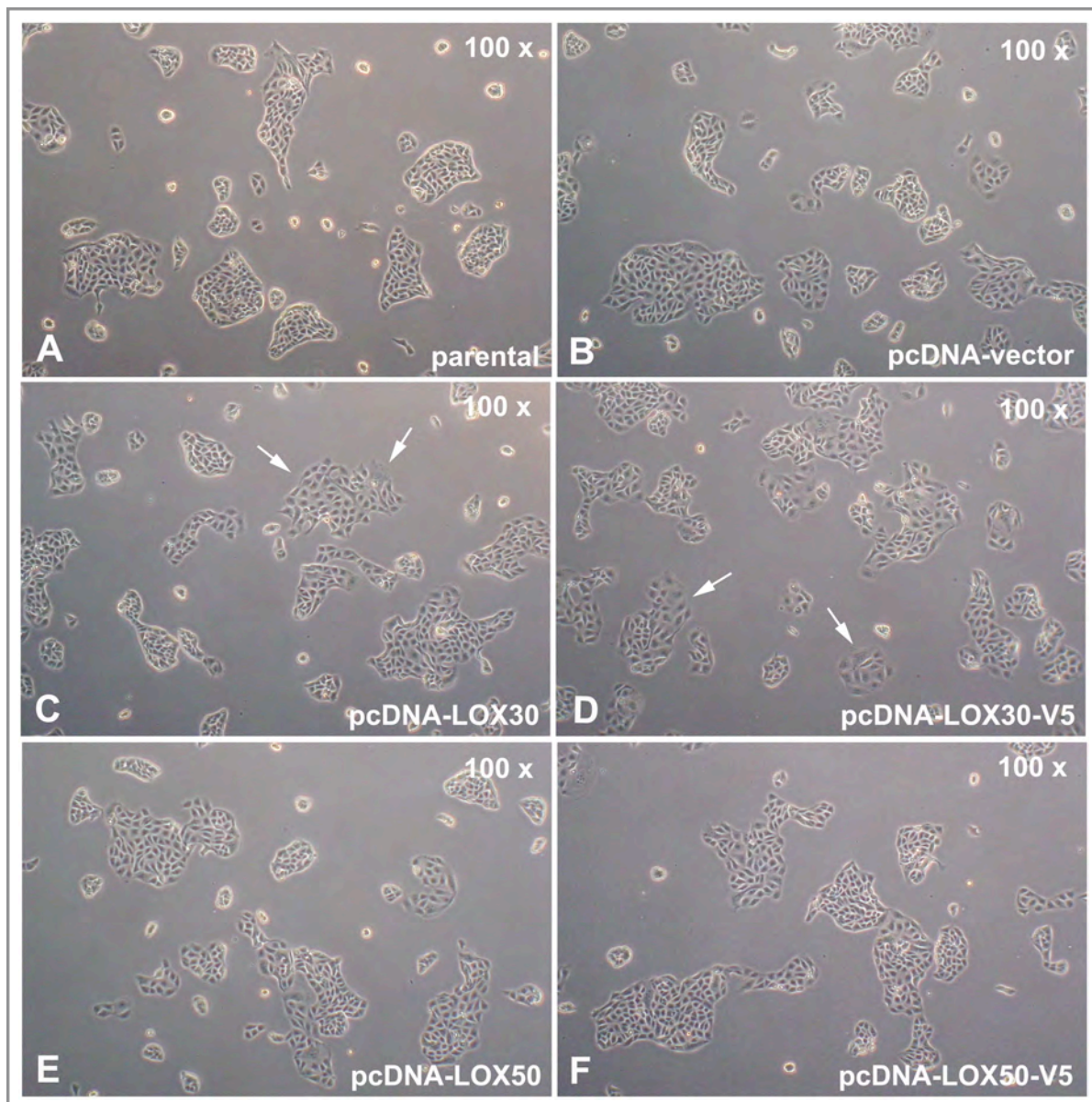
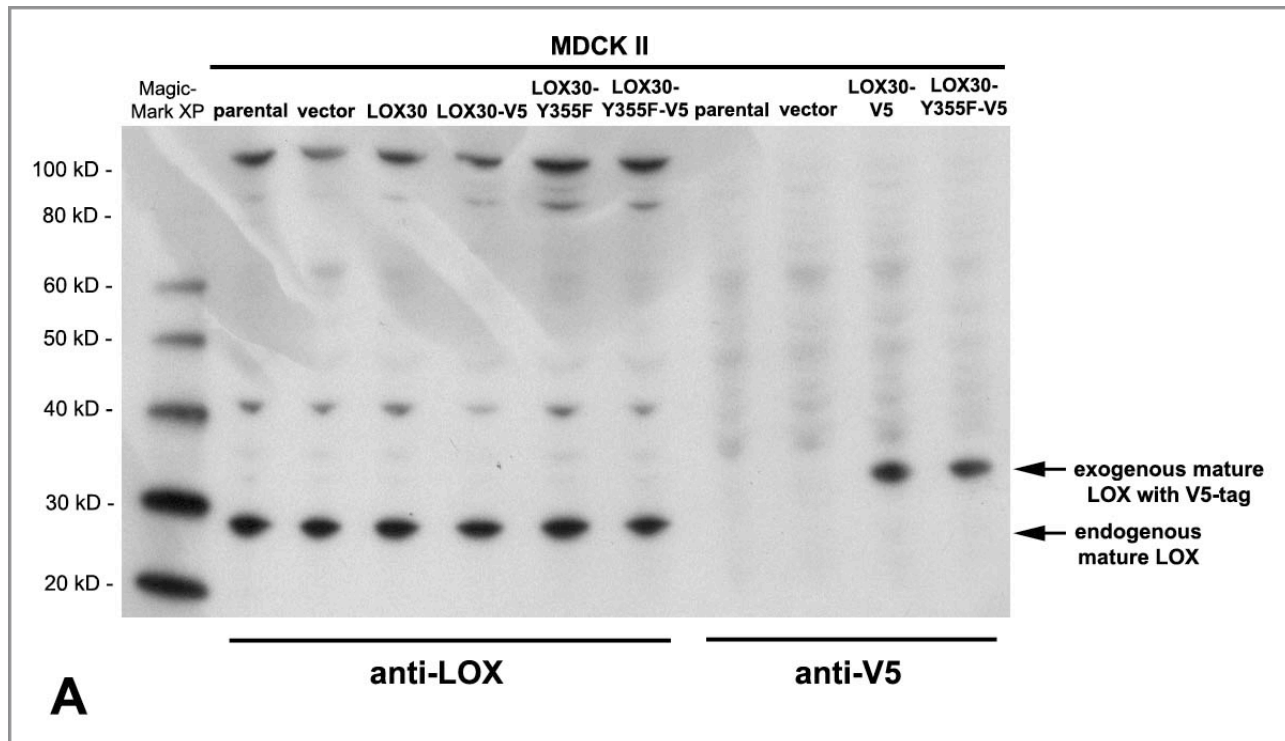


Figure 35. Morphology of stable MDCK II pcDNA-LOX cell lines.

MDCK II cells were transfected with (B) pcDNA-vector, (C) pcDNA-LOX30 construct, (D) pcDNA-LOX30-V5 construct, (E) pcDNA-LOX50 construct and (F) pcDNA-LOX50-V5 construct. After selection of stable clones with G418 for two weeks, clonal populations were propagated. Images were taken with a Zeiss Axiovert 25 brightfield microscope.

Results

Notably, cells of LOX50 and LOX50-V5 clones did not seem to exhibit visible phenotype differences compared to the parental and vector-expressing control cell lines (Figure 35 E and F). Following phenotypic evaluation, all stable cell lines were assessed by western blot analysis for expression of the transfected LOX constructs. Western blots with cell lysates of MDCK II cells transfected with the mature LOX constructs did only reveal expression of endogenous mature LOX when probed with the anti-LOX antibody (Figure 36 A, left panel). However, when using the anti-V5 antibody, cell lines carrying the constructs with V5-tagged mature LOX showed a clear signal above 30 kD indicating the expression of exogenous mature LOX (Figure 36 A, right panel). This observation may suggest that the anti-LOX antibody did not recognize exogenous mature LOX which was expressed from the transfected constructs. Furthermore, these results imply that mature LOX from constructs without the V5-tag may be expressed and present in these cell lines but cannot be detected by the anti-LOX antibody. This hypothesis is indirectly supported by RT-PCR data where human LOX primers amplified the expected fragment in all cell lines transfected with the mature LOX constructs but not in the parental and vector-only expressing cells which express only the endogenous dog LOX (data not shown). In addition, western blots were stripped and re-probed with anti-GAPDH antibody as an internal standard confirming equal amounts of protein were loaded for each sample (Figure 36 B).



Results

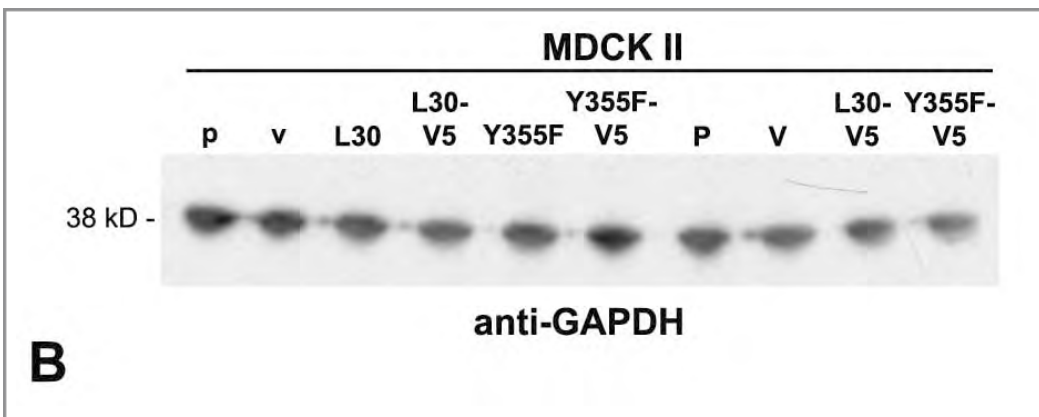


Figure 36. Examination of pcDNA-LOX30 expression in stable transfected MDCK cell lines by western blot analysis.

Protein extracts of MDCK-LOX30 cells were prepared from cell lysates. 20 µg of total protein were loaded for each sample. Western blots were probed with (A) anti-LOX (left panel) and anti-V5 (right panel) antibody to assess expression of the pcDNA-LOX30 construct. Blots were re-probed with (B) anti-GAPDH antibody as an internal standard for equal loading of the samples.

Western blots also verified expression of exogenous LOX in MDCK II cells that were transfected with full-length LOX constructs (Figure 37). As expected, the anti-LOX antibody detected endogenous mature 30 kD LOX in both, cell lysates and conditioned cell medium, of parental MDCK II cells and all transfected, cell lines (Figure 37 A). Furthermore, in conditioned cell medium of cell lines carrying the constructs with full-length LOX, signals above 30 kD were seen in polyclonal populations #1 and #2 of LOX50 and in polyclonal populations #3 and #4 of LOX50-V5 transfected cells, suggesting the detection of exogenous mature LOX. In addition, strong signals between 50 kD and 60 kD in conditioned cell medium indicated the presence of exogenous proLOX. Interestingly, the molecular weight of these bands was significantly higher compared to the expected size of ~ 50 kD for human proLOX. Alternatively, these signals could also represent dimers of exogenous mature LOX instead. The expected molecular weight for a dimer consisting of two 30 kD mature LOX monomers would match almost exactly the observed signals. Considering the highly insoluble properties of LOX and its known tendency to form aggregates {Herbert Kagan, personal communication} the formation of such dimers could be favored under the increasing concentration of mature LOX in these over expressing cell lines. However, the observed 60 kD bands seen in conditioned cell medium may also represent glycosylated forms of the secreted exogenous proLOX. In this case it remains still puzzling why these bands are not seen in cell lysates.

Results

The expression of V5-tagged LOX was confirmed when western blots with protein extracts of MDCK II cells transfected with LOX50-V5 constructs were probed with the anti-V5 antibody (Figure 37 B). A strong double band just above 50 kD was detected in cell lysates reflecting the slightly elevated size of V5-tagged proLOX. In addition, a very strong signal around 60 kD in media fractions indicated the presence of glycosylated and secreted V5-tagged LOX. A band above 30 kD in conditioned cell medium suggested that V5-tagged proLOX was also correctly processed by BMP-1 into the mature form within the extracellular space.

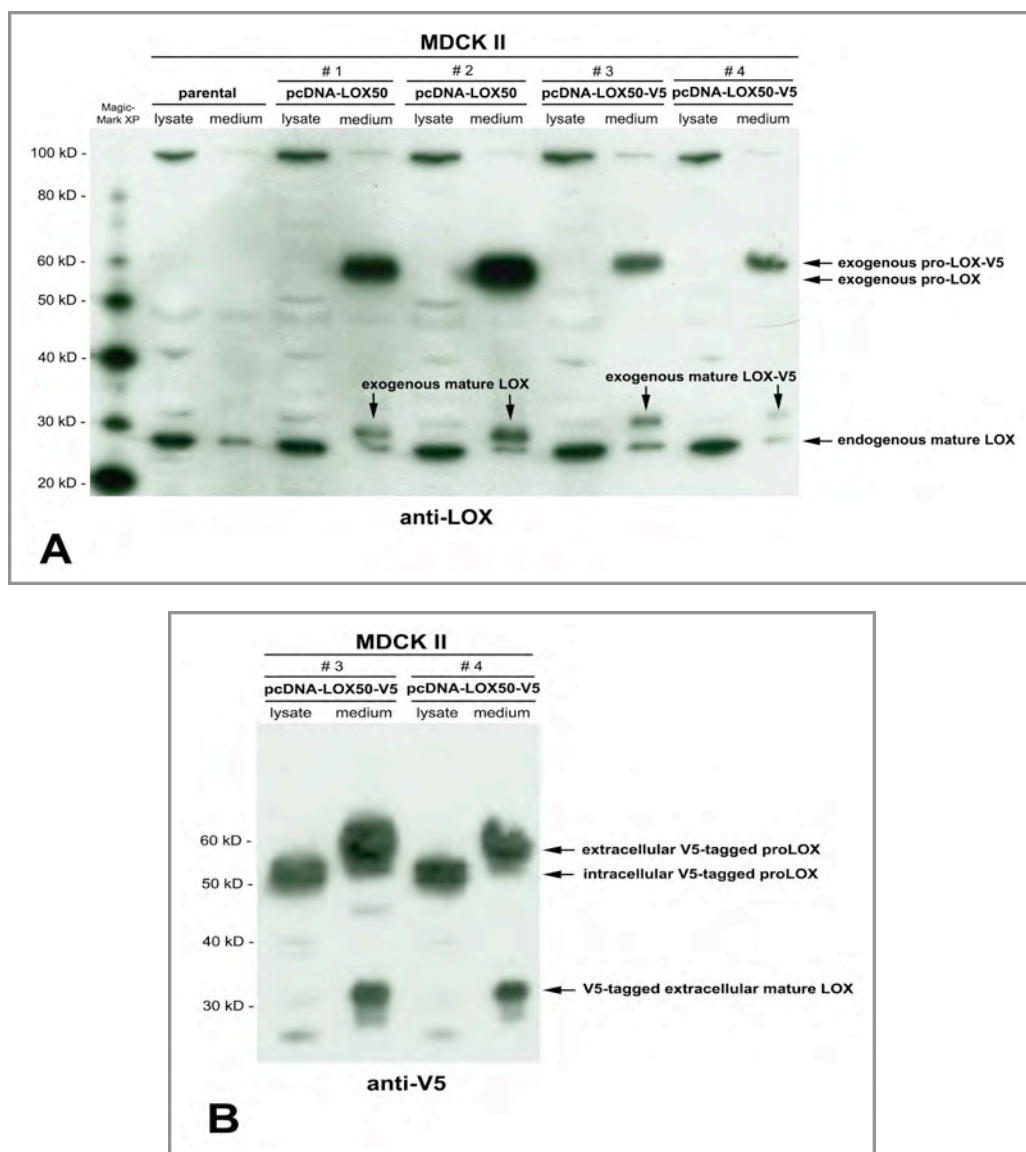


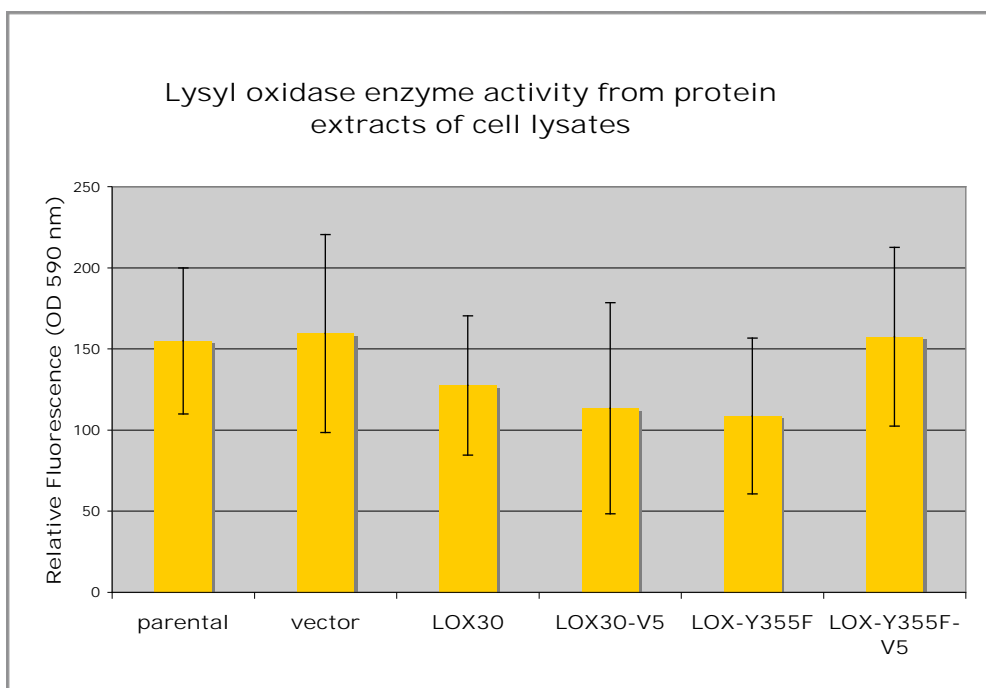
Figure 37. Examination of pcDNA-LOX50 expression in stable transfected MDCK cell lines by western blot analysis.

Protein extracts of MDCK-LOX50 cells were prepared from cell lysates and conditioned cell medium. 20 µg of total protein were loaded for each sample. Western blots were probed with (A) anti-LOX and (B) anti-V5 antibody for verification of LOX50-EGFP expression.

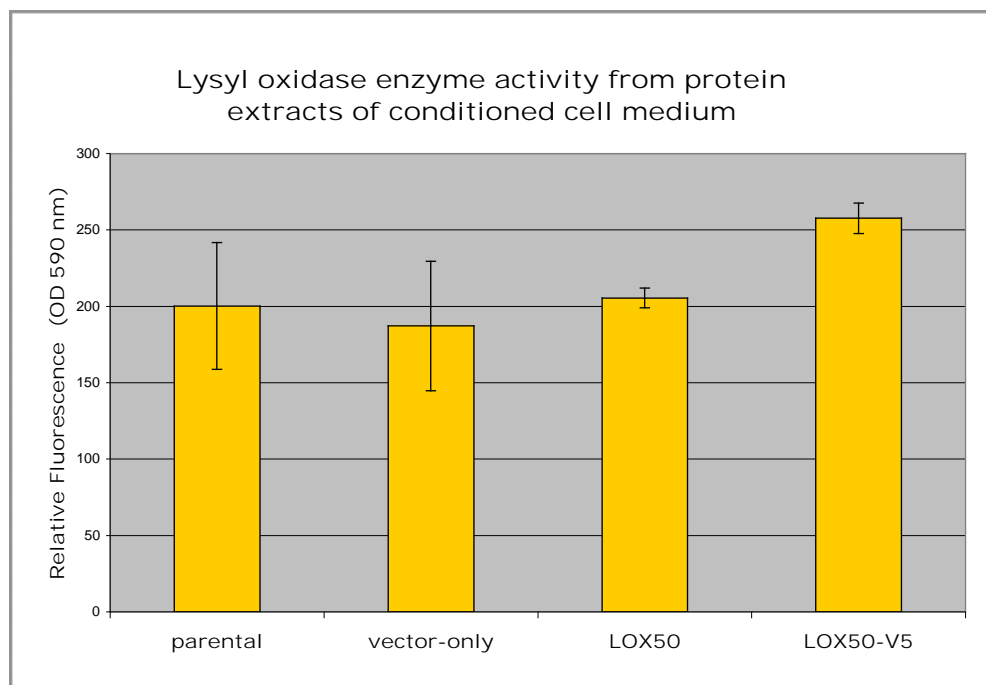
Results

After successful over-expression of intra- and extracellular mature LOX, it was intriguing to test whether the exogenous expressed LOX does possess catalytic activity. In the case of MDCK II cell lines expressing the transfected mature LOX inside the cell, activity measurements were performed with cell lysates to determine if active LOX was accumulating in the cytoplasm (Figure 38 A). The detected activity levels were relatively low and displayed a high degree of variability within each sample as indicated by the big error bars. Furthermore, the activity levels in parental MDCK II cells and the vector-only expressing cell line were higher compared to the cell lines expressing the mature LOX constructs. Also, cell lines transfected with catalytically inactive mature LOX (LOX-Y355F) did not exhibit lower activity levels compared to cells carrying the active form (LOX30). The detection of enzyme activity from mature LOX in the cytoplasm has been already difficult for endogenous mature LOX in the parental MDCK II cell line (Results 1.1). As discussed previously the lack of activity does not necessarily mean that mature LOX is not active in the cytoplasm. It is possible that other sources of hydrogen peroxide in the cytoplasm mask the amount that is generated by LOX activity. However, it was expected to overcome this signal-to-noise ratio problem in cell lines that over-express mature LOX in the cytoplasm. It is also possible that intracellular mature LOX is kept in an inactive state by an unknown mechanism, possibly through interaction(s) with other proteins. In contrast, activity assays with conditioned cell medium of cell lines over-expressing extracellular mature LOX showed a minor increase in LOX-activity compared to the parental cell line (Figure 38 B). This suggests that at least part of the exogenous expressed mature LOX in conditioned cell medium may exhibit catalytic activity. Still, based on the amount of exogenous LOX observed by western blot analysis it was surprising not to detect more enzyme activity compared to the parental cell line.

Results



A



B

Figure 38. BAPN-inhibitable lysyl oxidase enzyme activity in conditioned cell medium of pcDNA-LOX expressing MDCK II cells.

100 µg of total protein from (A) cell lysates and (B) conditioned cell medium of pcDNA-LOX transfected cell lines were assayed for BAPN-inhibitable lysyl oxidase enzyme activity using 1, 5-diaminopentane as a synthetic substrate.

Results

Summary

In this part of the dissertation two approaches were undertaken to over-express catalytically active LOX in MDCK II cells. The first strategy comprised expression of mature and full-length LOX as a fusion protein with EGFP at the C-terminus (Table 8).

Expression construct	Location	LOX activity compared to parental MDCK cells	Morphology compared to parental MDCK cells
pEGFP-LOX30	not detected	not measured	same
pEGFP-LOX50	extracellular	similar	elongated, fibroblast-like
pcDNA-LOX30	intracellular	similar	slightly flattened
pcDNA-LOX30-V5	intracellular	similar	slightly flattened
pcDNA-LOX50	extracellular	similar	epithelial
pcDNA-LOX50-V5	extracellular	similar	epithelial

Table 8. Qualitative characteristics of stable MDCK-LOX cell lines.

Listed are the names of the respective expression constructs, location of the expressed protein, detected lysyl oxidase enzyme activity (in comparison to the parental cell line) and the morphological phenotype.

The expression of intracellular 30 kD mature LOX-EGFP was not successful, as it did not yield a detectable protein for yet unknown reasons. Expression of 50 kD full-length LOX-EGFP resulted in an 80-85 kD proLOX-EGFP fusion protein that was detected by western blot and immunofluorescence analysis. In western blots a weak signal at 60 kD was also observed in conditioned cell medium that might correspond to the processed mature LOX-EGFP form. However, activity assays did not reveal an increase in LOX activity compared to parental cells implying that the observed phenotype in LOX50-EGFP cells may not be related to over-expression of the LOX-EGFP fusion protein. Although it is also possible that the morphological phenotype change was induced by LOX but independent from its catalytic activity, for example through interaction with (an)other protein(s).

As a second approach mature and full-length LOX constructs containing C-terminal V5-tags were generated and successfully over-expressed in MDCK II cells (Table 3). Cell lines over-expressing 30 kD mature LOX in the cytoplasm did not yield higher LOX activity than controls although a mild morphological phenotype was observed in these cells. Over-expression of 50 kD full-length LOX in MDCK II cells resulted in significant amounts of extracellular mature LOX as examined by western blot analysis. The level of lysyl oxidase enzyme activity in extracellular medium fractions was slightly elevated compared to control cell lines.

Results

However, MDCK-LOX50 cell lines did not show morphological changes in their phenotype indicating that over-expression of extracellular mature LOX may not have an obvious influence on the epithelial phenotype of MDCK II cells.

For both strategies it has been proven difficult to express recombinant mature LOX that does possess detectable enzyme activity. This may be partially related to assay conditions, at least in case of intracellular LOX activity measurements, but may also reflect a general problem to generate active recombinant LOX protein, an observation supported by results from other laboratories as well (personal communication with Drs. Kagan, Kirschmann and Sommer).

IV. Discussion and future perspectives

This project provides the first detailed studies on the role of the extracellular matrix enzyme LOX in epithelial cells. Initially, an *in vitro* model system was established that allowed the investigation of LOX in epithelia using two well-characterized epithelial cell lines. In the second part it was tested whether this *in vitro* model is capable to recapitulate epithelial phenotype changes observed during cancer progression that may be in particular related to the function of LOX. Furthermore, the third part addressed the question whether LOX over-expression has an effect on the epithelial phenotype in normal epithelial cells.

Initially, an *in vitro* model system was established to study the role of LOX in normal epithelial cells. Using the MDCK II and MCF-10A cell lines, it was demonstrated for the first time that epithelial cells have the ability to express catalytically active LOX {published in Jansen & Csiszar, 2007}. Mature LOX protein and enzyme activity were detected in conditioned cell medium of both cell lines suggesting that epithelial tissues may contribute to the crosslinking formation in collagen and elastin fibers within the extracellular matrix. In addition, using western blot and immunofluorescence analysis, we detected unexpectedly even larger amounts of mature LOX in the cytoplasm of these cells. Cytoplasmic localization of the mature 30 kD protein has not been reported before and was a surprising discovery raising the question for a novel intracellular function. It is also of particular interest whether mature LOX present in the cytoplasm of these cells does possess catalytic activity. Despite tremendous efforts we were not able to recover significant LOX activity from cytoplasmic fractions with the current standard assay system. These findings could indicate that mature LOX is not catalytically active in the cytoplasm, for example as a result from interactions with other proteins that may keep it in an inactive conformation. A yeast-two-hybrid screen performed in our laboratory identified several cytoplasmic proteins that could potentially interact with LOX (Fogelgren & Csiszar, unpublished data). However, these potential interactions have to be confirmed and the possible impact on the function of LOX is subject of ongoing investigations in a collaborating group {D. Kirschmann, personal communication}. The yeast-two-hybrid screen also identified several extracellular proteins as potential LOX-interacting partners. Among those was fibronectin that in subsequent biochemical studies has been confirmed to physically interact with LOX {Fogelgren et al., 2005}.

Discussion

Interestingly, this interaction did not have an inhibitory effect on LOX catalytic activity but rather seems to act as a scaffold promoting processing of LOX within the extracellular matrix {Fogelgren et al., 2005}.

However, the lack of LOX activity in cytoplasmic fractions could also be a result of the method that is applied in the current standard assay for activity measurements {Palamakumbura & Trackman, 2002}. The principle of this assay is based on the detection of LOX-generated hydrogen peroxide, a side-product of the catalytic reaction. The assay has been used successfully for years to measure LOX activity within the extracellular space, e.g. conditioned cell medium. However, the biochemical environment in the cytoplasm is very different and other intracellular sources generating hydrogen peroxide could mask the produced hydrogen peroxide amounts generated by LOX. For example, hydrogen peroxide is a side-product of the respiration chain in mitochondria where superoxide radicals are converted into hydrogen peroxide spontaneously or through enzymatic catalysis of superoxide dismutase (SOD) {Rhee et al., 2005}. A second intracellular source is NADPH oxidase, which is mainly activated through tyrosine receptor kinase signaling, also resulting in hydrogen peroxide generation by spontaneous or SOD-mediated conversion of reactive oxygen species {Chiarugi & Cirri, 2003}. On the other hand, the amount of hydrogen peroxide resulting from physiological sources is probably reduced in the lysed cytoplasmic fractions that are used for LOX activity assays. The reaction mixture for activity measurements contains urea at a final concentration of 1.2 M, which most likely leads to disruption of most physiological signaling cascades due to inactivation of proteins through denaturation. But hydrogen peroxide could be also generated as a consequence of oxidative degradation processes that occur in cytoplasmic fractions while LOX activity measurements are performed. Altogether, these potential sources of hydrogen peroxide can impede the specific detection of LOX-generated hydrogen peroxide during intracellular activity measurements.

Another interesting aspect of the detection of mature LOX in the cytoplasm of MDCK II and MCF-10A cells is the question whether proLOX, at least in epithelial cells, can be processed inside the cell. In the literature the conversion of the pro-enzyme into the mature form by cleavage of the pro-peptide is only described for the extracellular space {Cronshaw et al., 1995; Panchenko et al, 1996; Uzel et al., 2001}. Our study provided indirect evidence for intracellular processing of LOX as the mature form of BMP-1, the major known processing enzyme of proLOX, was not only detected in conditioned cell medium of MDCK II and MCF-10A cells but also in cytoplasmic fractions.

Discussion

Alternatively, processed mature LOX could enter the cytoplasm from the extracellular space through a yet unknown mechanism. Kagan and colleagues have demonstrated the “proof of principle” for this hypothesis when they investigated the role of mature LOX inside the nucleus of vascular smooth muscle cells in the late 1990s. In those studies, purified and fluorescently labeled mature LOX protein was added to the cell culture medium and then subsequently detected inside the nucleus of these cells, suggesting it must have passed the plasma membrane and the nuclear envelope in order to enter the nucleus {Li et al., 1997; Nellaiappan et al., 2000}. Furthermore, it was shown that LOX retained catalytic activity within the nucleus. The molecular events of how LOX has entered the cells have never been elucidated but competitive inhibition of fluorescently labeled LOX by the addition of unlabeled LOX implies that its cellular uptake is mediated by an active transport mechanism.

Another novel finding was the observation of an approximately 35 kD signal, in addition to the 30 kD band of mature LOX, in western blots with cytoplasmic fractions of MCF-10A cells. Due to the size difference of only ~ 5 kD it could possibly represent a post-translational modified, e.g. phosphorylated, form of the mature protein. Previous analysis of the amino acid sequence of LOX revealed several potential phosphorylation sites close to the BMP-1 cleavage site at the N-terminus of the mature protein {K. Fong, personal communication}. However, solid experimental evidence for the phosphorylation of LOX is still missing except for initial data from a preliminary study. Using an in vitro phosphorylation assay, where LOX was artificially over-expressed in NIH3T3 fibroblasts, phosphatase treatment diminished a putative phosphorylated band of LOX compared to controls {A. Ikramuddin, personal communication}. But these data have not been confirmed by a precise biochemical analysis of the potential phosphorylation sites involved. For a long time researchers in the field have speculated about post-translational modifications, such as phosphorylation, of mature LOX. Interestingly, this signal was not detected in MDCK II cells but may be due to the presence of high EGF and IGF concentrations in the culture medium of MCF-10A cells. Clearly, the detection of intracellular mature LOX opens up new avenues for future LOX research, raising the possibility to discover novel (intracellular) functions and new substrates of this versatile matrix enzyme. It remains to be seen in the future, if further biochemical and cell biology studies addressing the role of intracellular LOX can shed more light on this area of research.

Discussion

In the second part of this thesis project, it was possible to recapitulate the observed up-regulation of LOX during cancer progression by applying a well-characterized *in vitro* EMT assay. Using western blot analysis, we detected elevated LOX protein levels after the induction of scattering in MDCK II cells. Quantitative real-time PCR analysis revealed a more than two-fold increase of LOX mRNA copy numbers suggesting transcriptional up-regulation as the cause of increased LOX expression. These results show that our epithelial *in vitro* model is under defined conditions capable to reflect key features of tumor progression *in vivo*. This is important as the interest to study the function of LOX in epithelia is also motivated by the goal to obtain further insights into the mechanistic role of LOX during cancer progression. Increased LOX mRNA levels have been also detected by differential gene expression analysis in metastatic breast cancer cell lines and then later also by microarray analysis in hypoxic cancer cell lines with increased metastatic potential {Kirschmann et al., 1999; Denko et al., 2003}. Immunohistochemistry studies with breast cancer tissue arrays confirmed elevated LOX expression on the protein level as well {Payne et al., 2005}. One more recent study provided evidence that in hypoxic tumor tissues transcriptional up-regulation of LOX is mediated by hypoxia-inducible factor 1 (HIF-1) {Erler et al., 2006}. In contrast, conditions during the scatter assay with MDCK II cells were rather normoxic, implying that transcription of the LOX gene during EMT in cancer might be also up-regulated by alternative means. Numerous growth factors have been shown to induce EMT by initiating conserved transcription programs leading to a loss of epithelial and a gain of mesenchymal, and therefore migratory, characteristics in epithelial cells {reviewed in Thiery, 2002}. Notably, TGF-beta is one of the growth factors inducing EMT and has been shown to increase LOX mRNA levels in several fibrogenic cell types, i.e., vascular smooth muscle cells, lung fibroblasts and osteoblastic cells {Boak et al., 1994; Feres-Filho et al., 1995; Gacheru et al., 1997}. Future studies will have to clarify the molecular mechanisms and the players of the EMT transcriptome involved that result in increased transcription activity of LOX.

In this context it is of interest that LOXL2, another member of the lysyl oxidase gene family, has been recently demonstrated to promote Snail-mediated EMT in MDCK II cells {Peinado et al., 2005}. The data suggests that LOXL2 increases protein stability of the Snail transcription factor through modification of two lysine residues that are critical for its proteolytic degradation. These results raise the possibility for potentially novel cytoplasmic substrates of LOX as well.

Discussion

In the third part of this study, it was tested whether over-expression of LOX alters the epithelial phenotype of MDCK II cells. Both, intra- and extracellular over-expression of the mature protein was performed. Two strategies, using different tags, were developed to achieve this goal and each of those will be discussed separately. The tags were used to distinguish endogenous LOX in MDCK II cells from stably transfected exogenous LOX.

First, LOX was over-expressed as an EGFP-fusion protein. Intracellular expression of a mature LOX30-EGFP construct did not yield a detectable protein for unknown reasons. It can be speculated whether the construct was not successfully integrated into the genome or whether the LOX30-EGFP fusion gene was not successfully expressed. For the latter case, it is possible that either the mRNA transcript or the expressed protein did not pass intrinsic quality control mechanisms and became subject to pre-translational mRNA decay or to post-translational degradation {Isken & Masquat, 2007; Herbert & Molinari, 2007}. As mature LOX and EGFP have almost the same molecular weight (30 kD) correct protein folding may have been affected by steric hindrance. The relatively large size of EGFP could also have prevented access of a chaperon that may stabilize the conformation of intracellular mature LOX. Expression of a full-length LOX50-EGFP construct resulted in a secreted ~ 85 kD protein that was detected independently by LOX and GFP antibodies and corresponded to the calculated size of the LOX50-EGFP fusion protein. In addition, a weak signal of approximately 60 kD was detected that might represent the mature fusion protein. The analyzed subclone of this cell line displayed a strong mesenchymal morphology although cells were still growing in clusters and maintaining adhesive cell-cell contacts as indicated by E-cadherin expression. However, we did not detect increased LOX activity from conditioned cell medium of this subclone and the signal of the processed LOX50-EGFP fusion protein was relatively weak. Therefore it is questionable if the observed phenotype is a direct consequence of LOX over-expression. Due to the random genomic integration of the construct, it is also possible that the function of other genes may have been affected resulting in the altered morphology. At the same time it cannot be excluded that LOX induced the morphological phenotype independent of its amine oxidase activity as well.

The second approach comprised over-expression of mature and full-length V5-tagged LOX constructs in MDCK II cells. We decided to use the V5-tag because it is very small, only 1.5 kD, and has therefore in comparison to the 30 kD EGFP protein a smaller potential to affect the native conformation of LOX by steric means. Over-expression of mature LOX seems to have a mild effect on the epithelial phenotype in MDCK II cells as cell lines transfected with the mature LOX

Discussion

construct showed slightly flattened cell shapes. In contrast, the morphology from stable cell lines expressing the full-length construct was not different from parental MDCK II cells. These results suggest that the intracellular mature LOX protein but not the extracellular form may affect the epithelial phenotype. Despite the detection of exogenous intracellular and extracellular mature LOX by western blot analysis we were not able to detect increased LOX activity compared to parental cells. Although intracellular measurement of LOX activity may be difficult due to other potential hydrogen peroxide sources as discussed previously, it was expected to overcome the signal-to-noise ratio by constitutive LOX over-expression under the CMV promoter. Therefore it was even more surprising that cell lines expressing full-length constructs did not yield increased LOX activity although significant amounts of processed exogenous mature LOX were detected by western blot analysis in conditioned cell medium of these cell lines. It is also unlikely that the V5-tag has influenced the catalytic ability of LOX as cell lines over-expressing untagged constructs did not yield increased activity either. The generation of recombinant LOX with catalytic activity has been a challenge for a long time in the field. Until today there is only one publication reporting successful generation of recombinant active LOX from *E. coli* inclusion bodies {Jung et al., 2003}. However, these results have not been reproducible yet in our and other laboratories {B. Fogelgren & P. Trackman, personal communication}. The difficulties to express recombinant active LOX in this and other studies may result in part from its biochemical properties. Researchers have observed from early on that LOX is highly insoluble in aqueous buffer solutions such as PBS {Kagan et al., 1979}. Starting at moderate concentrations LOX has the tendency to form multimers and sometimes becomes even visible as amorphous precipitates in the solution. This is also the main reason why purified LOX is traditionally solubilized in buffers containing high concentrations of urea {Sullivan & Kagan, 1982}. In conclusion, difficulties to express and detect recombinant active LOX in this study do also reflect a general problem to master the unique biochemical properties of this protein.

The lack of a morphological change in cell lines transfected with V5-tagged full-length LOX is another hint that the strong phenotype observed in one subclone of LOX50-EGFP cells was not caused by exogenously expressed LOX. In fact the data obtained in this study imply that over-expression of LOX in normal epithelial cells may have not the same consequence as in their malignant counterparts. Transfection of LOX into non-invasive breast cancer cells increased their invasive potential as determined by migration assays and was reversible in a dose-dependent manner upon treatment with BAPN {Kirschmann et al., 2002; Payne et al., 2005}.

Discussion

Invasive breast cancer cell lines with high endogenous LOX expression levels displayed a greatly reduced invasiveness *in vitro* and a decreased metastatic spread in orthotopic tumors *in vivo* after inhibition of LOX with BAPN or specific siRNAs {Payne et al., 2005; Erler et al., 2006}. These studies provided strong evidence that LOX is capable to induce a migratory and invasive phenotype in cancer cells. However, cancer cells have acquired numerous mutations throughout their lifespan that altogether do account for their altered cell behavior. In contrast, normal epithelial cells could have regulatory mechanisms in place that are able to compensate over-expression of LOX thereby maintaining their normal epithelial characteristics.

This study demonstrated for the first time that epithelial cells produce catalytically active LOX. Furthermore, it presents compelling evidence that mature LOX is not only present in the extracellular space but also expressed in the cytoplasm of this cell type. Studies presented in this dissertation research have reinforced that more knowledge about the biochemical properties of LOX would greatly facilitate research efforts on the cell biology of this protein. To further investigate the function of intracellular LOX, a novel assay to measure intracellular LOX activity may be needed. Ideally, this assay would not rely on the detection of hydrogen peroxide due to its high abundance in the cytoplasm. An important step that remains to be investigated is whether the function of intracellular LOX in epithelial cells is related to its role during cancer metastasis. However, research on the role of intracellular LOX certainly has the potential to pave the way for new areas of exciting research and discoveries of this multifunctional protein.

V. Abstract

The aim of the first part of my PhD project was to investigate the role of the extracellular matrix enzyme lysyl oxidase (LOX) in epithelial cells and its potential implications for cancers of epithelial origin.

Using two well-characterized epithelial cell lines, i.e. MDCK II and MCF-10A, an *in vitro* model system was established to study the function of LOX in epithelia. For the first time the presence of mature LOX protein was demonstrated within cytoplasmic fractions. In addition, the enzyme was found to be secreted from the cells and BAPN-inhibitable LOX enzymatic activity was detected in concentrated fractions of conditioned cell medium. This result suggests that epithelial cells can express catalytically active LOX. Notably, extracellular expression and enzymatic activity of LOX were significantly elevated in post-confluent compared to pre-confluent cell cultures. This finding may indicate that LOX expression is elevated in differentiated epithelia. Although large amounts of mature LOX protein were observed in cytoplasmic fractions by western blotting, it was not possible to recover intracellular BAPN-inhibitable LOX enzymatic activity.

LOX protein expression was shown to increase during scattering of MDCK II cells after hepatocyte growth factor (HGF) treatment. This process recapitulates important cellular characteristics of tumor metastasis *in vivo*. The higher LOX protein level correlated with a two-fold increase of LOX mRNA in HGF-treated compared to control cells as revealed by quantitative PCR. Therefore, the scatter assay may represent a suitable model system to study the recently reported role of LOX during cancer progression *in vitro*.

Two strategies were followed to generate stable MDCK II lines that express recombinant LOX under a CMV promoter in order to determine whether constitutive LOX over-expression can induce changes of the epithelial phenotype. The first strategy comprised transfection of LOX-EGFP constructs. However, this approach did not yield detectable amounts of recombinant protein. Steric hindrance of the relatively large EGFP-tag (30 kD) may be a reason for the failure to express LOX-EGFP fusion proteins. Nevertheless, one clone transfected with full-length LOX-EGFP displayed an elongated morphology that resembled mesenchymal cells. The second approach used LOX-V5 expression constructs. Neither intra- nor extracellular expression of LOX induced significant phenotypical/morphological changes in MDCK II cells.

Abstract

In addition, no increase of LOX enzyme activity was detected in either, cytoplasmic fractions or conditioned cell medium of stably transfected cell lines. The difficulties in expressing recombinant LOX in this study represents a general challenge of the field and may result from its biochemical properties as well as the lack of more specific and sensitive assays to reliably determine its catalytic activity.

Even though preliminary, the results of this study can serve as a promising basis for future investigations with the goal to decipher the precise function of LOX in epithelial cells.

VI. Zusammenfassung

Das Ziel des ersten Teils der vorliegenden Dissertation war es die Rolle des extrazellulären Matrix Enzyms Lysyl Oxidase (LOX) in Epithelzellen zu untersuchen, sowie die daraus resultierenden Implikationen für Krebsarten epithelialen Ursprungs.

Unter Anwendung der beiden gut charakterisierten Zelllinien MDCK II und MCF-10A, wurde ein *in vitro* Modellsystem für Studien zur Funktion von LOX in Epithelien etabliert. Zum ersten Mal wurde die Präsenz des reifen LOX Proteins in zytoplasmatischen Fraktionen nachgewiesen. Außerdem konnte in beiden Zelllinien gezeigt werden, dass das Enzym in den extrazellulären Bereich sekretiert wird und BAPN-inhibierbare Enzymaktivität konnte in Überständen von konditioniertem Zellkulturmedium gemessen werden. Dieses Resultat lässt darauf schließen, dass Epithelzellen katalytisch aktives LOX Protein exprimieren können. Interessanterweise war die extrazelluläre LOX Expression und Enzymaktivität deutlich höher in post-konfluenten als in präkonfluenten Zellkulturen. Dies könnte ein Hinweis darauf sein, dass LOX in differenzierten Epithelien verstärkt exprimiert wird. Obwohl größere Mengen von prozessiertem LOX Protein bei Western-Blot Analysen auch in zytoplasmatischen Fraktionen gefunden wurden, konnte keine intrazelluläre BAPN-inhibierbare LOX Enzymaktivität nachgewiesen werden.

Eine erhöhte LOX Protein Expression in MDCK II Zellen wurde nach Behandlung mit dem Wachstumsfaktor HGF während des sogenannten „Scattering“ (Auflösung des epithelialen Zellverbandes) beobachtet. Dieser Prozess rekapituliert wichtige Merkmale der Metastasenbildung von Tumoren *in vivo*. Zusätzlich wurde durch quantitative PCR Analysen gezeigt, dass die erhöhten LOX Protein Mengen ebenfalls mit einem zweifachen Anstieg der LOX mRNA Transkripte in HGF-behandelten versus unbehandelten Zellen korrelierten. Deshalb könnte der „Scatter-Assay“ als geeignetes *in vitro* Modellsystem für die Untersuchung der Funktion von LOX während der Metastasenbildung von Krebsarten epithelialen Ursprungs dienen.

Des Weiteren wurden zwei Strategien verfolgt, um stabile MDCK II Zelllinien zu generieren, die rekombinantes LOX Protein unter der Kontrolle eines CMV Promoters exprimieren. Ziel war es zu untersuchen, ob eine konstitutive Überexprimierung Änderungen im epithelialen Phänotyp induzieren würde. Die erste Strategie umfaßte die Transfektion von LOX-EGFP Konstrukten. Allerdings resultierte dieser Ansatz nicht in detektierbaren Mengen von rekombinantem Protein.

Zusammenfassung

Sterische Hinderung durch das relativ große EGFP-Tag (30 kD) könnten ein Grund dafür sein, dass eine detektierbare Expression von LOX-EGFP Fusionsproteinen gescheitert ist. Dennoch zeigte ein selekterter Klon, der mit einem LOX-EGFP Konstrukt transfiziert war, eine Morphologie, die mesenchymalen Zellen ähnelt. Beim zweiten strategischen Ansatz wurden LOX-V5 Expressionsvektoren verwendet. Weder die intra- noch die extrazelluläre Überexprimierung von LOX mit diesen Konstrukten resultierte in einer signifikanten phänotypischen oder morphologischen Änderung der MDCK II Zellen. Es konnte auch keine erhöhte LOX Enzymaktivität in zytoplasmatischen Fraktionen oder konditionierten Zellkulturmedium Überständen von stabil transfizierten Zelllinien nachgewiesen werden. Die in dieser Studie beobachteten Schwierigkeiten, rekombinantes LOX Protein zu exprimieren, stellen ein generelles Problem des Forschungsfeldes dar und liegen vermutlich zumindest teilweise an den biochemischen Eigenschaften dieses Proteins, sowie dem Fehlen eines spezifischeren und sensitiveren Assays zum zuverlässigen Nachweis seiner katalytischen Aktivität.

Obwohl die Ergebnisse dieser Studie nur als vorläufig zu betrachten sind, können Sie als vielversprechende Basis für zukünftige Untersuchungen dienen, mit dem Ziel die präzise Funktion von LOX in Epithelzellen zu entschlüsseln.

VII. Literature

Asuncion L, Fogelgren B, Fong KS, Fong SF, Kim Y, Csiszar K. A novel human lysyl oxidase-like gene (LOXL4) on chromosome 10q24 has an altered scavenger receptor cysteine rich domain. *Matrix Biol.* 2001 Nov;20(7):487-91.

Bazan JF. Structural design and molecular evolution of a cytokine receptor superfamily. *Proc Natl Acad Sci U S A.* 1990 Sep;87(18):6934-8.

Bedell-Hogan D, Trackman P, Abrams W, Rosenbloom J, Kagan H. Oxidation, cross-linking, and insolubilization of recombinant tropoelastin by purified lysyl oxidase. *J Biol Chem.* 1993 May 15;268(14):10345-50.

Boak AM, Roy R, Berk J, Taylor L, Polgar P, Goldstein RH, Kagan HM. Regulation of lysyl oxidase expression in lung fibroblasts by transforming growth factor-beta 1 and prostaglandin E2. *Am J Respir Cell Mol Biol.* 1994 Dec;11(6):751-5.

Bradford MM. A rapid and sensitive method for the quantitation of microgram quantities of protein utilizing the principle of protein-dye binding. *Anal Biochem.* 1976 May 7;72:248-54.

Bublil EM, Yarden Y. The EGF receptor family: spearheading a merger of signaling and therapeutics. *Curr Opin Cell Biol.* 2007 Apr;19(2):124-34.

Butler E, Hardin J, Benson S. The role of lysyl oxidase and collagen crosslinking during sea urchin development. *Exp Cell Res.* 1987 Nov;173(1):174-82.

Chalfie M, Tu Y, Euskirchen G, Ward WW, Prasher DC. Green fluorescent protein as a marker for gene expression. *Science.* 1994 Feb 11;263(5148):802-5.

Chiarugi P, Cirri P. Redox regulation of protein tyrosine phosphatases during receptor tyrosine kinase signal transduction. *Trends Biochem Sci.* 2003 Sep;28(9):509-14.

Contente S, Kenyon K, Rimoldi D, Friedman RM. Expression of gene rrg is associated with reversion of NIH 3T3 transformed by LTR-c-H-ras. *Science.* 1990 Aug 17;249(4970):796-8.

Contente S, Kenyon K, Sriraman P, Subramanyan S, Friedman RM. Epigenetic inhibition of lysyl oxidase transcription after transformation by ras oncogene. *Mol Cell Biochem.* 1999 Apr;194(1-2):79-91.

Literature

Cronshaw AD, Fothergill-Gilmore LA, Hulmes DJ. The proteolytic processing site of the precursor of lysyl oxidase. *Biochem J.* 1995 Feb 15;306 (Pt 1):279-84.

Csiszar K, Entersz I, Trackman PC, Samid D, Boyd CD. Functional analysis of the promoter and first intron of the human lysyl oxidase gene. *Mol Biol Rep.* 1996;23(2):97-108.

Csiszar K. Lysyl oxidases: a novel multifunctional amine oxidase family. *Prog Nucleic Acid Res Mol Biol.* 2001;70:1-32.

Csiszar K, Fong SF, Ujfalusi A, Krawetz SA, Salvati EP, Mackenzie JW, Boyd CD. Somatic mutations of the lysyl oxidase gene on chromosome 5q23.1 in colorectal tumors. *Int J Cancer.* 2002 Feb 10;97(5):636-42.

Debnath J, Muthuswamy SK, Brugge JS. Morphogenesis and oncogenesis of MCF-10A mammary epithelial acini grown in three-dimensional basement membrane cultures. *Methods.* 2003 Jul;30(3):256-68.

Denko N, Wernke-Dollries K, Johnson AB, Hammond E, Chiang CM, Barton MC. Hypoxia actively represses transcription by inducing negative cofactor 2 (Dr1/DrAP1) and blocking preinitiation complex assembly. *J Biol Chem.* 2003 Feb 21;278(8):5744-9.

Dodson JW, Hay ED. Secretion of collagenous stroma by isolated epithelium grown in vitro. *Exp Cell Res.* 1971 Mar;65(1):215-20.

Erler JT, Bennewith KL, Nicolau M, Dornhöfer N, Kong C, Le QT, Chi JT, Jeffrey SS, Giaccia AJ. Lysyl oxidase is essential for hypoxia-induced metastasis. *Nature.* 2006 Apr 27;440(7088):1222-6.

Feres-Filho EJ, Choi YJ, Han X, Takala TE, Trackman PC. Pre- and post-translational regulation of lysyl oxidase by transforming growth factor-beta 1 in osteoblastic MC3T3-E1 cells. *J Biol Chem.* 1995 Dec 22;270(51):30797-803.

Fidler IJ. The pathogenesis of cancer metastasis: the 'seed and soil' hypothesis revisited. *Nat Rev Cancer.* 2003 Jun;3(6):453-8.

Fogelgren B, Polgár N, Szauter KM, Ujfaludi Z, Laczkó R, Fong KS, Csiszar K. Cellular fibronectin binds to lysyl oxidase with high affinity and is critical for its proteolytic activation. *J Biol Chem.* 2005 Jul 1;280(26):24690-7.

Gacheru SN, Trackman PC, Shah MA, O'Gara CY, Spacciapoli P, Greenaway FT, Kagan HM. Structural and catalytic properties of copper in lysyl oxidase. *J Biol Chem.* 1990 Nov 5;265(31):19022-7.

Literature

Gacheru SN, Thomas KM, Murray SA, Csiszar K, Smith-Mungo LI, Kagan HM. Transcriptional and post-transcriptional control of lysyl oxidase expression in vascular smooth muscle cells: effects of TGF-beta 1 and serum deprivation. *J Cell Biochem.* 1997 Jun 1;65(3):395-407.

Giampuzzi M, Botti G, Cilli M, Gusmano R, Borel A, Sommer P, Di Donato A. Down-regulation of lysyl oxidase-induced tumorigenic transformation in NRK-49F cells characterized by constitutive activation of ras proto-oncogene. *J Biol Chem.* 2001 Aug 3;276(31):29226-32.

Giampuzzi M, Oleggini R, Di Donato A. Altered adhesion features and signal transduction in NRK-49F cells transformed by down-regulation of lysyl oxidase. *Biochim Biophys Acta.* 2003 Apr 11;1647(1-2):239-44.

Giampuzzi M, Oleggini R, Albanese C, Pestell R, Di Donato A. beta-catenin signaling and regulation of cyclin D1 promoter in NRK-49F cells transformed by down-regulation of the tumor suppressor lysyl oxidase. *Biochim Biophys Acta.* 2005 Sep 30;1745(3):370-81.

Gordon MK, Olsen BR. The contribution of collagenous proteins to tissue-specific matrix assemblies. *Curr Opin Cell Biol.* 1990 Oct;2(5):833-8.

Gumbiner BM. Regulation of cadherin-mediated adhesion in morphogenesis. *Nat Rev Mol Cell Biol.* 2005 Aug;6(8):622-34.

Hämäläinen ER, Kemppainen R, Kuivaniemi H, Tromp G, Vaheri A, Pihlajaniemi T, Kivirikko KI. Quantitative polymerase chain reaction of lysyl oxidase mRNA in malignantly transformed human cell lines demonstrates that their low lysyl oxidase activity is due to low quantities of its mRNA and low levels of transcription of the respective gene. *J Biol Chem.* 1995 Sep 15;270(37):21590-3.

Hay ED. Development of the vertebrate cornea. *Int Rev Cytol.* 1980;63:263-322.

Hay ED. The mesenchymal cell, its role in the embryo, and the remarkable signaling mechanisms that create it. *Dev Dyn.* 2005 Jul;233(3):706-20.

Hayashi K, Fong KS, Mercier F, Boyd CD, Csiszar K, Hayashi M. Comparative immunocytochemical localization of lysyl oxidase (LOX) and the lysyl oxidase-like (LOXL) proteins: changes in the expression of LOXL during development and growth of mouse tissues. *J Mol Histol.* 2004 Nov;35(8-9):845-55.

Helfand BT, Chang L, Goldman RD. Intermediate filaments are dynamic and motile elements of cellular architecture. *J Cell Sci.* 2004 Jan 15;117(Pt 2):133-41.

Literature

Hebert DN, Molinari M. In and out of the ER: protein folding, quality control, degradation, and related human diseases. *Physiol Rev.* 2007 Oct;87(4):1377-408.

Höckel M, Vaupel P. Tumor hypoxia: definitions and current clinical, biologic, and molecular aspects. *J Natl Cancer Inst.* 2001 Feb 21;93(4):266-76.

Hornstra IK, Birge S, Starcher B, Bailey AJ, Mecham RP, Shapiro SD. Lysyl oxidase is required for vascular and diaphragmatic development in mice. *J Biol Chem.* 2003 Apr 18;278(16):14387-93.

Huang Y, Dai J, Tang R, Zhao W, Zhou Z, Wang W, Ying K, Xie Y, Mao Y. Cloning and characterization of a human lysyl oxidase-like 3 gene (hLOXL3). *Matrix Biol.* 2001 Apr;20(2):153-7.

Huber MA, Kraut N, Beug H. Molecular requirements for epithelial-mesenchymal transition during tumor progression. *Curr Opin Cell Biol.* 2005 Oct;17(5):548-58.

Isken O, Maquat LE. Quality control of eukaryotic mRNA: safeguarding cells from abnormal mRNA function. *Genes Dev.* 2007 Aug 1;21(15):1833-56.

Jalkanen S, Salmi M. Cell surface monoamine oxidases: enzymes in search of a function. *EMBO J.* 2001 Aug 1;20(15):3893-901.

Jansen MK, Csiszar K. Intracellular localization of the matrix enzyme lysyl oxidase in polarized epithelial cells. *Matrix Biol.* 2007 Mar;26(2):136-9.

Jeay S, Pianetti S, Kagan HM, Sonenshein GE. Lysyl oxidase inhibits ras-mediated transformation by preventing activation of NF-kappa B. *Mol Cell Biol.* 2003 Apr;23(7):2251-63.

Jourdan-Le Saux C, Le Saux O, Donlon T, Boyd CD, Csiszar K. The human lysyl oxidase-related gene (LOXL2) maps between markers D8S280 and D8S278 on chromosome 8p21.2-p21.3. *Genomics.* 1998 Jul 15;51(2):305-7.

Jourdan-Le Saux C, Tomsche A, Ujfalusi A, Jia L, Csiszar K. Central nervous system, uterus, heart, and leukocyte expression of the LOXL3 gene, encoding a novel lysyl oxidase-like protein. *Genomics.* 2001 Jun 1;74(2):211-8.

Jung ST, Kim MS, Seo JY, Kim HC, Kim Y. Purification of enzymatically active human lysyl oxidase and lysyl oxidase-like protein from Escherichia coli inclusion bodies. *Protein Expr Purif.* 2003 Oct;31(2):240-6.

Kagan HM, Sullivan KA, Olsson TA 3rd, Cronlund AL. Purification and properties of four species of lysyl oxidase from bovine aorta. *Biochem J.* 1979 Jan 1;177(1):203-14.

Literature

Kagan HM, Williams MA, Williamson PR, Anderson JM. Influence of sequence and charge on the specificity of lysyl oxidase toward protein and synthetic peptide substrates. *J Biol Chem.* 1984 Sep 25;259(18):11203-7.

Kagan HM, Trackman PC. Properties and function of lysyl oxidase. *Am J Respir Cell Mol Biol.* 1991 Sep; 5(3):206-10.

Kagan HM, Li W. Lysyl oxidase: properties, specificity, and biological roles inside and outside of the cell. *J Cell Biochem.* 2003 Mar 1;88(4):660-72.

Kalluri R, Neilson EG. Epithelial-mesenchymal transition and its implications for fibrosis. *J Clin Invest.* 2003 Dec;112(12):1776-84.

Kanda T, Sullivan KF, Wahl GM. Histone-GFP fusion protein enables sensitive analysis of chromosome dynamics in living mammalian cells. *Curr Biol.* 1998 Mar 26;8(7):377-85.

Kaneda A, Wakazono K, Tsukamoto T, Watanabe N, Yagi Y, Tatematsu M, Kaminishi M, Sugimura T, Ushijima T. Lysyl oxidase is a tumor suppressor gene inactivated by methylation and loss of heterozygosity in human gastric cancers. *Cancer Res.* 2004 Sep 15;64(18):6410-5.

Kang Y, Massagué J. Epithelial-mesenchymal transitions: twist in development and metastasis. *Cell.* 2004 Aug 6;118(3):277-9.

Kay BK, Williamson MP, Sudol M. The importance of being proline: the interaction of proline-rich motifs in signaling proteins with their cognate domains. *FASEB J.* 2000 Feb;14(2):231-41.

Kenyon K, Contente S, Trackman PC, Tang J, Kagan HM, Friedman RM. Lysyl oxidase and rrg messenger RNA. *Science.* 1991 Aug 16;253(5021):802.

Kenyon K, Modi WS, Contente S, Friedman RM. A novel human cDNA with a predicted protein similar to lysyl oxidase maps to chromosome 15q24-q25. *J Biol Chem.* 1993 Sep 5;268(25):18435-7.

Kim Y, Boyd CD, Csiszar K. A new gene with sequence and structural similarity to the gene encoding human lysyl oxidase. *J Biol Chem.* 1995 Mar 31;270(13):7176-82.

Kirschmann DA, Seftor EA, Nieva DR, Mariano EA, Hendrix MJ. Differentially expressed genes associated with the metastatic phenotype in breast cancer. *Breast Cancer Res Treat.* 1999 May;55(2):127-36.

Literature

Kirschmann DA, Seftor EA, Fong SF, Nieva DR, Sullivan CM, Edwards EM, Sommer P, Csiszar K, Hendrix MJ. A molecular role for lysyl oxidase in breast cancer invasion. *Cancer Res.* 2002 Aug 1;62(15):4478-83.

Knott L, Bailey AJ. Collagen cross-links in mineralizing tissues: a review of their chemistry, function, and clinical relevance. *Bone.* 1998 Mar;22(3):181-7.

Kosonen T, Uriu-Hare JY, Clegg MS, Keen CL, Rucker RB. Incorporation of copper into lysyl oxidase. *Biochem J.* 1997 Oct 1;327 (Pt 1):283-9.

Kuivaniemi H, Korhonen RM, Vaheri A, Kivirikko KI. Deficient production of lysyl oxidase in cultures of malignantly transformed human cells. *FEBS Lett.* 1986 Jan 20;195(1-2):261-4.

Laczko R, Szauter KM, Jansen MK, Hollosi P, Muranyi M, Molnar J, Fong KS, Hinek A, Csiszar K. Active lysyl oxidase (LOX) correlates with focal adhesion kinase (FAK)/paxillin activation and migration in invasive astrocytes. *Neuropathol Appl Neurobiol.* 2007 Dec;33(6):631-43.

Laemmli UK. Cleavage of structural proteins during the assembly of the head of bacteriophage T4. *Nature.* 1970 Aug 15;227(5259):680-5.

Lazarus HM, Cruikshank WW, Narasimhan N, Kagan HM, Center DM. Induction of human monocyte motility by lysyl oxidase. *Matrix Biol.* 1995 Dec;14(9):727-31.

Li W, Liu G, Chou IN, Kagan HM. Hydrogen peroxide-mediated, lysyl oxidase-dependent chemotaxis of vascular smooth muscle cells. *J Cell Biochem.* 2000 Jun 12;78(4):550-7.

Li W, Nellaiappan K, Strassmaier T, Graham L, Thomas KM, Kagan HM. Localization and activity of lysyl oxidase within nuclei of fibrogenic cells. *Proc Natl Acad Sci U S A.* 1997 Nov 25;94(24):12817-22.

Mariani TJ, Trackman PC, Kagan HM, Eddy RL, Shows TB, Boyd CD, Deak SB. The complete derived amino acid sequence of human lysyl oxidase and assignment of the gene to chromosome 5 (extensive sequence homology with the murine ras revision gene). *Matrix.* 1992 Jun;12(3):242-8.

Mäki JM, Kivirikko KI. Cloning and characterization of a fourth human lysyl oxidase isoenzyme. *Biochem J.* 2001 Apr 15;355(Pt 2):381-7.

Mäki JM, Tikkanen H, Kivirikko KI. Cloning and characterization of a fifth human lysyl oxidase isoenzyme: the third member of the lysyl oxidase-related subfamily with four scavenger receptor cysteine-rich domains. *Matrix Biol.* 2001 Nov;20(7):493-6.

Literature

Mäki JM, Räsänen J, Tikkanen H, Sormunen R, Mäkikallio K, Kivirikko KI, Soininen R. Inactivation of the lysyl oxidase gene Lox leads to aortic aneurysms, cardiovascular dysfunction, and perinatal death in mice. *Circulation*. 2002 Nov 5;106(19):2503-9.

Mäki JM, Sormunen R, Lippo S, Kaarteenaho-Wiik R, Soininen R, Myllyharju J. Lysyl oxidase is essential for normal development and function of the respiratory system and for the integrity of elastic and collagen fibers in various tissues. *Am J Pathol*. 2005 Oct;167(4):927-36.

Mbeunkui F, Metge BJ, Shevde LA, Pannell LK. Identification of differentially secreted biomarkers using LC-MS/MS in isogenic cell lines representing a progression of breast cancer. *J Proteome Res*. 2007 Aug;6(8):2993-3002.

McKAY GF, LALICH JJ, SCHILLING ED, STRONG FM. A crystalline "lathyrus factor" from *Lathyrus odoratus*. *Arch Biochem Biophys*. 1954 Oct;52(2):313-22.

Mecham RP. Elastin synthesis and fiber assembly. *Ann N Y Acad Sci*. 1991;624:137-46.

Mecham, RP. The extracellular matrix: an overview. *Springer 1st edition* (2011).

Min C, Kirsch KH, Zhao Y, Jeay S, Palamakumbura AH, Trackman PC, Sonenshein GE. The tumor suppressor activity of the lysyl oxidase propeptide reverses the invasive phenotype of Her-2/neu-driven breast cancer. *Cancer Res*. 2007 Feb 1;67(3):1105-12.

Mullis K, Faloona F, Scharf S, Saiki R, Horn G, Erlich H. Specific enzymatic amplification of DNA in vitro: the polymerase chain reaction. *Cold Spring Harb Symp Quant Biol*. 1986;51 Pt 1:263-73.

Nagan N, Kagan HM. Modulation of lysyl oxidase activity toward peptidyl lysine by vicinal dicarboxylic amino acid residues. Implications for collagen cross-linking. *J Biol Chem*. 1994 Sep 2;269(35):22366-71.

Nagaraja GM, Othman M, Fox BP, Alsaber R, Pellegrino CM, Zeng Y, Khanna R, Tamburini P, Swaroop A, Kandpal RP. Gene expression signatures and biomarkers of noninvasive and invasive breast cancer cells: comprehensive profiles by representational difference analysis, microarrays and proteomics. *Oncogene*. 2006 Apr 13;25(16):2328-38.

Narayanan AS, Siegel RC, Martin GR. Stability and purification of lysyl oxidase. *Arch Biochem Biophys*. 1974 May;162(1):231-7.

Nellaippian K, Risitano A, Liu G, Nicklas G, Kagan HM. Fully processed lysyl oxidase catalyst translocates from the extracellular space into nuclei of aortic smooth-muscle cells. *J Cell Biochem*. 2000 Sep 14;79(4):576-82.

Literature

Nelson CM, Bissell MJ. Of extracellular matrix, scaffolds, and signaling: tissue architecture regulates development, homeostasis, and cancer. *Annu Rev Cell Dev Biol.* 2006;22:287-309.

Nelson JM, Diegelmann RF, Cohen IK. Effect of beta-aminopropionitrile and ascorbate on fibroblast migration. *Proc Soc Exp Biol Med.* 1988 Jul;188(3):346-52.

Noblesse E, Cenizo V, Bouez C, Borel A, Gleyzal C, Peyrol S, Jacob MP, Sommer P, Damour O. Lysyl oxidase-like and lysyl oxidase are present in the dermis and epidermis of a skin equivalent and in human skin and are associated to elastic fibers. *J Invest Dermatol.* 2004 Mar;122(3):621-30.

O'DELL BL, HARDWICK BC, REYNOLDS G, SAVAGE JE. Connective tissue defect in the chick resulting from copper deficiency. *Proc Soc Exp Biol Med.* 1961 Nov;108:402-5.

O'Dell BL, Elsden DF, Thomas J, Partridge SM, Smith RH, Palmer R. Inhibition of the biosynthesis of the cross-links in elastin by a lathyrogen. *Nature.* 1966 Jan 22;209(5021):401-2.

Olsen BR, Reginato AM, Wang W. Bone development. *Annu Rev Cell Dev Biol.* 2000;16:191-220.

Palamakumbura AH, Trackman PC. A fluorometric assay for detection of lysyl oxidase enzyme activity in biological samples. *Anal Biochem.* 2002 Jan 15;300(2):245-51.

Palamakumbura AH, Jeay S, Guo Y, Pischon N, Sommer P, Sonenshein GE, Trackman PC. The propeptide domain of lysyl oxidase induces phenotypic reversion of ras-transformed cells. *J Biol Chem.* 2004 Sep 24;279(39):40593-600.

Panchenko MV, Stetler-Stevenson WG, Trubetskoy OV, Gacheru SN, Kagan HM. Metalloproteinase activity secreted by fibrogenic cells in the processing of prolysyl oxidase. Potential role of procollagen C-proteinase. *J Biol Chem.* 1996 Mar 22;271(12):7113-9.

Payne SL, Fogelgren B, Hess AR, Seftor EA, Wiley EL, Fong SF, Csiszar K, Hendrix MJ, Kirschmann DA. Lysyl oxidase regulates breast cancer cell migration and adhesion through a hydrogen peroxide-mediated mechanism. *Cancer Res.* 2005 Dec 15;65(24):11429-36.

Peinado H, Del Carmen Iglesias-de la Cruz M, Olmeda D, Csiszar K, Fong KS, Vega S, Nieto MA, Cano A, Portillo F. A molecular role for lysyl oxidase-like 2 enzyme in snail regulation and tumor progression. *EMBO J.* 2005 Oct 5;24(19):3446-58.

Literature

Pinnell SR, Martin GR. The cross-linking of collagen and elastin: enzymatic conversion of lysine in peptide linkage to alpha-amino adipic-delta-semialdehyde (allysine) by an extract from bone. *Proc Natl Acad Sci U S A.* 1968 Oct;61(2):708-16.

Postovit LM, Abbott DE, Payne SL, Wheaton WW, Margaryan NV, Sullivan R, Jansen MK, Csiszar K, Hendrix MJ, Kirschmann DA. Hypoxia/reoxygenation: a dynamic regulator of lysyl oxidase-facilitated breast cancer migration. *J Cell Biochem.* 2008 Apr 1;103(5):1369-78.

Prockop DJ, Sieron AL, Li SW. Procollagen N-proteinase and procollagen C-proteinase. Two unusual metalloproteinases that are essential for procollagen processing probably have important roles in development and cell signaling. *Matrix Biol.* 1998 Feb;16(7):399-408.

Quondamatteo F. Assembly, stability and integrity of basement membranes in vivo. *Histochem J.* 2002 Aug-Sep;34(8-9):369-81.

Ren C, Yang G, Timme TL, Wheeler TM, Thompson TC. Reduced lysyl oxidase messenger RNA levels in experimental and human prostate cancer. *Cancer Res.* 1998 Mar 15;58(6):1285-90.

Resnick D, Pearson A, Krieger M. The SRCR superfamily: a family reminiscent of the Ig superfamily. *Trends Biochem Sci.* 1994 Jan;19(1):5-8.

Rhee SG, Kang SW, Jeong W, Chang TS, Yang KS, Woo HA. Intracellular messenger function of hydrogen peroxide and its regulation by peroxiredoxins. *Curr Opin Cell Biol.* 2005 Apr;17(2):183-9.

Riesen FK, Rothen-Rutishauser B, Wunderli-Allenspach H. A ZO1-GFP fusion protein to study the dynamics of tight junctions in living cells. *Histochem Cell Biol.* 2002 Apr;117(4):307-15.

Rizzuto R, Brini M, Pizzo P, Murgia M, Pozzan T. Chimeric green fluorescent protein as a tool for visualizing subcellular organelles in living cells. *Curr Biol.* 1995 Jun 1;5(6):635-42.

Saito H, Papaconstantinou J, Sato H, Goldstein S. Regulation of a novel gene encoding a lysyl oxidase-related protein in cellular adhesion and senescence. *J Biol Chem.* 1997 Mar 28;272(13):8157-60.

Saltiel AR, Pessin JE. Insulin signaling pathways in time and space. *Trends Cell Biol.* 2002 Feb;12(2):65-71.

Sarrias MR, Grønlund J, Padilla O, Madsen J, Holmskov U, Lozano F. The Scavenger Receptor Cysteine-Rich (SRCR) domain: an ancient and highly conserved protein module of the innate immune system. *Crit Rev Immunol.* 2004;24(1):1-37.

Literature

Savage JE, Bird DW, Reynolds G, O'Dell BL. Comparison of copper deficiency and lathyrism in turkey poulets. *J Nutr.* 1966 Jan;88(1):15-25.

Siegel RC, Pinnell SR, Martin GR. Cross-linking of collagen and elastin. Properties of lysyl oxidase. *Biochemistry.* 1970 Nov 10;9(23):4486-92.

Siegel RC. Biosynthesis of collagen crosslinks: increased activity of purified lysyl oxidase with reconstituted collagen fibrils. *Proc Natl Acad Sci U S A.* 1974 Dec;71(12):4826-30.

Simons K, Fuller SD. Cell surface polarity in epithelia. *Annu Rev Cell Biol.* 1985;1:243-88.

Skinner J, Bounacer A, Bond JA, Haughton MF, deMicco C, Wynford-Thomas D. Opposing effects of mutant ras oncogene on human fibroblast and epithelial cell proliferation: implications for models of human tumorigenesis. *Oncogene.* 2004 Aug 5;23(35):5994-9.

Smith-Mungo LI, Kagan HM. Lysyl oxidase: properties, regulation and multiple functions in biology. *Matrix Biol.* 1998 Feb;16(7):387-98.

Southern JA, Young DF, Heaney F, Baumgärtner WK, Randall RE. Identification of an epitope on the P and V proteins of simian virus 5 that distinguishes between two isolates with different biological characteristics. *J Gen Virol.* 1991 Jul;72 (Pt 7):1551-7.

Stassar MJ, Devitt G, Brosius M, Rinnab L, Prang J, Schradin T, Simon J, Petersen S, Kopp-Schneider A, Zöller M. Identification of human renal cell carcinoma associated genes by suppression subtractive hybridization. *Br J Cancer.* 2001 Nov 2;85(9):1372-82.

Stassen FL. Properties of highly purified lysyl oxidase from embryonic chick cartilage. *Biochim Biophys Acta.* 1976 Jun 7;438(1):49-60.

Stoker M, Gherardi E, Perryman M, Gray J. Scatter factor is a fibroblast-derived modulator of epithelial cell mobility. *Nature.* 1987 May 21-27;327(6119):239-42.

Sullivan KA, Kagan HM. Evidence for structural similarities in the multiple forms of aortic and cartilage lysyl oxidase and a catalytically quiescent aortic protein. *J Biol Chem.* 1982 Nov 25;257(22):13520-6.

Takahara K, Lyons GE, Greenspan DS. Bone morphogenetic protein-1 and a mammalian tolloid homologue (mTld) are encoded by alternatively spliced transcripts which are differentially expressed in some tissues. *J Biol Chem.* 1994 Dec 23;269(51):32572-8.

Tanzer ML. Experimental lathyrism. *Int Rev Connect Tissue Res.* 1965;3:91-112.

Literature

Thiery JP. Epithelial-mesenchymal transitions in tumour progression. *Nat Rev Cancer.* 2002 Jun;2(6):442-54.

Trackman PC, Zoski CG, Kagan HM. Development of a peroxidase-coupled fluorometric assay for lysyl oxidase. *Anal Biochem.* 1981 May 15;113(2):336-42.

Trackman PC, Bedell-Hogan D, Tang J, Kagan HM. Post-translational glycosylation and proteolytic processing of a lysyl oxidase precursor. *J Biol Chem.* 1992 Apr 25;267(12):8666-71.

Tsien RY. The green fluorescent protein. *Annu Rev Biochem.* 1998;67:509-44.

Uzel MI, Scott IC, Babakhanlou-Chase H, Palamakumbura AH, Pappano WN, Hong HH, Greenspan DS, Trackman PC. Multiple bone morphogenetic protein 1-related mammalian metalloproteinases process pro-lysyl oxidase at the correct physiological site and control lysyl oxidase activation in mouse embryo fibroblast cultures. *J Biol Chem.* 2001 Jun 22;276(25):22537-43.

Veal EA, Day AM, Morgan BA. Hydrogen peroxide sensing and signaling. *Mol Cell.* 2007 Apr 13;26(1):1-14.

Wang SX, Mure M, Medzihradsky KF, Burlingame AL, Brown DE, Dooley DM, Smith AJ, Kagan HM, Klinman JP. A crosslinked cofactor in lysyl oxidase: redox function for amino acid side chains. *Science.* 1996 Aug 23;273(5278):1078-84.

Wang SX, Nakamura N, Mure M, Klinman JP, Sanders-Loehr J. Characterization of the native lysine tyrosylquinone cofactor in lysyl oxidase by Raman spectroscopy. *J Biol Chem.* 1997 Nov 14;272(46):28841-4.

Ward TH, Lippincott-Schwartz J. The uses of green fluorescent protein in mammalian cells. *Methods Biochem Anal.* 2006;47:305-37.

Wessel GM, McClay DR. Gastrulation in the sea urchin embryo requires the deposition of crosslinked collagen within the extracellular matrix. *Dev Biol.* 1987 May;121(1):149-65.

Wu M, Min C, Wang X, Yu Z, Kirsch KH, Trackman PC, Sonenshein GE. Repression of BCL2 by the tumor suppressor activity of the lysyl oxidase propeptide inhibits transformed phenotype of lung and pancreatic cancer cells. *Cancer Res.* 2007 Jul 1;67(13):6278-85.

Yap AS, Crampton MS, Hardin J. Making and breaking contacts: the cellular biology of cadherin regulation. *Curr Opin Cell Biol.* 2007 Oct;19(5):508-14.

Literature

Yarden Y, Sliwkowski MX. Untangling the ErbB signalling network. *Nat Rev Mol Cell Biol.* 2001 Feb;2(2):127-37.

Yeaman C, Grindstaff KK, Hansen MD, Nelson WJ. Cell polarity: Versatile scaffolds keep things in place. *Curr Biol.* 1999 Jul 15;9(14):R515-7.

Yurchenco PD, Amenta PS, Patton BL. Basement membrane assembly, stability and activities observed through a developmental lens. *Matrix Biol.* 2004 Jan;22(7):521-38.

Teil 2:

„Gene expression signatures of circulating peripheral blood cells associated with early-onset coronary artery disease“

Durchführung der experimentellen Arbeiten am
Cardiovascular Research Center, University of Hawaii, Honolulu

vorgelegt von
Matthias Jansen

Köln, im Februar 2012

Table of contents

I. Introduction	4
1.1 Significance of cardiovascular disease for modern western societies	4
1.2 A brief historical perspective of atherosclerosis research	4
Figure 1. Scheme of the mevalonate pathway leading to cholesterol biosynthesis (A) and chemical structure of cholesterol (B).	6
1.3 A morphological and anatomical view on development and progression of atherosclerosis	7
Figure 2. Schematic depiction of a low density lipoprotein (LDL) particle.	8
Figure 3. Stages of atherosclerotic plaque development in the coronary artery.	9
1.4 Inflammatory processes during atherosclerosis	10
Figure 4. Immune cell recruitment and activation at atherosclerotic lesion sites.	12
Figure 5. Rupture of a vulnerable plaque.	14
Figure 6. Stable plaque phenotype.	15
1.5 Circulating blood cells and their potential significance in atherosclerosis	16
Figure 7. Adhesion of platelets to vascular endothelium (A) and adhesion of platelets to monocytes (B).	19
1.6 Systems biology and the analysis of the atherosclerotic phenotype	20
Figure 8. Workflow of the critical steps during a microarray experiment.	22
Figure 9. Schematic illustration of the SAGE protocol.	24
1.7 Working hypothesis and experimental approach of the second thesis project	26
II. Material and Methods	27
1. Study subjects	27
2. RNA purification	28
3. Microarray hybridization	29
4. Data analysis	29
5. Real-time PCR	30
III. Results	31
3.1 The study cohorts	31
Table 1. Clinical characteristics of early myocardial infarction (EMI) and medicated control (MCON) subjects.	31

Table of contents

3.2 Two step sample quality control analysis	32
3.3 Analysis of differential gene expression in circulating blood cells of patients with early-onset coronary artery disease	32
Figure 10. Microarray sample quality control and detection of differentially expressed genes.	34
Figure 11. Clustered heatmap and principal component analysis (PCA) of all differentially expressed genes identified by the LOTEST algorithm in EMI compared to MCON samples.	35
3.4 Application of gene ontology databases to identify functional gene expression signatures in circulating blood cells associated with coronary artery disease (CAD)	36
3.5 Ingenuity Pathway Analysis (IPA) identifies inflammatory gene expression signatures and immune imbalance in EMI samples	36
Table 2. The top four networks identified by Ingenuity Pathway Analysis (IPA).	37
Figure 12. Ingenuity Network 1.	39
Table 3. Differentially expressed genes of Ingenuity Network 1 with reported function in cardiovascular disease and/or inflammation.	40
Figure 13. Ingenuity Network 2.	43
Table 4. Differentially expressed genes of Ingenuity Network 2 with reported function in cardiovascular disease and/or inflammation.	44
Figure 14. Ingenuity Network 3.	47
Table 5. Differentially expressed genes of Ingenuity Network 3 with reported function in cardiovascular disease and/or inflammation.	48
Figure 15. Ingenuity Network 4.	51
Table 6. Differentially expressed genes of Ingenuity Network 4 with reported function in cardiovascular disease and/or inflammation.	52
3.6 PANTHER identifies differentially expressed genes associated with the immune response as the most significant functional category in EMI samples	53
Table 7. Ontological analysis of differentially expressed genes using PANTHER.	54
Table 8. Differentially expressed genes of the PANTHER „Biological Process“ category Immunity and Defense with reported function in cardiovascular disease and/or inflammation.	56
Figure 16. Clustered heatmap of genes from the biological process category “Immunity and defense” identified by PANTHER.	57
3.7 Examination of mRNA expression levels from selected differentially expressed genes in EMI individuals using quantitative real-time PCR	58
Figure 17. Average microarray expression levels (A) and relative quantities determined by quantitative real-time PCR of selected candidate genes (B).	59
Summary	60

Table of contents

IV. Discussion	61
1. The phenotype of early-onset coronary artery disease is reflected in gene expression signatures of circulating blood cells	61
1.1 Critical features of experimental design and differential expression analysis	61
1.2 Over-representation of pro-inflammatory gene expression changes in EMI subjects	64
Table 9. Potential candidate genes involved in immune regulation that separate the atherosclerotic phenotype between EMI and control individuals based on differential expression analysis.	64
1.3 Over-representation of pro-atherogenic gene expression changes in EMI subjects	68
Table 10. Potential candidate genes involved in diverse biological functions that separate the atherosclerotic phenotype between EMI and control individuals based on differential expression analysis.	68
2. Potential impact of cardiac-related medication on gene expression profiles in the study cohort	71
3. Significance of the study results	73
Table 11. Overlapping functions within the gene expression signature between the study of Sinnaeve et al. and our results.	74
Table 12. Overlapping functions within the gene expression signature between the study of Wingrove et al. and our results.	75
V. Abstract	77
VI. Zusammenfassung	78
VII. Literature	80
VIII. Acknowledgements	104
IX. Erklärung	105

I. Introduction

1.1 Significance of cardiovascular disease for modern western societies

Cardiovascular disease is the leading cause for mortality in developed countries and based on the „Global Burden Disease Study“ predicted to become the pre-eminent health problem worldwide (Murray & Lopez, 1997). Most commonly manifested as myocardial infarction (MI), it accounts for approximately one out of three deaths in the United States (Cutler et al., 2006). By the late 1940s, atherosclerosis resulting in ischaemic heart disease was recognized as the major cause for death in the United States and led to increased efforts towards the identification of underlying mechanism(s) and subsequent prevention measures (Levy & Thom, 1998). Until the 1970s, atherosclerosis was considered a lipid storage disease based on numerous experimental and clinical evidence (Gofman et al., 1950; Ross & Harker, 1976). During the 1970s and 1980s, the dominating influence of vascular biology led to an increased focus on growth factors and smooth muscle cell proliferation (Ross, 1979). The concept of atherosclerosis as an inflammatory disease has emerged in the 1990s due to the notion that atherosclerotic plaques, besides lipids and vascular cell types do also contain immune cells such as leukocytes (Jonasson et al., 1986; Libby, 2002). The economic burden of cardiovascular disease is substantial and causes the European Union over € 150 billion and the United States more than € 300 billion of annual direct as well as indirect costs (Leal et al., 2006; Thom et al., 2006). In comparison, the annual costs of all cancer treatments in the United States make up about 50 % of those from cardiovascular disease. Most importantly, the economic impact is not only exerted on a country's healthcare system but also as a loss of productivity in companies and a loss of income for affected individuals (Gaziano, 2007).

1.2 A brief historical perspective of atherosclerosis research

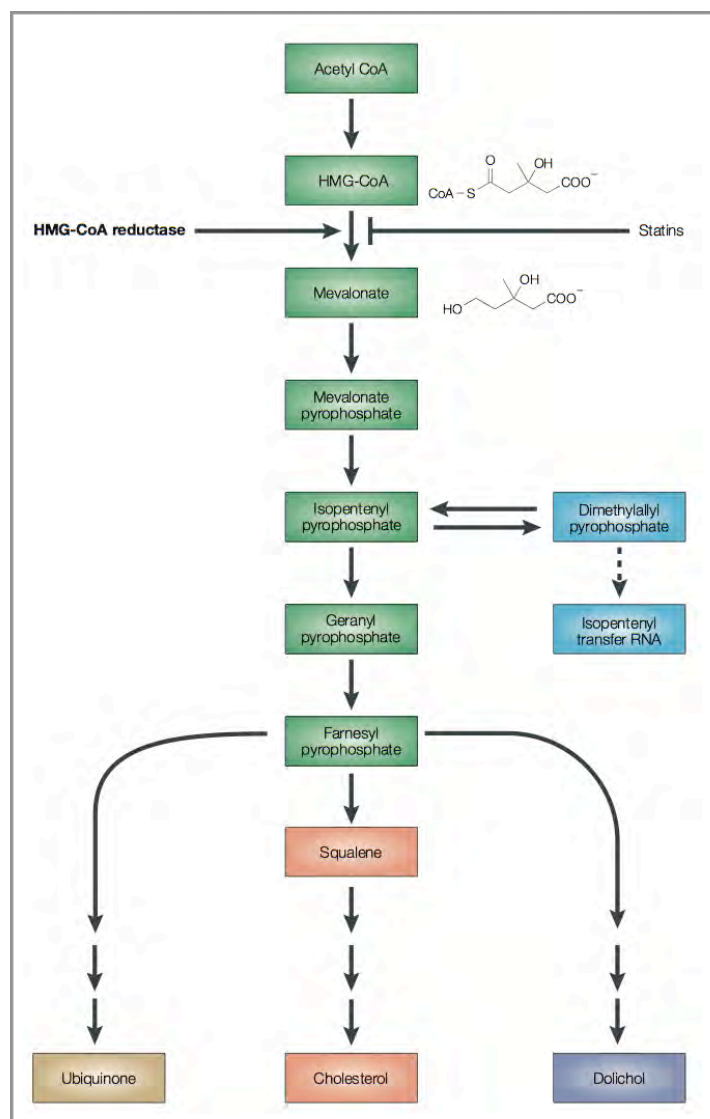
Although it has become an epidemic only in the modern world, the occurrence of atherosclerosis dates back to ancient times. The English pioneer of Paleopathology Sir Marc Ruffer described in 1911 arterial changes in an Egyptian mummy that were suggestive of atherosclerosis (Ruffer M, 1911). This observation was confirmed in the early 1960s using modern immunohistochemical techniques that identified lipid deposits, reduplication of the internal elastic lamina and calcification in arteries of Egyptian mummies (Sandison, 1962).

Introduction

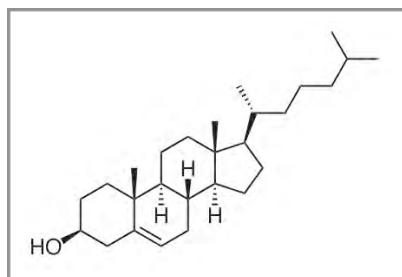
However, the first detailed scientific description of an atherosclerotic degenerated arterial wall seems to date back to 1804 when the Italian surgeon and anatomist Antonio Scarpa speculated metabolic processes to be the cause for this pathological observation. Nevertheless, Albrecht von Haller was in 1755 the first to introduce the term „atheroma“ (greek = porridge) for degenerative processes of the intimal layer within the arterial wall. In the 19th century a debate erupted of whether these arterial changes are induced by inflammation or simply the result of timely degeneration. Most of the pathologists followed Carl Rokitanski who considered atherosclerosis as a purely degenerative process characterized by connective tissue accumulation and calcification in the intimal layer of arteries. Notably, the German pathologist Rudolf Virchow assumed chronic inflammation as the underlying cause of atheroma that he designated „chronic endarteritis deformans“. However, Virchow also considered that lipid accumulation was only a late manifestation of the disease. Finally, the term „atherosclerosis“ was introduced in 1904 by Marchand to refer to the degenerative process of the inner arterial layer (Leibowitz, 1970).

Until the beginning of the 20th century atherosclerosis research remained purely descriptive. The first breakthrough towards a mechanistic assessment came in 1908 when the Russian scientist Alexander Ignatowski showed that feeding rabbits with a diet of egg yolk and milk resulted in experimental atherosclerosis (Ignatowski, 1908). The experiments were confirmed by Anitschkov and Chalatov in 1913 who obtained the same results by supplementing rabbit food with pure cholesterol (Anitschkow & Chalatov, 1913). This was the beginning of the lipid theory of atherosclerosis that dominated the research field for most of the 20th century. This view was for the first time adapted in the 1970s when Russel Ross developed the „response to injury“ hypothesis that attributed a major role for the endothelium and smooth muscle cells in atherogenesis (Ross et al., 1977). The second breakthrough emerged in the 1990s with the generation of mouse models for atherosclerosis based on homologous recombination techniques. Genetically engineered mice lacking Apolipoprotein E and/or LDL receptor developed atherosclerotic lesions similar to those observed in humans and therefore opened a new era of research at a mechanistic level (Ishibashi et al., 1994; Nakashima et al., 1994). Due to increasing evidence of immune system involvement in all stages of the disease, Ross reshaped in 1999 his „response to injury“ hypothesis towards the view of atherosclerosis as a „chronic inflammatory disease“ (Ross, 1999). As of today, it is widely accepted that atherosclerosis is a multifactorial disease converging on the interplay of excess cholesterol, inflammation and the vascular response to both of those factors (Rocha & Libby, 2009).

Introduction



A



B

Figure 1. Scheme of the mevalonate pathway leading to cholesterol biosynthesis (A) and chemical structure of cholesterol (B).

(A) Statins interfere with cholesterol synthesis through inhibition of HMG-CoA reductase, the key enzyme in the second step of the pathway (from Tobert JA, *Nature Reviews Drug Discovery* 2; 517-526. July 2003).

(B) Notably, the amphipathic properties of cholesterol result from one hydrophilic hydroxyl group and from the hydrophobic hydrocarbon backbone containing four saturated hydrocarbon rings that are characteristic for all steroids (from p. 167 „Taschenatlas der Biochemie“, Koolman & Röhm).

1.3 A morphological and anatomical view on development and progression of atherosclerosis

Cholesterol is an essential component of the cell membrane. It provides the phospholipid bilayer of membranes rigidity to withstand mechanical forces. As for all lipids the biosynthesis pathway begins with activated acetic acid (Acetyl-CoA) and results in the characteristic steroid core module of cholesterol (Figure 1). It is mainly produced in the liver but to some extent also in other organs such as the intestine and the skin. Most of the cholesterol is incorporated into cell membranes contributing to their structural integrity. In addition, it is converted into bile acids that support intestinal digestion and a small fraction of cholesterol serves as a template for the synthesis of steroid hormones such as cortisol. Different lipoprotein complexes that differ in their protein and lipid composition transport cholesterol via the circulation into the tissues. The most significant carrier for cholesterol is low density lipoprotein (LDL) that consists of a lipid rich core surrounded by an amphipathic lipid layer inserted with apolipoprotein B (Figure 2). These proteins are important as they mediate binding to receptors for cellular uptake of cholesterol. Lipids are mainly hydrophobic molecules and would be insoluble within the hydrophilic blood stream. Therefore lipoprotein complexes facilitate the transport of an otherwise insoluble cargo through the circulation system. A characteristic manifestation of atherosclerosis is the formation of atherosclerotic plaques or lesions (also known as atheroma) in blood vessels (Figure 3). Normal arteries have a typical trilaminar structure. The endothelium is in direct contact with the blood and rests upon a basement membrane. The tunica intima consists of smooth muscle cells scattered within the extracellular matrix. An internal elastic lamina separates the intimal layer from the tunica media that contains multiple layers of smooth muscle cells embedded in a collagen- and elastin-containing matrix. Finally, the adventitia encloses the arterial wall towards the surrounding tissue. Excess levels of cholesterol can lead to the formation of early lesions, also called fatty streaks. They are characterized by a lipid-rich core embedded in the intimal layer and an enlargement of the artery in an outward direction. Yet the normal size of the arterial lumen remains (almost) constant. Notably, fatty streaks are still reversible and prevalent in young individuals and were even found in fetal aortas of neonates (Berenson et al., 1998; Napoli et al., 1997). Mature plaques develop when smooth muscle cells migrate from the tunica media past the internal elastic lamina into the tunica intima and/or subendothelial space. Mature plaques can occur as two different phenotypes: „vulnerable“ and „stable“ plaques. Vulnerable plaques contain a large lipid pool along with many inflammatory cells and a thin fibrous cap of extracellular matrix components.

Introduction

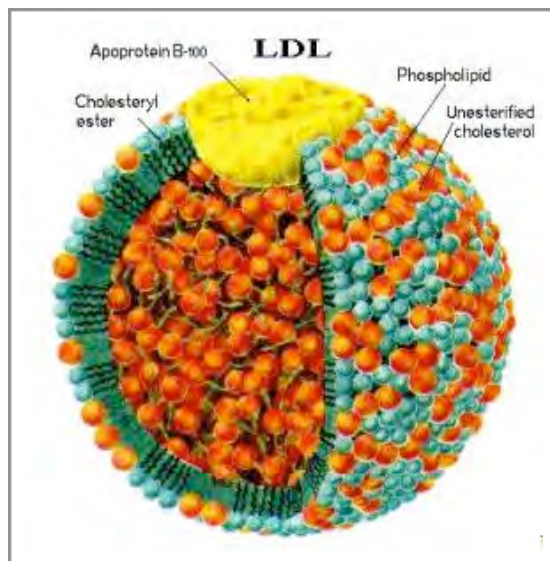


Figure 2. Schematic depiction of a low density lipoprotein (LDL) particle.

A hydrophobic core containing cholestryl esters is covered with amphipathic lipids embedding apolipoprotein B (from www.foodspace.wordpress.com).

Introduction

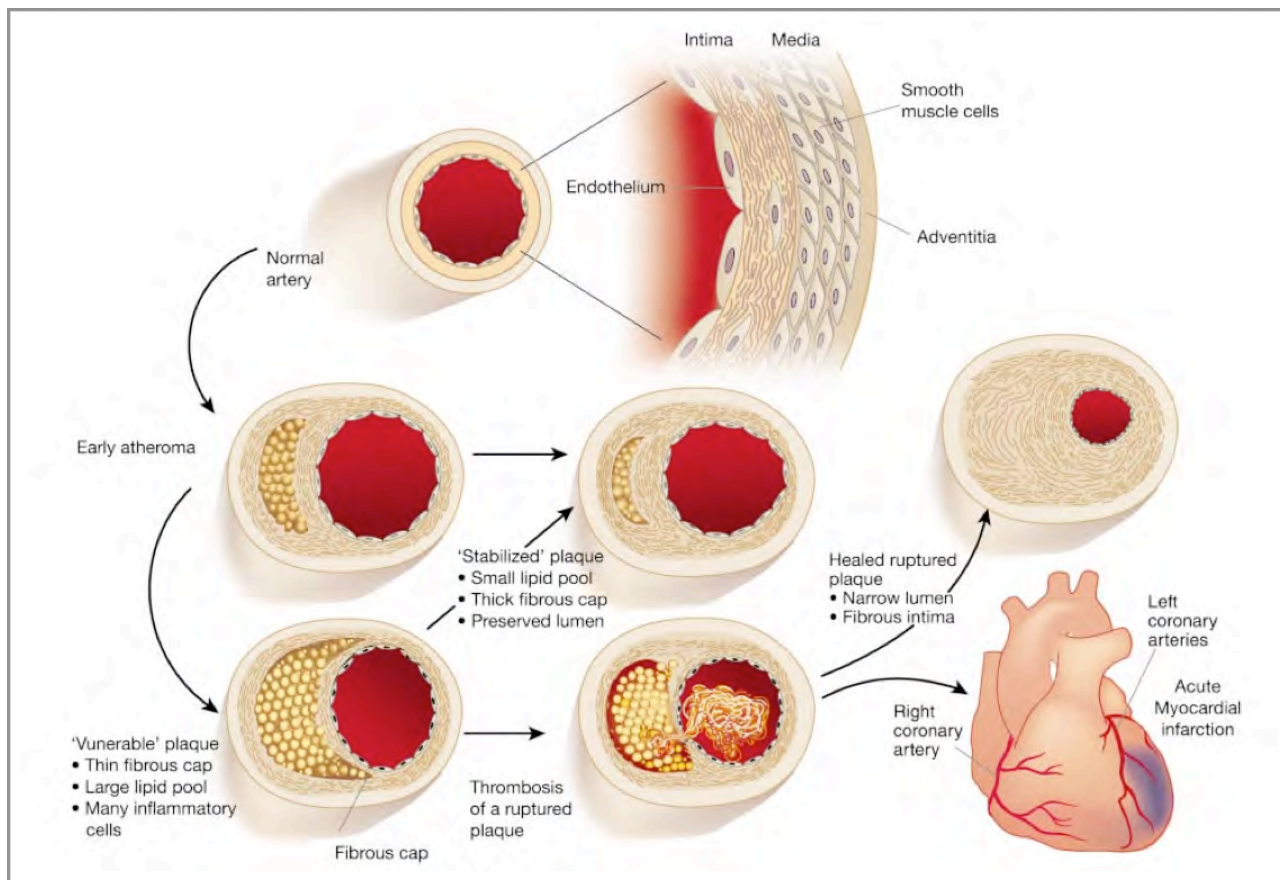


Figure 3. Stages of atherosclerotic plaque development in the coronary artery.

Normal arteries have a trilaminar structure consisting of an endothelium lining the arterial lumen, the tunica intima and the tunica media (displayed in the enlargement). The intimal layer contains mesenchymal cells scattered in an extracellular matrix and the medial layer comprises several layers of smooth muscle cells. In addition, arteries are covered by a surrounding adventitial layer. Early atherosclerotic plaques are characterized by lipid accumulation in the intimal layer. Further lipid accumulation and inflammatory processes can lead to vulnerable plaques with a thin fibrous cap. This cap might rupture resulting in thrombosis and possibly myocardial infarction. The arterial lumen at the site of a healed ruptured plaque is significantly narrowed due to fibrous tissue accumulation in the intimal layer. In contrast, stabilized plaques contain a small lipid pool and a thick fibrous cap that is usually resistant to physical rupture (from Libby P, *Nature* **420**; 868-871. Dec 2002).

Introduction

This plaque phenotype is prone to physical rupture with subsequent thrombus formation and might result in artery occlusion and myocardial infarction. In case of a non-fatal cardiovascular event, the ruptured plaque can heal but is often accompanied by massive expansion of smooth muscle cells and extracellular matrix deposits in the intimal layer and thereby reduces the arterial lumen. In contrast, a stable plaque is characterized by a small lipid pool, low amounts of inflammatory cells and a thick fibrous cap that is rich in collagen. This plaque phenotype usually remains quiescent unless inflammatory stimulation triggers conversion into a vulnerable plaque.

1.4 Inflammatory processes during atherosclerosis

As of today it has become evident that inflammation is a critical feature from early to late stages of atherosclerosis. Poole and Florey observed already in the 1950s that soon after feeding rabbits a cholesterol diet, leukocytes would attach to and cross the intact endothelium into the intimal layer of the arterial wall (Poole & Florey, 1958). Experimental animal studies in the 1990s have eventually revealed the molecular basis for immune-cell recruitment during the initiation of atherosclerosis. Leukocyte adhesion molecules, in particular vascular cell-adhesion molecule 1 (VCAM-1), mediate attachment of monocytes and T-cells on endothelial cells lining the arterial lumen and initiate their subsequent penetration into the intimal layer (Cybulsky & Gimbrone, 1991) (Figure 4 A). In addition, other adhesion molecules including E-selectin and P-selectin seem to be involved in monocyte attachment to the endothelium (Dong et al., 1998). Leukocytes enter the intimal layer through passage between intact endothelial cell junctions, a process that is referred to as diapedesis. This directed migration is mediated by a chemotactic gradient built of various cytokines. For example, monocyte chemoattractant protein-1 (MCP-1) is secreted by vascular endothelial cells and can recruit mononuclear phagocytes into nascent atheroma (Gu et al., 1998; Boring et al., 1998). The inflammatory activation of the endothelium can result from several stimuli. Excess cholesterol seems to be the major initiating trigger in both, animal models and humans, as atherosclerosis is practically absent in human populations with cholesterol levels below 150 mg/dl but gradually increases with elevated serum cholesterol (Campbell et al., 1998; Stamler et al., 1986). Cholesterol sequestered in LDL particles can freely penetrate the intimal layer of the arterial wall where it becomes susceptible to oxidative modification by reactive oxygen species and/or extracellular enzymes (Williams & Tabas, 1998).

Introduction

Oxidized LDL (oxLDL) induces monocyte chemoattractant protein 1 (MCP-1) expression in endothelial cells thereby attracting monocytes (Navab et al., 1996). Accordingly, expression of the corresponding receptor CCR2 on monocytes is also stimulated by hypercholesterolemia (Han et al., 1999). Another stimulus may be hypertension resulting in shear stress within the arterial lumen that can also contribute to expression of inflammatory genes in endothelial cells (Topper & Gimbrone, 1999). In fact, endothelial cells in culture that are exposed to shear stress mimicking arterial blood flow, display elevated expression of several leukocyte adhesion molecules (Dai et al., 2004).

Once monocytes have entered the intimal layer they differentiate into macrophages under the influence of macrophage colony-stimulating factor (M-CSF) secreted by endothelial cells and smooth muscle cells (Figure 4 B) (Rajavashisth et al., 1998). Macrophages can undergo a second conversion into „foam cells“ whose name results from the massive accumulation of lipids within cytoplasmic droplets. In the presence of oxLDL, macrophages start expressing scavenger receptors that initiate the conversion into foam cells by allowing cellular uptake and clearance of modified LDL particles from the system (Febraio et al., 2000; Suzuki et al., 1997). Internalized oxLDL is subject to lysosomal degradation and antigen presentation of degraded fragments on the cell surface via MHC class II molecules can result in activation of T-cells (Nicoletti et al., 1999).

T-cells are critical inflammatory regulators of atherogenesis through diverse actions (Figure 4 C). Upon activation via antigen presentation (e.g. oxLDL) and stimulation by cytokines such as interleukin 12 (IL-12) secreted from macrophages they can differentiate into T helper 1 (Th1) cells (Uyemura et al., 1996). Th1 cells produce potent pro-inflammatory cytokines including IFN- γ and TNF- α that reinforce the inflammatory cascade by prompting macrophages and vascular cells to secrete additional pro-inflammatory mediators (Frostegard et al., 1999). Furthermore, Th1-mediated immune responses increase endothelial permeability and expression of adhesion molecules on endothelial cells resulting in recruitment of additional inflammatory cells (Figure 4 D). In fact, it seems that antigen-presenting cells (e.g. dendritic cells) may travel from atherosclerotic plaques to the thymus where they activate memory and effector T-cells that undergo clonal expansion before traveling back to the lesion site (Angeli et al., 2004). Another key player among pro-inflammatory cytokines is CD40 ligand (CD40LG), a member of the tumor necrosis factor (TNF) family, that is expressed by most cell types present in atherosclerotic lesions (Mach et al., 1997a). CD40LG signaling triggers inflammatory activation of T-cells, macrophages, endothelial cells and smooth muscle cells and is not only characterized by cytokine production but also results in expression of matrix metalloproteinases (MMPs) and procoagulant tissue factor (Mach et al., 1997b).

Introduction

The latter two are important mediators during plaque rupture as MMPs degrade the fibrous extracellular matrix cap that stabilizes the mature plaque and tissue factor triggers thrombocytic aggregation of platelets once the blood gains access to the lipid core (Libby & Aikawa, 2002).

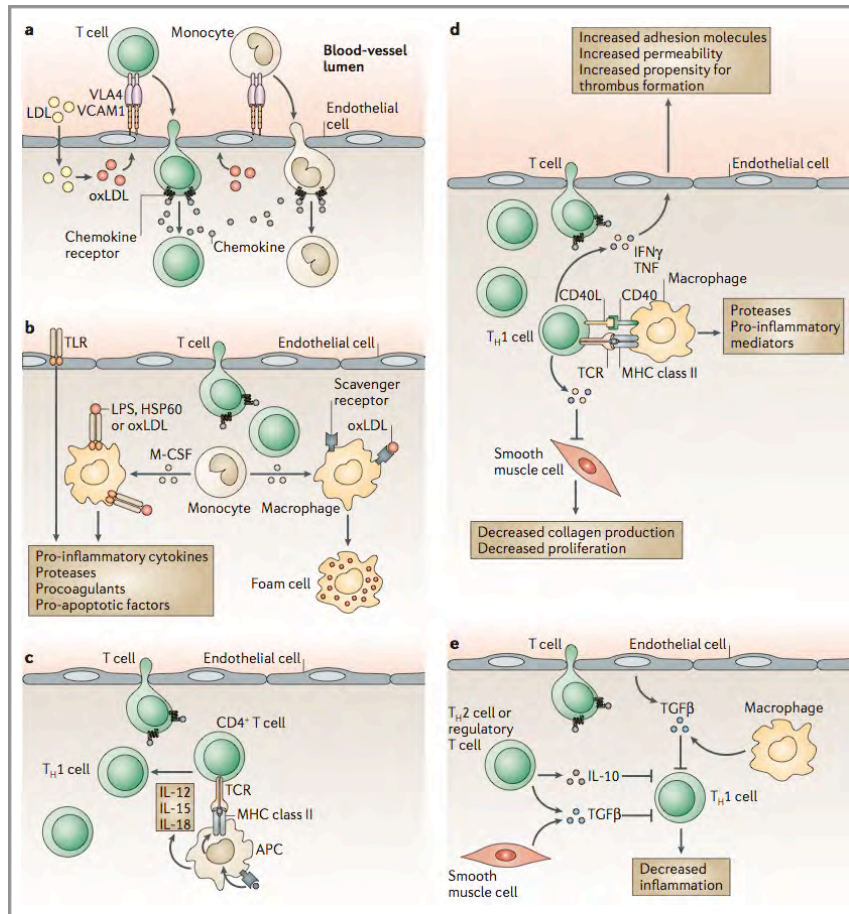


Figure 4. Immune cell recruitment and activation at atherosclerotic lesion sites.

(a) LDL particles enter the intimal layer where they are subject to oxidative modification. Leukocytes bind to adhesion molecules (e.g. VCAM-1) on the surface of endothelial cells and then pass through the endothelial layer following a chemokine gradient. (b) Monocytes differentiate under the influence of M-CSF into macrophages. In response to oxLDL macrophages undergo foam cell conversion thereby accumulating lipids in their cytoplasm. In addition, macrophages can present antigens of degraded fragments of oxLDL, lipopolysaccharides (LPS) or heat shock proteins (HSP60) on their surface. (c) T-cells become activated through antigen presenting cells (APC), express the cell surface marker CD4 and can differentiate into Th1 cells in the presence of interleukins (e.g. IL-12). (d) Th1 cells mediate pro-inflammatory signals in atherosclerotic plaques. They secrete interferon gamma (IFN- γ) and tumor necrosis factor (TNF) further activating the endothelium and inhibiting smooth muscle cell proliferation. In addition, Th1 cells can trigger inflammatory cascades in macrophages through CD40 ligand signaling. (e) Th2 cells mediate anti-inflammatory signals in atherosclerotic plaques. They produce interleukin 10 (IL-10) and transforming growth factor beta (TGF β) that both inhibit Th1 cell responses and stimulate smooth muscle cell proliferation and differentiation (from Hansson & Libby, *Nat Rev Immun* 6; 508-519. July 2006).

Introduction

Persistent inflammation at atherosclerotic lesion sites results on one hand in a lipid-rich core and on the other hand in a fibrous cap that is thin and fragile due to smooth muscle cell inhibition and MMP-mediated extracellular matrix degradation (Figure 5). This imbalance renders the plaque vulnerable to physical rupture and is the main cause for thrombocytic occlusions that can lead to ischemia in coronary arteries and eventually to myocardial infarction, the most adverse cardiovascular event (Virmani et al., 2002). In addition to plaque disruption by fracture of the fibrous cap two other mechanisms are discussed as initiating events for atherothrombosis. First, steady plaque erosion driven by endothelial desquamation, possibly as a result of apoptosis, may expose sub-endothelial collagen and von Willebrandt factor that promote platelet aggregation (Farb et al., 1996; Durand et al., 2004). Second, it is speculated that microvessels generated in atheromas as a result of neo-angiogenesis may be more fragile and therefore prone to micro-hemorrhage (de Boer et al., 1999).

However, mature plaques can also exhibit a stable phenotype that is characterized by a small lipid core with a thick fibrous cap and seems to be supported by T helper 2 (Th2) cell immune responses (Figure 4E and Figure 6). This T-cell subpopulation secretes interleukin 10 (IL-10) and transforming growth factor beta (TGF- β) that both suppress pro-inflammatory processes mediated by Th1 cells including production of IL-12 and IFN- γ (Mallat et al., 1999; Mallat et al., 2001). Most importantly, TGF- β stimulates proliferation of smooth muscle cells that produce and secrete collagen fibrils thereby adding tensile strength and resilience to the fibrous cap (Lutgens et al., 2002). Stable plaque phenotypes often develop as a consequence of the healing process after a resolved plaque rupture. However, increased extracellular matrix synthesis and fibrous tissue accumulation cause expansion of the intimal layer and come as mentioned earlier at the price of reducing the arterial lumen and thereby decrease blood flow capacity.

Introduction

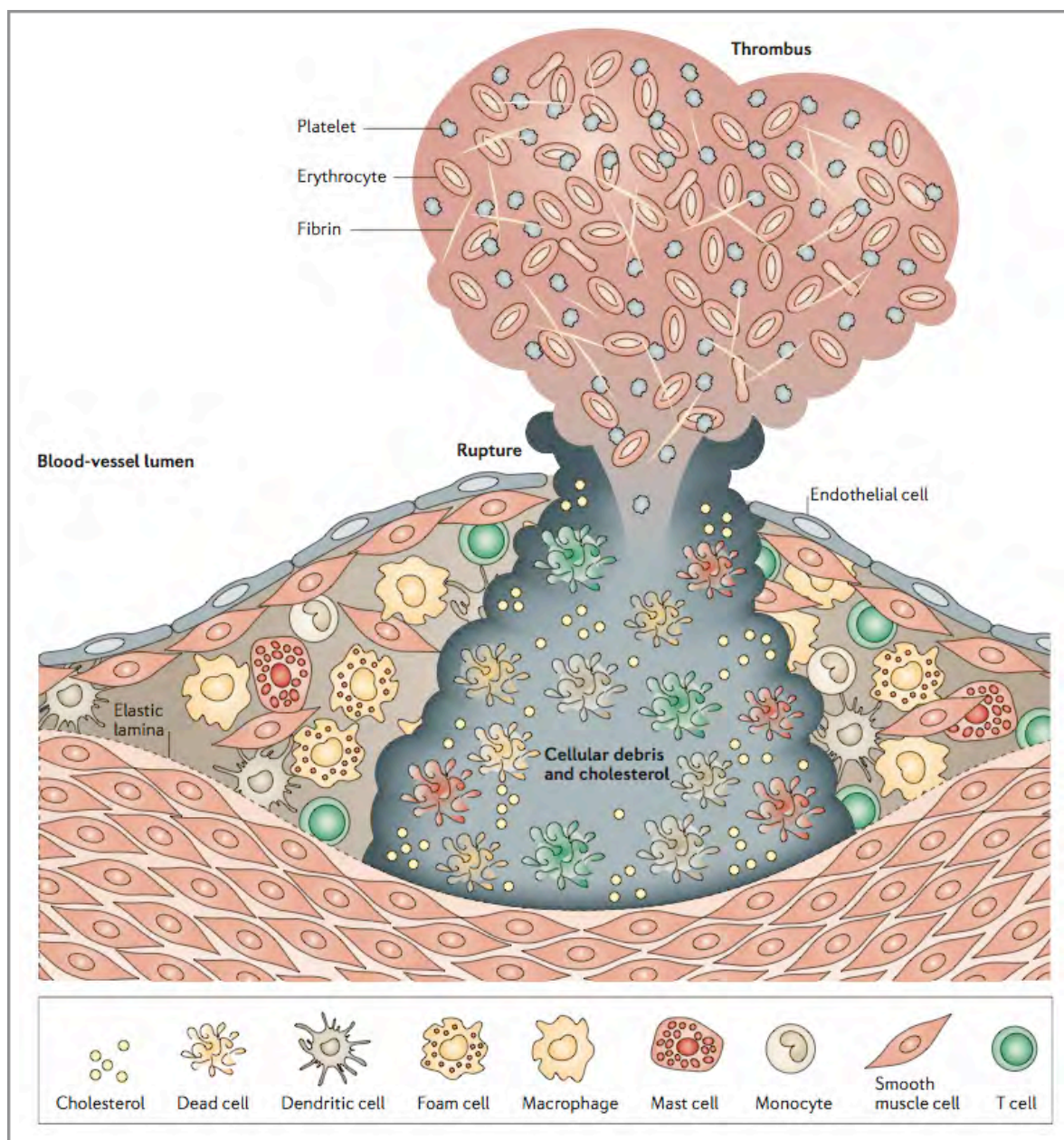


Figure 5. Rupture of a vulnerable plaque.

Persistent inflammatory signals from immune cells within the plaque induce secretion of matrix metalloproteinases (MMPs) and inhibit collagen synthesis by smooth muscle cells. The result is a plaque with a thin fibrous cap that may eventually fissure upon mechanical shear stress from the arterial blood flow. The release of cellular debris and cholesterol from the plaque interior into the arterial lumen leads to platelet aggregation and can result in thrombosis. Arterial occlusion due to thrombus formation might cause ischaemia and - depending on location and duration - subsequent myocardial infarction (from Hansson & Libby, *Nat Rev Immun* 6; 508-519. July 2006).

Introduction

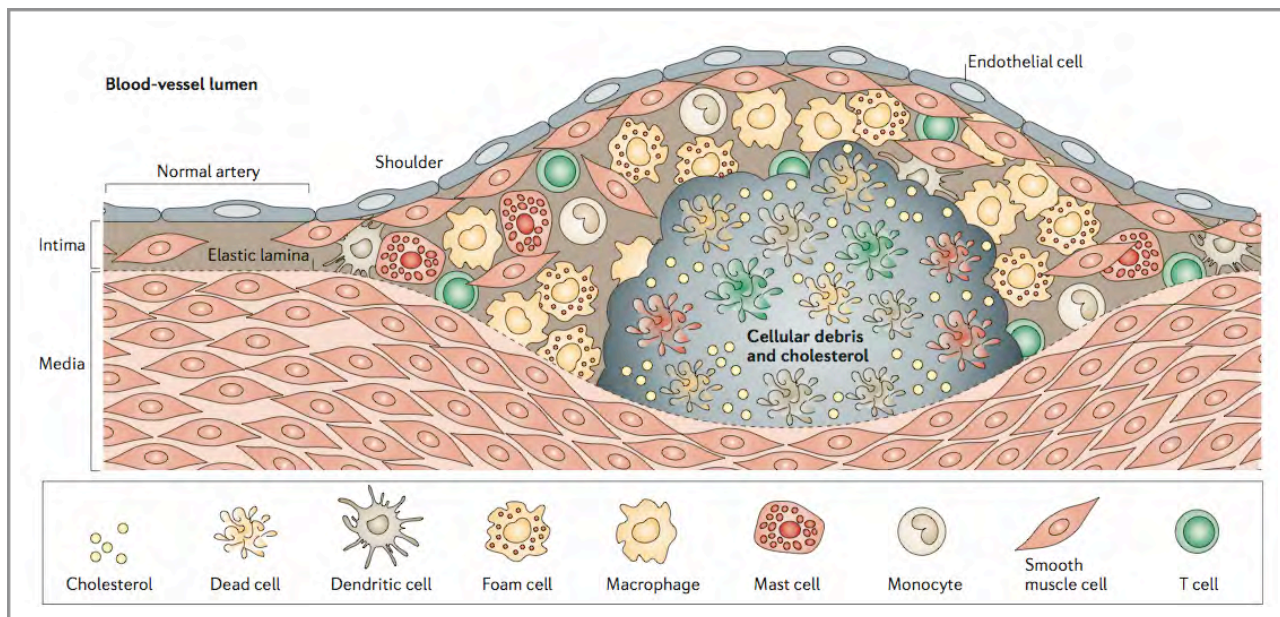


Figure 6. Stable plaque phenotype.

The plaque contains a lipid-rich core consisting of cholesterol and cellular debris from degenerated cells and is covered by a thick fibrous cap made up by smooth muscle cells and a tight meshwork of collagen fibrils (not shown). The intact plaque is sealed against the arterial lumen by an endothelial layer. Diverse immune cell types including monocytes, macrophages and T-cells reside within the plaque and may affect its phenotype by secretion of cytokines, proteases, thrombotic molecules and vasoactive substances (from Hansson & Libby, *Nat Rev Immun* **6**; 508-519. July 2006).

1.5 Circulating blood cells and their potential significance in atherosclerosis

Infiltrating immune cells from the circulation are a hallmark of atherosclerotic plaque development at the lesion site and set the stage for inflammatory processes in atherosclerosis (Libby, 2002). Approximately 40% of the cells in human atherosclerotic plaques express macrophage markers, about 10% are T-cells and almost 50% are vascular smooth muscle cells (Jonasson et al., 1986). Interestingly, the actual ratio of immune cells in the plaque that represent resident cells of the vessel wall versus cells originating from the circulation is not known. Even vascular endothelial cells and smooth muscle cells at atherosclerotic lesion sites have been shown to originate at least in part from circulating bone marrow-derived precursors (Saiura et al., 2001; Werner & Nickenig, 2007). These observations indicate that plaques are throughout the disease process in dynamic exchange with the circulation and are modulated by stimuli from not only their local micro- but also the systemic environment.

Circulating monocytes appear to be a major source of macrophages in plaques where they can further transition into cholesterol-loaded foam cells (Smith et al., 1995; Suzuki et al., 1997; Febbraio et al., 2000). Furthermore, recent studies have demonstrated that in particular a pro-inflammatory subset of circulating monocytes expressing the surface marker P-selectin glycoprotein ligand 1 (PSGL-1) accumulates in atherosclerotic plaques (An et al., 2008). Circulating monocytes apparently represent a heterogenous population of immune cells but the distinct functions of different monocyte subsets in atherosclerosis remain to be resolved (Woolard & Geissmann, 2010). Interestingly, monocytes are not only recruited to but may also emigrate from atherosclerotic lesion sites back into the circulation (Llodra et al., 2004). However, the underlying mechanism(s) that control monocyte traffic in and out of plaques, as well as the functional significance of this observation are unknown. In conclusion, monocytes seem to exhibit a high degree of plasticity within their local environment. In addition, within plaques they are also capable to differentiate into dendritic cells upon cytokine stimulation by granulocyte macrophage colony stimulating factor (GM-CSF) (Geissmann et al., 2003).

Dendritic cells (DCs) can originate from monocytes (myeloid) as well as from lymphoid progenitors and comprise a small fraction of leukocytes (0,3 %). DCs serve mainly as antigen-presenting cells thereby modulating the adaptive immune response. There are resident DCs within the vascular wall but also circulating DCs in the blood stream. During atherosclerotic progression the number of circulating DCs decreases whereas the numbers in vulnerable plaques increase (Yilmaz et al., 2006). Notably, oxidized LDL promotes differentiation of monocytes into dendritic

Introduction

cells, a process that is inhibited by statins, a potent class of cholesterol-lowering drugs (Perrin-Cocon et al., 2001; Yilmaz et al., 2004). Furthermore, in response to high cholesterol levels DCs seem to travel back from atherosclerotic lesion sites to lymphoid tissues where they may induce clonal expansion of auto-reactive T-cells against oxLDL epitopes (Angeli et al., 2004).

Mast cells represent another small but potentially important subset of leukocytes that enter atherosclerotic plaques from the circulation and may contribute to disease progression. Originating from myeloid progenitor cells, mast cells are involved in inflammatory and hypersensitivity reactions of the immune system (Hofmann & Abraham, 2009). Upon stimulation they can release vasoactive substances (e.g. histamine and leukotrienes), proteolytic enzymes (e.g. tryptase and chymase), pro-inflammatory cytokines (e.g. TNF- α = tumor necrosis factor- α) and growth factors (e.g. PAF = platelet activating factor) that are all stored within cytoplasmic granules. Mast cells are activated in response to antigen binding to Immunoglobulin E (IgE), components of the complement cascade and excess cholesterol of which the latter two are found in atherosclerotic plaques (Niculescu & Rus, 2004; Baumruker et al., 2003). Mast cells are present in atherosclerotic lesion sites from early to late stages of the disease process but specifically in rupture-prone regions of vulnerable plaques (Kartinen et al., 1994). Proteolytic enzymes secreted by mast cells are thought to degrade the fibrous cap leading to plaque stabilization whereas release of TNF- α from secretory granules may act on macrophages and T cells amplifying the inflammatory cascade (Johnson et al., 1998; Kartinen et al., 1996). In conclusion, mast cells seem to enhance pro-atherogenic events throughout the disease process.

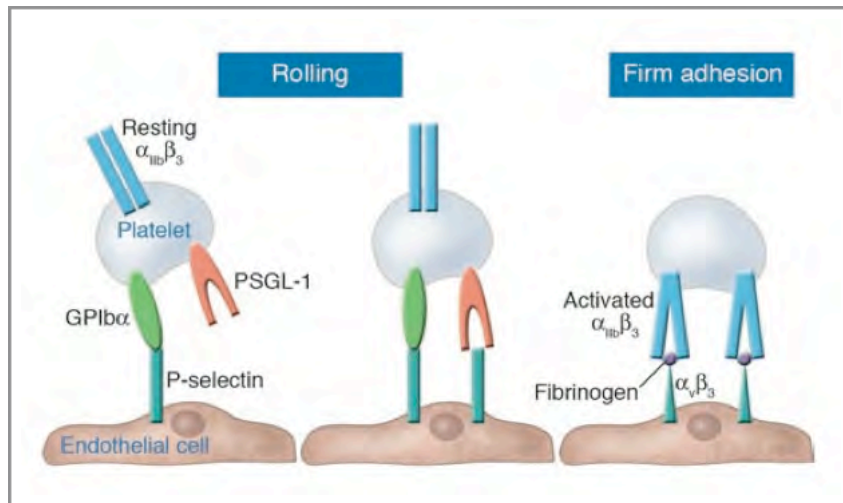
Although circulating platelets are mostly recognized for their central role during hemostasis, studies within the last decade attribute a significant impact for this anucleate cell type on atherosclerotic disease development and progression (May et al, 2008). The role of platelets during thrombus formation after rupture of atherosclerotic plaques is well understood (Bhatt & Topol, 2003). However, accumulating evidence strongly suggests that platelets contribute to early stages of atherogenesis as well. About a decade ago, studies have demonstrated that adhesion of circulating platelets to the endothelium is critical for atherosclerotic plaque development (Massberg et al., 2002). Platelets not only adhere to endothelial cells but also to leukocytes and may in particular facilitate recruitment of monocytes to the vascular wall thereby promoting plaque formation (Huo et al., 2003). Platelet attachment to the endothelium is thought to occur via a two-step process that includes interaction of P-selectin glycoprotein ligand 1 (PSGL-1) and integrins with corresponding receptors on target cells (Figure 7 A) (Romo et al., 1999; Frenette et al., 2000).

Introduction

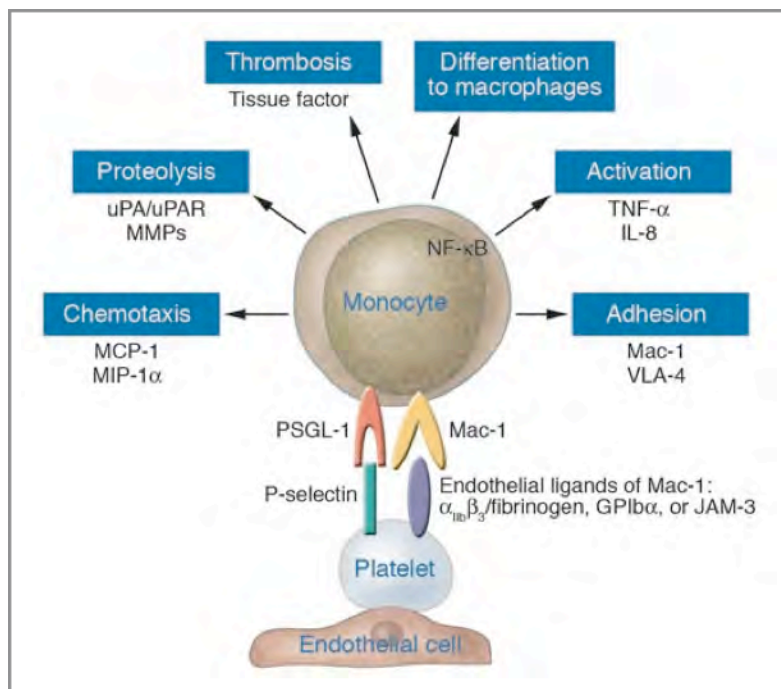
Monocytes are bound similarly through adhesion receptors on the cell surface (Figure 7 B). According to the current concept, platelets may be activated upon chemical (e.g. cytokines, oxLDL) and/or physical (e.g. hypertension) stimulation and modulate diverse inflammatory processes contributing to an atherogenic milieu at the vascular wall (May et al., 2008). For example, secretion of interleukin-1 β (IL-1 β) by platelets induces expression of pro-inflammatory cytokines and leukocyte adhesion molecules in endothelial cells (Hawrylowicz et al., 1991; Gawaz et al., 2000). Similarly, platelet-derived CD40 ligand triggers expression of leukocyte chemoattractants and adhesion receptors in endothelial cells (Henn et al., 1998). Furthermore, platelet factor 4 (PF4) a chemokine unique for platelets has been shown to promote hypercholesterolemia by inhibition of LDL uptake via the LDL receptor on one hand and to induce foam cell formation by uptake of oxidized LDL via scavenger receptors in macrophages on the other hand (Sachais et al., 2002; Nassar et al., 2003). In conclusion, the significance of platelets in atherosclerosis may go far beyond the involvement in thrombus formation during acute cardiovascular events. It seems as if the role of this cell type as inflammatory modulator is at least as important during early stages of the disease process.

In summary, circulating immune cells and platelets patrol within the blood stream and may act as both, primary sensors and effectors, of the atherosclerotic coronary artery disease phenotype. Therefore, circulating blood cells as an entity do represent an attractive target to investigate the cellular interplay between the plaque site and systemic influences with the aim to identify novel biomarkers and yet unknown mechanisms of atherosclerosis.

Introduction



A.



B.

Figure 7. Adhesion of platelets to vascular endothelium (A) and adhesion of platelets to monocytes (B).
(A) Initially, platelets tether to endothelial cells via interaction of the cell surface ligands GPIba and PSGL-1 with P-selectin. Firm adhesion is mediated via integrin $\alpha_{IIb}\beta_3$ binding of platelets with $\alpha_v\beta_3$ integrins on endothelial cells. **(B)** Platelet binding to monocytes through adhesion molecules can induce transcription programs that result in diverse downstream signaling events (from Gawaz et al., *J Clin Invest.* 2005 Dec;115 (12):3378-84.).

1.6 Systems biology and the analysis of the atherosclerotic phenotype

One of the fundamental aims in biology is to understand the complexity of organisms and to decipher the underlying molecular mechanisms of cell function. Despite the breakthroughs of modern biochemistry and molecular biology since the mid 20th century that were enabling the investigation of single genes and proteins, it has remained a daunting task to analyze multifactorial and complex phenotypes at the systemic level. Soon it became evident that phenotypes result from characteristic gene expression signatures involving simultaneous and coordinated expression patterns of many genes. With the rise of the genome sequencing era in the 1990s, genome sequences from many organisms became accessible. Yet researchers did not have the technology in their hands to analyze the expression of more than a few genes at a time. It was originally a competitive sequencing technique that yielded rapidly a powerful technology for whole genome expression profiling. Sequencing by hybridization (SBH) was proposed as an alternative approach to *de novo* DNA sequencing and utilized short oligonucleotide probes of defined sequence to search for complementary sequences on an unknown target DNA (Strezoska et al., 1991). A significant improvement was achieved by Stephen Fodor and colleagues. They reversed the configuration and attached oligonucleotide probes to an array surface that could be hybridized to known target DNAs of interest (Fodor et al., 1991; Pease et al., 1994). Due to fluorescent labeling, the hybridization pattern directly revealed the identity of all complementary probes. An important prerequisite for this approach was the development of a photolithographic combinatorial chemistry strategy that allowed the synthesis of oligonucleotide probes on the surface of miniaturized arrays. Initially, a matrix of 256 spatially defined oligonucleotide probes was generated. Nowadays, capacities of probing short oligonucleotides - usually 60mers - representing the genes of entire genomes on microarrays are realized. Notably, sequence specificity has been demonstrated down to single base pair mismatches emphasizing the accuracy and stringency of the method (Chee et al., 1996). Over the last decade microarrays have become a widely used tool for genome-wide expression profiling between two phenotypic states (e.g. disease vs non-disease). Although the financial costs for the equipment to carry out microarray experiments remain high, most researchers have nowadays access to this technology due to the establishment of core facilities at many research centers. As of today, commercially available arrays feature the genes of entire genomes from diverse model organisms, including mice and man, thereby allowing assessment of the complete transcriptome of a tissue or cell type of interest. The procedure itself starts with the extraction of total RNA from cells or tissues, for example from a healthy and a diseased tissue (Figure 8).

Introduction

mRNA is then labeled by fluorescent or chemiluminescent dyes for later detection of hybridization between complementary samples and probes on the microarray. In addition, template RNA may be amplified by in vitro transcription. Samples are then hybridized to the array and fluorescence or chemiluminescence of bound probes is detected with a scanner. Signal intensities are normalized and subsequently analyzed with detection algorithms for differential gene expression patterns. Significance and functional grouping of differentially expressed genes can be assessed using biological knowledgebases. Finally, candidate genes are validated by independent techniques such as quantitative PCR. Besides expression profiling, microarray analysis is also used for the detection of single nucleotide polymorphisms (SNPs) due to high sequence specificity of the hybridization between samples and probes. In addition, a second competitive gene expression profiling technique emerged in the 1990s called serial analysis of gene expression (SAGE). This method was introduced by Kinzler and coworkers and is based on two basic principles (Velculescu et al., 1995). First, a cleavage site for a restriction enzyme at a fixed distance from the poly(A) tail allows specific detection of mRNA transcripts. Second, the sequence identity of extracted transcript fragments is determined by primary sequencing reactions. Altogether, the SAGE procedure encompasses multiple enzymatic, PCR amplification, purification and cloning steps that are finalized by a sequencing reaction. It starts with the purification of mRNA on solid phase oligo(dT) beads followed by subsequent cDNA synthesis (Figure 9). The cDNA is then digested with a restriction enzyme, that is also called anchoring enzyme (AE), to reveal the closest 3'-cleavage site with respect to the poly(A) tail of a given transcript. A commonly used anchoring enzyme is *Nla*III recognizing a 4 bp cleavage site that is predicted to occur every 256 bp and is therefore likely to be present on most mRNA species. In the next step, the sample is equally divided and then ligated to two different linkers. Both linkers are recognized by an restriction enzyme, also called the tagging enzyme (TE), that cuts 10 bp 3' from the anchoring enzyme yielding a transcript fragment known as the SAGE tag. The SAGE tags are then ligated to form ditags and amplified by PCR using primers designed against the known linker sequences. Following PCR amplification the ditags are released from the linker, become serially ligated creating concatenates that are cloned and finally sequenced. The initial data analysis comprises two essential steps: 1) Examining the sequence identity of the SAGE tags. 2) Identification of the corresponding genes by comparison to a reference database. Relative expression levels can be calculated by dividing the unique tag count by the total tags sequenced. The fold change of gene expression changes between two sample groups is determined by the ratio of tags between libraries.

Introduction

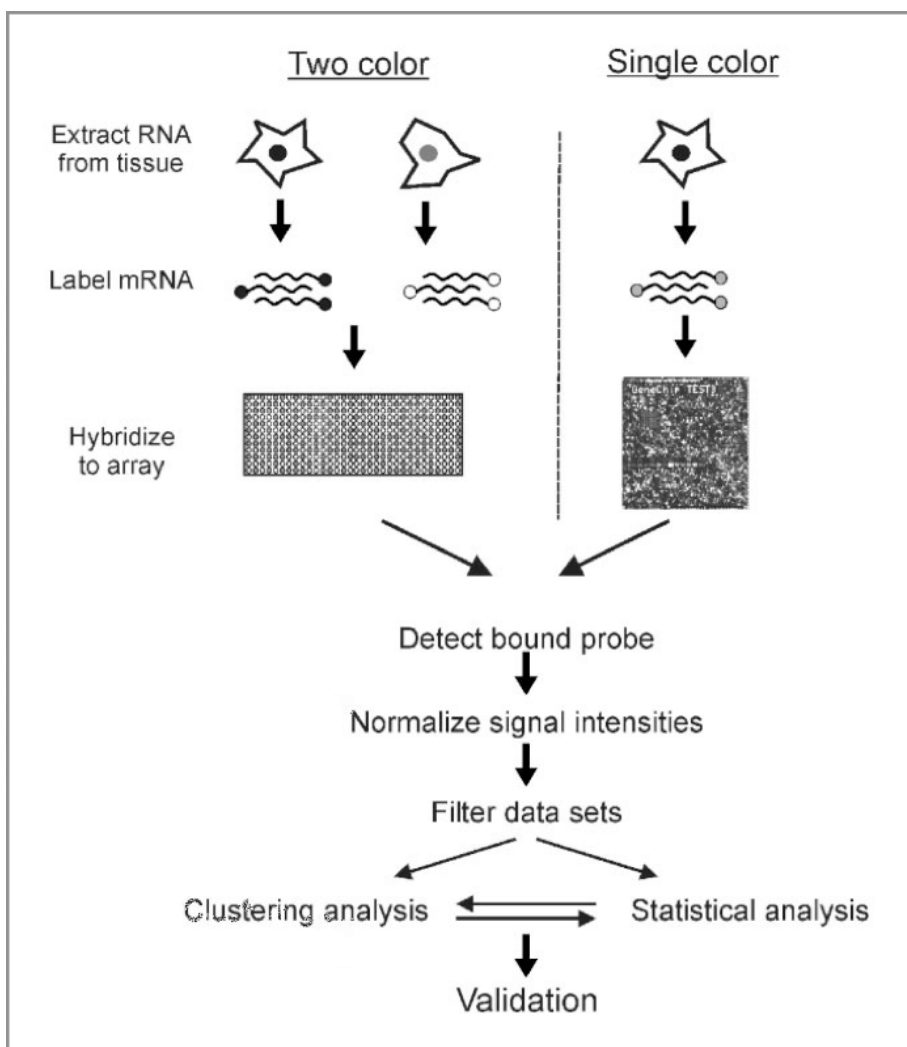


Figure 8. Workflow of the critical steps during a microarray experiment.

mRNA is purified from cells or tissue(s) of interest and subsequently labeled for later chemiluminescent or fluorescent detection. The labeling process may also involve amplification of the template RNA (not shown). Labeled mRNA is then hybridized onto the microarray where it binds specifically to complementary DNA sequences (competitively for two-color arrays; non-competitively for single-color arrays). Bound sequences are detected and identified according to their position on the array. Signal intensities are then normalized to enable interarray comparisons. Normalized data sets are subjected to computational analysis yielding a list of differentially expressed transcripts that may be further analyzed using biological knowledgebases. Finally, candidate genes are validated with alternative methods, for example by quantitative PCR (from Cook & Rosenzweig, *Circ Res* 91(7):559-64. October 2002).

Introduction

There are subtle differences between expression profiling based on microarray versus SAGE analysis. The latter technique seems to be slightly more sensitive as less starting material is needed. Microarray experiments require typically the preparation of at least a few nanograms of total RNA. In contrast, only a few cells are technically sufficient to perform a SAGE analysis due to the PCR amplification step. In addition, the SAGE technique has the advantage that no prior sequence information of the interrogated sample is needed whereas hybridization on microarrays can be only performed against known oligonucleotide probes (Velculescu et al., 2000). However, with several genomes - including the human genome - being sequenced and annotated this has not been a major obstacle anymore for the past decade. A strength of microarray experiments is, they do require less time and effort especially with regard to the efficient semi-automated commercial setups that have been developed in recent years.

Both, the SAGE and microarray technology, have greatly contributed to the field of functional genomics that aims to understand the relationship between the genome of an organism and its phenotype. Whole genome measurement technologies have also paved the way for the feasibility of systems biology approaches that attempt to elucidate not only the molecular components but also their interactions within networks of a cell type, tissue or entire organism (Tegner et al., 2007). Due to the large amount of data from whole genome expression profiling studies, computational analysis including the use of biological knowledgebases has become a prerequisite for data mining (Kitano, 2002). Synergistic use of bioinformatics and whole genome technologies has yielded novel conceptual approaches for systems biology such as reverse engineering that can be viewed as a „process of identifying gene networks from whole genome data using an underlying computational model“ (Tegner et al., 2003).

Introduction

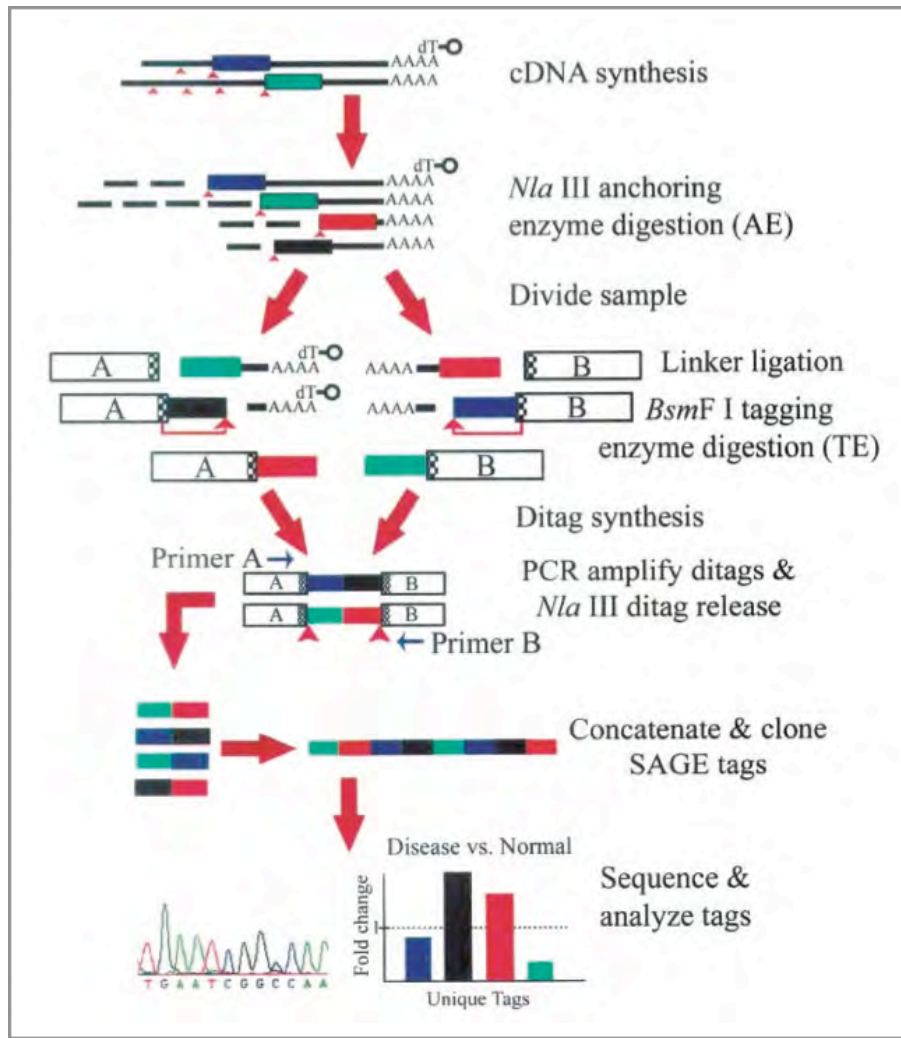


Figure 9. Schematic illustration of the SAGE protocol.

Double-stranded cDNA is synthesized on mRNA templates bound to oligo(dT) beads (circles). Digestion with the anchoring enzyme (AE) exposes the 3' most restriction site. The resulting fragments are equally divided and ligated to different linkers (A and B) yielding the SAGE tag. The SAGE tags are then blunted-ended and ligated to ditags, PCR amplified with primers against the linkers, ligated to concatenates, cloned and finally sequenced (from Patino et al., *Circ Res* 91(7):565-69. October 2002).

Introduction

Systems biology studies in the genomics era were first conducted in prokaryotic organisms and yeast but have been extended to mammalian models in recent years (Gardner et al., 2003; Mustacchi et al., 2006; Basso et al., 2005; Calvano et al., 2005). This „bottom-up“ approach, moving from relatively simple to more complex model systems, has been a common and successful strategy in life science research. For example, basic mechanisms of gene regulation were initially discovered in peas, fruit flies and bacteria and then applied and extended to mammalian systems (Mendel, 1950; Morgan, 1911; Jacob & Monod, 1961). However, Tegner and colleagues propose in parallel a „top-down“ approach that starts with a phenotype (e.g. a multifactorial disease) in humans or animal models and narrows down to „simple“ cellular models (Tegner et al., 2007). Reverse engineering may thereby be used to identify „principal networks“ in complex traits that comprise most of the key interactions between their molecular components. These networks, representing sub-phenotypes, can then be further delineated and most importantly also manipulated in appropriate cellular model systems. Manipulation can encompass a variety of measures including gene silencing or specific inhibition of their respective proteins.

Coronary artery disease (CAD) resulting from atherosclerosis is a multifactorial disease based on genetic predisposition(s) and environmental pressures (Watkins & Farrall, 2006). It is therefore an excellent example for a complex trait that may be amenable to a systems biology approach. CAD is a degenerative inflammatory disease of the arterial wall leading to the formation of atherosclerotic plaques that can eventually cause adverse clinical events such as myocardial infarction. From the systems biology perspective, a key assumption is that the CAD phenotype must be in some way also represented by the components (e.g. cells, metabolites and proteins) that are most affected by the disease. These components presumably reflect the environmental influences filtered through the genetic composition of an individual. Over years, lifestyle factors such as food intake and stress were believed to alter gene expression patterns related to lipid metabolism and inflammation, both of which are known factors contributing to the disease phenotype (Glass & Witztum, 2001). However, current knowledge about atherosclerosis is largely a fragmented picture based on single candidate gene approaches (e.g. knock-outs) and individual risk factors (e.g. inflammatory markers). Therefore, whole genome measurement technologies such as microarray expression profiling together with computer-assisted modeling of biological knowledgebases harbor the potential to unravel systemic gene regulatory networks of the CAD phenotype at the mRNA level.

1.7 Working hypothesis and experimental approach of the second thesis project

Atherosclerosis has once been defined as a lipid storage disease but is now widely recognized as a chronic inflammatory condition of the arterial vessel wall. So far research has largely focused on the atherosclerotic lesion site including resident vascular cell types and infiltrating immune cells that both contribute to the development and progression of atherosclerotic plaques (Hansson & Libby, 2006). Circulating blood cells are the source for many inflammatory cell types within the plaque and represent an interface between immune system and atherosclerotic lesion(s). However, whether circulating blood cells themselves do reflect and possibly contribute to the disease phenotype is poorly understood (Kang et al., 2006). Therefore, this study aimed to investigate the whole blood transcriptome from CAD patients using a systems biology approach by microarray expression profiling and subsequent biological knowledgebase-assisted analysis of differentially expressed genes. In the first step a small but prospectively matched study cohort was assembled that featured individuals diagnosed with atherosclerotic coronary artery disease and healthy control subjects. Whole blood samples were collected and total mRNA from circulating blood cells was prepared for hybridization onto whole genome microarrays. A novel algorithm designed for the detection of heterogenous and sparse signals was used for differential expression analysis. Biological knowledgebases were then applied to identify networks and functional groups within the differentially expressed genes. Finally, candidate genes representing different functional categories were validated by quantitative PCR.

II. Material and Methods

1. Study subjects

Following a protocol that was reviewed and approved by the Veterans Administration Pacific Islands Healthcare System (VAPIHCS), the University of Hawaii IRB and the United States Army Medical Research and Materiel Command Human Research Protection Office, age and ethnicity matched groups of subjects that had no evidence of chronic or active infectious or autoimmune diseases were recruited. Using a relational data warehouse, developed at VAPIHCS to mirror its clinical database (VistA) (Advani et al., 1999, Proc AMIA Symp, 653-7), eligible patients were electronically identified as having diagnoses and clinical laboratory results appropriate for enrollment based upon the inclusion and exclusion criteria listed below.

Inclusion criteria for the two age, gender and ethnicity-matched study groups were as follows: 1) Individuals diagnosed with early-onset coronary artery disease (EMI) that had an ICD-9 code for myocardial infarction (MI) before age 50 but at least more than 6 months prior to screening and enrollment. These individuals were undergoing standard post-MI therapy and were taking any of a specific set of cardiac-related medication classes including acetylic salicylic acid (aspirin), angiotensin converting enzyme (ACE) inhibitors, angiotensin receptor type 1 blockers, β -adrenoceptor blockers and 3-hydroxy-3-methylglutaryl coenzyme A reductase inhibitors (statins). 2) Medicated control individuals (MCON) did not have an ICD-9 code for myocardial infarction but were taking any combination of these medications.

Criteria for exclusion were 1) treatment of active infection within the last month, 2) a clinical history of chronic infection or rheumatologic disease, 3) active use of non-steroidal anti-inflammatory drugs, 4) laboratory evidence of active infectious or autoimmune disease, 5) a history of an MI within the last 6 months, 6) an absolute monocyte count < 125 cells/ μ l within the last year, 7) anemia defined as hemoglobin < 10 g/dL or HCT $< 30\%$ within the last year (CAD subjects were excluded if their hemoglobin levels were < 11 g/dL or HCT $< 33\%$), 8) CRP ≥ 2.0 mg/dL or ESR ≥ 30 mm/hr. In addition, potential subjects with active pregnancy or dementia were excluded. Finally, subjects with severe active mental illness were excluded based upon review of the medical record. All eligible subjects were invited to be screened for enrollment. After giving informed consent, eligible subjects were given a detailed medical history questionnaire to record baseline characteristics, such as past medical history, medication use and habits.

Material and methods

All subjects screened also underwent routine clinical laboratory testing, which included a complete blood count with differential, comprehensive metabolic profile, erythrocyte sedimentation rate and C-reactive protein level. Eligible subjects that were not excluded during the screening process were invited to return for a second blood draw, when 80 ml of blood was collected for RNA extraction. This process yielded two study groups (EMI and MCON) with 10 subjects in each group.

2. RNA purification

Total RNA was isolated from peripheral blood drawn from the study subjects using the Qiagen PAXgene RNA Kit (Valencia, CA) according to the manufacturer's instructions. Briefly, blood was incubated in PAXgene Blood RNA Tubes at room temperature for 2 h to ensure complete lysis of blood cells and subsequent stabilization of RNA. Nucleic Acids were then pelleted for 10 minutes at 4000 g and washed once in RNase-free water. The pellet was resuspended and incubated with Proteinase K for 10 minutes at 55 °C. Remaining cell debris and proteins were removed by centrifugation at 20.000 g for three minutes through a shredder spin column. Flow-through was transferred into a RNA spin column and binding conditions were adjusted by adding half the volume ethanol. DNA was removed by treatment with DNase I for 15 minutes at room temperature. After several washing steps RNA was eluted twice in 40 µl elution buffer. Up to 70 % of whole blood mRNA consists of globin transcripts that were removed subsequently with Ambion GLOBINclear Reduction Kit (Foster City, CA). Briefly, biotinylated globin probes were hybridized to purified whole blood RNA and globin transcripts were depleted with streptavidin magnetic beads. Final RNA concentration was determined with a NanoDrop ND-100 Spectrophotometer (Wilmington, DE). RNA quality was assessed using the RNA LabChip Kits on an Agilent Bioanalyzer 2100 (Santa Clara, CA). Samples with a RNA integrity number (RIN) of ≥ 7 were further processed for microarray hybridization. The RIN is a score on a scale from 1 to 10 determined by Agilent Bioanalyzer software using an algorithm that is based on the data of 1300 electropherograms of total eukaryotic RNA ranging from completely degenerated (score = 1) up to highly intact (score = 10) samples. In addition to ribosomal ratios this procedure allows quality assessment of total RNA with respect to the complete electrophoretic trace (Imbeaud et al., 2005; Schroeder et al., 2006).

3. Microarray hybridization

1 µg of total RNA from each sample was processed using Applied Biosystems NanoAmp RT-IVT Labeling Kit (Foster City, CA) to generate digoxigenin (DIG, Roche)-labeled cRNA for microarray hybridizations. Double-stranded cDNA was synthesized from RNA template and in vitro-transcribed resulting in approximately 100-fold amplified DIG-labeled cRNA. 10 µg of cRNA from each sample were hybridized onto Applied Biosystems Human Survey Genome Microarray 2.0 (Foster City, CA) containing 32,878 probes for the interrogation of 29,098 genes, of which 21 % have been curated only by Celera Genomics and 79 % were based on public databases. After hybridization each microarray was scanned with an Applied Biosystems 1700 Chemiluminescent Microarray Analyzer (Foster City, CA). Chemiluminescent images from each microarray were auto-gridded, then spot and spatially normalized. Chemiluminescent signals were quantified, corrected for background and the final images and feature data were processed using the Applied Biosystems 1700 Chemiluminescent Microarray Analyzer software v1.1. Data and images were collected through an automated process for each microarray using the ABI 1700 Analyzer platform. Each biological sample of this study was assayed and analyzed on a single microarray as previous work in our laboratory and by others has consistently demonstrated limited variability between technical replicates (Shi et al., 2006).

4. Data analysis

A novel detection algorithm that utilizes a localized version of statistical testimation (LOTEST) was used to detect a global signal for differential gene expression between cases (EMI) and controls (MCON) (Okimoto, 2006). First, the data output from each microarray was vectorized to form a column of an expression data matrix where the control and EMI samples segregated into two disjoint groups (Figure 10 A). Each row of the data matrix represents the expression profile of a gene across the control and EMI sample groups. The data matrix was then quantile normalized to suppress low-frequency systematic (experimental) error and log₂ transformed to equalize variation (fold change) over intensity (expression). A Ratio-Intensity (RI) scatter plot of mean log₂ ratio (MLR) versus mean log₂ expression (MLE) was generated where each gene was represented by a point in (MLR/MLE) space (Figure 10 C). Genes with similar mean log₂ expression levels were grouped across the x-axis in 51 quantile bins, where each bin contained approximately 650 genes.

Material and methods

Statistical testimation based on the Donoho-Johnstone Universal Threshold (DJUT) was computed for each bin to detect genes that were differentially expressed (Donoho & Johnstone, 1994, Sabatti et al., 2002). The genes that exceeded the DJUT for each bin, together, formed a global estimate of the signal for differential gene expression between EMI and control samples. The LOTEST algorithm can be viewed as a localized „test-and-estimate“ (testimation) procedure to detect a sparse signal of differential expression - embedded in additive Gaussian noise - that simultaneously controls for multiple comparisons. Localized testimation for the detection of differentially expressed genes has been implemented in a web-based software application called **Microarray ANalysis of INtensities and RatIos** (MANINI) that is publicly available on the internet for registered academic users at <http://crchbioinfo.org/CRCHXpress>. The resulting list of differentially expressed genes identified by the LOTEST algorithm was further analyzed using row-clustered heatmaps and principal component analysis (PCA) (Fig. 11). Ingenuity Pathway Analysis (Ingenuity Systems, Inc, Redwood City, CA) and PANTHER (www.pantherdb.org) knowledgebases were used to identify sets of functionally related genes and signaling pathways that were overrepresented in the list of differentially expressed genes. The overrepresented pathways defined subsets of genes that were likely to have functional relevance to early MI. The genes contained in significant IPA networks and PANTHER functional categories were depicted in row-clustered heatmaps and were further analyzed by visual inspection for consistency of expression levels in order to discriminate truly differentially expressed genes between EMI and control samples. These discriminatory genes were used to define a set of candidate genes with significance for atherosclerotic coronary artery disease.

5. Real-time PCR

Candidate genes for potential biomarkers were further validated by quantitative real-time PCR analysis. 1 µg of total RNA from selected samples was reverse transcribed into cDNA using Superscript III cDNA Synthesis Kit from Invitrogen (Carlsbad, CA) according to the manufacturer's instructions. 100 ng of cDNA template for each sample were amplified with Applied Biosystems TaqMan Gene Expression Assays for the corresponding gene and Applied Biosystems TaqMan Gene Expression Master Mix according to the manufacturer's instructions (Foster City, CA). All samples were assayed in triplicates. Gene expression values were calculated relative to GAPDH levels (as an internal standard) using the $2^{-\Delta\Delta CT}$ method (Livak & Schmittgen, 2001; Schmittgen & Livak, 2008).

Results

III. Results

3.1 The study cohorts

To analyze global gene expression profiles in circulating blood cells of patients with early onset coronary artery disease 10 subjects with early myocardial infarction (EMI) were recruited. Using their age and ethnicity data, a matched cohort of 10 medicated control subjects (MCON) without a known diagnosis of coronary artery disease or EMI was assembled. Each group comprised two black, four asian and 4 caucasian patients with ages ranging from 43 to 60 (Table 1). Neither mean body weight (approximately 92 kg) nor body mass index (29) was different between the groups. Values for traditional cardiac risk factors, such as hypertension, diabetes, hyperlipidemia, cigarette use, and family history of heart disease, were similar across the study groups. Comparing the clinical laboratory results also revealed no significant differences among the groups (data not shown). From each patient one whole blood sample was available for RNA extraction and subsequent microarray analysis.

	EMI (n=10)	MCON (n=10)	p-value
Age, average±SD, y	51.5±5.79	51.5±5.79	1.0000
Ethnicity, %			
Black	20	20	1.0000
Asian	40	40	1.0000
Caucasian	40	40	1.0000
Weight±SD, kg	89.5±13.0	94.6±15.1	0.1873
Body Mass Index ±SD	28.7±4.6	29.7±3.5	0.7103
Hypertension, %	50	70	0.6831
Diabetes mellitus, %	30	20	1.0000
Hyperlipidemia, %	80	70	1.0000
Smoking status, %	20	10	1.0000
Family history, %	10	10	0.4795

Table 1. Clinical characteristics of early myocardial infarction (EMI) and medicated control (MCON) subjects.

Depicted are for each study group the clinical parameters age, ethnicity, body weight & body mass index as well as the history of hypertension, diabetes, hyperlipidemia, smoking status and history of cardiovascular disease, respectively. p-values were calculated from the t-test for continuous variables and the McNemar's test for categorical covariates.

Results

3.2 Two step sample quality control analysis

Purified RNA samples with an RNA integrity number (RIN) of 7 were deemed sufficient for downstream processing and microarray analysis (see also Material & Methods). All 20 samples (MCON and EMI) revealed a RIN > 7, and therefore were processed for microarray hybridization (data not shown). To evaluate the quality of microarray hybridization, the raw data were tested using box-and-whisker plots and histograms (Figure 10 A and B). From the box plot diagram it is obvious that sample MCON 4 produced increased amounts of outliers and a strongly decreased interquartile range compared to all other samples (Fig. 10 A). Histogram analysis revealed similar distributions of the expression data for all samples with the exception of MCON 4 (Fig. 10 B). Due to the high likelihood that there was a technical or experimental problem with sample MCON 4, it was excluded from further data analysis. Therefore, the final dataset available for differential expression analysis included 10 EMI samples and 9 MCON samples.

3.3 Analysis of differential gene expression in circulating blood cells of patients with early-onset coronary artery disease

The LOTEST algorithm, a localized „test-and-estimate“ procedure for detecting a sparse signal embedded in additive Gaussian noise, was used to analyze differential gene expression between the EMI and MCON groups (Okimoto, 2006). A Ratio-Intensity (RI) scatter plot of mean log₂ ratio (MLR) versus mean log₂ expression (MLE) was generated where each gene was represented by a point in (MLR/MLE) space (Fig. 10 C). Genes with similar mean log₂ expression levels were grouped across the x-axis in 51 quantile bins (black and yellow stripes), where each bin contained approximately 650 genes. Assuming that only a small percentage of genes in a bin were truly differentially expressed, i.e., that the signal for differential expression was sparse, a threshold was computed for each bin based on the Donoho Johnstone universal threshold (DJUT) of wavelet denoising theory (Donoho & Johnstone, 1994; Sabatti et al., 2002). Using this approach, 1203 differentially expressed genes were detected between EMI and MCON samples with 664 genes up-regulated and 539 genes down-regulated in the EMI group (Figure 10 C).

The expression intensity (fold change) for each gene was plotted in a color-coded heatmap with genes numbered on the vertical axis and the corresponding MCON/EMI samples placed on the horizontal axis (Figure 11 A). In the heatmap, the expression data fall into four clusters with down-regulated genes of EMI samples located in the top half and up-regulated genes in the bottom half and vice versa for the MCON group.

Results

Furthermore, heatmap diagrams ensure visual identification of genes that display truly consistent expression patterns across the sample groups (EMI vs MCON). After visual inspection of the clustered heatmap containing all differentially expressed genes, 195 genes (panel of genes 540 to 735) were excluded from further analysis as most of the variation in expression for this set of genes was contributed by only two samples (EMI2 and EMI5). Downstream data analysis using the biological knowledgebases PANTHER and IPA revealed no significant functional grouping or pathway structure in these genes (data not shown).

In addition, principal component analysis (PCA), a mathematical procedure in multivariate analysis providing a lower dimensional picture of a complex data matrix, was performed (Pearson, 1901; Miranda et al., 2008). PCA is often used as a tool in exploratory data analysis to distinguish data according to their variance. Principal component analysis of the differentially expressed genes identified by the LOTEST algorithm clearly separated EMI from MCON individuals (Figure 11 B). Interestingly, PCA results also indicated that samples EMI2 (asian), EMI5 (caucasian) and EMI7 (caucasian) were distinct from the rest of the EMI group. The separation of EMI 2 and EMI 5 in PCA results may also be related to the differences observed in the expression patterns for the genes 540 to 735 as described above. PCA separates sample EMI 7 from the rest of the EMI group as well and EMI 7 also displays two patches of unique expression patterns in the top (genes 100 to 200) and bottom half (genes 1050 to 1100) compared to other EMI subjects (Figure 11 A).

Results

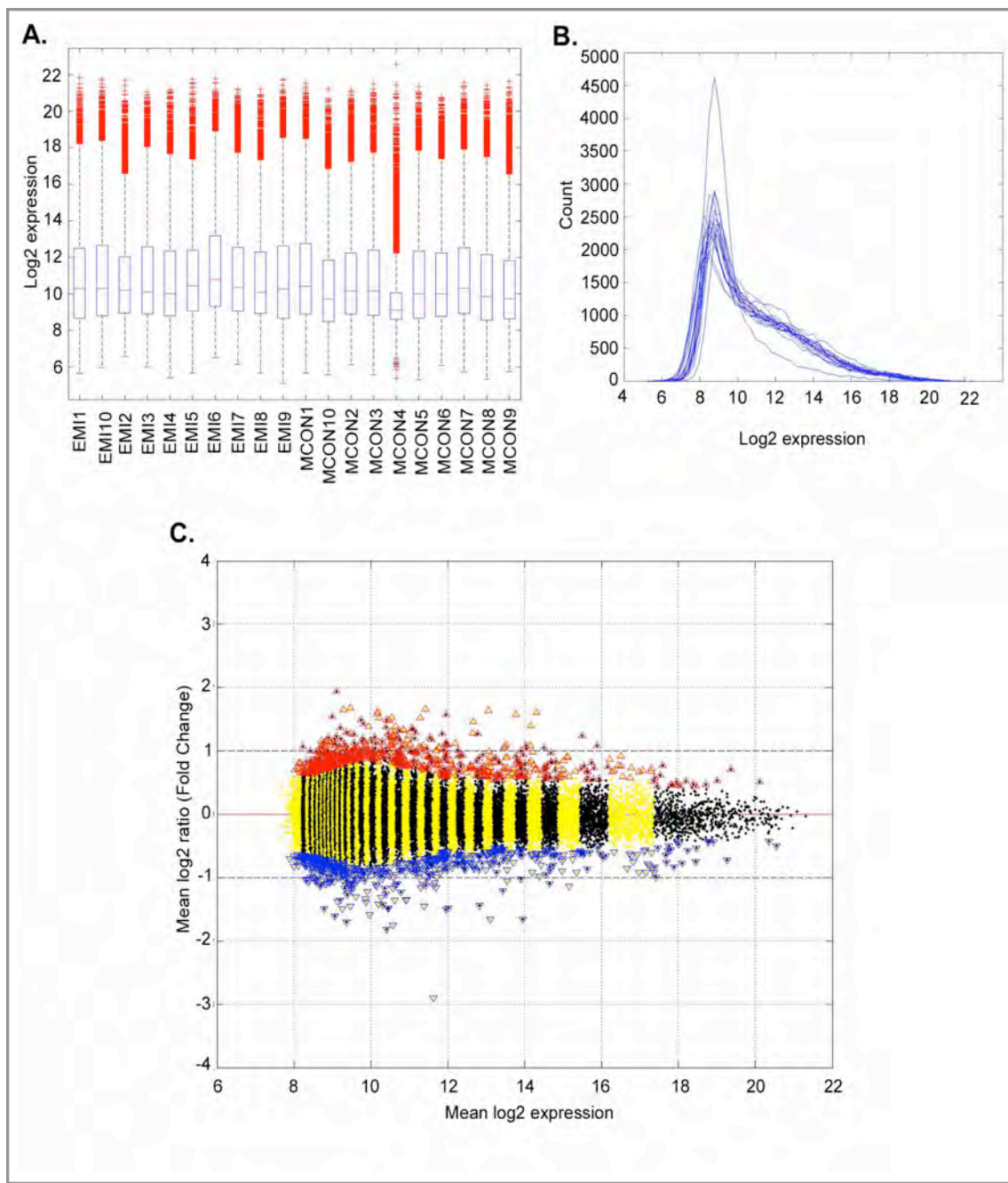


Figure 10. Microarray sample quality control and detection of differentially expressed genes.

(A) Box and whiskers plots of raw microarray data. Samples are depicted along the horizontal axis while log2 expression intensities for each gene are plotted on the vertical axis; the upper and lower ends of the box contain all genes between the first and third quartiles of log2 expression; the red line in each box represents the median log2 expression; the upper and lower ends of the dotted vertical lines represent outliers of log2 expression. **(B)** Histogram of raw microarray data, showing the number of genes with a given log2 expression intensity. **(C)** Ratio-intensity (RI) plot of the quantile normalized microarray data. The results of the LOTEST differential expression analysis are superimposed on the RI plot with fold change (ratio) of gene expression is plotted versus log2 expression (intensity). The vertical black and yellow stripes represent 51 sets of approximately 650 genes having similar levels of fluorescent intensity. The dots in red triangles show the up-regulated and the dots in blue triangles show the down-regulated genes.

Results

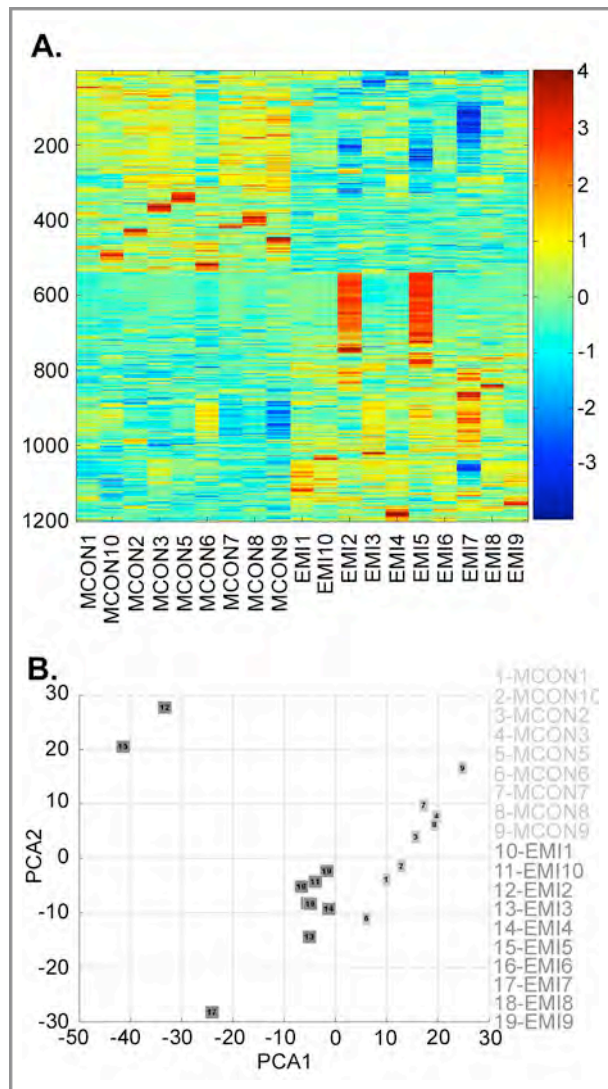


Figure 11. Clustered heatmap and principal component analysis (PCA) of all differentially expressed genes identified by the LOTESt algorithm in EMI compared to MCON samples.

(A) Clustered heatmap: genes are numbered on the vertical axis and the columns represent the specified subject. The color of each rectangle represents the expression value (as fold change) of a gene according to the color scale bar on the right. (B) Principal component analysis (PCA) of all differentially expressed genes separates the EMI (dark squares) from the MCON (bright squares) group.

Results

3.4 Application of gene ontology databases to identify functional gene expression signatures in circulating blood cells associated with coronary artery disease (CAD)

Clustered heatmap and principal component analyses describe overall changes in gene expression, but provide few insights into the biological processes and signaling networks involved in propagation and manifestation of a disease phenotype. Identifying the perturbed biological networks underlying a complex clinical phenotype such as coronary artery disease requires systematic analysis of the contributing gene functions based on known mammalian biology (Calvano et al., 2005). To identify functionally significant expression patterns in EMI subjects, the list of differentially expressed genes was further analyzed by screening gene ontology databases. Ontologies represent a formal structuring of knowledge that is ideally suited and amenable to computational analysis of complex data sets. In this study, web-based entry tools of the two biological knowledgebases IPA (Ingenuity Pathway Analysis) and PANTHER (Protein Analysis Through Evolutionary Relationships) were applied to analyze the obtained microarray expression data. These bioinformatics knowledgebases enable a new analytical approach that objectively examines large experimental data sets in order to identify significant functional patterns. Therefore, this methodology is in particular applicable to high-throughput platforms such as whole-genome microarray expression profiling. Furthermore, the original literature detailing the functional categories and interactions can be accessed to examine and verify the findings.

3.5 Ingenuity Pathway Analysis (IPA) identifies inflammatory gene expression signatures and immune imbalance in EMI samples

The IPA database from Ingenuity Systems is a unique resource that aims to identify networks of interacting genes representing functional modules within a microarray expression data set (www.ingenuity.com). These networks contain approximately 25 to 30 genes with a functional relationship and direct physical, transcriptional or enzymatic interactions based on manually curated findings of hundreds of thousands full-text articles in the peer-reviewed scientific literature. Every network is characterized by one or more hub genes that represent a central interface due to their multiple interactions with other genes.

The 1008 genes identified as differentially expressed by the LOTESt algorithm and their corresponding expression values were fed into the IPA database. The IPA algorithm detected four significant networks with 26 to 30 focus molecules each (Table 2).

Results

The network with the highest significance (score of 46) contained „Cell Death, Immunological Disease, Immune Response“ as top functions. The following networks with a score of 37 comprised also immunological themes such as „Immune and Lymphatic System Development and Function“ (network 3) but also diverse functions such as „Cell Morphology“, „Connective Tissue Development and Function“ (network 2) and „Cellular Assembly and Organization“ in network 4 (Table 2). Subsequent networks had scores below 25 and were therefore excluded from further analysis (data not shown). To evaluate consistency of gene expression patterns across the sample groups the top four networks were additionally analyzed using clustered heatmap diagrams. Criteria for consistency were matched if more than 50 % of subjects within EMI and MCON samples displayed a fold change in expression > 1 according to the color scale bar of the corresponding heatmap. This procedure was considered an important measure to identify false positives among the differentially expressed genes.

#	Top Functions	Score	Focus Molecules
1	Cell Death, Immunological Disease, Immune Response	46	30
2	Cell Morphology, Cellular Response to Therapeutics, Connective Tissue Development and Function	37	26
3	Cellular Function and Maintenance, Hematological System Development and Function, Immune and Lymphatic System Development and Function	37	26
4	Gene Expression, Cellular Assembly and Organization, Cellular Movement	37	26

Table 2. The top four networks identified by Ingenuity Pathway Analysis (IPA).

„Score“ is a ranking algorithm of IPA and „Focus Molecules“ indicates the number of genes within a network. Immunological functions are indicated in bold.

Network 1 contains a total of 28 genes of which 15 genes were up-regulated (top half) and 13 genes down-regulated (bottom half) in EMI subjects (Figure 12 B). The up-regulated FOS is the major hub gene of this network (Figure 12 A). However, visual inspection of the heatmap revealed that differential expression of FOS is only driven by individual EMI 7 (Figure 12 B, row 2). Genes that displayed a more consistent up-regulation across EMI samples were AHNAK (row 5), PTX3 (row 7), JAG1 (row 9), CRABP2 (row 11) and MLLT7 (row 14). AHNAK or desmyokin mediates in a complex with L-type Ca²⁺-channels activation of cytolytic T-cells that kill virally infected cells, tumor cells and potentially autoreactive T-cells (Matza et al., 2009). PTX3 or pentraxin 3 is a member of the pentraxin family and is a pro-inflammatory peptide of the innate immune system that results in complement activation (Botazzi et al., 2005).

Results

Similar to CRP (C-reactive Protein), PTX3 behaves as an acute phase protein with low blood levels under normal physiological conditions that increase rapidly during inflammatory processes. JAG1 or serrate is a Notch-ligand and a positive regulator of T-cell development, peripheral T-cell activation and effector cell differentiation (Yuan et al., 2010). CRABP2 is a retinoic acid binding protein with unknown function but increased levels were recently found in a murine model of degenerative joint disease (Welch et al., 2009). MLLT7 or Foxo4 belongs to the winged/helix forkhead family of transcription factors (Katoh & Katoh, 2004). Genes in network 1 that were down-regulated included CCI22 (row 16), S100B (row 17), CCR7 (row 20), TXNL2 (row 22), SNFT (row 23), TAGLN (row 24) and NOX4 (row 25). CCL22 or chemokine ligand 22 is a cytokine that acts chemotactic on monocytes, dendritic cells, natural killer cells and chronically activated T-cells (Gear & Camerini, 2003). S100B belongs to the S100 family of proteins containing 2 EF-hand calcium-binding motifs and is involved in diverse Ca^{2+} -dependent cytoplasmic signaling cascades (Donato, 2001). CCR7 encodes a chemokine receptor that is important for immune protection but also for immune tolerance as loss of expression results in multiple organ auto-immunity (Sanchez-Sanchez et al., 2006; Worbs & Förster, 2007). TXNL2 or PICOT (PKC-interacting cousin of thioredoxin) interacts with protein kinase C (PKC) via its thioredoxin homology domain and is a modulator T-cell receptor signaling (Isakov & Altman, 2002; Kato et al., 2008). SNFT or p21^{SNFT} is a basic leucine zipper transcription factor and inhibits IL-2 transcription, a major stimulator of T-cell activation (Iacobelli et al., 2000). Therefore, down-regulation of SNFT indicates increased IL2-levels in EMI subjects. TAGLN or transgelin encodes an acting-crosslinking protein, its disruption has been recently shown to enhance inflammation of the vasculature during atherosclerosis (Shen et al., 2010). NOX4 belongs to the family of NADPH oxidases and has been implicated in hypertension, vascular inflammation and atherosclerosis (Sedeek et al., 2009; Schröder, 2010; Lassegue & Griendling, 2010). In summary, the expression pattern of the represented genes in network 1 suggests an alert and active immune system with pro-inflammatory themes. Activating and pro-inflammatory factors of the immune response (AHNAK, PTX3, JAG1) were significantly up-regulated whereas antagonists of inflammation (SNFT, TAGLN) as well as an important inhibitor of auto-immunity (CCR7) were down-regulated within the EMI group compared to medicated control samples (Table 3).

Results

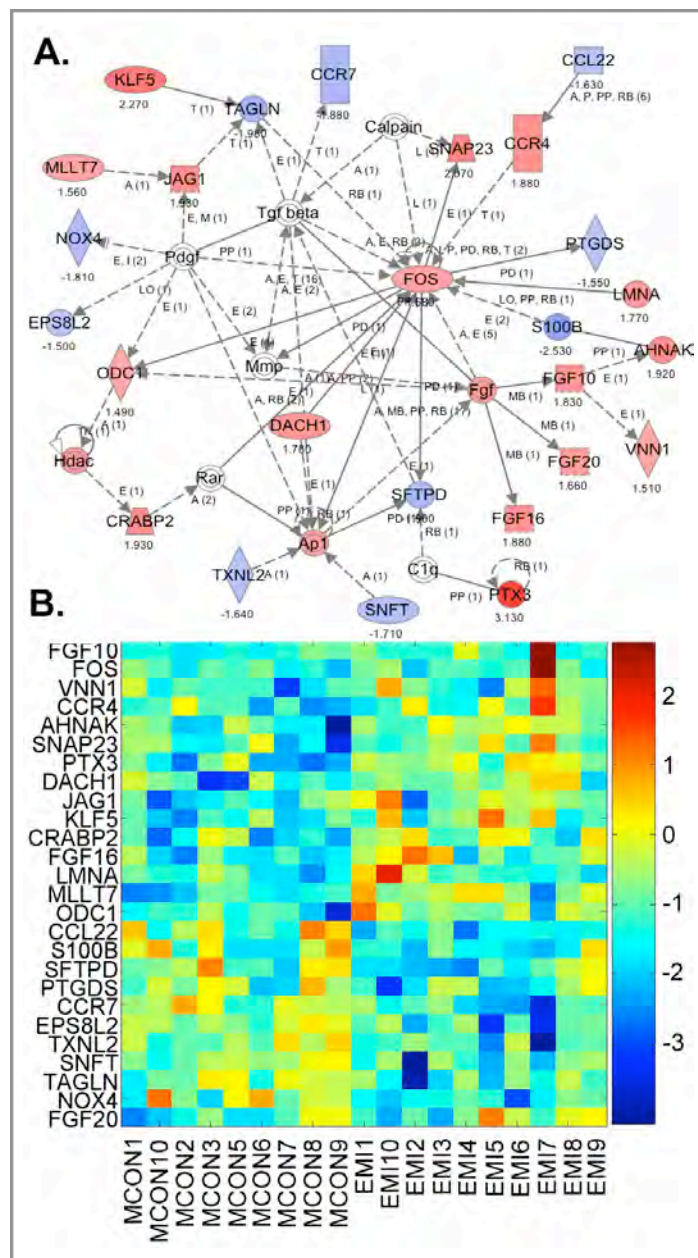


Figure 12. Ingenuity Network 1.

(A) Red color denotes up- and blue color down-regulation of a particular gene. Solid lines denote direct, dotted lines indirect interactions. Arrowheads indicate direction of interactions. The gene with the most connections (FOS) is defined as a hub-gene. Symbols: square = ligand, rectangle = receptor, circle = cytoplasmic protein, rhomboid = enzyme, oval = transcription factor. **B.** Clustered heatmap of genes contained in Ingenuity Network 1. The color of each square represents the expression value (as fold change) of a gene according to the color scale bar on the right.

Results

Gene Symbol	Reference
AHNAK	Matza et al., <i>Proc Natl Acad Sci U S A</i> 2009; 106:9785-9790.
PTX3	Botazzi et al., <i>Curr Opin Immunol</i> 2006 Feb;18(1):10-5.
JAG1	Guidos CJ, <i>J Exp Med</i> 2006; 203:2233-2237.
SNFT	Iacobelli et al., <i>J Immunol</i> 2000 Jul 15;165(2):860-8.
TAGLN	Shen et al., <i>Circ Res</i> 2010 Apr 30;106(8):1351-62.
CCR7	Worbs & Förster, <i>Trends Immunol</i> 2007 Jun;28(6):274-80.

Table 3. Differentially expressed genes of Ingenuity Network 1 with reported function in cardiovascular disease and/or inflammation.

Results

Network 2 consists of 30 genes where expression of 12 genes was increased and expression of 18 genes was decreased in EMI subjects (Figure 13). This network displays three major hub genes with PTPRC (protein tyrosine phosphatase receptor type) and BCL2L1 (BCL2-like 1) found up-regulated, and CD40LG (CD 40 ligand) down-regulated in EMI samples (Figure 13 A). PTPRC is a receptor type protein tyrosine phosphatase that is specifically expressed in hematopoietic cells and essential for positive regulation of T- and B-cell antigen receptor signaling (Hermiston & Zikherman, 2009). BCL2L1 is a member of the BCL-2 protein family and can be expressed as a long isoform inhibiting apoptosis and a short isoform activating apoptosis. More recently, BCL2L1 has been also implicated in autoimmunity mediated by B-cells (Dörner & Lipsky, 2006). The decreased CD40LG belongs to the TNF family, is expressed on activated T-cells and in conjunction with its receptor CD40 known as a major player in inflammatory and autoimmune diseases including atherosclerosis. Inhibition of CD40 signaling has been shown to stabilize atherosclerotic plaques and to attenuate the disease progress (Lutgens et al., 2007). Interestingly, in this study CD40LG was found down-regulated in EMI samples raising the question whether this observation reflects the disease phenotype or possibly the response to the high dose of anti-inflammatory medication received by these subjects. Among the genes in network 2 that were found consistently over-represented in EMI samples, the gene products of CAMP (cathelicidin antimicrobial peptide), LGALS3 (galectin-3) and IL12RB1 (interleukin 12 receptor beta 1 subunit) in particular exert pro-inflammatory actions of the immune system. CAMP is an antimicrobial peptide and acts as a chemoattractant for a wide range of immune cells including neutrophils, monocytes, mast cells and T-cells (Zanetti, 2004). LGALS3 is a pro-inflammatory beta-galactoside carbohydrate binding protein of the lectin family that is absent in resting T-cells and a positive mediator of acute and chronic inflammation (Rabinovich et al., 2002, Hsu et al., 2009, Henderson & Sethi, 2009). IL12RB1 encodes the beta-1 subunit of the IL-12 receptor that is mainly expressed on activated T-cells and natural killer cells and initiates signaling cascades triggered by interleukin-12 tuning the immune response to increased cytotoxicity (Trinchieri, 2003). ST6GAL1 (ST6 beta-galactosamide alpha-2,6-sialyltransferase 1) and MGST1 (microsomal glutathione S-transferase 1) were also found up-regulated in EMI subjects and are agonists of B-cell receptor signaling and involved in the homeostasis of oxidative stress, respectively (Collins et al., 2009; Schmidt-Krey et al., 2000). Interestingly, CD22 and PTPRCAP, both down-regulated in EMI samples, represent agonists of the up-regulated STGAL1 and PTPRC, respectively.

Results

CD22 belongs to the sialic acid binding family of lectins and serves as receptor of STGAL1 thereby inhibiting B-cell receptor signaling (O'Reilly & Paulson, 2009). Its down-regulation may suggest increased BCR signaling in EMI samples. PTPRCAP (protein tyrosine phosphatase receptor type associated protein) is thought to bind PTPRC dimers thereby promoting formation of active monomers (Takeda et al., 2004; Leitenberg et al., 2007). A decrease of PTPRCAP expression in EMI subjects could then indicate less PTPRC activity and subsequent decreased T-cell activity. SIT1 encodes a regulatory transmembrane adaptor protein that acts as a negative regulator of T-cell activation and was found decreased in EMI subjects (Simeoni et al., 2008). A set of eight (row 20-27) out of the 18 down-regulated genes in EMI samples of network 2 were interferon-inducible genes including a RNA helicase (DDX58 or RIG-1), a GTPase (MX1), a ubiquitin-like protein (ISG15) and a transcription factor (IRF7). ID3, an inhibitor of transcription through formation of non-functional DNA-binding dimers, was also down-regulated within the EMI group. Loss of expression is responsible for a phenotype similar to Sjögren's Syndrome that is characterized by auto-reactive immune cells against exocrine glands (Guo et al., 2010). The two down-regulated genes in EMI samples of network 2 with the most consistent expression pattern were PRSS3 and ITGAX. PRSS3 encodes a serine protease of the trypsin family and has been implicated in chronic pancreatitis (Rosendahl et al., 2010). ITGAX or CD11C represents the gene for a leukocyte-specific integrin and high expression levels have been associated with hypercholesterolemia in atherogenesis (Wu et al., 2009). The observed decrease of expression could be a side-effect of statin treatment that may reduce lipid levels in EMI patients. Taken together, network 2 suggests an increased activation status of the immune system in EMI subjects with potent pro-inflammatory mediators (CAMP, LGALS3) and B-/T-cell agonists (ST6GAL1, IL12RB1) up-regulated and on the other hand decreased expression of negative regulators of immune cell function (CD22, SIT1) and interferon-inducible genes (Table 4).

Results

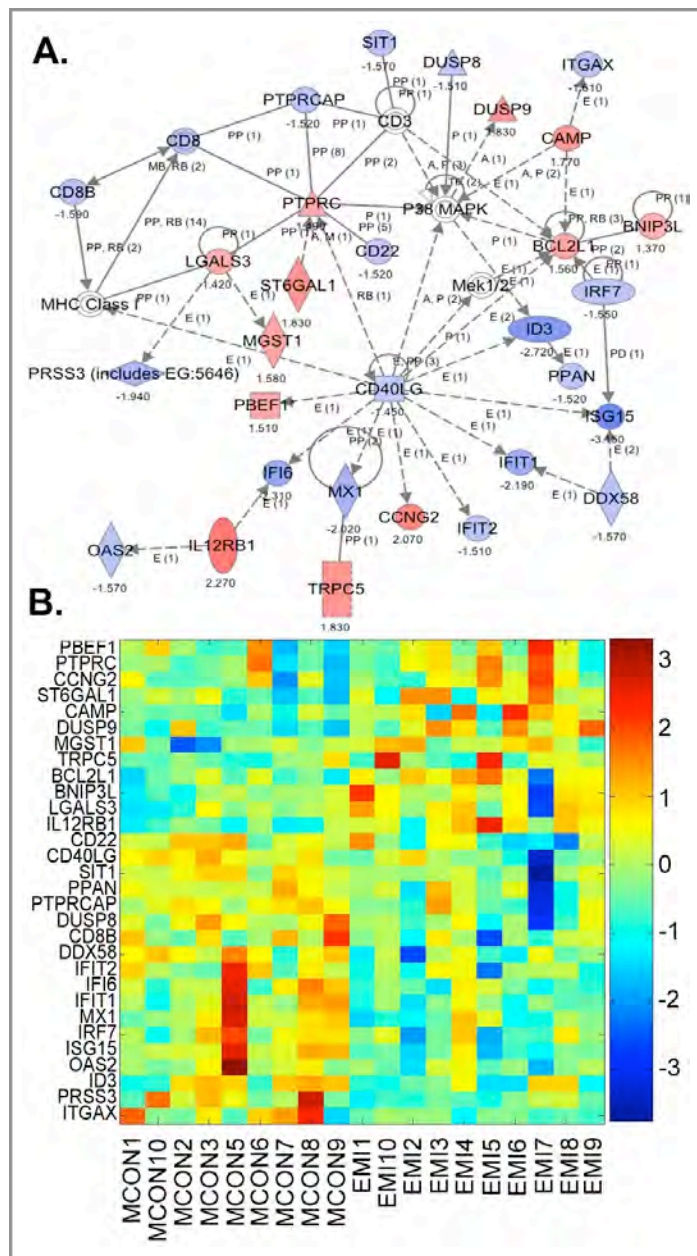


Figure 13. Ingenuity Network 2.

(A) Red color denotes up- and blue color down-regulation of a particular gene. Solid lines denote direct, dotted lines indirect interactions. Arrowheads indicate direction of interactions. Genes with many connections (PTPRC, BCL2L, CD40LG) are defined as hub-genes. Symbols: square = ligand, rectangle = receptor, circle = cytoplasmic protein, rhomboid = enzyme, oval = transcription factor. **(B)** Clustered heatmap of genes contained in Ingenuity Network 2. The color of each square represents the expression value (as fold change) of a gene according to the color scale bar on the right.

Results

Gene Symbol	References for function in cardiovascular disease and/or inflammation
CAMP	Zanetti M, <i>J Leukoc Biol</i> 2004 Jan;75(1):39-48.
LGALS3	Rabinovich et al., <i>Trends Immunol</i> 2002; 23 :313-320.
ST6GAL1	Collins et al., <i>Nat Immunol</i> 2006 Feb;7(2):199-206.
IL12RB1	Trinchieri et al., <i>Nat Rev Immunol</i> 2003; 3 :133-146.
CD22	O'Reilly & Paulson, <i>Trends Pharmacol Sci</i> 2009 May;30(5):240-8.
SIT1	Simeoni et al., <i>Trends Pharmacol Sci</i> 2009 May;30(5):240-8.

Table 4. Differentially expressed genes of Ingenuity Network 2 with reported function in cardiovascular disease and/or inflammation.

Results

Network 3 displays 26 genes with only 9 genes up-regulated but 17 genes down-regulated in the EMI group (Figure 14). There are two hub genes, IL8 and NRG1, both with increased expression in EMI samples (Figure 14 A). It has to be emphasized though that increased expression of interleukin-8 (IL8) is driven by only one individual (EMI7) and may therefore be not representative for the whole group (Figure 14 B). NRG1 or neuregulin 1 is a member of the growth factor family that binds to and activates ErbB receptor tyrosine kinase signaling. NRG1 has been implicated in neural development, synaptic plasticity and schizophrenia (Mei & Xiong, 2008). A recent report suggested also a role in immune system dysregulation of schizophrenic patients carrying genetic polymorphisms of the NRG1 gene (Marballi et al., 2010). The two up-regulated genes AEBP1 (adipocyte enhancer binding protein 1) and WNT5A have been both described as pro-inflammatory mediators of macrophages (Majdalawieh, 2010; Pereira et al. 2009). AEBP1 is a transcriptional repressor with carboxy-peptidase activity that has been reported as a novel atherogenic factor that increases NF-kappaB levels in macrophages leading to activation of pro-inflammatory gene cascades (Majdalawieh et al., 2006; Majdalawieh et al., 2007). Toll-like receptor-mediated expression of WNT5A has been shown as a key process for sustained inflammatory macrophage activation and was elevated upon microbial infection and in patients with acute sepsis (Blumenthal et al., 2006; Pereira et al., 2008). A platelet chemokine encoded by PPBP (row 5) or CXCL7 with elevated expression in EMI samples is the precursor of a strong chemoattractant and activator of neutrophils (Gleissner et al., 2008). Two genes not yet implicated in cardiovascular disease but with consistently elevated expression in EMI subjects were MIR16, a membrane-bound phosphodiesterase, and RNASE1, a secretory ribonuclease A (Zheng et al., 2003; Bai et al. 2009). Several of the genes that were found down-regulated within the EMI group are known antagonists of inflammation and auto-immunity or involved in lipid metabolism. NR1H4 is a farnesoid-sensing nuclear receptor involved in lipid and bile acid homeostasis and has been more recently also shown to counter-regulate inflammation and effector activities of the innate immune system (Li et al., 2007; Fiorucci et al., 2010). Expression of IL2RA or CD25, the alpha subunit of the interleukin-2 receptor, is crucial for suppressor T-cells that antagonize potential auto-immune reactions of the immune system (Shevach, 2002). CYP27A1, a cytochrome P450 member, promotes regression of atherosclerosis through cholesterol elimination (Luoma, 2008). LIPC, known as hepatic lipase, modifies lipids and lipid-binding proteins with observed pro- and anti-atherogenic effects depending on the cellular context (Zambon et al., 2003; Brown & Rader, 2007).

Results

LRP6, displaying decreased expression levels in EMI individuals, belongs to the family of low density lipoprotein receptors and defines together with frizzled a receptor complex for wnt signaling proteins (Manolagas & Almeida, 2007). A missense mutation in LRP6 that impairs wnt signaling has been identified in a family of iranian ancestry as the cause for autosomal dominant early-onset coronary artery disease with myocardial infarction prior to age 50 (Mani et al., 2007; Liu et al., 2008). The down-regulated HLA-DQA1 is a parologue of HLA class II molecules expressed in antigen-presenting cells. Interestingly, synthetic peptides of conserved HLA-DQA1 regions have been reported to inhibit priming and effector function of T lymphocytes *in vitro* and *in vivo* (Murphy et al., 1999; Zang & Murphy, 2005). AKAP12, decreased in EMI samples, represents the gene for a scaffolding protein in cell signaling that binds to protein kinase A (PKA) confining it to discrete locations within the cell (Wong & Scott, 2004). NOXA1 is an activator of NADPH oxidase 1, increased levels have been reported in atherosclerotic plaques (Niu et al., 2010). The down-regulated PTCH1 encodes a receptor for sonic hedgehog and has been implicated as a tumor suppressor gene (Toftgard, 2000). SP4, also decreased in EMI subjects, encodes a transcription factor whose knock-out mice display a heart failure phenotype due to defects in cardiomyocyte conduction (Nguyen-Tran et al., 2000). Altogether, the snapshot of differential gene expression in network 3 illustrates a picture where again pro-inflammatory genes (AEBP1, PPBP, WNT5A) are up-regulated. On the other hand, anti-inflammatory genes (NR1H4, HLA-DQA1) and genes that protect from auto-immunity (e.g. IL2RA) as well as factors that lower cholesterol levels (CYP27A1, LIPC, LRP6) were observed down-regulated in EMI subjects.

Results

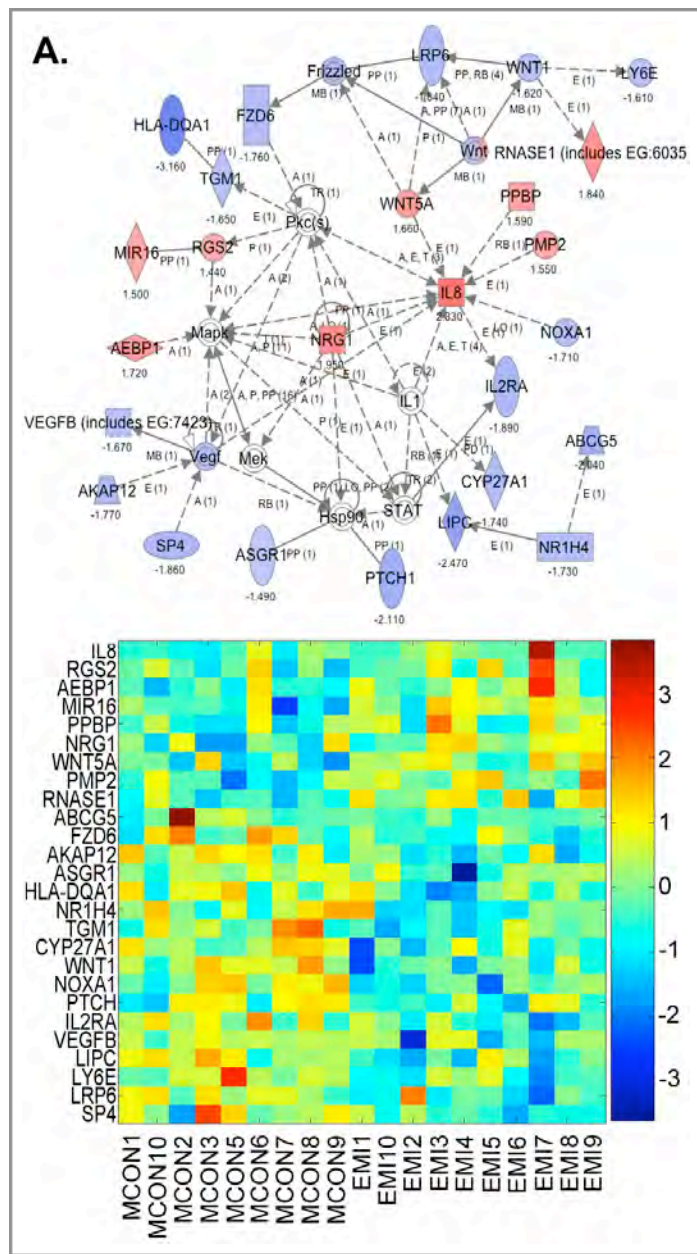


Figure 14. Ingenuity Network 3.

(A) Red color denotes up- and blue color down-regulation of a particular gene. Solid lines denote direct, dotted lines indirect interactions. Arrowheads indicate direction of interactions. Genes with most connections (IL8, NRG1) are defined as hub-genes. Symbols: square = ligand, rectangle = receptor, circle = cytoplasmic protein, rhomboid = enzyme, oval = transcription factor. **(B)** Clustered heatmap of Ingenuity Network 3. The color of each square represents the expression value (as fold change) of a gene according to the color scale bar on the right.

Results

Gene Symbol	References for function in cardiovascular disease
AEBP1	Majdalawieh et al., <i>Proc Natl Acad Sci U S A</i> 2006 Feb 14;103(7):2346-51.
PPBP	Gleissner et al., <i>Arterioscler Thromb Vasc Biol</i> 2008 Nov;28(11):1920-7.
WNT5A	Pereira et al., <i>Curr Atheroscler Rep</i> 2009 May;11(3):236-42.
NR1H4	Fiorucci et al., <i>Curr Mol Med</i> 2010 Aug 1;10(6):579-95.
HLA-DQA1	Murphy et al., <i>J Clin Invest</i> 1999 Mar;103(6):859-67.
IL2RA	Shevach, <i>Nat Rev Immunol</i> 2002 Jun;2(6):389-400.
CYP27A1	Luoma, <i>Eur J Clin Pharmacol</i> 2008 Sep;64(9):841-50.
LIPC	Zambon et al., <i>Curr Opin Lipidol</i> 2003 Apr;14(2):179-89.
LRP6	Mani et al., <i>Science</i> 2007 Mar 2;315(5816):1278-82.

Table 5. Differentially expressed genes of Ingenuity Network 3 with reported function in cardiovascular disease and/or inflammation.

Results

Network 4 contains 26 genes of which 17 were over-represented and 9 were under-represented within the EMI group. The first central hub gene in this network is PCAF, or p300/CBP-associated factor, that is connected with two circadian clock genes (NPAS2, CLOCK), the tumor suppressor gene BRCA2 and the histone methyl transferase gene MLL2 (Figure 15). PCAF, up-regulated in EMI samples, encodes a histone acetyl transferase involved in post-translational modification of lysine residues in histone and cardiac sarcomer proteins (Gupta et al., 2008; Dekker & Haisma, 2009). Most recently, a genetic variation in the promotor region of PCAF has been linked to reduced vascular morbidity and mortality during coronary artery disease in a major epidemiological study with three large patient cohorts (Pons et al., 2011). In addition, PCAF was detected up-regulated in a transcriptome analysis during the anti-inflammatory response of macrophages (Pereira et al., 2010). The down-regulated NPAS encodes a basic-helix-loop helix (bLHL) transcription factor that has been linked to hypertension and to altered circadian rhythm of cardiac β 3-adrenoceptor activity following myocardial infarction (Englund et al., 2009; Zhou et al., 2010). The CLOCK gene, under-represented in EMI subjects, also belongs to bLHL transcription factors and loss of expression is associated with metabolic syndromes including diabetes (Kovac et al., 2009; Marcheva et al., 2010). BRCA2, consistently down-regulated in EMI samples, has a crucial function during the homologous recombination pathway for DNA double-strand repair (Badie et al., 2010). The up-regulated MLL2, a histone methyl transferase, is involved in transcriptional regulation of beta-globin and estrogen receptor genes. It was also identified as the cause for Kabuki syndrome, a rare hereditary disorder characterized by intellectual disability and a distinct dysmorphic facial appearance (Ng et al., 2010; Paulussen et al., 2010). The second hub gene of network 4 is the up-regulated HDAC2 that besides a connection with PCAF and BRCA2 is also connected with ZBTB32. As a histone deacetylase and therefore antagonist of histone acetyl transferases (e.g. PCAF), HDAC2 forms transcriptional repressor complexes and has been shown to suppress inflammation in lung tissue during chronic obstructive pulmonary disease (COPD) (Barnes, 2009; Krämer, 2009). ZBTB32, under-represented in EMI samples, seems to attenuate immune responses as a negative regulator of T-cell activation and proliferation (Miaw et al., 2004; Piazza et al., 2004).

Two up-regulated genes (PIP5K2A, SNCA) and one down-regulated gene (IL1RAPL2) in EMI samples are implicated in central nervous system function. PIP5K2A encodes a unique kinase that generates phosphatidyl inositol bisphosphate and is genetically linked to schizophrenia (Rethelyi et al., 2010).

Results

SNCA or alpha-synuclein inhibits phospholipase D 2 selectively and is a major component of accumulating inclusion bodies in several neurodegenerative disorders including Parkinson's disease and Alzheimer's disease (Norris et al., 2009). IL1RAPL2, or interleukin 1 receptor accessory protein-like 2, is associated with x-linked mental retardation (Bahi et al., 2003). Among the nine genes in Network 4 with decreased expression levels in EMI samples were also BIN1 and SOX6 that both regulate L-type calcium channel function in cardiac myocytes as scaffolding protein and transcription factor, respectively (Hong et al., 2010, Cohen-Barak et al., 2003). Finally, two genes (ABCE1, KLHL2) that were found up-regulated and down-regulated in EMI individuals, respectively, have been associated with auto-immunity. ABCE1, an ABC transporter, has been implicated in systemic lupus erythematosus (SLE) and KLHL2, a transcription factor, has been reported as an auto-antigen in Sjögren's Syndrome an auto-immune disease of the salivary glands (Deng et al., 2006; Uchida et al., 2005).

In summary, the prevailing theme of differentially expressed genes in network 4 features transcriptional regulation including circadian clock transcription factors (CLOCK, NPAS2), genes involved in DNA and histone modification (MLL2, PCAF, HDAC2, BRCA2), transcription factors implicated in immune system function (KLHL2, ZBTB32) but also genes that have been known in the context of central nervous system function (PIP5K2A, SNCA).

Results

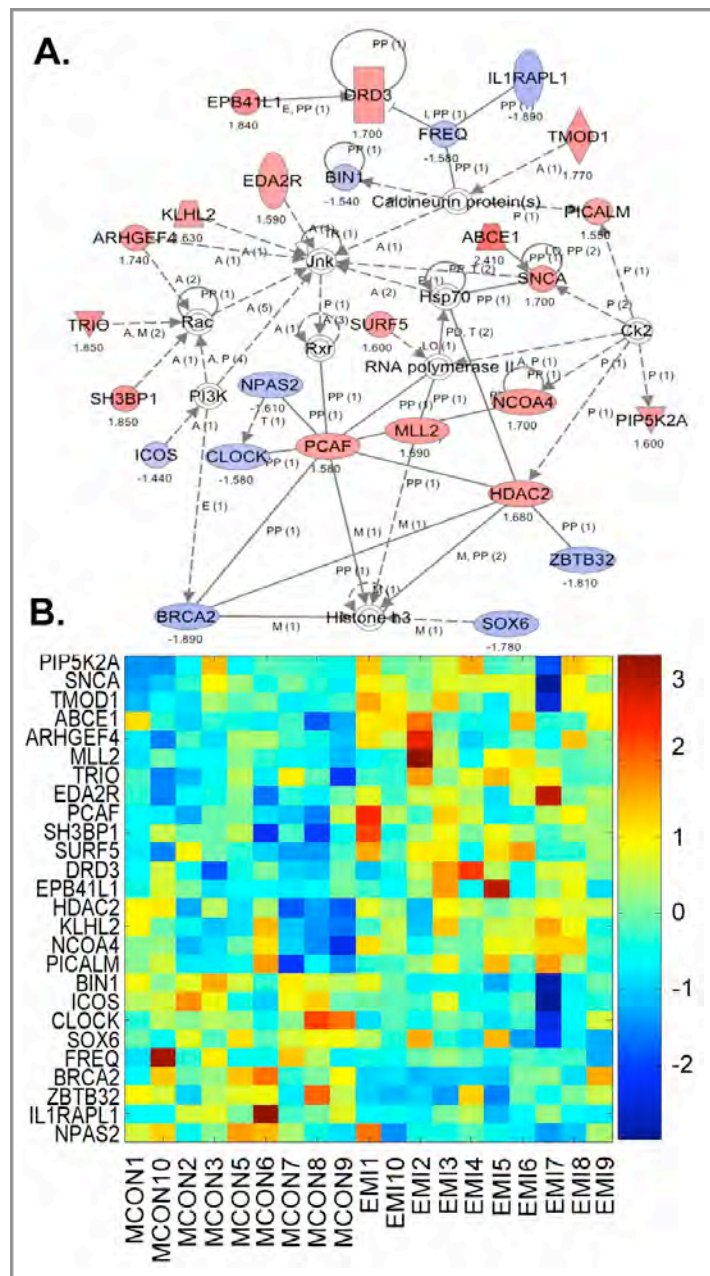


Figure 15. Ingenuity Network 4.

(A) Red color denotes up- and blue color down-regulation of a particular gene. Solid lines denote direct, dotted lines indirect interactions. Arrowheads indicate direction of interactions. Genes with many connections (PCAF, HDAC2) are defined as hub-genes. Symbols: square = ligand, rectangle = receptor, circle = cytoplasmic protein, rhomboid = enzyme, oval = transcription factor. **(B)** Clustered heatmap of Ingenuity Network 4. The color of each square represents the expression value (as fold change) of a gene according to the color scale bar on the right.

Results

Gene Symbol	References for function in cardiovascular disease
CLOCK	Marcheva et al., <i>Nature</i> 2010 Jul 29;466(7306):627-31.
NPAS2	Zhou et al., <i>Basic Res Cardiol</i> 2010 Jul 27.
MLL2	Ng et al., <i>Nat Genet</i> 2010 Sep;42(9):790-3.
PCAF	Gupta et al., <i>J Biol Chem</i> 2008 Apr 11;283(15):10135-46.
HDAC2	Krämer, <i>Trends Pharmacol Sci</i> 2009 Dec;30(12):647-55.
BRCA2	Badie et al., <i>Nat Struct Mol Biol</i> . 2010 Dec;17(12):1461-9.
ABCE1	Deng et al., <i>Mol Immunol</i> 2006 Mar;43(9):1497-507.
KLHL2	Uchida et al., <i>Mutagenesis</i> 2010 Jul;25(4):365-9.
ZBTB32	Piazza et al., <i>Mol Cell Biol</i> 2004 Dec;24(23):10456-69.
PIP5K2A	Rethelyi et al., <i>Am J Med Genet B Neuropsychiatr Genet</i> 2010 Apr 5;153B(3):792-801.
SNCA	Norris et al., <i>Curr Top Dev Biol</i> 2004;60:17-54.

Table 6. Differentially expressed genes of Ingenuity Network 4 with reported function in cardiovascular disease and/or inflammation.

Results

3.6 PANTHER identifies differentially expressed genes associated with the immune response as the most significant functional category in EMI samples

The PANTHER database also classifies genes according to their function based on electronically and manually curated scientific publications (Thomas et al., 2003). However, rather than detecting networks of interacting genes, PANTHER provides an expression analysis tool for microarray data interpretation where gene lists from experimental data sets are assigned to functional categories such as „Biological Process“ and „Molecular Function“ (Thomas et al., 2006). „Biological Process“ describes the biological system of the corresponding gene product, for example glyceraldehyde 3-phosphate dehydrogenase (GAPDH) is involved in carbohydrate metabolic processes. „Molecular Function“ is the function that a gene product performs on its molecular target, e.g. the enzyme GAPDH exerts oxidoreductase activity.

Biological Process. Of the 1008 genes detected by the LOTEST algorithm, 965 were represented within the PANTHER database (Table 7). Ontological analysis revealed „Immunity and defense“ ($p = 1.4E-05$) as the most significant parent category in Biological Process with a set of 90 detected genes. Interestingly, the significance was almost exclusively assigned to the 56 down-regulated genes ($p = 1.39E-05$) and not within the 34 up-regulated genes ($p = 1.00E-00$) of the EMI group. The sub-categories of the biological process „Immunity and defense“ were „Interferon-mediated immunity“, „Cytokine/chemokine mediated immunity“ and „B-cell and antibody-mediated immunity“. Eight down-regulated genes in sub-category „Interferon-mediated immunity“ displayed the highest significance ($p = 5.72E-03$) and were also detected by Ingenuity analysis in network 2 (Figure 16). Seven genes of sub-category „Cytokine/chemokine-mediated immunity“ were over-represented ($p = 6.23E-01$) and 10 genes of sub-category „B-cell- and antibody-mediated immunity“ were under-represented ($p = 1.21E-01$) with a less significant correlation in EMI samples. However, both themes were also represented across Ingenuity networks 1 to 4. The subsequent parent categories were scored less significant but five up-regulated genes in category „Nitrogen Metabolism“ ($p = 6.73E-03$) and 84 genes in category „Signal transduction“ ($p = 7.04E-03$) showed significant p-values.

Molecular Function. The parent-category „Defense/immunity protein“ displayed the highest significance ($p = 9.99E-02$) but almost exclusively within the 23 under-represented genes of the EMI group ($p = 2.12E-03$). A certain level of significance was also found in six down-regulated genes of the sub-category „Immunoglobulin“ ($4.65E-01$) in EMI samples.

Results

*REFLIST (25909)	All genes (965)				Up regulated genes (456)				Down regulated genes (509)				
	#	exp.	P-value	#	exp.	P-value	#	exp.	P-value	#	exp.	P-value	
Biological Process													
Immunity and defense	1393	90	51.88	+	1.40E-05	34	24.52	+	1.00E+00	56	27.37	+	1.39E-05
<i>Interferon-mediated immunity</i>	62	9	2.31	+	9.37E-02	1	1.09	-	1.00E+00	8	1.22	+	5.72E-03
<i>Cytokine/chemokine mediated immunity</i>	113	11	4.21	+	5.86E-01	7	1.99	+	6.23E-01	4	2.22	+	1.00E+00
<i>B-cell- and antibody-mediated immunity</i>	148	13	5.51	+	6.39E-01	3	2.6	+	1.00E+00	10	2.91	+	1.21E-01
Nitrogen metabolism	30	5	1.12	+	1.79E-01	5	0.53	+	6.73E-03	0	0.59	-	1.00E+00
<i>Nitrogen utilization</i>	5	3	0.19	+	1.35E-01	3	0.09	+	1.53E-02	0	0.1	-	1.00E+00
Protein metabolism and modification	3063	107	114.08	-	1.00E+00	49	53.91	-	1.00E+00	58	60.17	-	1.00E+00
<i>Protein biosynthesis</i>	692	34	25.77	+	1.00E+00	8	12.18	-	1.00E+00	26	13.59	+	2.20E-01
Small molecule transport	136	9	5.07	+	1.00E+00	8	2.39	+	4.62E-01	1	2.67	-	1.00E+00
Receptor mediated endocytosis	108	9	4.02	+	1.00E+00	8	1.9	+	1.52E-01	1	2.12	-	1.00E+00
Signal transduction	3259	138	121.38	+	1.00E+00	84	57.36	+	7.04E-03	54	64.03	-	1.00E+00
Molecular Function													
Defense/immunity protein	467	30	17.39	+	9.99E-02	7	8.22	-	1.00E+00	23	9.17	+	2.12E-03
<i>Immunoglobulin</i>	70	6	2.61	+	1.00E+00	0	1.23	-	1.00E+00	6	1.38	+	4.65E-01
Nucleic acid binding	2897	114	107.9	+	1.00E+00	42	50.99	-	1.00E+00	72	56.91	+	6.60E-01
<i>Translation elongation factor</i>	37	6	1.38	+	5.88E-01	6	0.65	+	1.18E-02	0	0.73	-	1.00E+00
Ribosomal protein	579	35	21.57	+	6.95E-01	9	10.19	-	1.00E+00	26	11.37	+	1.80E-02
Growth factor	115	10	4.28	+	1.00E+00	8	2.02	+	1.84E-01	2	2.26	-	1.00E+00
Transfer/carrier protein	329	14	12.25	+	1.00E+00	12	5.79	+	4.39E-01	2	6.46	-	1.00E+00

Table 7. Ontological analysis of differentially expressed genes using PANTHER.

Categories in italics are sub-categories of the parent-categories. Yellow highlight denotes the categories within „Biological Process“ and „Molecular Function“ containing the most significant numbers of differentially expressed genes. *Reference list containing all genes on the ABI microarray. + denotes overrepresentation, - denotes underrepresentation, # denotes number of genes detected. Bonferroni correction was used for multiple comparisons.

Results

A clustered heatmap of the genes detected within the most significant PANTHER category „Immunity and Defense“ (Biological Process) was generated for further expression analysis (Figure 16). Notably, many of the differentially expressed genes that have been previously identified by Ingenuity analysis were also found in the PANTHER database. They include the hub genes of network 2 (CD40LG), network 1 (FOS) and network 3 (IL8). In addition, the down-regulated IL2RA and CCR7, previously detected in Ingenuity networks 3 and 1 were identified by PANTHER as well. Both genes encode members of the cytokine receptor family and are crucial for maintenance of self-tolerance and for suppression of auto-immunity (Shevach, 2002; Worbs & Förster, 2007). The up-regulated genes JAG1, CAMP, PTX3 and LGALS3 encode peptides of the pro-inflammatory cascade that were also picked up by Ingenuity networks 1 and 2.

However, PANTHER analysis also identified additional genes distinct from Ingenuity results (Table 8). GSTT1, consistently down-regulated in EMI individuals, encodes a member of the Glutathione-S-transferase family of enzymes that plays a major role in the detoxification of reactive oxygen species and xenobiotics (Bolt & Thier, 2006). The GSTT1 null allele, a common genetic polymorphism that impairs catalytic activity, has been associated with coronary artery disease in several major epidemiological studies and was independent of the ethnic background (Maciel et al., 2009; Tang et al., 2010; Wang et al., 2010). Five genes whose expression levels were over-represented in EMI samples included IFNGR1, VAV3, MARCO, IL5RA and IKBKB, all of them are known mediators of inflammation during the innate and/or adaptive immune response. The IFNGR1 gene product comprises the ligand-binding chain of the interferon-gamma receptor and initiates interferon-mediated inflammatory signals at the cell surface of immune cells. IFNGR1 levels were recently found increased in a subset of limited systemic sclerosis patients with pulmonary arterial hypertension (Pendergrass et al., 2010). VAV3 belongs to the guanine nucleotide exchange factors (GEFs) and is critical for signaling during T-cell activation (Tybulewicz, 2005). MARCO, encoding a class A macrophage scavenger receptor with collagenous structure, is a differentiation marker for monocytic-derived cell lineages such as macrophages and dendritic cells (Sarrias et al., 2004). In macrophages MARCO is thought to mediate lipid influx promoting their conversion into foam cells that were detected in atherosclerotic plaques (Platt et al., 2002). Increased MARCO expression was also found in a mouse model for cerebral artery occlusion suggesting a role during ischaemic processes as they also occur during atherosclerotic processes leading to infarction (Milne et al., 2005).

Results

The up-regulated IL5RA, encoding the alpha subunit of the interleukin 5 receptor, has been associated with increased serum antibody levels, expansion of eosinophil numbers in the blood and eosinophil infiltration into various tissues (Adachi & Alam, 1998; Takatsu et al., 2009). The increased IKBKB encodes a positive regulator of NF-kappaB-mediated pro-inflammatory gene expression in immune cells and is a target for inhibitor treatment of chronic inflammatory disorders such as rheumatoid arthritis, inflammatory bowel diseases and chronic obstructive pulmonary disease (Perkins, 2007; Strnad & Burke, 2007). In summary, PANTHER analysis identified immune response relevant genes and therein those mediating inflammation as the major feature within the global expression signal of the EMI group. Notably, this observation largely confirms our Ingenuity results (see section 3.5) reinforcing the potential significance of immunity for the disease phenotype.

Gene Symbol	References for function in cardiovascular disease
GSTT1	Wang et al., <i>Mutagenesis</i> 2010 Jul;25(4):365-9.
IFNGR1	Pendergrass et al., <i>PLoS One</i> 2010 Aug 17;5(8):e12106.
VAV3	Tybulewicz, <i>Curr Opin Immunol</i> 2005 Jun;17(3):267-74.
MARCO	Platt et al., <i>Int Rev Cytol</i> 2002;212:1-40.
IL5RA	Takatsu et al., <i>Adv Immunol</i> 2009;101:191-236.
IKBKB	Strnad & Burke, <i>Trends Pharmacol Sci</i> 2007 Mar;28(3):142-8.

Table 8. Differentially expressed genes of the PANTHER „Biological Process“ category *Immunity and Defense* with reported function in cardiovascular disease and/or inflammation.

Results

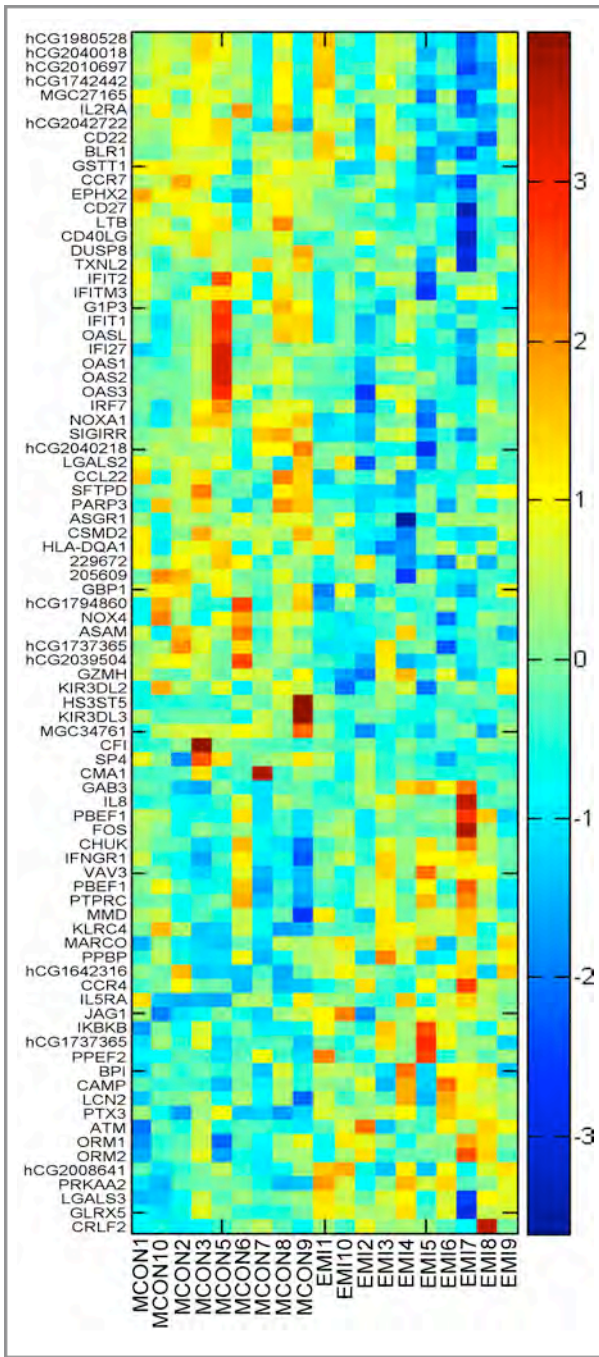


Figure 16. Clustered heatmap of genes from the biological process category “Immunity and defense” identified by PANTHER.

Expression of genes depicted in the top zone (row 1-53) is down-regulated within the EMI group, expression of genes in the bottom zone (row 54-85) is up-regulated within the EMI group. The color of each square represents the expression value (as fold change) of a gene according to the color scale bar on the right.

3.7 Examination of mRNA expression levels from selected differentially expressed genes in EMI individuals using quantitative real-time PCR

The expression level for every single gene of a sample that was hybridized to a microarray was calculated and normalized in a complex workflow. An algorithm integrated into the manufacturers software allowed normalization of a multitude of control samples with known quantities distributed across the array surface. But even before microarray hybridization the primary RNA sample is subjected to a labeling procedure including synthesis of cDNA and *in vitro* transcription of cRNA that could possibly differ from the quantities of the original sample.

Therefore, quantitative real-time PCR was performed to test whether the expression intensities observed during microarray analysis could be reproduced by an independent technique. A set of selected candidate genes implicated in inflammation and/or cardiovascular disease that were found either up- or down-regulated within the EMI group was analyzed. The aim of these experiments was to compare quantitative expression trends between microarray and qPCR results. The criteria for gene selection were consistency of expression within the sample groups (EMI vs MCON) and representation of the most prominent functional categories detected during microarray analysis (Figure 17 A). The pro-inflammatory category was represented by the genes encoding PTX3, LGALS3 and CAMP. Agonists of T-cell activation were represented by IL12RB1 and JAG1. IL2RA and CCR7 represented genes with a link to auto-immunity. GSTT1 serves as an cellular antioxidant that protects from atherosclerosis. NGFR represented a pro-apoptotic antagonist of lymphocytes. All of the selected genes were assayed in triplicates using TaqMan probes on reverse transcribed RNA samples from two individuals representing the expression trend of the respective sample group. Quantitative real-time PCR analysis revealed in particular two findings. First, the expression trends observed during microarray analysis were confirmed (Figure 17 B). However, the absolute expression intensities measured by quantitative PCR were not necessarily identical with those of the microarray analysis. This may be due to the fact that qPCR results were normalized against the expression level of only one housekeeping gene (GAPDH) whereas microarray expression values were calculated in a normalization workflow containing multiple technical and spatial features during array analysis. One exception is PTX3 whose expression levels were found on average more than two-fold up-regulated in EMI samples in microarray analysis but showed only 20 % up-regulation in qPCR results (Figure 17 A and B, top panel). In this case MCON samples displayed similar mRNA levels compared to microarray analysis whereas expression levels of EMI samples differed by more than 40 % (data not shown).

Results

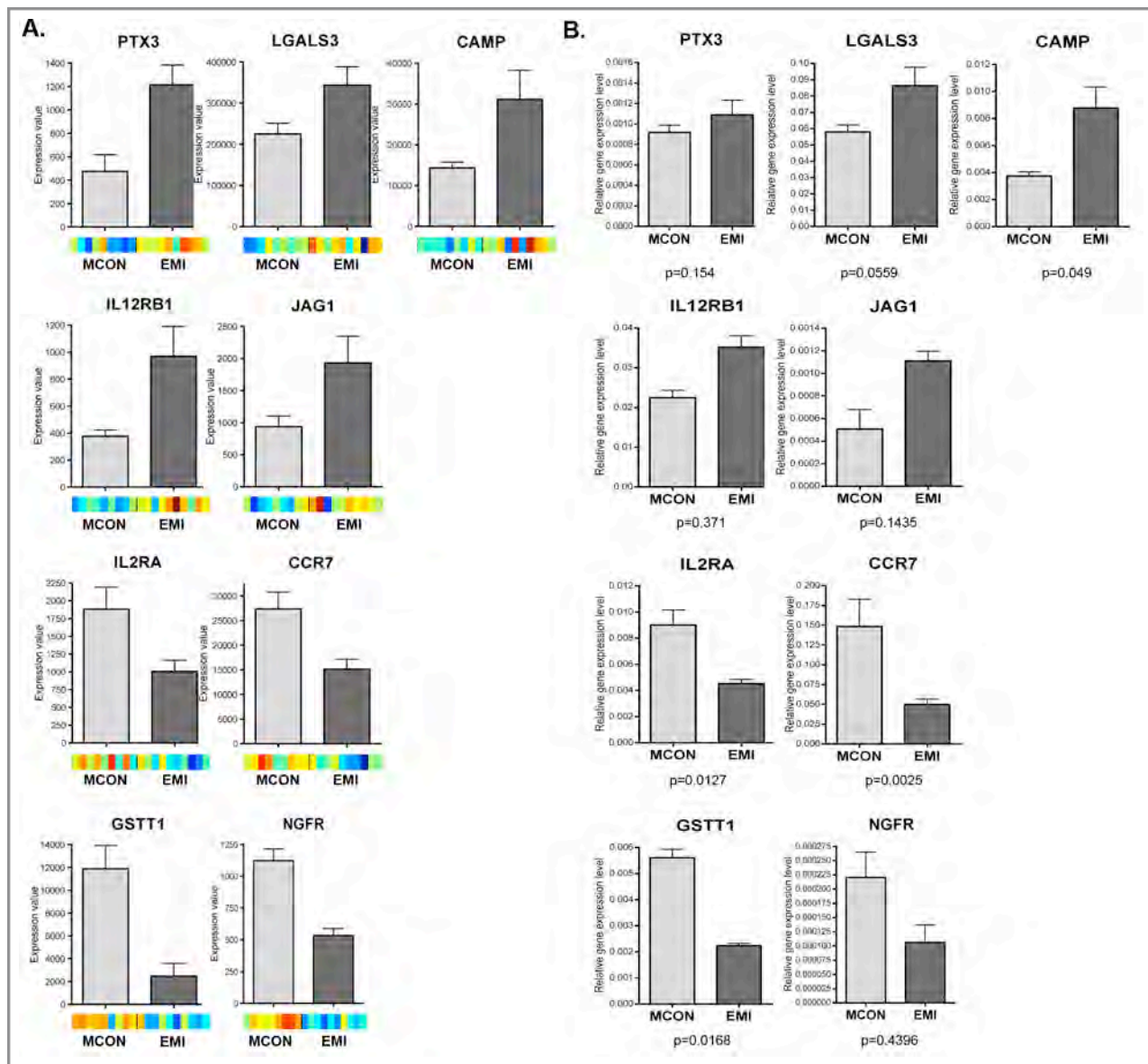


Figure 17. Average microarray expression levels (A) and relative quantities determined by quantitative real-time PCR of selected candidate genes (B).

PTX3, LGALS3 and CAMP are pro-inflammatory molecules, IL12RB and JAG1 are T-lymphocyte agonists, CCR7 and IL2RA prevent autoimmune reactions, GSTT1 is an antioxidant protective against atherosclerosis, and NGFR is pro-apoptotic to lymphocytes. **(A)** On the clustered heat map strips, blue hues represent down- and red hues up-regulation. **(B)** Confirming quantitative real-time PCR analysis of mRNA levels of the same genes.

Results

Summary

Whole-genome expression profiling of circulating blood cells from subjects with early-onset coronary artery disease identified inflammatory themes associated with the immune response as the predominant signature within all differentially expressed genes detected by the LOTEST algorithm. Functional analysis using the gene ontology databases Ingenuity Pathway Analysis and PANTHER revealed a pool of identical genes that were found within their networks and functional categories, respectively, reinforcing the significance of these genes within the global expression pattern that distinguishes subjects with early myocardial infarction (EMI) from medicated control subjects (MCON). Quantitative real-time PCR of selected candidate genes confirmed the expression trends of microarray analysis. Furthermore, the results of this microarray study also suggest that inflammatory processes continue in EMI individuals despite therapeutical anti-inflammatory medication.

IV. Discussion

In the second part of my PhD project, the transcriptome of circulating peripheral blood cells from healthy subjects and patients with early-onset coronary artery disease was analyzed for differential gene expression patterns. Data were assessed by hybridization of microarrays and subsequent quantification of fluorescence signals. *In silico* methods were applied to identify functional groups according to gene ontology terms within the differential gene expression signatures. Finally, a selection of candidate genes distinguishing case (EMI) and control (MCON) groups was additionally examined using quantitative PCR.

1. The phenotype of early-onset coronary artery disease is reflected in gene expression signatures of circulating blood cells

Using whole genome expression profiling, this study provides evidence that features of the coronary artery disease phenotype are imprinted into the gene expression profile of circulating blood cells. Microarray analysis using the LOTEST algorithm detected 1008 genes that were differentially expressed in EMI subjects. An integrated functional analysis approach based on Ingenuity Pathway Analysis and PANTHER biological knowledgebases revealed overrepresentation of genes involved in inflammatory processes mediated by the immune system within the EMI group.

1.1 Critical features of experimental design and differential expression analysis

The multiethnic study cohort representing African-americans, Caucasians and Asians comprised 10 individuals in each of the case (EMI) and control group (MCON). Compared to epidemiological studies that cover large patient cohorts with thousands of individuals this may seem a low number of study subjects. Indeed, studies with a broad epidemiological scope would need larger sample sizes in order to obtain unequivocal results. However, the aim of this study was to test a novel microarray data analysis method suitable to reliably identify differentially expressed genes that would distinguish the phenotype of cases from controls. We hypothesized that fundamental signals for differential expression associated with early-onset coronary artery disease can be tracked down with relatively few samples in an appropriate experimental setting.

Discussion

A clinical database of the Veterans Administration Pacific Islands Healthcare System (VAPHICS) containing tens of thousands of patients enabled us to assemble a valid small-scale study group with most prospectively matched individuals based on age, ethnicity and clinically relevant parameters for the disease phenotype.

A crucial challenge for the analysis of whole genome microarray data is the detection of relatively weak signal(s) within a noisy background of thousands of genes being simultaneously expressed with similar expression levels (Chelly et al. 1989; Butte, 2002). As the phenotype of atherosclerotic coronary artery disease is multifactorial and a result of both, environmental and genetic influences, we not only expected a noisy but also heterogeneous signals consisting of multiple signal components for differential expression. LOTEST, a novel detection algorithm applying a „localized test and estimate“ procedure was implemented for microarray data analysis (Okimoto, 2006). Based on the principles of estimation theory, this algorithm applies spatial adaptation and thresholding to the fold change values of genes with similar expression using the Donoho Johnstone Universal Threshold (DJUT) in order to detect weak and sparse signals for differential expression (Donoho & Johnstone, 1994; Sabatti et al., 2002).

In contrast, detection algorithms commonly used for differential expression analysis of microarray data are typically based on the *t*-test such as the Significance Analysis of Microarrays (SAM) (Tusher et al., 2001). These traditional methods of linear statistics rely on adequate sample numbers and assume that differential expression (DE) is consistent within a sample class but significantly different between two sample classes. However, this signal model may be inappropriate in situations where true DE genes are rare and sample heterogeneity and complexity of the phenotype result in DE patterns that are highly variable over the samples of a microarray experiment (Donoho & Jin, 2008). In fact, comparison of SAM and LOTEST performance on simulated and actual microarray data demonstrated that SAM picked up only homogenous single-component signals whereas LOTEST detected heterogeneous multi-component signals (G. Okimoto, personal communication). LOTEST analysis of microarray data from this study cohort detected a total of 1203 differentially expressed genes from 32,878 probes representing 29,098 genes on a human genome survey array. However, the probability to generate false positives from a background of tens of thousands of genes on the array remains significant. To address this issue we implemented an additional tool in order to make the analysis workflow more robust. Color-coded heatmap diagrams enabled visual verification or falsification of genes specified as differentially expressed by the LOTEST algorithm (Eisen et al., 1998).

Discussion

Why is this important? The initial heatmap diagram of all 1203 differentially expressed genes immediately revealed a patch of 195 genes that was driven by only two individuals within the case group (EMI2 and EMI7, Figure 11 A). Downstream *in silico* analysis using Ingenuity and PANTHER knowledgebases confirmed there was no functional significance within this set of 195 genes. In conclusion, complementing statistical analysis by heatmap diagrams provides a powerful control measure to evaluate expression patterns during the course of the analysis workflow. This may in particular be true for studies with low sample numbers where statistical confidence is decreased by definition.

Two recent studies investigating the transcriptome of peripheral blood cells in coronary artery disease correlated stringent gene expression thresholds with specific features of the clinical phenotype. The first study determined differential expression by setting an arbitrary threshold at > 1.3 fold difference between clinical phenotypes as defined by the extent of coronary stenosis (Wingrove et al., 2008). The second study applied a threshold by calculating a correlation coefficient between gene expression values and a stringent CAD-Index as defined by number and severity of lesions and diseased vessels (Sinnaeve et al., 2009). In summary, both studies applied criteria for DE analysis that reflect a typical linear relationship. As outlined above, approaches based on linear assumptions may limit the capability for the detection of rare, weak and heterogenous signals consisting of multiple signal components. In contrast, the net we casted in this microarray study to detect differential expression patterns used adaptive statistics based on DJUT thresholding to correlate variable gene expression values with the CAD phenotype as defined by myocardial infarction prior to age 50 (Okimoto, 2006). Besides different microarray platforms and individual sample handling these differences in the analysis approach may account for the limited overlap in terms of the identified genes between our and other studies. In conclusion, neither one nor the other approach may be better but they are likely to detect fundamentally different signals of differential expression. Notably, there are similarly few DE gene overlaps between other studies for which the reasons are not fully understood and may involve ethnic and/or environmental differences of the study cohorts at different geographical locations.

1.2 Over-representation of pro-inflammatory gene expression changes in EMI subjects

In the second step of analysis, functional groups of genes were identified using additional *in silico* methods. The two gene ontology databases IPA and PANTHER unravelled a heterogenous signal within the gene expression signature of circulating blood cells in EMI subjects representing a broad spectrum of inflammatory processes (Table 9). Notably, most positive regulators of inflammation were over-represented whereas negative regulators were under-represented in the disease group. Furthermore, inflammatory themes could be divided into subgroups representing the innate and adaptive immune system and in many cases differentially expressed genes even indicated the contributing cell-type(s).

Immunological context	Genes	References
Antimicrobial host defense	PTX3↑, CAMP↑, LGALS3↑	Botazzi et al., 2006; Zanetti, 2004; Rabinovich et al., 2002
T-cell signaling	AHNAK1↑, JAG1↑, SNFT↓, CD40LG↓, IL12RB1↑, SIT1↓, HLA-DQA1↓, ZBTB32↓, VAV3↑	Matza et al., 2009; Guidos, 2006; Iacobelli et al., 2000; Lutgens et al., 2007; Trinchieri et al., 2003; Simeoni et al., 2009; Murphy et al., 1999; Piazza et al., 2004; Tybulewicz, 2005
Auto-immunity	CCR7↓, ID3↓, IL2RA↓	Worbs & Fröster, 2007; Maruyama et al., 2011; Shevach, 2002
Macrophages	AEBP1, WNT5A↑, MARCO↑	Majdalawieh et al., 2006; Blumenthal et al., 2006; Arredouani & Kobzik, 2004
Granulocytes	PPBP↑, IL5RA↑	Gleissner et al., 2008; Adachi & Alam, 1998
Vascular inflammation	TAGLN↓, NOX4↓	Feil et al., 2004; Brandes & Schröder, 2008
IFN-γ-signaling	IFNGR1↑	Leon & Zuckerman, 2005
IFN-inducible genes	RIG-I↓, IFIT2↓, IFI6↓, IFIT1↓, MX1↓, IRF7↓, ISG15↓, OAS2↓	Haller et al., 2007; Taniguchi et al., 2001; Parker & Porter, 2004; Fensterl & Sen, 2011; Jeon et al., 2010; Eskildsen et al., 2003; Berchthold et al., 2008

Table 9. Potential candidate genes involved in immune regulation that separate the atherosclerotic phenotype between EMI and control individuals based on differential expression analysis.

Arrow ↑ = up-regulated in EMI group; arrow ↓ = down-regulated in EMI group

Discussion

The up-regulated pro-inflammatory genes PTX3, CAMP and LGALS3 encode antimicrobial peptides and are potent mediators of the innate immune response. PTX3 encodes the prototypic long pentraxin 3 that activates the classical pathway of complement activation in response to microbial infection and facilitates pathogen recognition by macrophages and dendritic cells (Garlanda et al., 2002; Nauta et al., 2003). In addition, increased blood levels of PTX3 as inflammatory marker even outperformed the diagnostic and prognostic value of c-reactive protein (CRP) for myocardial infarction in CAD patients (Peri et al., 2000; Latini et al., 2004). CAMP is a strong chemoattractant for neutrophils, monocytes, and T-cells and induces degranulation of mast cells as well as transcriptional alterations in macrophages (Zanetti, 2004). LGALS3 belongs to the lectin family of carbohydrate-binding proteins and is a key component not only during the initial host defense against microbes but also during chronic inflammation as a potent agonist of T-cell function (Henderson & Sethi, 2009; Hsu et al., 2009).

It is well known that phospholipids of oxidized low density lipoproteins (oxLDL) are recognized as antigens by the immune system during atherosclerosis (Stemme et al., 1995). Furthermore, cross-reactivity has been observed between oxLDL and epitopes from microbial pathogens such as *streptococcus* and *chlamydia* (Kol et al., 1998; Shaw et al., 2000). Therefore, elevated transcript levels of antimicrobial peptides may indicate ongoing molecular mimicry where factors of the antimicrobial host defense are induced by endogenous oxLDL molecules in EMI individuals.

Differential expression of a set of at least eight genes (AHNAK, JAG1, SNFT, IL12RB1, SIT1, HLA-DQA1, ZBTB32 and VAV3) indicates increased T-cell activation in EMI subjects. T-cell populations play a major role in the regulation of the innate and adaptive immune response during inflammatory processes in both, early and late stages of atherosclerosis (Hansson & Libby, 2006). This could explain why most inflammatory genes that were detected in our analysis account for activated T-cells. These eight genes encode a broad range of proteins including adaptor molecules (AHNAK, SIT1), ligands (JAG1), transcription factors (SNFT, ZBTB32), cytokine receptors (IL12RB1), major histocompatibility complex (MHC) proteins (HLA-DQA1) and guanine nucleotide exchange factor (GEF) signaling molecules (VAV3). However, based on their differential expression pattern in EMI subjects they do all have in common to promote T-cell activation. T-cells become activated in response to oxLDL particles, differentiate and produce secreted cytokines including IFN- γ (Frostegard et al., 1999). Paracrine crosstalk with effector cell types results for example in macrophage activation (Hansson & Libby, 2006). Activated macrophages produce additional cytokines and pro-thrombotic mediators again reinforcing the pro-inflammatory cascade.

Discussion

Altogether, the putative T-cell gene expression signature detected in EMI individuals could be considered a positive feedback-loop system that seems to maintain the inflammatory response in EMI individuals.

Expression of the genes CCR7, IL2RA and ID3 was found decreased in EMI samples. This is an interesting observation considering that loss of expression for each of the three genes has reportedly resulted in substantial autoimmune reactions. For CCR7 it has been demonstrated that knock-out mice were prone to the development of generalized multi-organ autoimmunity (Worbs & Förster, 2007). The auto-immune phenotype was characterized by lymphocytic infiltrations into several organs in addition to the presence of circulating auto-antibodies against a multitude of tissue-specific antigens (Davalos-Misslitz et al., 2007). IL2RA (also called CD25), the gene encoding the interleukin-2 receptor α -chain, is a marker for a small population of suppressor T-cells that maintain self-tolerance within the immune system (Shevach, 2002). Knock-out mice of ID3, a DNA-binding inhibitor, display T-cell-mediated autoimmune reactions to salivary glands a phenotype similar to Sjögren's Syndrome (Li et al., 2004). A most recent study demonstrated that ID3 is also crucial for expression of Foxp3 which itself is an important transcription factor of suppressor T-cells (Maruyama et al., 2011). With respect to our findings these data raise the question whether self-tolerance in EMI subjects may be compromised or even indicate auto-immunity as an ongoing disease feature in EMI individuals.

AEBP1, WNT5A and MARCO, all over-represented in EMI samples, have been reported as pro-inflammatory mediators in macrophages, that represent a potent phagocytic cell population of monocytic origin. AEBP1 is known to be expressed in macrophages where it promotes inflammatory signals and atherosclerotic foam cell formation (Majdalawieh et al., 2006). The effects seem to be mediated via I κ B- α inhibition resulting in increased NF- κ B activity (Majdalawieh et al., 2007). Toll-like receptor-mediated WNT5A expression is a key process for sustained inflammatory macrophage activation upon microbial stimuli (Blumenthal et al., 2006). In addition, WNT5A was increased in individuals with sepsis implicating its relevance in systemic inflammation (Perreira et al., 2009). MARCO belongs to the class A scavenger receptor family that is expressed on macrophages and also implicated in foam cell conversion during atherosclerosis (Arredouani & Kobzik, 2004). Interestingly, MARCO was identified as the major binding receptor for unopsonized particles and bacteria in human lung alveolar macrophages (Arredouani et al., 2005). In conclusion, elevated transcript levels of AEBP1, WNT5A and MARCO could be an indicator of increased macrophage-induced inflammation in EMI individuals.

Discussion

The two up-regulated genes, PPBP and IL5RA, are known to exert effects on the behavior of specific granulocyte subpopulations. PPBP (or CXCL7), is the most abundant platelet chemokine and its proteolytically cleaved variant NAP-2 is a strong neutrophil chemoattractant (Harter et al., 1994; Gleissner et al., 2008). IL5RA encodes the α -chain of the interleukin-5 receptor and is strongly expressed on activated eosinophils (Adachi & Alam, 1998). IL-5 signaling is critical for growth, activation and survival of eosinophils. Furthermore, increased IL-5 signal transduction results in expansion of eosinophil numbers in the blood and eosinophil infiltration into various tissues (Takatsu et al., 2009). Taken together, up-regulated PPBP and IL5RA in EMI subjects may indicate increased activity of granulocyte subpopulations that represent powerful phagocytic cells of the innate immune response.

Down-regulation of TAGLN and NOX4, as observed in EMI subjects, has been implicated in vascular inflammation during atherosclerosis. TAGLN (or SM22) was known as a gene for a smooth muscle-cell specific cytoskeletal protein with unknown function when a study was published demonstrating that loss of expression in hypercholesterolemic mice resulted in increased atherosclerotic lesions (Feil et al., 2004). In addition, disruption of TAGLN enhances arterial inflammation in response to injury (Shen et al., 2010). NOX4 belongs to the NADPH oxidase family that influences diverse physiological processes in the vasculature through production of reactive oxygen species (ROS) in response to a variety of stimuli (Brandes & Schröder, 2008). Whereas some NOX isoforms are associated with inflammatory macrophages in atherosclerotic plaques, NOX4 seems to be restricted to vascular smooth muscle cells (Sorescu et al., 2002). Furthermore, NOX4 is required for the differentiated phenotype of smooth muscle cells in the vasculature (Clempus et al., 2007). Therefore, NOX4 seems important for normal physiological function of the vascular system and may even prevent inflammatory processes. In conclusion, decreased transcript levels of both, TAGLN and NOX4, could indicate enhanced arterial inflammation in EMI individuals.

Finally, transcript levels of IFNGR1 encoding the ligand-binding chain of the interferon gamma receptor were significantly increased within the EMI group. IFN- γ -signaling plays a central role in the crosstalk between innate and adaptive immune response during inflammatory processes in atherosclerosis (Leon & Zuckerman, 2005). For example, IFN- γ is secreted by T-cells in atherosclerotic plaques leading to macrophage activation. Knock-out studies for IFN- γ or its receptor in animal models clearly suggest a potentiating role in atherosclerosis (Hansson & Libby, 2006).

Discussion

Expression of IFNGR1 was recently found increased in limited systemic sclerosis patients with pulmonary arterial hypertension (Pendergrass et al., 2010). Limited systemic sclerosis or scleroderma is a fibrotic autoimmune disease characterized by apoptosis of endothelial cells and smooth muscle cells in small blood vessels followed by inflammation and fibrotic deposition of extracellular matrix components (Gabrielli et al., 2009). Taken together, elevated IFNGR1 expression could be a sign of enhanced inflammatory crosstalk between components of the innate and adaptive immune system in EMI patients.

1.3 Over-representation of pro-atherogenic gene expression changes in EMI subjects

In addition, differentially expressed genes were observed in the EMI group that have not been reported in the context of inflammation but in other cellular processes implicated in atherosclerosis (Table 10).

Biological context	Genes	References
Cholesterol homeostasis	CYP27A1↓, LIPC↓, LRP6↓	Luoma, 2008; Zambon et al., 2003; Mani et al., 2007
Detoxification of reactive oxygen species	GSTT1↓	Hayes & Strange, 2000; Wang et al., 2010
Apoptosis	NGFR↓	Fiore et al., 2009
Cardiomyopathy	SP4↓, BIN1↓, SOX6↓	Nguyen-Tran et al., 2000; Muller et al., 2003; Hagiwara et al., 2000

Table 10. Potential candidate genes involved in diverse biological functions that separate the atherosclerotic phenotype between EMI and control individuals based on differential expression analysis.

Arrow ↑ = up-regulated in EMI group; arrow ↓ = down-regulated in EMI group

For example, three genes involved in cholesterol depletion were found significantly under-represented in EMI subjects. CYP27A1 belongs to the cytochrome P450 enzyme family and is involved in cholesterol oxidation as part of bile synthesis pathway. Since the conversion of cholesterol to bile acids is the major route for removing cholesterol from the body this protein is important for overall cholesterol homeostasis (Luoma, 2008).

Discussion

LIPC encodes a triglyceride lipase mainly expressed in the liver and serves the dual functions of triglyceride hydrolysis as well as a bridging factor for receptor-mediated cellular lipoprotein uptake. A common polymorphism in the promoter region resulting in decreased LIPC expression and subsequent enzyme activity is associated with an increased risk of atherosclerosis (Zambon et al., 2003). A missense mutation in LRP6, a member of the LDL receptor family, that results in loss of function has been recently demonstrated as the cause for autosomal dominant early-onset coronary artery disease (CAD) in an iranian family (Mani et al., 2007, Liu et al., 2008). Interestingly, many individuals of the family carrying the mutation develop CAD with subsequent myocardial infarction prior to age 50 which was one of the most important inclusion criteria for EMI subjects in this study. Decreased expression levels of LRP6 may therefore implicate impaired LDL clearance in EMI individuals of our study cohort. In conclusion, the down-regulation of three genes that are involved in the elimination of cholesterol indicates an imbalance of cholesterol homeostasis reflecting the disease phenotype. However, the observed expression pattern of cholesterol-regulating genes could at least in part also result from a possibly higher dose of cholesterol-lowering medication (statin) in the EMI group.

GSTT1 encodes an enzyme of the glutathione-S-transferase family that is known for its critical role in the detoxification of side products generated by reactive oxygen species (Bolt & Thier, 2006). In recent years, several major studies have shown that a common polymorphism resulting in a non-functional GSTT1 null allele is associated with hyperlipidemia, inflammation and myocardial infarction in patients with coronary artery disease independent of the ethnic background (Cornelis et al., 2007, Maciel et al., 2009, Tang et al., 2010, Wang et al., 2010). Interestingly, GSTT1 is one of the most consistent down-regulated genes in EMI subjects reflecting the results of the epidemiological studies cited above even within this small sample group. We assume that some of the EMI individuals may be carriers of the GSTT1 null allele as quantitative real-time PCR on a few samples from our study cohort did not yield detectable signals (data not shown). One of the known side effects of reactive oxygen species (ROS) is the generation of oxidized LDL, a feature with substantial significance for atherosclerosis (Hayes & Strange, 2000). In conclusion, decreased GSTT1 expression in EMI individuals could potentiate the pathophysiological effects of ROS on the CAD phenotype.

Discussion

NGFR is the gene encoding nerve growth factor receptor, a death receptor of the TNF receptor superfamily mediating apoptotic signals in neurons but also in cells of the immune system such as macrophages (Fiore et al., 2009). Therefore, decreased transcript levels of NGFR could reflect reduced apoptosis of immune cell populations in EMI subjects with the consequence of an overall increased immune response that obviously contributes to inflammatory processes during atherosclerosis.

An interesting finding of this study was the down-regulation of three genes implicated in cardiac myopathies. BIN1 is a scaffolding protein of L-type calcium channels in cardiac myocytes and genetic ablation results in perinatal lethal cardiomyopathy that is characterized by aberrant myofibril formation (Muller et al., 2003; Hong et al., 2010). SP4 encodes a transcription factor that is mainly expressed in ventricular myocytes. Its loss of expression in knock-out mice results in sudden death due to spontaneous ventricular tachycardia with a high incidence of atrioventricular block leading to cardiac arrest (Nguyen-Tran et al., 2000). At the molecular level, a decrease and mislocalization of connexins was identified as a cause for malignant arrhythmias. SOX6 is a transcription factor that is important for cardiac myocyte differentiation and its disruption leads also to sudden neonatal death due to atrioventricular blocks (Hagiwara et al., 2000). The molecular mechanism seems to involve suppression of the cardiac L-type Ca^{2+} channel alpha 1c subunit expression (Cohen-Barak et al., 2003). Expression levels for both, SP4 and SOX6, were decreased in cases and raise the question of whether cardiac myocytes in EMI subjects also display reduced transcript levels. For obvious reasons this is difficult to test in humans but the intriguing thought remains that circulating blood cells could possibly mirror the phenotype of cardiac tissue. In fact, it has been recently demonstrated that gene expression signatures in peripheral blood cells during atherosclerosis do reflect the gene expression patterns of an adjacent tissue, the atherosclerotic vasculature (Sinnaeve et al., 2009). However, the circulating blood stream is in direct contact with the vasculature and therefore makes interactions between those tissues more amenable. Nevertheless, it is quite puzzling that three genes, whose loss of expression in mice results in lethal cardiomyopathy, were found significantly down-regulated in EMI samples from our study cohort.

2. Potential impact of cardiac-related medication on gene expression profiles in the study cohort

All individuals of the EMI group, diagnosed with atherosclerotic coronary artery disease, have suffered myocardial infarction (MI) prior to age 50 and receive as a consequence standard post-MI therapeutical medication (see also Material & Methods). As any of these drugs could potentially affect gene expression profiles, we assembled a healthy control group that was treated with the same subset of medication. However, due to possible variations in the doses of applied medication some remaining variance in gene expression cannot be excluded. The following section will discuss this issue with regard to the identified differential expression profile within the obtained microarray data set of this study.

One of the surprising findings of this study was the decreased expression of CD40LG in EMI individuals. It was the major hub gene of Ingenuity Network 2 and was also detected within the PANTHER biological process category „Immunity and defense“ (Figure 13 A and Figure 16). CD40LG belongs to the tumor necrosis factor (TNF) family and signaling via its receptor CD40 results in NF- κ B mediated pro-inflammatory gene expression (Lievens et al., 2009). About a decade ago extensive studies demonstrated a major role for CD40LG and its receptor CD40 in promoting inflammation during atherosclerosis (Lutgens et al., 2007). Knock-out mice and inhibition of CD40LG by antibody treatment resulted in a decrease in atherosclerosis with a stable plaque phenotype that was rich in collagen and low in inflammatory cells (Mach et al., 1998; Lutgens et al., 1999; Lutgens et al., 2000). The role of CD40LG as a pro-inflammatory mediator in atherosclerosis was also confirmed in clinical studies (Lee et al., 1999; Heeschen et al., 2003). CD40LG is expressed on the surface of activated T-cells but the main source of soluble CD40 ligand are platelets (Graf et al., 1995; Henn et al., 1998). Furthermore, CD40LG binds to glycoprotein IIb/IIIa on platelets which promotes platelet aggregation and eventually leads to coagulation and thrombus formation (Andre et al., 2002). Interestingly, it is known that acetylsalicylic acid, the active ingredient of Aspirin, inactivates platelet function in part by irreversible glycoprotein IIb/IIIa modification and may thereby cease CD40LG production (Muhlestein, 2010). Therefore, possibly higher doses of Aspirin medication in cases compared to controls may account for decreased transcript levels of CD40LG in EMI individuals.

Discussion

In addition, there is substantial evidence that statins are capable to reduce expression of the CD40/CD40LG dyad via inhibition of IFN- γ signaling in a variety of atherogenic cell types (Arnaud et al., 2005). Statins are traditionally known as 3-hydroxy-3-methylglutaryl coenzyme A (HMG-CoA) reductase inhibitors that block a rate-limiting step in cholesterol biosynthesis (Alberts et al., 1980). Clinical studies in the 1990s have proven statins as the most efficient drugs to reduce serum cholesterol levels in atherosclerotic patients (Scandinavian Simvastatin Survival Study Group, 1994). During the last decade accumulating evidence emerged that statins also exert immunomodulatory and anti-inflammatory properties contributing to an improved clinical outcome in atherosclerosis (Downs et al., 1998; Tonkin et al., 2000; Nissen et al., 2005; Ridker et al., 2005). Benefits of statin therapy have actually been extended to other (auto-immune) inflammatory diseases such as multiple sclerosis and rheumatoid arthritis (McC Carey et al., 2004; Vollmer et al., 2004). Basic research has rendered some mechanistic insight on these pleiotropic effects and revealed HMG-CoA reductase dependent and independent actions of statin. Inhibition of HMG-CoA reductase does not only block cholesterol synthesis but also interferes with isoprenoid synthesis. Isoprenylation is crucial for post-translational modification and subsequent function of small GTPases of the Ras and Rho family (Hall, 1998). For example, inhibition of Rac1 prenylation and Rac1-mediated NAD(P)H oxidase activity by statins attenuates the production of reactive oxygen species (Takemoto et al., 2001; Wassmann, 2001). However, it is questionable whether the observed down-regulation of NOX4 in Ingenuity Network 2 is possibly related to statin treatment (Figure 13). An important finding is that statins inhibit IFN- γ -induced MHC-II expression in atherogenic cells such as monocytes and macrophages and, thus, act as direct repressors of MHC-II-mediated T-cell activation. Repression is independent of HMG-CoA reductase inhibition and occurs via attenuation of an inducible promoter of the transactivator CIITA (Kwak et al., 2000). Decreased transcript levels of HLA-DQA1, a MHC-II class gene, were indeed found in Ingenuity Network 3 and could therefore result from statin treatment. In contrast to classic MHC-II-mediated T-cell activation, HLA-DQA1 peptides seem to have inhibitory effects on T-cells though (Murphy et al., 1999; Zang & Murphy, 2005).

Several studies in mice and man demonstrated that statins also suppress the production of pro-atherogenic cytokines (e.g. IFN- γ , IL-12) and induce the production of anti-atherogenic cytokines (e.g. TGF- β) thereby shifting the immune response from a pro-inflammatory Th1 cell-mediated towards an anti-inflammatory Th2 cell-mediated phenotype (Youssef et al., 2002; Gegg et al., 2005; Rosenson et al., 1999; Shimada et al., 2004).

Discussion

Interestingly, the receptors for IL-12 and IFN- γ were found up-regulated during our differential expression analysis in Ingenuity Network 2 and PANTHER biological process category „Immunity and Defense“, respectively (Figure 13 and Figure 17). Increased transcript levels of these two cytokine receptors could in fact represent a response to statin-reduced IL-12 and IFN- γ expression thereby maintaining a pro-inflammatory Th1 cell-mediated immune response. Moreover, this implicates a mechanism for evasion of the disease phenotype from therapeutical medication and provides at least in part an explanation why the inflammatory signature is still persistent in EMI subjects. A possible decrease of IFN- γ levels due to statin treatment may be also the reason for the observed down-regulation of eight interferon-inducible genes in Ingenuity network 2 (Figure 13 and Table 9). Most of these genes encode either transcription factors or enzymes involved in DNA metabolism that have not been implicated in cardiovascular disease before. Altogether, the interference with IFN- γ and CD40 ligand signaling seems a critical feature of statin immunosuppressive effects. Obviously, both cytokines play a major role at the interface of cytokine crosstalk between atherogenic cells resulting in activation of T-cell populations that mediate pro-inflammatory effector functions.

3. Significance of the study results

This study used whole genome expression profiling and a systems biology analysis approach that together yielded a rich data set with potential candidate genes for early-onset coronary artery disease. A complex picture of robust and redundant inflammatory signatures within the EMI cohort emerged. The complexity of pathways was at least in part expected as the samples comprised pooled RNA from circulating blood cells including platelets and leukocytes (lymphocytes, granulocytes, monocytes). We decided to analyze initially the whole blood transcriptome as further separation into different leukocyte cell types could have affected the gene expression pattern. However, as a follow-up study it may be of interest to analyze cell fractions of lymphocytes, granulocytes and monocytes separately. The identified genes cover multiple functional aspects of inflammation but also revealed other features related to atherosclerosis such as cholesterol homeostasis (Table 9 and Table 10). However, among the diverse genes related to the innate and adaptive immune response were many that have been previously not reported in the context of atherosclerosis. In addition, there were new candidate genes without a documented function in cardiovascular disease and inflammation. Interestingly, only a few genes were found that encode for cytokines.

Discussion

This may reflect the phenotype but could also result from technical limitations as many growth factors are produced in low quantities and/or have a short half life in terms of their mRNA stability. Most cytokine genes are known to harbor AU-rich elements (AREs) in their 3' untranslated region (UTR) that confer to rapid mRNA decay, for example via a multiprotein complex called the exosome (Khabar, 2007; Hamilton et al., 2010).

The overlap of our candidate genes with those of other studies seems marginal at first. Two laboratories within the Cardiovascular Research Unit at Duke University have recently analyzed peripheral blood cell gene expression signatures in patients with coronary artery disease (CAD). In one study, comprising 222 subjects, a set of 160 differentially expressed genes predictive of the extent of CAD was identified. From these, one perfect match (NOX4) as well as six genes of gene/protein families (LGALS9, ABCC6, NOTCH2, IL2, SOX4, HDAC5) correlating to our candidate genes were detected (Table 11) (Sinnaeve et al., 2009).

Sinnaeve et al.	Corresponding candidate gene of this study	Biological function
NOX4 (NADPH oxidase)	NOX4 (Network 1 and PANTHER)	Vascular inflammation
LGALS9 (L-galectin)	LGALS3 (Network 2 and PANTHER)	Pro-inflammatory
ABCC6 (ABC transporter)	ABCG5 (Network 3)	Cholesterol depletion
NOTCH2 (notch ligand)	JAG1 (Network 1 and PANTHER)	T-cell activation
IL2 (cytokine)	CD40LG (Network 2)	Pro-inflammatory
SOX4 (transcription factor)	SOX6 (Network 4)	Cardiac development
HDAC5 (histone deacetylase)	HDAC2 (Network 4)	Lymphocyte differentiation

Table 11. Overlapping functions within the gene expression signature between the study of Sinnaeve et al. and our results.

Full name of the gene family is added in parentheses. Network plus number and/or PANTHER indicate the source within our ontological analysis.

Discussion

Another study, comprising a total of 243 subjects, identified 50 genes from microarray analysis (41 subjects) and 56 genes based on a literature search that correlated with the extent of coronary artery stenosis and were in addition validated by qPCR analysis in two independent patient cohorts comprising 95 subjects and 107 subjects, respectively (Wingrove et al., 2008). Out of these 106 identified genes, one exact match (MGST1) of the microarray pool and five validated genes (TNF, TNFRSF1B, IFNG, IL8RA, IL8RB) of the literature search did correspond to genes of cytokines and/or corresponding receptors in our potential candidate list (Table 12).

Wingrove et al.	Corresponding candidate gene of this study	Biological function
MGST1 (microsomal glutathione-S-transferase)	MGST1 (Network 2)	Oxidative stress
TNF, TNFRSF1B (tumor necrosis factor / receptor)	CD40LG (Network 2)	Pro-inflammatory
IFNG (interferon-γ)	IFNGR1 (PANTHER)	Pro-inflammatory
IL8RA, IL8RB (interleukin receptor)	IL12RB1 (Network 2)	Pro-inflammatory

Table 12. Overlapping functions within the gene expression signature between the study of Wingrove et al. and our results.

Full name of the gene family is added in parentheses. Network plus number and/or PANTHER indicate the source within our ontological analysis.

Taken together, our and other studies display at least a partial overlap in terms of the identified inflammatory profiles and their respective cytokine signaling pathways. Notably, expression levels of CD40LG were not found elevated in those studies either, possibly as a result of similar medication (e.g. aspirin and statins) of the patient cohorts. In conclusion, there is a certain degree of consistency between microarray data with respect to the functional categories embedded in the gene expression signatures.

The use of genome-wide expression profiling in order to investigate the underlying phenotype of atherosclerosis has started at the beginning of this millennium. However, these studies have almost exclusively addressed the vasculature and therein atherosclerotic plaques (Bijnens et al., 2006).

Discussion

Most studies were performed using animal models as well as human tissue samples and revealed diverse individual genes and/or pathways that confirmed the prevailing knowledge of atherosclerosis as an inflammatory disease (Hiltunen et al., 2002; Archacki et al., 2003; King et al., 2005; Lutgens et al., 2005; Tabibiazar et al., 2005). At the time when this investigation was initiated, to our knowledge no comprehensive microarray study was published that had analyzed gene expression signatures of whole blood in atherosclerotic coronary artery disease. Hence, it was of outstanding interest to answer the question whether circulating blood cells would mirror the phenotype of vascular tissue. Based on the findings of this study the answer seems to be, yes. In addition, our results are supported by the two recently published studies of the Duke Medical Center (Wingrove et al., 2008; Sinnaeve et al., 2009). Both studies demonstrated a correlation of gene expression signatures in circulating blood cells with the CAD phenotype. Furthermore, Sinnaeve and colleagues were able to show that gene expression patterns in peripheral blood cells actually correlated with those from tissue samples of atherosclerotic vasculature from an independent patient cohort.

The future perspective of the present investigation is to further validate genes from our candidate list in larger epidemiological studies but also in basic research. Testing of individual genes in larger patient cohorts would add statistical significance and could be in addition used to investigate potential genetic causes for reduced expression as observed in some of the detected genes. One of the limitations of microarray analysis remains the inability to distinguish whether decreased transcript levels of a specific gene result from genetic or epigenetic influences. For example, the gene GSTT1 is deleted in a relatively high percentage of the human population and was also identified with decreased expression in EMI individuals during our analysis (Bolt & Thier, 2006). Genes successfully validated in large scale studies could eventually qualify as biomarkers that may serve as diagnostic indicators of the atherosclerotic phenotype. Complementary, it would be interesting to further assess candidate genes in basic research using functional studies at the molecular level in the diverse cell types implicated in atherosclerosis. By gaining mechanistic insight this approach could lead to the identification of new targets for therapeutical drug development. In conclusion, genome-wide expression profiling is a powerful tool that can serve as an unbiased high-throughput approach to discover new candidate genes for phenotypes with a multifactorial background such as atherosclerotic coronary artery disease.

Abstract

V. Abstract

The aim of the second part of my PhD project was to identify differential gene expression signatures in circulating blood cells that are associated with coronary artery disease.

Using a microarray-based whole genome expression profiling approach the transcriptome of circulating peripheral blood cells from individuals diagnosed with atherosclerotic coronary artery disease (CAD) was analyzed. The study cohort was assembled from a large clinical database hosted by the Veterans Administration Pacific Islands Healthcare System (VAPHICS). Samples from patients with early myocardial infarction (MI) prior to age 50 and clinically diagnosed with CAD were compared to a healthy control group treated with the same cardiac-related medication. Gene expression profiles from whole blood mRNA samples that were depleted for β -globin transcripts was assessed by microarray analysis. A novel algorithm called LOTEST that was specifically designed to detect heterogenous and sparse signals embedded within gaussian noise, identified 1203 differentially expressed genes between patients and controls. Out of these, 195 genes were excluded from downstream analysis as they were represented by only two individuals within the patient group. The gene ontology databases „Protein Analysis Through Evolutionary Relationships“ (PANTHER) and „Ingenuity Pathway Analysis“ (IPA) were then applied to analyze functional grouping within the identified differential gene expression pattern. The analysis revealed over-representation of genes that are associated with inflammation and immune system function. A list of potential candidate genes with the most consistent expression pattern across the sample groups was confirmed by quantitative real-time PCR analysis and included up-regulated pro-inflammatory genes (PTX3, LGALS3, CAMP), down-regulated anti-inflammatory genes (IL12RB1, JAG1), decreased expression of genes that protect from auto-immunity (IL2RA, CCR7) and genes not previously implicated in immune system function (GSTT1, NGFR). The results of this study suggest persistent ongoing inflammation in CAD patients of the study cohort despite treatment with anti-inflammatory medication.

The outcome of this small-scale study can serve as a basis for future investigations in order to discover new biomarkers and/or potential targets for drug development against so far unknown disease mechanism(s). Certainly, the realization of these tasks would require substantial epidemiological and basic research efforts.

VI. Zusammenfassung

Das Ziel des zweiten Teils dieser Dissertation war die Identifizierung von Genen in zirkulierenden Blutzellen, deren differentielles Expressionsmuster mit dem Phänotyp der koronaren Herzkrankheit korreliert.

Unter Verwendung eines Microarray-basierten Ansatzes wurde das gesamte Transkriptom aus peripher zirkulierenden Blutzellen von Patienten mit koronarer Herzkrankheit im Vergleich zu einer gesunden Kontrollgruppe analysiert. Die Teilnehmer der vorliegenden Studie wurden aus einer klinischen Datenbank des „Veterans Administration Pacific Islands Healthcare System“ (VAPHICS) ausgewählt. Proben von Patienten, die vor Erreichen des 50. Lebensjahres einen Herzinfarkt erlitten haben, und bei denen eine klinisch diagnostizierte koronare Herzkrankheit vorlag, wurden mit einer gesunden Kontrollgruppe verglichen, die die gleichen Medikamente einnahm. Genexpressionsprofile von mRNA Proben aus Gesamtblut, die zuvor von beta-Globin Transkripten bereinigt waren, wurden anhand von Microarray-Analysen untersucht. Ein neuer Algorithmus mit dem Namen LOTEST, der speziell drauf ausgerichtet ist heterogene und seltene Signale in einem starken Gaußschen Hintergrundrauschen zu detektieren, identifizierte 1203 differentiell exprimierte Gene zwischen Patienten und Kontrollindividuen. Davon wurden 195 Gene von der nachfolgenden Datenanalyse ausgeschlossen, da dieses Signal nur in zwei Individuen der Patientengruppe repräsentiert war. Die beiden Gen-Ontologie Datenbanken „Protein Analysis Through Evolutionary Relationships“ (PANTHER) und „Ingenuity Pathway Analysis“ (IPA) wurden nachfolgend angewandt um mögliche funktionelle Gruppierungen in der differentiellen Genexpressionssignatur zu analysieren. Die Analyse ergab eine Überrepräsentierung von Genen, die mit Entzündungsmechanismen und der Funktion des Immunsystems assoziiert sind. Eine Liste von potentiellen Kandidatengenen, deren Expressionsmuster in den jeweiligen Studiengruppen besonders homogen war, konnte durch quantitative PCR Analysen bestätigt werden. Diese Kandidatengene umfassen hochregulierte entzündungsfördernde Gene (PTX3, LGALS3, CAMP), herunterregulierte entzündungshemmende Gene (IL12RB1, JAG1), abgeschwächte Expression von Genen, die vor Autoimmunreaktionen schützen (IL2RA, CCR7), sowie Gene, die vorher nicht im Kontext der Funktion des Immunsystems bekannt waren. Die Ergebnisse dieser Studie deuten darauf hin, dass trotz medikamentöser Behandlung mit Entzündungshemmern, ein persistenter Entzündungsstatus bei Patienten mit koronarer Herzkrankheit vorliegt.

Zusammenfassung

Das Resultat dieser im kleinen Maßstab angelegten Studie kann als Basis für zukünftige Untersuchungen dienen, deren Zielsetzung es ist neue Biomarker und/oder potentielle Zielgene für die Entwicklung von neuen Medikamenten gegen bislang unbekannte Mechanismen der koronaren Herzkrankheit zu finden. Diese ambitionierten Ziele erfordern jedoch weitere substantielle Anstrengungen auf den Gebieten der Grundlagen- sowie der epidemiologischen Forschung.

VII. Literature

Adachi T, Alam R. The mechanism of IL-5 signal transduction. *Am J Physiol.* 1998 Sep;275(3 Pt 1):C623-33.

Alberts AW, Chen J, Kuron G, Hunt V, Huff J, Hoffman C, Rothrock J, Lopez M, Joshua H, Harris E, Patchett A, Monaghan R, Currie S, Stapley E, Albers-Schonberg G, Hensens O, Hirshfield J, Hoogsteen K, Liesch J, Springer J. Mevinolin: a highly potent competitive inhibitor of hydroxymethylglutaryl-coenzyme A reductase and a cholesterol-lowering agent. *Proc Natl Acad Sci U S A.* 1980 Jul;77(7):3957-61.

An G, Wang H, Tang R, Yago T, McDaniel JM, McGee S, Huo Y, Xia L. P-selectin glycoprotein ligand-1 is highly expressed on Ly-6Chi monocytes and a major determinant for Ly-6Chi monocyte recruitment to sites of atherosclerosis in mice. *Circulation.* 2008 Jun 24;117(25):3227-37.

André P, Prasad KS, Denis CV, He M, Papalia JM, Hynes RO, Phillips DR, Wagner DD. CD40L stabilizes arterial thrombi by a beta3 integrin--dependent mechanism. *Nat Med.* 2002 Mar;8(3):247-52.

Angeli V, Llodrá J, Rong JX, Satoh K, Ishii S, Shimizu T, Fisher EA, Randolph GJ. Dyslipidemia associated with atherosclerotic disease systemically alters dendritic cell mobilization. *Immunity.* 2004 Oct;21(4):561-74.

Anitschkow N, Chalakov S. Ueber experimentelle Cholesterinstearose. *Zbl allg Path path Anat.* 1913 24: 1-9.

Arnaud C, Braunersreuther V, Mach F. Toward immunomodulatory and anti-inflammatory properties of statins. *Trends Cardiovasc Med.* 2005 Aug;15(6):202-6.

Badie S, Escandell JM, Bouwman P, Carlos AR, Thanasoula M, Gallardo MM, Suram A, Jaco I, Benitez J, Herbig U, Blasco MA, Jonkers J, Tarsounas M. BRCA2 acts as a RAD51 loader to facilitate telomere replication and capping. *Nat Struct Mol Biol.* 2010 Dec;17(12):1461-9.

Bahi N, Friocourt G, Carrié A, Graham ME, Weiss JL, Chafey P, Fauchereau F, Burgoyne RD, Chelly J. IL1 receptor accessory protein like, a protein involved in X-linked mental retardation, interacts with Neuronal Calcium Sensor-1 and regulates exocytosis. *Hum Mol Genet.* 2003 Jun 15;12(12):1415-25.

Literature

Bai X, Liang Z, Zhao S, Liu X, Zhu M, Wu Z, Yu M. The porcine ANG, RNASE1 and RNASE6 genes: molecular cloning, polymorphism detection and the association with haematological parameters. *Mol Biol Rep.* 2009 Nov;36(8):2405-11.

Barnes PJ. Role of HDAC2 in the pathophysiology of COPD. *Annu Rev Physiol.* 2009;71:451-64. Review.

Basso K, Margolin AA, Stolovitzky G, Klein U, Dalla-Favera R, Califano A. Reverse engineering of regulatory networks in human B cells. *Nat Genet.* 2005 Apr;37(4):382-90.

Baumrucker T, Csonga R, Pursch E, Pfeffer A, Urtz N, Sutton S, Bofill-Cardona E, Cooke M, Prieschl E. Activation of mast cells by incorporation of cholesterol into rafts. *Int Immunol.* 2003 Oct;15(10):1207-18.

Berchtold S, Manncke B, Klenk J, Geisel J, Autenrieth IB, Bohn E. Forced IFIT-2 expression represses LPS induced TNF-alpha expression at posttranscriptional levels. *BMC Immunol.* 2008 Dec 24;9:75.

Bhatt DL, Topol EJ. Scientific and therapeutic advances in antiplatelet therapy. *Nat Rev Drug Discov.* 2003 Jan;2(1):15-28.

Bijnens AP, Lutgens E, Ayoubi T, Kuiper J, Horrevoets AJ, Daemen MJ. Genome-wide expression studies of atherosclerosis: critical issues in methodology, analysis, interpretation of transcriptomics data. *Arterioscler Thromb Vasc Biol.* 2006 Jun;26(6):1226-35.

Berenson GS, Srinivasan SR, Nicklas TA. Atherosclerosis: a nutritional disease of childhood. *Am J Cardiol.* 1998 Nov 26;82(10B):22T-29T.

Blumenthal A, Ehlers S, Lauber J, Buer J, Lange C, Goldmann T, Heine H, Brandt E, Reiling N. The Wingless homolog WNT5A and its receptor Frizzled-5 regulate inflammatory responses of human mononuclear cells induced by microbial stimulation. *Blood.* 2006 Aug 1;108(3):965-73.

Bolt HM, Thier R. Relevance of the deletion polymorphisms of the glutathione S-transferases GSTT1 and GSTM1 in pharmacology and toxicology. *Curr Drug Metab.* 2006 Aug;7(6):613-28.

Boring L, Gosling J, Cleary M, Charo IF. Decreased lesion formation in CCR2^{-/-} mice reveals a role for chemokines in the initiation of atherosclerosis. *Nature.* 1998 Aug 27;394(6696):894-7.

Bottazzi B, Garlanda C, Salvatori G, Jeannin P, Manfredi A, Mantovani A. Pentraxins as a key component of innate immunity. *Curr Opin Immunol.* 2006 Feb;18(1):10-5.

Literature

Brown RJ, Rader DJ. Lipases as modulators of atherosclerosis in murine models. *Curr Drug Targets.* 2007 Dec;8(12):1307-19.

Butte A. The use and analysis of microarray data. *Nat Rev Drug Discov.* 2002 Dec;1(12):951-60.

Campbell TC, Parpia B, Chen J. Diet, lifestyle, and the etiology of coronary artery disease: the Cornell China study. *Am J Cardiol.* 1998 Nov 26;82(10B):18T-21T.

Chelly J, Concorde JP, Kaplan JC, Kahn A. Illegitimate transcription: transcription of any gene in any cell type. *Proc Natl Acad Sci U S A.* 1989 Apr;86(8):2617-21.

Cohen-Barak O, Yi Z, Hagiwara N, Monzen K, Komuro I, Brilliant MH. Sox6 regulation of cardiac myocyte development. *Nucleic Acids Res.* 2003 Oct 15;31(20):5941-8.

Collins BE, Smith BA, Bengtson P, Paulson JC. 2006. *Ablation of CD22 in ligand-deficient mice restores B cell receptor signaling.* *Nat Immunol.* 2006 Feb;7(2):199-206.

Cornelis MC, El-Sohemy A, Campos H. GSTT1 genotype modifies the association between cruciferous vegetable intake and the risk of myocardial infarction. *Am J Clin Nutr.* 2007 Sep;86(3):752-8.

Cutler JA, Thom TJ, Roccella E. Leading causes of death in the United States. *JAMA.* 2006 Jan 25;295(4):383-4

Cybulsky MI, Gimbrone MA Jr. Endothelial expression of a mononuclear leukocyte adhesion molecule during atherogenesis. *Science.* 1991 Feb 15;251(4995):788-91.

Cybulsky MI, Iiyama K, Li H, Zhu S, Chen M, Iiyama M, Davis V, Gutierrez-Ramos JC, Connally PW, Milstone DS. A major role for VCAM-1, but not ICAM-1, in early atherosclerosis. *J Clin Invest.* 2001 May;107(10):1255-62.

Dai G, Kaazempur-Mofrad MR, Natarajan S, Zhang Y, Vaughn S, Blackman BR, Kamm RD, García-Cerdeña G, Gimbrone MA Jr. Distinct endothelial phenotypes evoked by arterial waveforms derived from atherosclerosis-susceptible and -resistant regions of human vasculature. *Proc Natl Acad Sci U S A.* 2004 Oct 12;101(41):14871-6.

Davalos-Misslitz AC, Rieckenberg J, Willenzon S, Worbs T, Kremmer E, Bernhardt G, Förster R. Generalized multi-organ autoimmunity in CCR7-deficient mice. *Eur J Immunol.* 2007 Mar;37(3):613-22.

Literature

de Boer OJ, van der Wal AC, Teeling P, Becker AE. Leucocyte recruitment in rupture prone regions of lipid-rich plaques: a prominent role for neovascularization? *Cardiovasc Res.* 1999 Feb;41(2):443-9.

Dekker FJ, Haisma HJ. Histone acetyl transferases as emerging drug targets. *Drug Discov Today.* 2009 Oct;14(19-20):942-8.

Deng YJ, Huang ZX, Zhou CJ, Wang JW, You Y, Song ZQ, Xiang MM, Zhong BY, Hao F. Gene profiling involved in immature CD4+ T lymphocyte responsible for systemic lupus erythematosus. *Mol Immunol.* 2006 Mar;43(9):1497-507.

Donato R. RAGE: a single receptor for several ligands and different cellular responses: the case of certain S100 proteins. *Curr Mol Med.* 2007 Dec;7(8):711-24.

Dong ZM, Chapman SM, Brown AA, Frenette PS, Hynes RO, Wagner DD. The combined role of P- and E-selectins in atherosclerosis. *J Clin Invest.* 1998 Jul 1;102(1):145-52.

Donoho, DL & Johnstone IM. Ideal spatial adaptation by wavelet shrinkage. *Biometrika* 1994 Aug, 3 (81): 425-455.

Donoho D, Jin J. Higher criticism thresholding: Optimal feature selection when useful features are rare and weak. *Proc Natl Acad Sci U S A.* 2008 Sep 30;105(39):14790-5.

Downs JR, Clearfield M, Weis S, Whitney E, Shapiro DR, Beere PA, Langendorfer A, Stein EA, Kruyer W, Gotto AM Jr. Primary prevention of acute coronary events with lovastatin in men and women with average cholesterol levels: results of AFCAPS/TexCAPS. Air Force/Texas Coronary Atherosclerosis Prevention Study. *JAMA.* 1998 May 27;279(20):1615-22.

Durand E, Scoazec A, Lafont A, Boddaert J, Al Hajzen A, Addad F, Mirshahi M, Desnos M, Tedgui A, Mallat Z. In vivo induction of endothelial apoptosis leads to vessel thrombosis and endothelial denudation: a clue to the understanding of the mechanisms of thrombotic plaque erosion. *Circulation.* 2004 Jun 1;109(21): 2503-6.

Eisen MB, Spellman PT, Brown PO, Botstein D. Cluster analysis and display of genome-wide expression patterns. *Proc Natl Acad Sci U S A.* 1998 Dec 8;95(25):14863-8.

Englund A, Kovanen L, Saarikoski ST, Haukka J, Reunanen A, Aromaa A, Lönnqvist J, Partonen T. NPAS2 and PER2 are linked to risk factors of the metabolic syndrome. *J Circadian Rhythms.* 2009 May 26;7:5.

Literature

Eskildsen S, Justesen J, Schierup MH, Hartmann R. Characterization of the 2'-5'-oligoadenylate synthetase ubiquitin-like family. *Nucleic Acids Res.* 2003 Jun 15;31(12):3166-73.

Farb A, Burke AP, Tang AL, Liang TY, Mannan P, Smialek J, Virmani R. Coronary plaque erosion without rupture into a lipid core. A frequent cause of coronary thrombosis in sudden coronary death. *Circulation.* 1996 Apr 1;93(7):1354-63.

Febbraio M, Podrez EA, Smith JD, Hajjar DP, Hazen SL, Hoff HF, Sharma K, Silverstein RL. Targeted disruption of the class B scavenger receptor CD36 protects against atherosclerotic lesion development in mice. *J Clin Invest.* 2000 Apr;105(8):1049-56.

Feil S, Hofmann F, Feil R. SM22alpha modulates vascular smooth muscle cell phenotype during atherogenesis. *Circ Res.* 2004 Apr 16;94(7):863-5.

Fensterl V, Sen GC. The ISG56/IFIT1 gene family. *J Interferon Cytokine Res.* 2011 Jan;31(1):71-8.

Fiorucci S, Cipriani S, Mencarelli A, Renga B, Distrutti E, Baldelli F. Counter-regulatory role of bile acid activated receptors in immunity and inflammation. *Curr Mol Med.* 2010 Aug 1;10(6):579-95.

Fodor SP, Read JL, Pirrung MC, Stryer L, Lu AT, Solas D. Light-directed, spatially addressable parallel chemical synthesis. *Science.* 1991 Feb 15;251(4995):767-73.

Fodor SP, Rava RP, Huang XC, Pease AC, Holmes CP, Adams CL. Multiplexed biochemical assays with biological chips. *Nature.* 1993 Aug 5;364(6437):555-6.

Frenette PS, Denis CV, Weiss L, Jurk K, Subbarao S, Kehrel B, Hartwig JH, Vestweber D, Wagner DD. P-Selectin glycoprotein ligand 1 (PSGL-1) is expressed on platelets and can mediate platelet-endothelial interactions in vivo. *J Exp Med.* 2000 Apr 17;191(8):1413-22.

Friesel R, Komoriya A, Maciag T. Inhibition of endothelial cell proliferation by gamma-interferon. *J Cell Biol.* 1987 Mar;104(3):689-96.

Frostegård J, Ulfgren AK, Nyberg P, Hedin U, Swedenborg J, Andersson U, Hansson GK. Cytokine expression in advanced human atherosclerotic plaques: dominance of pro-inflammatory (Th1) and macrophage-stimulating cytokines. *Atherosclerosis.* 1999 Jul;145(1):33-43.

Gardner TS, di Bernardo D, Lorenz D, Collins JJ. Inferring genetic networks and identifying compound mode of action via expression profiling. *Science.* 2003 Jul 4;301(5629):102-5.

Literature

Gawaz M, Brand K, Dickfeld T, Pogatsa-Murray G, Page S, Bogner C, Koch W, Schömig A, Neumann F. Platelets induce alterations of chemotactic and adhesive properties of endothelial cells mediated through an interleukin-1-dependent mechanism. Implications for atherosclerosis. *Atherosclerosis*. 2000 Jan;148(1):75-85.

Gaziano TA. Reducing the growing burden of cardiovascular disease in the developing world. *Health Affairs*. 2007; 26 (1): 13-24.

Gear AR, Camerini D. Platelet chemokines and chemokine receptors: linking hemostasis, inflammation, and host defense. *Microcirculation*. 2003 Jun;10(3-4):335-50.

Gegg ME, Harry R, Hankey D, Zambarakji H, Pryce G, Baker D, Adamson P, Calder V, Greenwood J. Suppression of autoimmune retinal disease by lovastatin does not require Th2 cytokine induction. *J Immunol*. 2005 Feb 15;174(4):2327-35.

Geissmann F, Jung S, Littman DR. Blood monocytes consist of two principal subsets with distinct migratory properties. *Immunity*. 2003 Jul;19(1):71-82.

Gleissner CA, von Hundelshausen P, Ley K. Platelet chemokines in vascular disease. *Arterioscler Thromb Vasc Biol*. 2008 Nov;28(11):1920-7.

Gofman JW, Lindgren F, Elliott h, Mantz W, Hewitt J, Strisower B, Herring V, Lyon TP. The role of lipids and lipoproteins in atherosclerosis. *Science*. 1950 Feb 17;111(2877):166-71.

Gordon S, Taylor PR. Monocyte and macrophage heterogeneity. *Nat Rev Immunol*. 2005 Dec;5(12):953-64.

Graf D, Müller S, Korthäuer U, van Kooten C, Weise C, Krocze RA. A soluble form of TRAP (CD40 ligand) is rapidly released after T cell activation. *Eur J Immunol*. 1995 Jun;25(6):1749-54.

Gu L, Okada Y, Clinton SK, Gerard C, Sukhova GK, Libby P, Rollins BJ. Absence of monocyte chemoattractant protein-1 reduces atherosclerosis in low density lipoprotein receptor-deficient mice. *Mol Cell*. 1998 Aug;2(2):275-81.

Gupta MP, Samant SA, Smith SH, Shroff SG. HDAC4 and PCAF bind to cardiac sarcomeres and play a role in regulating myofilament contractile activity. *J Biol Chem*. 2008 Apr 11;283(15):10135-46.

Härter L, Petersen F, Flad HD, Brandt E. Connective tissue-activating peptide III desensitizes chemokine receptors on neutrophils. Requirement for proteolytic formation of the neutrophil-activating peptide 2. *J Immunol*. 1994 Dec 15;153(12):5698-708.

Literature

Hagiwara N, Klewer SE, Samson RA, Erickson DT, Lyon MF, Brilliant MH. Sox6 is a candidate gene for p100H myopathy, heart block, and sudden neonatal death. *Proc Natl Acad Sci U S A.* 2000 Apr 11;97(8):4180-5.

Hall A. Rho GTPases and the actin cytoskeleton. *Science.* 1998 Jan 23;279(5350):509-14.

Hamilton T, Novotny M, Pavicic PJ Jr, Herjan T, Hartupee J, Sun D, Zhao C, Datta S. Diversity in post-transcriptional control of neutrophil chemoattractant cytokine gene expression. *Cytokine.* 2010 Oct-Nov;52(1-2):116-22.

Han KH, Han KO, Green SR, Quehenberger O. Expression of the monocyte chemoattractant protein-1 receptor CCR2 is increased in hypercholesterolemia. Differential effects of plasma lipoproteins on monocyte function. *J Lipid Res.* 1999 Jun;40(6):1053-63.

Hansson GK, Libby P. The immune response in atherosclerosis: a double-edged sword. *Nat Rev Immunol.* 2006 Jul;6(7):508-19.

Hansson GK, Hellstrand M, Rymo L, Rubbia L, Gabbiani G. Interferon gamma inhibits both proliferation and expression of differentiation-specific alpha-smooth muscle actin in arterial smooth muscle cell. *J Exp Med.* 1989 Nov 1;170(5):1595-608.

Hawrylowicz CM, Howells GL, Feldmann M. Platelet-derived interleukin 1 induces human endothelial adhesion molecule expression and cytokine production. *J Exp Med.* 1991 Oct 1;174(4):785-90.

Hayes JD, Strange RC. Glutathione S-transferase polymorphisms and their biological consequences. *Pharmacology.* 2000 Sep;61(3):154-66.

Heeschen C, Dimmeler S, Hamm CW, van den Brand MJ, Boersma E, Zeiher AM, Simoons ML; CAPTURE Study Investigators. Soluble CD40 ligand in acute coronary syndromes. *N Engl J Med.* 2003 Mar 20;348(12):1104-11.

Henderson NC, Sethi T. The regulation of inflammation by galectin-3. *Immunol Rev.* 2009 Jul;230(1):160-71.

Henn V, Slupsky JR, Gräfe M, Anagnostopoulos I, Förster R, Müller-Berghaus G, Kroczek RA. CD40 ligand on activated platelets triggers an inflammatory reaction of endothelial cells. *Nature.* 1998 Feb 5;391 (6667):591-4.

Literature

Hermiston ML, Zikherman J, Zhu JW. CD45, CD148, and Lyp/Pep: critical phosphatases regulating Src family kinase signaling networks in immune cells. *Immunol Rev.* 2009 Mar;228(1):288-311.

Hofmann AM, Abraham SN. New roles for mast cells in modulating allergic reactions and immunity against pathogens. *Curr Opin Immunol.* 2009 Dec;21(6):679-86.

Hong TT, Smyth JW, Gao D, Chu KY, Vogan JM, Fong TS, Jensen BC, Colecraft HM, Shaw RM. BIN1 localizes the L-type calcium channel to cardiac T-tubules. *PLoS Biol.* 2010 Feb 16;8(2):e1000312.

Huo Y, Schober A, Forlow SB, Smith DF, Hyman MC, Jung S, Littman DR, Weber C, Ley K. Circulating activated platelets exacerbate atherosclerosis in mice deficient in apolipoprotein E. *Nat Med.* 2003 Jan;9(1):61-7.

Hsu DK, Chen HY, Liu FT. Galectin-3 regulates T-cell functions. *Immunol Rev.* 2009 Jul;230(1):114-27.

Iacobelli M, Wachsman W, McGuire KL. Repression of IL-2 promoter activity by the novel basic leucine zipper p21SNFT protein. *J Immunol.* 2000 Jul 15;165(2):860-8.

Ignatowski A. Wirkung der tierischen Nahrung auf den Kaninchenorganismus. *Ber Milit-med Akad.* 1908 16:154-176.

Imbeaud S, Graudens E, Boulanger V, Barlet X, Zaborski P, Eveno E, Mueller O, Schroeder A and Auffray C. Towards standardization of RNA quality assessment using user-independent classifiers of microcapilaary electrophoresis traces. *Nucl. Acids Res.* 2005 33 (6): e56.

Isakov N, Witte S, Altman A. PICOT-HD: a highly conserved protein domain that is often associated with thioredoxin and glutaredoxin modules. *Trends Biochem Sci.* 2000 Nov;25(11):537-9.

Ishibashi S, Herz J, Maeda N, Goldstein JL, Brown MS. The two-receptor model of lipoprotein clearance: tests of the hypothesis in "knockout" mice lacking the low density lipoprotein receptor, apolipoprotein E, or both proteins. *Proc Natl Acad Sci U S A.* 1994 May 10;91(10):4431-5.

JACOB F, MONOD J. Genetic regulatory mechanisms in the synthesis of proteins. *J Mol Biol.* 1961 Jun; 3:318-56.

Jakobsson PJ, Morgenstern R, Mancini J, Ford-Hutchinson A, Persson B. Membrane-associated proteins in eicosanoid and glutathione metabolism (MAPEG). A widespread protein superfamily. *Am J Respir Crit Care Med.* 2000 Feb;161(2 Pt 2):S20-4.

Literature

Johnson JL, Jackson CL, Angelini GD, George SJ. Activation of matrix-degrading metalloproteinases by mast cell proteases in atherosclerotic plaques. *Arterioscler Thromb Vasc Biol.* 1998 Nov;18(11):1707-15.

Kaartinen M, Penttilä A, Kovanen PT. Accumulation of activated mast cells in the shoulder region of human coronary atheroma, the predilection site of atheromatous rupture. *Circulation.* 1994 Oct;90(4):1669-78.

Kaartinen M, Penttilä A, Kovanen PT. Mast cells in rupture-prone areas of human coronary atheromas produce and store TNF-alpha. *Circulation.* 1996 Dec 1;94(11):2787-92.

Kato N, Motohashi S, Okada T, Ozawa T, Mashima K. PICOT, protein kinase C theta-interacting protein, is a novel regulator of FcepsilonRI-mediated mast cell activation. *Cell Immunol.* 2008 Jan;251(1):62-7.

Katoh M, Katoh M. Human FOX gene family. *Int J Oncol.* 2004 Nov;25(5):1495-500.

Khabar KS. Rapid transit in the immune cells: the role of mRNA turnover regulation. *J Leukoc Biol.* 2007 Jun;81(6):1335-44.

Kitano H. Computational systems biology. *Nature.* 2002 Nov 14;420(6912):206-10.

Kol A, Sukhova GK, Lichtman AH, Libby P. Chlamydial heat shock protein 60 localizes in human atheroma and regulates macrophage tumor necrosis factor-alpha and matrix metalloproteinase expression. *Circulation.* 1998 Jul 28;98(4):300-7.

Kovac J, Husse J, Oster H. A time to fast, a time to feast: the crosstalk between metabolism and the circadian clock. *Mol Cells.* 2009 Aug 31;28(2):75-80.

Kozaki K. Identification of specific autoantigens in Sjögren's syndrome by SEREX. *Immunology.* 2005 Sep; 116(1):53-63.

Krämer OH. HDAC2: a critical factor in health and disease. *Trends Pharmacol Sci.* 2009 Dec;30(12):647-55.

Kwak B, Mulhaupt F, Myit S, Mach F. Statins as a newly recognized type of immunomodulator. *Nat Med.* 2000 Dec;6(12):1399-402.

Lassègue B, Griendling KK. NADPH oxidases: functions and pathologies in the vasculature. *Arterioscler Thromb Vasc Biol.* 2010 Apr;30(4):653-61.

Literature

Latini R, Maggioni AP, Peri G, Gonzini L, Lucci D, Mocarelli P, Vago L, Pasqualini F, Signorini S, Soldateschi D, Tarli L, Schweiger C, Fresco C, Cecere R, Tognoni G, Mantovani A. Lipid Assessment Trial Italian Network (LATIN) Investigators. Prognostic significance of the long pentraxin PTX3 in acute myocardial infarction. *Circulation*. 2004 Oct 19;110(16):2349-54.

Leal J, Luengo-Fernández R, Gray A, Petersen S, Rayner M. Economic burden of cardiovascular diseases in the enlarged European Union. *Eur Heart J*. 2006 Jul;27(13):1610-9.

Lee Y, Lee WH, Lee SC, Ahn KJ, Choi YH, Park SW, Seo JD, Park JE. CD40L activation in circulating platelets in patients with acute coronary syndrome. *Cardiology*. 1999;92(1):11-6.

Leibowitz J. The History of Coronary Artery Disease. London: *Wellcome Institute of the History of Medicine*, 1970.

Leitenberg D, Falahati R, Lu DD, Takeda A. CD45-associated protein promotes the response of primary CD4 T cells to low-potency T-cell receptor (TCR) stimulation and facilitates CD45 association with CD3/TCR and lck. *Immunology*. 2007 Aug;121(4):545-54.

Leon ML, Zuckerman SH. Gamma interferon: a central mediator in atherosclerosis. *Inflamm Res*. 2005 Oct;54(10):395-411.

Levy D, Thom TJ. Death rates from coronary disease--progress and a puzzling paradox. *N Engl J Med*. 1998 Sep 24;339(13):915-7.

Li H, Dai M, Zhuang Y. A T cell intrinsic role of Id3 in a mouse model for primary Sjogren's syndrome. *Immunity*. 2004 Oct;21(4):551-60.

Li YT, Swales KE, Thomas GJ, Warner TD, Bishop-Bailey D. Farnesoid X receptor ligands inhibit vascular smooth muscle cell inflammation and migration. *Arterioscler Thromb Vasc Biol*. 2007 Dec;27(12):2606-11.

Libby P, Aikawa M. Stabilization of atherosclerotic plaques: new mechanisms and clinical targets. *Nat Med*. 2002 Nov;8(11):1257-62.

Lievens D, Eijgelaar WJ, Biessen EA, Daemen MJ, Lutgens E. The multi-functionality of CD40L and its receptor CD40 in atherosclerosis. *Thromb Haemost*. 2009 Aug;102(2):206-14.

Liu W, Mani S, Davis NR, Sarrafzadegan N, Kavathas PB, Mani A. Mutation in EGFP domain of LDL receptor-related protein 6 impairs cellular LDL clearance. *Circ Res*. 2008 Nov 21;103(11):1280-8.

Literature

Livak KJ, Schmittgen TD. Analysis of relative gene expression data using real-time quantitative PCR and the 2(-Delta Delta C(T)) Method. *Methods*. 2001 Dec;25(4):402-8.

Llodrá J, Angeli V, Liu J, Trogan E, Fisher EA, Randolph GJ. Emigration of monocyte-derived cells from atherosclerotic lesions characterizes regressive, but not progressive, plaques. *Proc Natl Acad Sci U S A*. 2004 Aug 10;101(32):11779-84.

Luoma PV. Cytochrome P450 and gene activation--from pharmacology to cholesterol elimination and regression of atherosclerosis. *Eur J Clin Pharmacol*. 2008 Sep;64(9):841-50.

Lutgens E, Gorelik L, Daemen MJ, de Muinck ED, Grewal IS, Koteliansky VE, Flavell RA. Requirement for CD154 in the progression of atherosclerosis. *Nat Med*. 1999 Nov;5(11):1313-6.

Lutgens E, Cleutjens KB, Heeneman S, Koteliansky VE, Burkly LC, Daemen MJ. Both early and delayed anti-CD40L antibody treatment induces a stable plaque phenotype. *Proc Natl Acad Sci U S A*. 2000 Jun 20;97(13):7464-9.

Lutgens E, Gijbels M, Smook M, Heeringa P, Gotwals P, Koteliansky VE, Daemen MJ. Transforming growth factor-beta mediates balance between inflammation and fibrosis during plaque progression. *Arterioscler Thromb Vasc Biol*. 2002 Jun 1;22(6):975-82.

Lutgens E, Lievens D, Beckers L, Donners M, Daemen M. CD40 and its ligand in atherosclerosis. *Trends Cardiovasc Med*. 2007 May;17(4):118-23.

Mach F, Schönbeck U, Sukhova GK, Bourcier T, Bonnefoy JY, Pober JS, Libby P. Functional CD40 ligand is expressed on human vascular endothelial cells, smooth muscle cells, and macrophages: implications for CD40-CD40 ligand signaling in atherosclerosis. *Proc Natl Acad Sci U S A*. 1997 Mar 4;94(5):1931-6.

Mach F, Schönbeck U, Bonnefoy JY, Pober JS, Libby P. Activation of monocyte/macrophage functions related to acute atheroma complication by ligation of CD40: induction of collagenase, stromelysin, and tissue factor. *Circulation*. 1997 Jul 15;96(2):396-9.

Mach F, Schönbeck U, Sukhova GK, Atkinson E, Libby P. Reduction of atherosclerosis in mice by inhibition of CD40 signalling. *Nature*. 1998 Jul 9;394(6689):200-3.

Majdalawieh A, Zhang L, Fukui IV, Rader DJ, Ro HS. Adipocyte enhancer-binding protein 1 is a potential novel atherogenic factor involved in macrophage cholesterol homeostasis and inflammation. *Proc Natl Acad Sci U S A*. 2006 Feb 14;103(7):2346-51.

Literature

Majdalawieh A, Zhang L, Ro HS. Adipocyte enhancer-binding protein-1 promotes macrophage inflammatory responsiveness by up-regulating NF-kappaB via IkappaBalph negative regulation. *Mol Biol Cell.* 2007 Mar;18(3):930-42.

Majdalawieh A, Ro HS. Regulation of IkappaBalph function and NF-kappaB signaling: AEBP1 is a novel proinflammatory mediator in macrophages. *Mediators Inflamm.* 2010;2010:823821.

Mallat Z, Besnard S, Duriez M, Deleuze V, Emmanuel F, Bureau MF, Soubrier F, Esposito B, Duez H, Fievet C, Staels B, Duverger N, Scherman D, Tedgui A. Protective role of interleukin-10 in atherosclerosis. *Circ Res.* 1999 Oct 15;85(8):e17-24.

Mallat Z, Gojova A, Marchiol-Fournigault C, Esposito B, Kamaté C, Merval R, Fradelizi D, Tedgui A. Inhibition of transforming growth factor-beta signaling accelerates atherosclerosis and induces an unstable plaque phenotype in mice. *Circ Res.* 2001 Nov 9;89(10):930-4.

Mani A, Radhakrishnan J, Wang H, Mani A, Mani MA, Nelson-Williams C, Carew KS, Mane S, Najmabadi H, Wu D, Lifton RP. LRP6 mutation in a family with early coronary disease and metabolic risk factors. *Science.* 2007 Mar 2;315(5816):1278-82.

Manolagas SC, Almeida M. Gone with the Wnts: beta-catenin, T-cell factor, forkhead box O, and oxidative stress in age-dependent diseases of bone, lipid, and glucose metabolism. *Mol Endocrinol.* 2007 Nov;21(11):2605-14.

Marballi K, Quinones MP, Jimenez F, Escamilla MA, Raventós H, Soto-Bernardini MC, Ahuja SS, Walss-Bass C. In vivo and in vitro genetic evidence of involvement of neuregulin 1 in immune system dysregulation. *J Mol Med.* 2010 Nov;88(11):1133-41.

Marcheva B, Ramsey KM, Buhr ED, Kobayashi Y, Su H, Ko CH, Ivanova G, Omura C, Mo S, Vitaterna MH, Lopez JP, Philipson LH, Bradfield CA, Crosby SD, JeBailey L, Wang X, Takahashi JS, Bass J. Disruption of the clock components CLOCK and BMAL1 leads to hypoinsulinaemia and diabetes. *Nature.* 2010 Jul 29;466(7306):627-31.

Maruyama T, Li J, Vaque JP, Konkel JE, Wang W, Zhang B, Zhang P, Zamarron BF, Yu D, Wu Y, Zhuang Y, Gutkind JS, Chen W. Control of the differentiation of regulatory T cells and T(H)17 cells by the DNA-binding inhibitor Id3. *Nat Immunol.* 2011 Jan;12(1):86-95.

Massberg S, Brand K, Grüner S, Page S, Müller E, Müller I, Bergmeier W, Richter T, Lorenz M, Konrad I, Nieswandt B, Gawaz M. A critical role of platelet adhesion in the initiation of atherosclerotic lesion formation. *J Exp Med.* 2002 Oct 7;196(7):887-96.

Literature

Matza D, Badou A, Jha MK, Willinger T, Antov A, Sanjabi S, Kobayashi KS, Marchesi VT, Flavell RA. Requirement for AHNAK1-mediated calcium signaling during T lymphocyte cytosis. *Proc Natl Acad Sci U S A.* 2009 Jun 16;106(24):9785-90.

May AE, Seizer P, Gawaz M. Platelets: inflammatory firebugs of vascular walls. *Arterioscler Thromb Vasc Biol.* 2008 Mar;28(3):s5-10.

McCarey DW, McInnes IB, Madhok R, Hampson R, Scherbakov O, Ford I, Capell HA, Sattar N. Trial of Atorvastatin in Rheumatoid Arthritis (TARA): double-blind, randomised placebo-controlled trial. *Lancet.* 2004 Jun 19;363(9426):2015-21.

Mei L, Xiong WC. Neuregulin 1 in neural development, synaptic plasticity and schizophrenia. *Nat Rev Neurosci.* 2008 Jun;9(6):437-52.

Miaw SC, Kang BY, White IA, Ho IC. A repressor of GATA-mediated negative feedback mechanism of T cell activation. *J Immunol.* 2004 Jan 1;172(1):170-7.

Milne SA, McGregor AL, McCulloch J, Sharkey J. Increased expression of macrophage receptor with collagenous structure (MARCO) in mouse cortex following middle cerebral artery occlusion. *Neurosci Lett.* 2005 Jul 22-29;383(1-2):58-62.

MENDEL G. Gregor Mendel's letters to Carl Nägeli, 1866-1873. *Genetics.* 1950 Sep;35(5:2):1-29.

Morgan TH. THE ORIGIN OF FIVE MUTATIONS IN EYE COLOR IN DROSOPHILA AND THEIR MODES OF INHERITANCE. *Science.* 1911 Apr 7;33(849):534-7.

Muhlestein JB. Effect of antiplatelet therapy on inflammatory markers in atherothrombotic patients. *Thromb Haemost.* 2010 Jan;103(1):71-82.

Muller AJ, Baker JF, DuHadaway JB, Ge K, Farmer G, Donover PS, Meade R, Reid C, Grzanna R, Roach AH, Shah N, Soler AP, Prendergast GC. Targeted disruption of the murine Bin1/Amphiphysin II gene does not disable endocytosis but results in embryonic cardiomyopathy with aberrant myofibril formation. *Mol Cell Biol.* 2003 Jun;23(12):4295-306.

Murphy B, Magee CC, Alexander SI, Waaga AM, Snoeck HW, Vella JP, Carpenter CB, Sayegh MH. Inhibition of allorecognition by a human class II MHC-derived peptide through the induction of apoptosis. *J Clin Invest.* 1999 Mar;103(6):859-67.

Literature

Murray CJ, Lopez AD. Global mortality, disability, and the contribution of risk factors: Global Burden of Disease Study. *Lancet.* 1997 May 17;349(9063):1436-42.

Mustacchi R, Hohmann S, Nielsen J. Yeast systems biology to unravel the network of life. *Yeast.* 2006 Feb; 23(3):227-38.

Nakashima Y, Plump AS, Raines EW, Breslow JL, Ross R. ApoE-deficient mice develop lesions of all phases of atherosclerosis throughout the arterial tree. *Arterioscler Thromb.* 1994 Jan;14(1):133-40.

Napoli C, D'Armiento FP, Mancini FP, Postiglione A, Witztum JL, Palumbo G, Palinski W. Fatty streak formation occurs in human fetal aortas and is greatly enhanced by maternal hypercholesterolemia. Intimal accumulation of low density lipoprotein and its oxidation precede monocyte recruitment into early atherosclerotic lesions. *J Clin Invest.* 1997 Dec 1;100(11):2680-90.

Nassar T, Sachais BS, Akkawi S, Kowalska MA, Bdeir K, Leitersdorf E, Hiss E, Ziporen L, Aviram M, Cines D, Poncz M, Higazi AA. Platelet factor 4 enhances the binding of oxidized low-density lipoprotein to vascular wall cells. *J Biol Chem.* 2003 Feb 21;278(8):6187-93.

Navab M, Berliner JA, Watson AD, Hama SY, Territo MC, Lusis AJ, Shih DM, Van Lenten BJ, Frank JS, Demer LL, Edwards PA, Fogelman AM. The Yin and Yang of oxidation in the development of the fatty streak. A review based on the 1994 George Lyman Duff Memorial Lecture. *Arterioscler Thromb Vasc Biol.* 1996 Jul;16(7):831-42.

Ng SB, Bigham AW, Buckingham KJ, Hannibal MC, McMillin MJ, Gildersleeve HI, Beck AE, Tabor HK, Cooper GM, Mefford HC, Lee C, Turner EH, Smith JD, Rieder MJ Yoshiura K, Matsumoto N, Ohta T, Niikawa N, Nickerson DA, Bamshad MJ. Exome sequencing identifies MLL2 mutations as a cause of Kabuki syndrome. *Nat Genet.* 2010 Sep;42(9):790-3.

Nguyên-Trân VT, Kubalak SW, Minamisawa S, Fiset C, Wollert KC, Brown AB, Ruiz-Lozano P, Barrere-Lemaire S, Kondo R, Norman LW, Gourdie RG, Rahme MM, Feld GK, Clark RB, Giles WR, Chien KR. A novel genetic pathway for sudden cardiac death via defects in the transition between ventricular and conduction system cell lineages. *Cell.* 2000 Sep 1;102(5):671-82.

Nicoletti A, Caligiuri G, Törnberg I, Kodama T, Stemme S, Hansson GK. The macrophage scavenger receptor type A directs modified proteins to antigen presentation. *Eur J Immunol.* 1999 Feb;29(2):512-21.

Niculescu F, Rus H. The role of complement activation in atherosclerosis. *Immunol Res.* 2004;30(1):73-80.

Literature

Nissen SE, Tuzcu EM, Schoenhagen P, Crowe T, Sasiela WJ, Tsai J, Orazem J, Magorien RD, O'Shaughnessy C, Ganz P. Reversal of Atherosclerosis with Aggressive Lipid Lowering (REVERSAL) Investigators. Statin therapy, LDL cholesterol, C-reactive protein, and coronary artery disease. *N Engl J Med.* 2005 Jan 6;352(1):29-38.

Niu XL, Madamanchi NR, Vendrov AE, Tchivilev I, Rojas M, Madamanchi C, Brandes RP, Krause KH, Humphries J, Smith A, Burnand KG, Runge MS. Nox activator 1: a potential target for modulation of vascular reactive oxygen species in atherosclerotic arteries. *Circulation.* 2010 Feb 2;121(4):549-59.

Norris EH, Giasson BI, Lee VM. Molecular mechanisms of alpha-synuclein neurodegeneration. Alpha-synuclein: normal function and role in neurodegenerative diseases. *Curr Top Dev Biol.* 2004;60:17-54.

Okimoto GS. On the analysis of microarray data with applications to cancer and cardiovascular disease. *Doctoral thesis* 2006; University of Hawaii at Manoa, Honolulu.

O'Reilly MK, Paulson JC. Siglecs as targets for therapy in immune-cell-mediated disease. *Trends Pharmacol Sci.* 2009 May;30(5):240-8.

Parker N, Porter AC. Identification of a novel gene family that includes the interferon-inducible human genes 6-16 and ISG12. *BMC Genomics.* 2004 Jan 19;5(1):8.

Paulussen AD, Stegmann AP, Blok MJ, Tserpelis D, Posma-Velter C, Detisch Y, Smeets EE, Wagemans A, Schrander JJ, van den Boogaard MJ, van der Smagt J, van Haeringen A, Stolte-Dijkstra I, Kerstjens-Frederikse WS, Mancini GM, Wessels MW, Hennekam RC, Vreeburg M, Geraedts J, de Ravel T, Fryns JP, Smeets HJ, Devriendt K, Schrander-Stumpel CT. MLL2 mutation spectrum in 45 patients with Kabuki syndrome. *Hum Mutat.* 2011 Feb;32(2):E2018-25.

Pease AC, Solas D, Sullivan EJ, Cronin MT, Holmes CP, Fodor SP. Light-generated oligonucleotide arrays for rapid DNA sequence analysis. *Proc Natl Acad Sci U S A.* 1994 May 24;91(11):5022-6.

Pendergrass SA, Hayes E, Farina G, Lemaire R, Farber HW, Whitfield ML, Lafyatis R. Limited systemic sclerosis patients with pulmonary arterial hypertension show biomarkers of inflammation and vascular injury. *PLoS One.* 2010 Aug 17;5(8):e12106.

Peri G, Introna M, Corradi D, Iacutti G, Signorini S, Avanzini F, Pizzetti F, Maggioni AP, Moccetti T, Metra M, Cas LD, Ghezzi P, Sipe JD, Re G, Olivetti G, Mantovani A, Latini R. PTX3, A prototypical long pentraxin, is an early indicator of acute myocardial infarction in humans. *Circulation.* 2000 Aug 8;102(6):636-41.

Literature

Perkins ND. 2007. Integrating cell-signalling pathways with NF-kappaB and IKK function. *Nat Rev Mol Cell Biol.* 2007 Jan;8(1):49-62.

Pereira CP, Bachli EB, Schoedon G. The wnt pathway: a macrophage effector molecule that triggers inflammation. *Curr Atheroscler Rep.* 2009 May;11(3):236-42.

Pereira CP, Bachli EB, Schaer DJ, Schoedon G. Transcriptome analysis revealed unique genes as targets for the anti-inflammatory action of activated protein C in human macrophages. *PLoS One.* 2010 Oct 15;5(10):e15352.

Perrin-Cocon L, Agaugué S, Coutant F, Masurel A, Bezzine S, Lambeau G, André P, Lotteau V. Secretory phospholipase A2 induces dendritic cell maturation. *Eur J Immunol.* 2004 Aug;34(8):2293-302.

Piazza F, Costoya JA, Merghoub T, Hobbs RM, Pandolfi PP. Disruption of PLZP in mice leads to increased T-lymphocyte proliferation, cytokine production, and altered hematopoietic stem cell homeostasis. *Mol Cell Biol.* 2004 Dec;24(23):10456-69.

Platt N, Haworth R, Darley L, Gordon S. The many roles of the class A macrophage scavenger receptor. *Int Rev Cytol.* 2002;212:1-40.

Pons D, Trompet S, de Craen AJ, Thijssen PE, Quax PH, de Vries MR, Wierda RJ, van den Elsen PJ, Monraats PS, Ewing MM, Heijmans BT, Slagboom PE, Zwinderian AH, Doevedans PA, Tio RA, de Winter RJ, de Maat MP, Iakoubova OA, Sattar N, Shepherd J, Westendorp RG, Jukema JW; also on behalf of the PROSPER; WOSCOPS and GENDER study groups*. Genetic variation in PCAF, a key mediator in epigenetics, is associated with reduced vascular morbidity and mortality: evidence for a new concept from three independent prospective studies. *Heart.* 2011 Jan;97(2):143-50.

Poole JC, Florey HW. Changes in the endothelium of the aorta and the behaviour of macrophages in experimental atheroma of rabbits. *J Pathol Bacteriol.* 1958 Jul;75:2454-251.

Rabinovich GA, Baum LG, Tinari N, Paganelli R, Natoli C, Liu FT, Iacobelli S. Galectins and their ligands: amplifiers, silencers or tuners of the inflammatory response? *Trends Immunol.* 2002 Jun;23(6):313-20.

Rajavashisth T, Qiao JH, Tripathi S, Tripathi J, Mishra N, Hua M, Wang XP, Loussararian A, Clinton S, Libby P, Lusis A. Heterozygous osteopetrosis (op) mutation reduces atherosclerosis in LDL receptor-deficient mice. *J Clin Invest.* 1998 Jun 15;101(12):2702-10.

Literature

Réthelyi JM, Bakker SC, Polgár P, Czobor P, Strengman E, Pásztor PI, Kahn RS, Bitter I. Association study of NRG1, DTNBP1, RGS4, G72/G30 and PIP5K2A with schizophrenia and symptom severity in a Hungarian sample. *Am J Med Genet B Neuropsychiatr Genet.* 2010 Apr 5;153B(3):792-801.

Ridker PM, Cannon CP, Morrow D, Rifai N, Rose LM, McCabe CH, Pfeffer MA, Braunwald E; Pravastatin or Atorvastatin Evaluation and Infection Therapy-Thrombolysis in Myocardial Infarction 22 (PROVE IT-TIMI 22) Investigators. C-reactive protein levels and outcomes after statin therapy. *N Engl J Med.* 2005 Jan 6;352(1):20-8.

Rocha VZ, Libby P. Obesity, inflammation, and atherosclerosis. *Nat Rev Cardiol.* 2009 Jun;6(6):399-409.

Romo GM, Dong JF, Schade AJ, Gardiner EE, Kansas GS, Li CQ, McIntire LV, Berndt MC, López JA. The glycoprotein Ib-IX-V complex is a platelet counterreceptor for P-selectin. *J Exp Med.* 1999 Sep 20;190(6):803-14.

Rosendahl J, Teich N, Kovacs P, Szmola R, Blüher M, Gress TM, Hoffmeister A, Keim V, Löhr M, Mössner J, Nickel R, Ockenga J, Pfützer R, Schulz HU, Stumvoll M, Wittenburg H, Sahin-Tóth M, Witt H. Complete analysis of the human mesotrypsinogen gene (PRSS3) in patients with chronic pancreatitis. *Pancreatology.* 2010;10(2-3):243-9.

Rosenson RS, Tangney CC, Casey LC. Inhibition of proinflammatory cytokine production by pravastatin. *Lancet.* 1999 Mar 20;353(9157):983-4.

Ross R, Harker L. Hyperlipidemia and atherosclerosis. *Science.* 1976 Sep 17;193(4258):1094-100.

Ross R. The arterial wall and atherosclerosis. *Annu Rev Med.* 1979;30:1-15.

Ross R, Glomset J, Harker L. Response to injury and atherogenesis. *Am J Pathol.* 1977 Mar;86(3):675-84.

Ross R. Atherosclerosis--an inflammatory disease. *N Engl J Med.* 1999 Jan 14;340(2):115-26.

Ruffer M. On arterial lesions found in Egyptian mummies(158 BC-AD 525) *J Pathol Bact.* 1911 15: 453-462.

Sabatti C, Karsten SL, Geschwind DH. Thresholding rules for recovering a sparse signal from microarray experiments. *Math Biosci.* 2002 March; 176 (1):17-34.

Literature

Sachais BS, Kuo A, Nassar T, Morgan J, Kariko K, Williams KJ, Feldman M, Aviram M, Shah N, Jarett L, Poncz M, Cines DB, Higazi AA. Platelet factor 4 binds to low-density lipoprotein receptors and disrupts the endocytic machinery, resulting in retention of low-density lipoprotein on the cell surface. *Blood*. 2002 May 15;99(10):3613-22.

Sánchez-Sánchez N, Riol-Blanco L, Rodríguez-Fernández JL. The multiple personalities of the chemokine receptor CCR7 in dendritic cells. *J Immunol*. 2006 May 1;176(9):5153-9.

Saiura A, Sata M, Hirata Y, Nagai R, Makuuchi M. Circulating smooth muscle progenitor cells contribute to atherosclerosis. *Nat Med*. 2001 Apr;7(4):382-3.

Sandison A. Degenerative vascular disease in the Egyptian mummy. *Med Hist*. 1962 6: 77-81.

Sarrias MR, Grønlund J, Padilla O, Madsen J, Holmskov U, Lozano F. The Scavenger Receptor Cysteine-Rich (SRCR) domain: an ancient and highly conserved protein module of the innate immune system. *Crit Rev Immunol*. 2004;24(1):1-37.

Schmidt-Krey I, Mitsuoka K, Hirai T, Murata K, Cheng Y, Fujiyoshi Y, Morgenstern R, Hebert H. The three-dimensional map of microsomal glutathione transferase 1 at 6 Å resolution. *EMBO J*. 2000 Dec 1;19(23):6311-6.

Schmittgen TD, Livak KJ. Analyzing real-time PCR data by the comparative C(T) method. *Nat Protoc*. 2008;3(6):1101-8.

Schröder K. Isoform specific functions of Nox protein-derived reactive oxygen species in the vasculature. *Curr Opin Pharmacol*. 2010 Apr;10(2):122-6.

Schroeder A, Mueller O, Stocker S, Salowsky R, Leiber M, Gassmann M, Lightfoot S, Menzel W, Granzow M and Ragg T. The RIN: an RNA integrity number for assigning integrity values to RNA measurements. *BMC Mol. Biol*. 2006 7: 3.

Sedeek M, Hébert RL, Kennedy CR, Burns KD, Touyz RM. Molecular mechanisms of hypertension: role of Nox family NADPH oxidases. *Curr Opin Nephrol Hypertens*. 2009 Mar;18(2):122-7.

Seko Y, Cole S, Kasprzak W, Shapiro BA, Ragheb JA. The role of cytokine mRNA stability in the pathogenesis of autoimmune disease. *Autoimmun Rev*. 2006 May;5(5):299-305.

Shaw PX, Hörrkö S, Chang MK, Curtiss LK, Palinski W, Silverman GJ, Witztum JL. Natural antibodies with the T15 idiotype may act in atherosclerosis, apoptotic clearance, and protective immunity. *J Clin Invest*. 2000 Jun;105(12):1731-40.

Literature

Shen J, Yang M, Ju D, Jiang H, Zheng JP, Xu Z, Li L. Disruption of SM22 promotes inflammation after artery injury via nuclear factor kappaB activation. *Circ Res.* 2010 Apr 30;106(8):1351-62.

Shendure J. Exome sequencing identifies MLL2 mutations as a cause of Kabuki syndrome. *Nat Genet.* 2010 Sep;42(9):790-3.

Shevach EM. CD4+ CD25+ suppressor T cells: more questions than answers. *Nat Rev Immunol.* 2002 Jun;2(6):389-400.

Shi L, Reid LH, Jones WD, Shippy R, Warrington JA, Baker SC, Collins PJ, de Longueville F, Kawasaki ES, Lee KY, Luo Y, Sun YA, Willey JC, Setterquist RA, Fischer GM, Tong W, Dragan YP, Dix DJ, Frueh FW, Goodsaid FM, Herman D, Jensen RV, Johnson CD, Lobenhofer EK, Puri RK, Schrf U, Thierry-Mieg J, Wang C, Wilson M, Wolber PK, Zhang L, Amur S, Bao W, Barbacioru CC, Lucas AB, Bertholet V, Boysen C, Bromley B, Brown D, Brunner A, Canales R, Cao XM, Cebula TA, Chen JJ, Cheng J, Chu TM, Chudin E, Corson J, Corton JC, Croner LJ, Davies C, Davison TS, Delenstarr G, Deng X, Dorris D, Eklund AC, Fan XH, Fang H, Fulmer-Smentek S, Fuscoe JC, Gallagher K, Ge W, Guo L, Guo X, Hager J, Haje PK, Han J, Han T, Harbottle HC, Harris SC, Hatchwell E, Hauser CA, Hester S, Hong H, Hurban P, Jackson SA, Ji H, Knight CR, Kuo WP, LeClerc JE, Levy S, Li QZ, Liu C, Liu Y, Lombardi MJ, Ma Y, Magnuson SR, Maqsodi B, McDaniel T, Mei N, Myklebost O, Ning B, Novoradovskaya N, Orr MS, Osborn TW, Papallo A, Patterson TA, Perkins RG, Peters EH, Peterson R, Philips KL, Pine PS, Pusztai L, Qian F, Ren H, Rosen M, Rosenzweig BA, Samaha RR, Schena M, Schroth GP, Shchegrova S, Smith DD, Staedtler F, Su Z, Sun H, Szallasi Z, Tezak Z, Thierry-Mieg D, Thompson KL, Tikhonova I, Turpaz Y, Vallanat B, Van C, Walker SJ, Wang SJ, Wang Y, Wolfinger R, Wong A, Wu J, Xiao C, Xie Q, Xu J, Yang W, Zhang L, Zhong S, Zong Y, Slikker W Jr. The MicroArray Quality Control (MAQC) project shows inter- and intraplatform reproducibility of gene expression measurements. *Nat Biotechnol.* 2006 Sep;24(9):1151-61.

Shimada K, Miyauchi K, Daida H. Early intervention with atorvastatin modulates TH1/TH2 imbalance in patients with acute coronary syndrome: from bedside to bench. *Circulation.* 2004 May 11;109(18):e213-4.

Simeoni L, Lindquist JA, Smida M, Witte V, Arndt B, Schraven B. Control of lymphocyte development and activation by negative regulatory transmembrane adapter proteins. *Immunol Rev.* 2008 Aug;224:215-28.

Sinnaeve PR, Donahue MP, Grass P, Seo D, Vonderscher J, Chibout SD, Kraus WE, Sketch M Jr, Nelson C, Ginsburg GS, Goldschmidt-Clermont PJ, Granger CB. Gene expression patterns in peripheral blood correlate with the extent of coronary artery disease. *PLoS One.* 2009 Sep 14;4(9):e7037.

Literature

Sluimer JC, Kisters N, Cleutjens KB, Volger OL, Horrevoets AJ, van den Akker LH, Bijnens AP, Daemen MJ. Dead or alive: gene expression profiles of advanced atherosclerotic plaques from autopsy and surgery. *Physiol Genomics*. 2007 Aug 20;30(3):335-41.

Smith JD, Trogan E, Ginsberg M, Grigaux C, Tian J, Miyata M. Decreased atherosclerosis in mice deficient in both macrophage colony-stimulating factor (op) and apolipoprotein E. *Proc Natl Acad Sci U S A*. 1995 Aug 29;92(18):8264-8.

Stamler J, Wentworth D, Neaton JD. Is relationship between serum cholesterol and risk of premature death from coronary heart disease continuous and graded? Findings in 356,222 primary screenees of the Multiple Risk Factor Intervention Trial (MRFIT). *JAMA*. 1986 Nov 28;256(20):2823-8.

Stemme S, Faber B, Holm J, Wiklund O, Witztum JL, Hansson GK. T lymphocytes from human atherosclerotic plaques recognize oxidized low density lipoprotein. *Proc Natl Acad Sci U S A*. 1995 Apr 25;92(9):3893-7.

Stoecklin G, Anderson P. Posttranscriptional mechanisms regulating the inflammatory response. *Adv Immunol*. 2006;89:1-37.

Strnad J, Burke JR. IkappaB kinase inhibitors for treating autoimmune and inflammatory disorders: potential and challenges. *Trends Pharmacol Sci*. 2007 Mar;28(3):142-8.

Suzuki H, Kurihara Y, Takeya M, Kamada N, Kataoka M, Jishage K, Ueda O, Sakaguchi H, Higashi T, Suzuki T, Takashima Y, Kawabe Y, Cynshi O, Wada Y, Honda M, Kurihara H, Aburatani H, Doi T, Matsumoto A, Azuma S, Noda T, Toyoda Y, Itakura H, Yazaki Y, Kodama T, et al. A role for macrophage scavenger receptors in atherosclerosis and susceptibility to infection. *Nature*. 1997 Mar 20;386 (6622):292-6.

Takatsu K, Kouro T, Nagai Y. Interleukin 5 in the link between the innate and acquired immune response. *Adv Immunol*. 2009;101:191-236.

Takeda A, Matsuda A, Paul RM, Yaseen NR. CD45-associated protein inhibits CD45 dimerization and up-regulates its protein tyrosine phosphatase activity. *Blood*. 2004 May 1;103(9):3440-7.

Takemoto M, Node K, Nakagami H, Liao Y, Grimm M, Takemoto Y, Kitakaze M, Liao JK. Statins as antioxidant therapy for preventing cardiac myocyte hypertrophy. *J Clin Invest*. 2001 Nov;108(10):1429-37.

Literature

Tang JJ, Wang MW, Jia EZ, Yan JJ, Wang QM, Zhu J, Yang ZJ, Lu X, Wang LS. The common variant in the GSTM1 and GSTT1 genes is related to markers of oxidative stress and inflammation in patients with coronary artery disease: a case-only study. *Mol Biol Rep.* 2010 Jan;37(1):405-10.

Tegner J, Yeung MK, Hasty J, Collins JJ. Reverse engineering gene networks: integrating genetic perturbations with dynamical modeling. *Proc Natl Acad Sci U S A.* 2003 May 13;100(10):5944-9.

Tegnér J, Skogsberg J, Björkegren J. Thematic review series: systems biology approaches to metabolic and cardiovascular disorders. Multi-organ whole-genome measurements and reverse engineering to uncover gene networks underlying complex traits. *J Lipid Res.* 2007 Feb;48(2):267-77.

Thom T, Haase N, Rosamond W, Howard VJ, Rumsfeld J, Manolio T, Zheng ZJ, Flegal K, O'Donnell C, Kittner S, Lloyd-Jones D, Goff DC Jr, Hong Y, Adams R, Friday G, Furie K, Gorelick P, Kissela B, Marler J, Meigs J, Roger V, Sidney S, Sorlie P, Steinberger J, Wasserthiel-Smoller S, Wilson M, Wolf P. American Heart Association Statistics Committee and Stroke Statistics Subcommittee. Heart disease and stroke statistics--2006 update: a report from the American Heart Association Statistics Committee and Stroke Statistics Subcommittee. *Circulation.* 2006 Feb 14;113(6):e85-151.

Thomas PD, Campbell MJ, Kejariwal A, Mi H, Karlak B, Daverman R, Diemer K, Muruganujan A, Narechania A. PANTHER: a library of protein families and subfamilies indexed by function. *Genome Res.* 2003 Sep;13(9):2129-41.

Thomas PD, Kejariwal A, Guo N, Mi H, Campbell MJ, Muruganujan A, Lazareva-Ulitsky B. Applications for protein sequence-function evolution data: mRNA/protein expression analysis and coding SNP scoring tools. *Nucleic Acids Res.* 2006 Jul 1;34(Web Server issue):W645-50.

Toftgård R. Hedgehog signalling in cancer. *Cell Mol Life Sci.* 2000 Nov;57(12):1720-31.

Tonkin AM, Colquhoun D, Emberson J, Hague W, Keech A, Lane G, MacMahon S, Shaw J, Simes RJ, Thompson PL, White HD, Hunt D. Effects of pravastatin in 3260 patients with unstable angina: results from the LIPID study. *Lancet.* 2000 Dec 2;356(9245):1871-5.

Topper JN, Gimbrone MA Jr. Blood flow and vascular gene expression: fluid shear stress as a modulator of endothelial phenotype. *Mol Med Today.* 1999 Jan;5(1):40-6.

Trinchieri G. Interleukin-12 and the regulation of innate resistance and adaptive immunity. *Nat Rev Immunol.* 2003 Feb;3(2):133-46.

Literature

Tusher VG, Tibshirani R, Chu G. Significance analysis of microarrays applied to the ionizing radiation response. *Proc Natl Acad Sci U S A.* 2001 Apr 24;98(9):5116-21.

Tybulewicz VL. Vav-family proteins in T-cell signalling. *Curr Opin Immunol.* 2005 Jun;17(3):267-74.

Uchida K, Akita Y, Matsuo K, Fujiwara S, Nakagawa A, Kazaoka Y, Hachiya H, Naganawa Y, Oh-Iwa I, Ohura K, Saga S, Kawai T, Matsumoto Y, Shimozato K, Wang J, Zou L, Huang S, Lu F, Lang X, Han L, Song Z, Xu Z. Genetic polymorphisms of glutathione S-transferase genes GSTM1, GSTT1 and risk of coronary heart disease. *Mutagenesis.* 2010 Jul;25(4):365-9.

Uyemura K, Demer LL, Castle SC, Jullien D, Berliner JA, Gately MK, Warrier RR, Pham N, Fogelman AM, Modlin RL. Cross-regulatory roles of interleukin (IL)-12 and IL-10 in atherosclerosis. *J Clin Invest.* 1996 May 1;97(9):2130-8.

Virmani R, Burke AP, Farb A, Kolodgie FD. Pathology of the unstable plaque. *Prog Cardiovasc Dis.* 2002 Mar-Apr;44(5):349-56.

Velculescu VE, Zhang L, Vogelstein B, Kinzler KW. Serial analysis of gene expression. *Science.* 1995 Oct 20;270(5235):484-7.

Velculescu VE, Vogelstein B, Kinzler KW. Analysing uncharted transcriptomes with SAGE. *Trends Genet.* 2000 Oct;16(10):423-5.

Vollmer T, Key L, Durkalski V, Tyor W, Corboy J, Markovic-Plese S, Preiningerova J, Rizzo M, Singh I. Oral simvastatin treatment in relapsing-remitting multiple sclerosis. *Lancet.* 2004 May 15;363(9421):1607-8.

Wassmann S, Laufs U, Bäumer AT, Müller K, Konkol C, Sauer H, Böhm M, Nickenig G. Inhibition of geranylgeranylation reduces angiotensin II-mediated free radical production in vascular smooth muscle cells: involvement of angiotensin AT1 receptor expression and Rac1 GTPase. *Mol Pharmacol.* 2001 Mar;59(3):646-54.

Watkins H, Farrall M. Genetic susceptibility to coronary artery disease: from promise to progress. *Nat Rev Genet.* 2006 Mar;7(3):163-73.

Welch ID, Cowan MF, Beier F, Underhill TM. The retinoic acid binding protein CRABP2 is increased in murine models of degenerative joint disease. *Arthritis Res Ther.* 2009;11(1):R14.

Literature

Werner N, Nickenig G. Endothelial progenitor cells in health and atherosclerotic disease. *Ann Med.* 2007;39(2):82-90.

Williams KJ, Tabas I. The response-to-retention hypothesis of atherogenesis reinforced. *Curr Opin Lipidol.* 1998 Oct;9(5):471-4.

Wingrove JA, Daniels SE, Sehnert AJ, Tingley W, Elashoff MR, Rosenberg S, Buellesfeld L, Grube E, Newby LK, Ginsburg GS, Kraus WE. Correlation of peripheral-blood gene expression with the extent of coronary artery stenosis. *Circ Cardiovasc Genet.* 2008 Oct;1(1):31-8.

Wong W, Scott JD. AKAP signalling complexes: focal points in space and time. *Nat Rev Mol Cell Biol.* 2004 Dec;5(12):959-70.

Woppard KJ, Geissmann F. Monocytes in atherosclerosis: subsets and functions. *Nat Rev Cardiol.* 2010 Feb;7(2):77-86.

Worbs T, Förster R. A key role for CCR7 in establishing central and peripheral tolerance. *Trends Immunol.* 2007 Jun;28(6):274-80.

Wu H, Gower RM, Wang H, Perrard XY, Ma R, Bullard DC, Burns AR, Paul A, Smith CW, Simon SI, Ballantyne CM. Functional role of CD11c+ monocytes in atherogenesis associated with hypercholesterolemia. *Circulation.* 2009 May 26;119(20):2708-17.

Yilmaz A, Reiss C, Tantawi O, Weng A, Stumpf C, Raaz D, Ludwig J, Berger T, Steinkasserer A, Daniel WG, Garlichs CD. HMG-CoA reductase inhibitors suppress maturation of human dendritic cells: new implications for atherosclerosis. *Atherosclerosis.* 2004 Jan;172(1):85-93.

Yilmaz A, Weber J, Cicha I, Stumpf C, Klein M, Raithel D, Daniel WG, Garlichs CD. Decrease in circulating myeloid dendritic cell precursors in coronary artery disease. *J Am Coll Cardiol.* 2006 Jul 4;48(1):70-80.

Youssef S, Stüve O, Patarroyo JC, Ruiz PJ, Radosevich JL, Hur EM, Bravo M, Mitchell DJ, Sobel RA, Steinman L, Zamvil SS. The HMG-CoA reductase inhibitor, atorvastatin, promotes a Th2 bias and reverses paralysis in central nervous system autoimmune disease. *Nature.* 2002 Nov 7;420(6911):78-84.

Yuan JS, Kousis PC, Suliman S, Visan I, Guidos CJ. Functions of notch signaling in the immune system: consensus and controversies. *Annu Rev Immunol.* 2010 Mar;28:343-65.

Literature

Zambon A, Deeb SS, Pauletto P, Crepaldi G, Brunzell JD. Hepatic lipase: a marker for cardiovascular disease risk and response to therapy. *Curr Opin Lipidol.* 2003 Apr;14(2):179-89.

Zanetti M. Cathelicidins, multifunctional peptides of the innate immunity. *J Leukoc Biol.* 2004 Jan;75(1):39-48.

Zang W, Murphy B. Peptide-mediated immunosuppression. *Am J Ther.* 2005 Nov-Dec;12(6):592-9.

Zheng B, Berrie CP, Corda D, Farquhar MG. GDE1/MIR16 is a glycerophosphoinositol phosphodiesterase regulated by stimulation of G protein-coupled receptors. *Proc Natl Acad Sci U S A.* 2003 Feb 18;100(4):1745-50.

Zhou L, Zhang P, Cheng Z, Hao W, Wang R, Fang Q, Cao JM. Altered circadian rhythm of cardiac beta₃-adrenoceptor activity following myocardial infarction in the rat. *Basic Res Cardiol.* 2010 Jul 27.

VIII. Acknowledgements

First, I would like to thank Prof. Dr. Katalin Csiszar for giving me as an external PhD student the opportunity to conduct my experimental work in her laboratory at the Cardiovascular Research Center, University of Hawaii, Honolulu. She never let her students down (including myself) and provided a creative research environment that she generously guided with her scientific expertise.

I am thankful to Dr. Richard Girton for inviting me to a journey of an exciting microarray study dealing with a largely unexplored area of atherosclerosis research at a time when my initial PhD project seemed to cease in a dead end due to technical and methodical challenges.

Furthermore, I am greatly indebted to Prof. Dr. Arnd Baumann who has been my academic mentor at the University of Cologne since my early undergraduate studies. Without his support, my PhD endeavor overseas could not have been realized. In addition, his scientific advice throughout my dissertation was a tremendous gift.

I am thankful to everybody at the Cardiovascular Research Center (CVRC) for their support. Nowadays, scientific work has become increasingly an interdisciplinary team effort and I would like to thank in particular several people at CVRC for their help during my PhD projects. Dr. Ben Fogelgren for insightful discussions and for helping me to get familiar with the technical equipment at the research center, Dr. Keith Fong for introducing me into DNA cloning techniques, Dr. Kornelia Molnarne Szauter for her great support on the microarray study, Prof. Dr. Mark Goldman for valuable discussions and for teaching me the efficiency of well designed experiments, Dr. Gordon Okimoto for sharing his profound knowledge in bioinformatics, Linda Fong for her administrative support and last but not least Prof. Dr. Charles Boyd for guiding the Cardiovascular Research Center with great leadership and charisma through difficult times.

Most importantly, I want to thank Ulli for her infinite patience with a long-term PhD student.

IX. Erklärung

Ich versichere, dass ich die von mir vorgelegte Dissertation selbstständig angefertigt, die benutzten Quellen und Hilfsmittel vollständig angegeben und die Stellen der Arbeit - einschließlich Tabellen, Karten und Abbildungen-, die anderen Werken im Wortlaut oder dem Sinn nach entnommen sind, in jedem Einzelfall als Entlehnung kenntlich gemacht habe; dass diese Dissertation noch keiner anderen Fakultät oder Universität zur Prüfung vorgelegen hat; dass sie - abgesehen von unten angegebenen Teilpublikationen - noch nicht veröffentlicht worden ist sowie, dass ich eine solche Veröffentlichung vor Abschluß des Promotionsverfahrens nicht vornehmen werde.

Die Bestimmungen dieser Promotionsordnung sind mir bekannt. Die von mir vorgelegte Dissertation ist von Prof. Dr. Arnd Baumann (Universität zu Köln) und von Prof. Dr. Katalin Csiszar (University of Hawaii at Manoa, Honolulu) betreut worden.

Nachfolgend genannte Teilpublikationen liegen vor:

Jansen MK, Csiszar K. Intracellular localization of the matrix enzyme lysyl oxidase in polarized epithelial cells. *Matrix Biology* 2007, (2):136-9.

Szauter KM, Jansen MK, Okimoto G, Loomis M, Kimura JH, Heller M, Ku T, Tiirikainen M, Boyd CD, Csiszar K, Girton RA. Persistent inflammatory pathways associated with early-onset myocardial infarction in a medicated multiethnic hawaiian cohort. *Biochemistry Insights* 2011, (4): 13-27.

Köln, im Februar 2012

(Matthias Jansen)